

Network architecture and heme-responsive gene regulation of the two-component systems HrrSA and ChrSA

Marc Keppel

Schlüsseltechnologien / Key Technologies

Band / Volume 203

ISBN 978-3-95806-427-0

Forschungszentrum Jülich GmbH
Institut für Bio-und Geowissenschaften
Biotechnologie (IBG-1)

Network architecture and heme-responsive gene regulation of the two-component systems HrrSA and ChrSA

Marc Keppel

Schriften des Forschungszentrums Jülich
Reihe Schlüsseltechnologien / Key Technologies

Band / Volume 203

ISSN 1866-1807

ISBN 978-3-95806-427-0

Bibliografische Information der Deutschen Nationalbibliothek.
Die Deutsche Nationalbibliothek verzeichnet diese Publikation in der
Deutschen Nationalbibliografie; detaillierte Bibliografische Daten
sind im Internet über <http://dnb.d-nb.de> abrufbar.

Herausgeber
und Vertrieb: Forschungszentrum Jülich GmbH
 Zentralbibliothek, Verlag
 52425 Jülich
 Tel.: +49 2461 61-5368
 Fax: +49 2461 61-6103
 zb-publikation@fz-juelich.de
 www.fz-juelich.de/zb

Umschlaggestaltung: Grafische Medien, Forschungszentrum Jülich GmbH

Druck: Grafische Medien, Forschungszentrum Jülich GmbH

Copyright: Forschungszentrum Jülich 2019

Schriften des Forschungszentrums Jülich
Reihe Schlüsseltechnologien / Key Technologies, Band / Volume 203

D 61 (Diss. Düsseldorf, Univ., 2018)

ISSN 1866-1807
ISBN 978-3-95806-427-0

Vollständig frei verfügbar über das Publikationsportal des Forschungszentrums Jülich (JuSER)
unter www.fz-juelich.de/zb/openaccess.



This is an Open Access publication distributed under the terms of the [Creative Commons Attribution License 4.0](https://creativecommons.org/licenses/by/4.0/),
which permits unrestricted use, distribution, and reproduction in any medium, provided the original work is properly cited.

„Alle Dinge sind Gift, und nichts ist ohne Gift; allein die Dosis macht’s,
dass ein Ding kein Gift sei.“

Paracelsus (1493–1541)

The studies presented in this dissertation have been published or submitted for publication in the following articles and manuscripts:

Keppel M., Davoudi E., Gätgens C. and Frunzke J. (2018) Membrane Topology and Heme Binding of the Histidine Kinases HrrS and ChrS in *Corynebacterium glutamicum*. *Frontiers in Microbiology*. 2018;9:183. doi:10.3389/fmicb.2018.00183.

Keppel M.*, Piepenbreier H.*, Gätgens C., Fritz G. and Frunzke F. (2018) Toxic but Tasty - Temporal Dynamics and Network Architecture of Heme-Responsive Two-Component Signalling in *Corynebacterium glutamicum*. **In revision:** *Molecular Microbiology*

Keppel M.*, Davoudi C-F.*, Filipchuk A.*, Viets U., Pfeifer E., Polen T., Baumgart M., Bott M., and Frunzke J. (2018) HrrSA Orchestrates a Systemic Response to Heme and Determines Prioritization of Terminal Cytochrome Oxidase Expression. **Manuscript submitted.**

**These authors contributed equally to this work.*

Abbreviations

ATCC	American Type Culture Collection	HK	Histidine kinase
BHI(S)	Brain Heart Infusion (+ Sorbitol)	IPTG	Isopropyl-thio- β -D-galactopyranosid
CA	Catalytical domain	OD ₆₀₀	Optical density at 600 nm
ChAP-Seq	Chromatin affinity purification and sequencing	OPD	Output domain
ChIP	Chromatin immunoprecipitation	REC	Receiver domain
DNA	Deoxyribonucleic acid	RNA	Ribonucleic acid
DHP	Dimerization histidine phosphotransfer domain	RNA-Seq	RNA Sequencing
EMSA	Electrophoretic mobility shift assay	RR	Response regulator
e.g.	<i>exempli gratia</i>	TCS	Two-component system
<i>et al.</i>	<i>et alii</i>	TLS	Translation start side
etc.	<i>et cetera</i>	TSS	Transcription start site
eYFP	Enhanced yellow fluorescent protein	TMD	Transmembrane domain
		UV	Ultraviolet
		v/v	Volume per volume
		wt	Wild-type
		w/v	Weight per volume

Further abbreviations not included in this section are according to international standards, as, for example, listed in the author guidelines of the Journal of Cell Biology (<http://jcb.rupress.org/content/standard-abbreviations>).

Contents

1. Summary	1
2. Scientific context and key results of this thesis	2
2.1 Bacterial signal perception and transduction	2
2.1.1 Two-component signaling	3
2.2 Control of heme and iron homeostasis	8
2.2.1 The global relevance of iron	8
2.2.2 The regulation of iron homeostasis.....	9
2.2.3 Heme sensor systems.....	10
2.3 The heme-responsive two component systems HrrSA and ChrSA	14
2.3.1 Heme perception by the histidine kinases HrrS and ChrS	16
2.4 Heme-responsive gene regulation in <i>C. glutamicum</i>	18
2.4.1 Heme utilization vs. detoxification – a balancing act.....	19
2.5 Genome-wide profiling of the HrrSA regulon	23
2.5.1 Heme degradation and detoxification	24
2.5.2 The regulation of heme biosynthesis in <i>C. glutamicum</i>	24
2.5.3 The heme-dependent, HrrSA-mediated control of respiratory chain genes.....	27
2.5.4 Other targets of HrrSA.....	32
2.5.5 A glimpse into the unknown: HrrSA regulates several uncharacterized, cellular transport processes.....	34
2.5.6 The regulon of HrrSA and other global regulons: A comparison	38
2.6 Conclusion and outlook	40
3. Publications and manuscripts	44
3.1 Membrane Topology and Heme Binding of the Histidine Kinases HrrS and ChrS in <i>Corynebacterium glutamicum</i>	45
3.2 Toxic but Tasty - Temporal Dynamics and Network Architecture of Heme-Responsive Two-Component Signalling in <i>Corynebacterium glutamicum</i>	58
3.3 HrrSA Orchestrates a Systemic Response to Heme and Determines Prioritization of Terminal Cytochrome Oxidase Expression.	74

4. References	93
5. Appendix	102
5.1 Supplement “Membrane Topology and Heme Binding of the Histidine Kinases HrrS and ChrS”	108
5.2 Supplement “Toxic but Tasty - Temporal Dynamics and Network Architecture of Heme-Responsive Two-Component Signalling”	124
5.3 Supplement “HrrSA orchestrates a systemic response to heme and determines prioritization of terminal cytochrome oxidase expression”	145

1. Summary

Heme (iron bound protoporphyrin IX) is a versatile molecule that serves as the prosthetic group of various proteins, including hemoglobins, hydroxylases, catalases, peroxidases, and cytochromes. Because of its essential role in many cellular processes, such as electron transfer, respiration and oxygen metabolism, heme is synthesized and used by virtually all aerobic eukaryotic and prokaryotic species. As hemoglobin represents the most abundant iron reservoir in mammalian hosts and heme proteins are ubiquitously found in organic material, heme represents an important alternative source of iron for pathogenic and nonpathogenic bacteria alike. Despite its necessity for nearly all cellular life, elevated, intracellular heme levels are extremely toxic. To cope with this Janus-faced nature of heme, sophisticated regulatory systems have evolved to tightly balance its uptake, synthesis and utilization.

Remarkably, in several corynebacterial species, e.g. *Corynebacterium glutamicum* and *Corynebacterium diphtheriae*, two paralogous, heme-responsive two-component systems (TCSs), HrrSA and ChrSA, are dedicated to the coordinated control of heme homeostasis. Previous studies showed that, while HrrSA is required for utilization of heme as an alternative iron source by activating expression of a heme oxygenase (*hmuO*), ChrSA drives detoxification by induction of the *hrtBA* operon, which encodes a heme export system. Additionally, the histidine kinases (HKs) of both systems are able to phosphorylate both response regulators (RRs). This cross-talk is proofread by a specific phosphatase activity of the HKs.

In the framework of this PhD thesis, the signal perception, the temporal dynamics of heme-induced target gene activation and the constitution of the HrrSA regulon have been studied in detail. A comparative analysis of the membrane topology and the heme-binding characteristics of the HKs HrrS and ChrS revealed that while N-terminal sensing parts share only minor sequence similarity, both proteins are embedded into the cytoplasmic membrane *via* six α -helices and bind heme in a 1:1 stoichiometry per monomer. Alanine-scanning of conserved amino acid residues in the N-terminal sensor domain of HrrS revealed three aromatic residues (Y¹¹², F¹¹⁵, F¹¹⁸), which apparently contribute to heme binding and suggest an intra-membrane sensing mechanism of this HK. Exchange of the corresponding residues in ChrS and the resulting red shift of the Soret band of the heme-protein complex indicated, that in this HK, an altered set of ligands might contribute to binding in the triple mutant.

To understand how the particular regulatory network architecture of HrrSA and ChrSA shapes the dynamic response to heme, experimental reporter profiling was combined with a quantitative mathematical model. We found, that both HKs contribute to the fast onset of the detoxification response (*hrtBA*) upon stimulus perception and that the instant deactivation of the *hrtBA* promoter is achieved by a strong ChrS phosphatase activity upon stimulus decline. While the activation of the detoxification response is uncoupled from further factors, heme utilization (*hmuO*) is additionally governed by the global iron regulator DtxR, which integrates information on iron availability into the regulatory network.

Time-resolved and genome-wide monitoring of *in-vivo* promoter occupancy of HrrA revealed binding to more than 250 different genomic targets, which encode proteins associated with heme biosynthesis, the respiratory chain, oxidative stress response and cell envelope remodeling. Additionally, we found that in heme-rich environments, HrrA represses *sigC*, which encodes an activator of the *cydABCD* operon. Thereby, HrrA prioritizes the expression of genes encoding the cytochrome *bc₁-aa₃* supercomplex for the constitution of the respiratory chain.

In conclusion, this thesis provides comprehensive insights into the regulatory interplay of the HrrSA and ChrSA TCS shaping a systemic response to the versatile signaling molecule heme. Furthermore, for the first time, a time-resolved dataset of stimulus-dependent regulator binding and the resulting transcriptional changes grant global insight into heme-regulated gene expression in bacterial cells.

2. Scientific context and key results of this thesis

2.1 Bacterial signal perception and transduction

In diverse environments with an everchanging, unpredictable nutrient supply and the constant confrontation with harmful substances, the key to life is a fast recognition of extracellular and intracellular stimuli as well as a consequent adaptation at the level of gene expression. According to this principle, bacteria have evolved highly elaborate signaling systems to interact with environmental stimuli such as temperature gradients, occurrence of certain toxic or beneficial molecules, osmolarity, pH, and even light (Mascher *et al.*, 2006; Parkinson, 1993). The perception of these stimuli can ultimately lead to a variety of cellular outputs, ranging from an initiation of protective measures or metabolic adjustments to drastic responses, like the physical movement of a motile, bacterial cell towards a nutrient source or away from harmful conditions (Baker *et al.*, 2006). Furthermore, bacterial signaling systems can play an important role in the virulence of pathogenic strains, for example by sensing antibiotics and subsequently conferring resistance or by coordinating the timely expression of virulence factors (Chang *et al.*, 2018; Tiwari *et al.*, 2017). Thus, these systems represent an interesting target for the development of novel, medical treatment methods.

While a broad range of different signal transduction systems exist in bacteria, the fundamental principle is conserved. It consists of an initial signal detection, a subsequent processing of the stimulus (e.g. amplification or combination with additional inputs), the transduction, and finally the orchestration of an appropriate cellular output (Parkinson, 1993). Consequently, a minimum of two communication modules is needed to perform this task. These modules were termed transmitter and receiver by Parkinson *et al.* in 1992 (Parkinson and Kofoed, 1992).

For the simplest signal transduction pathways, a single protein carries both the input (transmitter) and the output (receiver) module. Classical prokaryotic transcriptional regulators, which act as one-component systems, represent these very prevalent systems. These regulators are suggested to be evolutionarily older than the more complex two-component systems (Ulrich *et al.*, 2005), which split transmitter and receiver domains into two proteins in signaling cascades.

The very fundamentals of bacterial gene control were discovered by François Jacob and Jacques Monod in the 1950s, after they studied the classical *Escherichia coli* LacI repressor, which binds a sugar molecule (stimulus/input) and consequently loses its repressing activity (output) (Jacob and Monod, 1961). Other classical examples for this type of regulators are

members of the TetR family that are involved in antibiotic resistance, metabolism, or quorum sensing (Cuthbertson and Nodwell, 2013).

Another group of general transcription factors, called sigma factors, are interchangeable subunits of prokaryotic RNA polymerases. Besides a primary sigma factor, needed for housekeeping functions of the cell, most bacteria possess a variety of alternative sigma factors that associate with the RNA polymerase under specific conditions or in response to certain stimuli and subsequently guide the polymerase to their target promoters (Davis *et al.*, 2017; Helmann, 1999). In doing so, a single sigma factor can regulate hundreds of genes and thereby, for example, impact the cellular metabolism, the general stress responses, the sporulation and the virulence of a particular strain (Ishihama, 2010; Kazmierczak *et al.*, 2005). In the case of extracytoplasmic-function (ECF) sigma factors, the activity of these proteins is often controlled by the interaction with so called anti-sigma factors (Mascher, 2013). This interaction can be reverted if the sigma factor is needed and the dissociation often occurs in response to a certain extracellular or intracellular stimulus (Helmann, 1999).

An alternative regulatory mechanism is RNA interference. This process is independent of a regulatory protein but instead, small RNAs bind to the mRNA of their target genes or even to their regulatory proteins in response to a stimulus and thereby inhibit gene expression (Storz *et al.*, 2011).

2.1.1 Two-component signaling

Two-component systems (TCSs) separate the transmitter and receiver modules and consist of two independent proteins with a conserved overall architecture (Figure 1). Upon interaction with a stimulus, an often membrane bound histidine kinase (HK, transmitter) undergoes autophosphorylation at a conserved histidine residue and subsequently catalyzes the phosphotransfer to a conserved aspartate residue of a cytoplasmatic response regulator (RR, receiver, (Capra and Laub, 2012; Mascher *et al.*, 2006; Stock *et al.*, 2000)). After phosphorylation, the RR becomes active and initiates an appropriate cellular output, commonly by binding promoter regions of target genes and acting as a transcription factor. In other cases, the output of an active RR is modulated by protein-protein interactions, e.g. in the case of chemotaxis regulation (Mascher *et al.*, 2006).

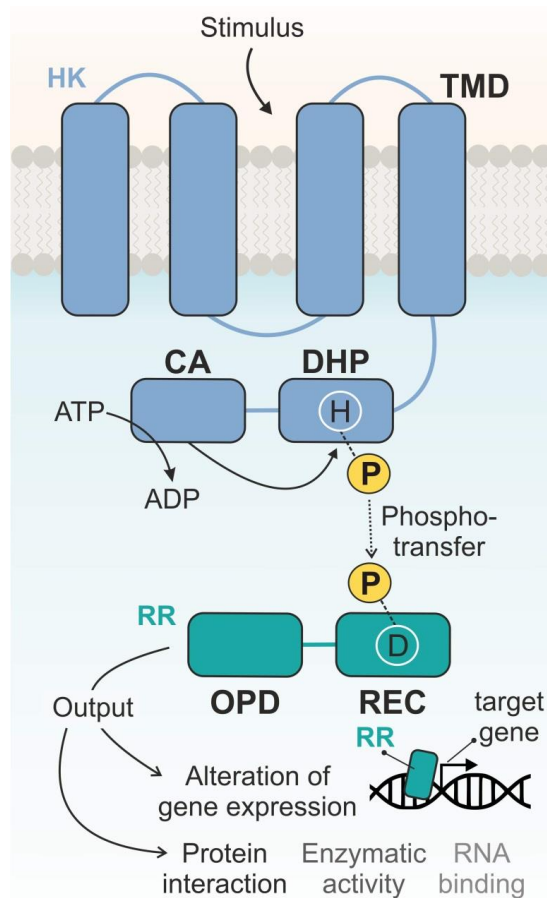


Figure 1: Architecture of a prototypical two-component system. An - often membrane bound - histidine kinase (HK, blue) interacts with the stimulus. Most commonly, this interaction takes place at the sensory domain, which is often located in or at the transmembrane domain (TMD) of the HK and which leads to intramolecular changes and activity of the catalytic domain (CA, stands for “catalytic and ATPase domain”). The CA mediates autophosphorylation of a conserved histidine residue (H) located in the dimerization and histidine phosphotransfer domain (DHP). Subsequently, the phosphate residue (yellow) is transferred to a conserved aspartate residue (D), located in the receiver domain (REC) of the cytoplasmic response regulator (RR, turquoise). The output domain (OPD) of the RR initiates the physiological output, for example by binding promoter regions of target genes and activating or repressing gene expression, by enzymatic activity or by protein-protein or protein-RNA interactions. Figure modified from (Jensen *et al.*, 2002)

While nearly every bacterial cell - with only few exceptions, such as some *Mycoplasma* species - contains multiple TCSs to regulate almost all aspects of its life (Capra and Laub, 2012; Mascher *et al.*, 2006), this type of signaling seems to be completely absent from well characterized members of the animal kingdom, such as *Homo sapiens*, *Drosophila melanogaster* and *Caenorhabditis elegans* (Wolanin *et al.*, 2002). However, in some eukaryotes, such as fungi and plants, a small number of TCSs has been described in the

past, which are involved in oxidative stress response, cell-cycle control or the sensing of osmotic stress (Catlett *et al.*, 2003; Santos and Shiozaki, 2001; Wolanin *et al.*, 2002).

2.1.1.1 Histidine kinases

Two-component systems allow the bacterial cell to react to vastly different stimuli. In these systems, HKs act as transient sensors and, by design, allow for a broad range of different inputs while maintaining a relatively simple and conserved architecture. A HK consists of – at least – two domains. The N-terminus of the enzyme contains an input domain, which is often membrane bound (transmembrane domain, TMD; Figure 1). This domain is responsible for the interaction with an individual stimulus, for example by binding a specific signaling molecule or by sensing a physical stimulation in the membrane (Mascher *et al.*, 2006). It is highly diverse, not only regarding the site of stimulus-interaction but also concerning the membrane anchoring.

The second domain of a HK is the C-terminal transmitter domain. This catalytic domain contains the dimerization and histidine phosphotransfer domain (DHP), a catalytical ATP binding domain (CA) and often either a PAS, a HAMP, or a GAF domain is located between the N-terminal TMD and the C-terminal transmitter domain (Galperin *et al.*, 2001; Galperin, 2005).

The transmitter domain becomes active in response to intramolecular changes after interaction of the sensor domain with its stimulus (Mascher *et al.*, 2006; Wolanin *et al.*, 2002). After subsequent autophosphorylation of the DHP domain, an active kinase (often present as a dimer) transfers the phosphate group to its cognate response regulator.

Besides phosphorylation, the dephosphorylation of the RR is crucial for a fast and transient response and the reset to the initial, inactive state after contact to a stimulus. The dephosphorylation can either be catalyzed by the RR itself (autophosphatase activity (Mascher *et al.*, 2006)) or be part of a negative regulation loop of the HK (phosphatase activity), preventing RR activity under the absence of the native stimulus. By regulating the activity of the two states of a hybrid kinase-phosphatase enzyme according to stimulus levels, a very transient and fast response can be achieved by the bacterial cell. A specific HK phosphatase activity, however, does not only allow a transient response but can help to maintain pathway specificity for a cognate HK-RR pair. A strong phosphatase activity can counteract unspecific, stimulus-independent RR activity in cases where the RR is phosphorylated by secondary sources, e.g. by non-cognate HKs or by molecular, intracellular phosphate donors such as acetylphosphate (McCleary and Stock, 1994).

The first phosphatase motifs were characterized in the CheC/CheX/FliY phosphatase family of *E. coli*. Pazy *et al.* (2010) reported a co-crystal structure of a CheX(HK)-CheY3(RR) complex, which was the snapshot of a dephosphorylation reaction. The phosphoryl group of CheY3 (HisKA subfamily) interacted with a helix of CheX, carrying a conserved ExxN motif. This motif was identified to be crucial for the dephosphorylation reaction. In the HK CheZ, which belongs to the HisKA_3 subfamily, an alternative DxxxQ phosphatase motif was identified (Silversmith, 2010). This interface was shown to be highly conserved among HKs of the HisKA_3 subfamily that contain a DHP domain (Willett and Kirby, 2012).

In both motifs, ExxN and DxxxQ, the polar residues asparagine (N) or glutamine (Q) are positioned to form a hydrogen bond with water molecules to allow an in-line attack of the phosphate (Silversmith, 2010), while the negatively charged residues aspartic acid (D) or glutamic acid (E) form salt bridges with residues in the RR (Pazy *et al.*, 2010; Zhao *et al.*, 2002).

Several high-resolution crystal structures of the cytoplasmic parts of HKs have been published, which greatly improved the knowledge on the molecular functionality of signal transduction (Albanesi *et al.*, 2009; Diensthuber *et al.*, 2013; Ferris *et al.*, 2012; Ferris *et al.*, 2014; Mechaly *et al.*, 2014). These studies proposed that a typical, intracellular DHP domain forms a bundle of four α -helices, with two helices from each HK monomer. Moreover, the conserved histidine residue is embedded into this structure and is located on the outer surface of helix 1 (Bhate *et al.*, 2015).

While the structure of C-terminal transmitter domains has been studied in detail for the last ten years, the architecture of HK sensory domains (TMDs) remained an enigma for the longest time, as the membrane localization of these parts diminishes the accessibility in structural analyses. Because of this, the recent publication of two crystal structures of the full-length nitrate/nitrite sensor kinase NarQ from *E. coli* represents a major scientific breakthrough (Gushchin *et al.*, 2017). A mutated ligand-free and a ligand-bound structure revealed, how stimulus perception (nitrate) induces significant rearrangements of the TMHs in the N-terminal sensor domain.

By combining liquid- and solid-state NMR, another recent study could impressively demonstrate that in the HK CitA, the binding of citrate as stimulus leads to contraction of the extracytoplasmic PAS domain (Salvi *et al.*, 2017). This movement in response to ligand interaction can also be speculated for other PAS-domains, as structures of DcuS and DctB suggest (Cheung and Hendrickson, 2008). While these studies proposed a mechanism of signal perception with a subsequent transduction to the catalytic kinase core for HKs with a

PAS domain, these mechanisms remain an important issue for future research on the majority of kinases that do not contain such a domain.

2.1.1.2 Response regulators

The cytoplasmatic RR of a TCS is phosphorylated at a conserved aspartate residue. This residue is located at the N-terminus of the protein, in a conserved, regulatory receiver domain (REC; Figure 1). For the majority of TCSs, the RR is phosphorylated in a direct interaction with the kinase, as described above. In a prototypical RR, phosphorylation of the N-terminal domain affects the activity of a C-terminal effector domain that shapes the cellular output (Stock *et al.*, 2000). Just like the input domains of HKs, the effector (output) domains of RRs are highly diverse and specifically adapted to the preferred way of regulation in response to the stimulus sensed by the HK. With more than 60 % however, the majority of effector domains binds to specific DNA sequences and directly influences target gene expression (Gao *et al.*, 2007; Stock *et al.*, 2000). Most RRs that act as direct transcriptional regulators, often feature a helix-turn-helix (HTH) motif (Aravind *et al.*, 2005) or, in rare cases, β -strands (Sidote *et al.*, 2008).

Apart from transcriptional regulation of an active RR, several enzymatic output domains have been described. For instance, proteins of the CheB family, which are involved in chemotaxis, harbor a C-terminal methyl-erectase as effector domain (West *et al.*, 1995) or PleD, which acts as a diguanylate cyclase, if activated (Chan *et al.*, 2004).

Other interesting output domains have been identified in the past, for example in the RR PhyR from *Methylobacterium extorquens*. PhyR consists of a prototypical REC domain combined with a C-terminal sigma factor-like output domain and is e.g. involved in stress responses of this bacterium (Galperin, 2010; Gourion *et al.*, 2006). The sigma-factor like domain can interact with an anti-sigma factor in a partner-switching mechanism leading to the release of the functional sigma factor, which subsequently recruits the RNA-polymerase to the promoters of stress-related genes (Francez-Charlot *et al.*, 2009).

In contrast to that, a more complex signal transduction can be achieved by combining two TCSs in a single pathway. These regulatory setups are called phosphorelays and integrate multiple signals from more than one TCS into a single phosphotransfer cascade. One example for this can be found in the regulation of sporulation in *Bacillus subtilis* (Burbulys *et al.*, 1991). Here, a phosphate is transferred between an His-Asp-His-Asp sequence. Two kinases (KinA and KinB) autophosphorylate in response to an extracellular stimulus and transfer the phosphoryl group to the first response regulator, Spo0F. Subsequently, an additional HK, Spo0B, receives the phosphate from Spo0F and transfers it to the last RR Spo0A, which then represses gene expression to shape the cellular output.

2.1.1.3 Stimulus perception of two-component systems

The sophisticated regulatory network architectures of two component systems evolved to cope with the drastic amount of crucial information in complex bacterial habitats. The act of sensing essential nutrients and the subsequent adjustment of metabolic pathways according to nutrient availability is one of the most important challenges in bacterial life. Here, two-component systems have the significant advantage that membrane bound histidine kinases are not limited to intracellular sensing but can also interact with certain stimuli extracellularly or even in the membrane (Keppel *et al.*, 2018b; Mascher *et al.*, 2006). Additionally, a variety of different output domains of cytoplasmic RRs enable nearly endless possibilities of genomic or phenotypic adaptation to the stimuli that are sensed by the HKs.

Well characterized examples for prototypical TCS from *E. coli* are the cytoplasmic NtrBC system, which is important for the regulation of nitrogen assimilation (Weiss *et al.*, 2002), the EnvZ/OmpR system, which can sense and initiate the response to changes in the extracellular osmolarity (Leonardo and Forst, 1996) and PhoBR, which senses availability of phosphate (Wanner and Chang, 1987). CitAB was discussed previously and regulates the citrate fermentation of *E. coli* and *Klebsiella pneumoniae* (Kaspar and Bott, 2002; Scheu *et al.*, 2012). Other TCSs can directly sense trace elements such as copper, zinc or iron. One example for this sensing is the iron-responsive FirRS system of nontypeable *Haemophilus influenzae*, which becomes active when the HK FirS interacts with ferrous iron or zinc in the periplasm. This system is speculated to be important for the pathogenicity of this bacterium (Steele *et al.*, 2012).

2.2 Control of heme and iron homeostasis

2.2.1 The global relevance of iron

With only few exceptions, the availability of iron molecules is critical to nearly all living organisms. Iron is involved in crucial, cellular processes like respiration and an essential part of [Fe-S] proteins like aconitases or fumarases, which catalyze reactions of the tricarboxylic acid (TCA) cycle (Cornelis *et al.*, 2011). Due to the poor solubility of Fe³⁺ and the role of Fe²⁺ in the Fenton/Haber-Weiss reaction, which produces harmful reactive oxygen species (Andrews *et al.*, 2003; Cornelis *et al.*, 2011), iron uptake needs to be tightly balanced with its sequestration and storage to prevent toxic concentrations.

In a review on the bacterial iron homeostasis, Andrews *et al.* (2003) define five general strategies of bacteria to appropriately manage their iron homeostasis. First, most bacteria possess high-affinity transporters in their membrane, to import iron or scavenge iron containing molecules from the environment, even if the concentrations are low (Andrews *et al.*, 2003). Additionally, bacterial cells often export ferric chelators (siderophores/hemophores) to bind iron ions or iron-containing heme molecules with a high affinity and subsequently scavenge them from the environment (Braun, 2001). The second strategy is the deposition of intracellular iron to allow for bacterial growth in times of iron scarcity (Andrews, 1998). Several iron storage mechanisms are applied by bacteria, including the prototypical ferritin, which is conserved between eukaryotes and prokaryotes and Dps, which is exclusively found in prokaryotes (Andrews *et al.*, 2003). In both cases, soluble ferrous iron is taken up by a multimeric protein complex, which consists of 24 monomers in case of ferritin and 12 in case of Dps. Two ferrous ions are bound to conserved residues in the single subunits and oxidized by O₂, leading to a di-ferric intermediate (Andrews *et al.*, 2003; Grant *et al.*, 1998). Subsequently, the ferric iron is stored either in a ferrihydrite core or in an amorphous ferric phosphate core, depending on phosphate availability. Besides ferritin or Dps, several bacterial species also harbor bacterioferritins that store iron in the form of heme molecules (Andrews *et al.*, 2003). As described earlier, Fe²⁺ molecules play a role in the formation of reactive oxygen species. To counteract this process, the third strategy to manage iron homeostasis is the expression of sophisticated resistance systems against redox stress (Andrews *et al.*, 2003). The fourth strategy is the downregulation of iron consuming processes in iron restrictive environments and the fifth strategy is the application of global iron-responsive regulatory systems that coordinate and fine-tune the expression of an extensive list of target genes involved in cellular iron homeostasis (Andrews *et al.*, 2003).

2.2.2 The regulation of iron homeostasis

Typically, iron homeostasis is regulated by global iron-dependent transcriptional regulators in the cytoplasm. The best characterized examples of global iron-dependent transcriptional regulators are DtxR and the ferric uptake regulator (Fur). Upon binding of a Fe²⁺ ion, Fur forms homodimers, which exhibit increased affinity for specific DNA sequences, called Fur-boxes, and repress e.g., iron acquisition genes by blocking the RNA polymerase (Lavrrar and McIntosh, 2003). In contrast, under iron deprivation, Fur is present in its iron-free form and thus, target genes of the iron-starvation regulon, iron uptake genes or storage genes are no longer repressed. Known targets for Fur proteins are e.g. the ferric citrate transport system (*fecABCDE*), the ferrichrome-iron receptor, encoded by *fhuA*, or *ftnA*, which is involved in iron storage (Carpenter *et al.*, 2009; Pohl *et al.*, 2003). In 2014, a genome wide binding study of Fur in *E. coli* extended the scope of its regulon beyond iron transport and storage (Seo *et*

al., 2014). Interestingly, the authors found direct Fur-mediated regulation of an enzyme of the TCA cycle, indicating a role of this regulator in the switch between fermentative pathways and oxidative phosphorylation in response to changing iron availability. Further examples for regulatory roles of Fur were postulated for biofilm formation, DNA synthesis and acidic stress response, highlighting the global impact of iron-dependent gene regulation in microbial systems (Seo *et al.*, 2014).

As long ago as 1936, Pappenheimer and Johnson reported the discovery, that the production of the diphtheria toxin in *Corynebacterium diphtheriae* is regulated by iron (Merchant and Spatafora, 2014; Pappenheimer and Johnson, 1936). Decades later, this finding was finally attributed to the function of the DtxR protein (diphtheria toxin repressor), which orchestrates iron-dependent gene expression in this important human pathogen. DtxR was however, not only described in the pathogen *C. diphtheriae* but later in the biotechnologically relevant soil bacterium *Corynebacterium glutamicum* (Boyd *et al.*, 1990; Schmitt and Holmes, 1991; Wennerhold and Bott, 2006). The regulator was found to be involved in i) iron acquisition, by repressing several transporters, including siderophore or heme transporter proteins, ii) in the storage of iron by activating ferritin (*ftn*) and *dps* expression and iii) in the assembly of iron-sulfur clusters by repressing the *suf* operon in *C. glutamicum*. Furthermore, DtxR binds in front of several genes that code for important transcriptional regulators, including *ripA*, which encodes a protein involved in regulation of iron-containing protein expression, and *hrrA*, encoding the RR of the HrrSA TCS (Frunzke *et al.*, 2011; Keppel *et al.*, 2018a; Wennerhold and Bott, 2006). The RR HrrA – and its target gene regulation – is a focus of this thesis.

With the growing number of sequenced bacterial genomes, various DtxR homologs have been identified since its first description, especially in Gram-positive pathogens. Amongst them are proteins like MntR from *Staphylococcus aureus* and *B. subtilis*, IdeR from *Mycobacterium tuberculosis* or SloR from *Streptococcus mutans* (Merchant and Spatafora, 2014). The link of these regulators to the virulence of the bacteria suggests that the level of iron is recognized as an important signal for the cell during infection (Merchant and Spatafora, 2014).

2.2.3 Heme sensor systems

Heme (iron bound protoporphyrin IX) is an essential molecule for nearly all aerobic cells, due to its role in critical cellular processes like electron transfer, respiration and oxygen metabolism (Ajioka *et al.*, 2006) and is synthesized and used by prokaryotes and eukaryotes alike (Ponka, 1999). It serves as important prosthetic group of cytochromes, hydroxylases, catalases, peroxidases, and hemoglobins (Layer *et al.*, 2010). Moreover, as hemoglobin is the most abundant reservoir of iron in the human body, host synthesized heme is often the only reliable source of iron for many pathogenic bacteria (Contreras *et al.*, 2014). In times of

iron deprivation however, not only pathogenic bacteria rely on the salvage of heme-bound iron. A broad variety of different, bacterial heme transporters and heme oxygenases that catalyze the degradation of heme (Wilks, 2002) testify to the importance of this molecule as alternative iron source, also for non-pathogenic lifecycles.

Similar to iron, however, heme causes severe toxicity at elevated levels. In human cells, the toxicity is speculated to partly originate from heme as an abundant source of redox-active iron, inducing the formation of reactive oxygen species and thereby damaging lipids, proteins, and the genomic DNA (Kumar and Bandyopadhyay, 2005). Additionally, heme is capable of promoting oxidation after aggregation in biological membranes thereby inducing cell lysis and was shown to catalyze the degradation of specific, small, mammalian proteins (Aft and Mueller, 1984). While studies concentrated on the toxic side effects of heme in eukaryotic cells, the mechanism of how this molecule affects bacterial cells is not conclusively unraveled (Anzaldi and Skaar, 2010). However, in our experiments, we could observe, that heme shows a much higher toxicity than corresponding iron concentrations, indicating that the central iron atom is not solely responsible for the toxic effect on bacterial cells. Furthermore, previous studies could demonstrate that certain non-iron metalloporphyrins (MPs) possess a strong antibacterial activity (Stojiljkovic *et al.*, 1999), additionally hinting at a general, iron-independent toxicity of certain porphyrin structures.

The absolute necessity of heme for prokaryotic and eukaryotic life, paired with its significant toxicity at high intracellular concentrations has led to the evolution of complex regulatory networks to equilibrate heme uptake and synthesis with its degradation and detoxification (Anzaldi and Skaar, 2010). In *Saccharomyces cerevisiae*, for example, the heme activator protein (Hap1) regulates genes, encoding various heme containing cytochromes, a catalase and flavohemoglobin in a heme-dependent manner (Figure 2A, (Hon *et al.*, 2005)). In this organism, important aerobic genes are directly activated by Hap1 while hypoxic genes are indirectly repressed by the activation of the ROX1 expression, which encodes a transcriptional repressor (Hickman and Winston, 2007). As the biosynthesis of heme is oxygen-dependent, *S. cerevisiae* utilizes this mechanism to indirectly sense hypoxia, *via* availability of heme (Zitomer *et al.*, 1997).

In mammalian cells, the activity of a conserved transcription factor named BTB and CNC homology 1 (BACH1, Figure 2B) is shaped by heme-binding (Ogawa *et al.*, 2001). This protein acts as a key player in the balancing of the cellular heme content by regulating *HMOX1*, which encodes a heme oxygenase (Sun *et al.*, 2002), as well as iron storage ferritin, a thioredoxin reductase (Hintze *et al.*, 2007), the NAD(P)H:menadione oxidoreductase 1 (Dhakshinamoorthy *et al.*, 2005) and more than 50 other target genes (Warnatz *et al.*, 2011).

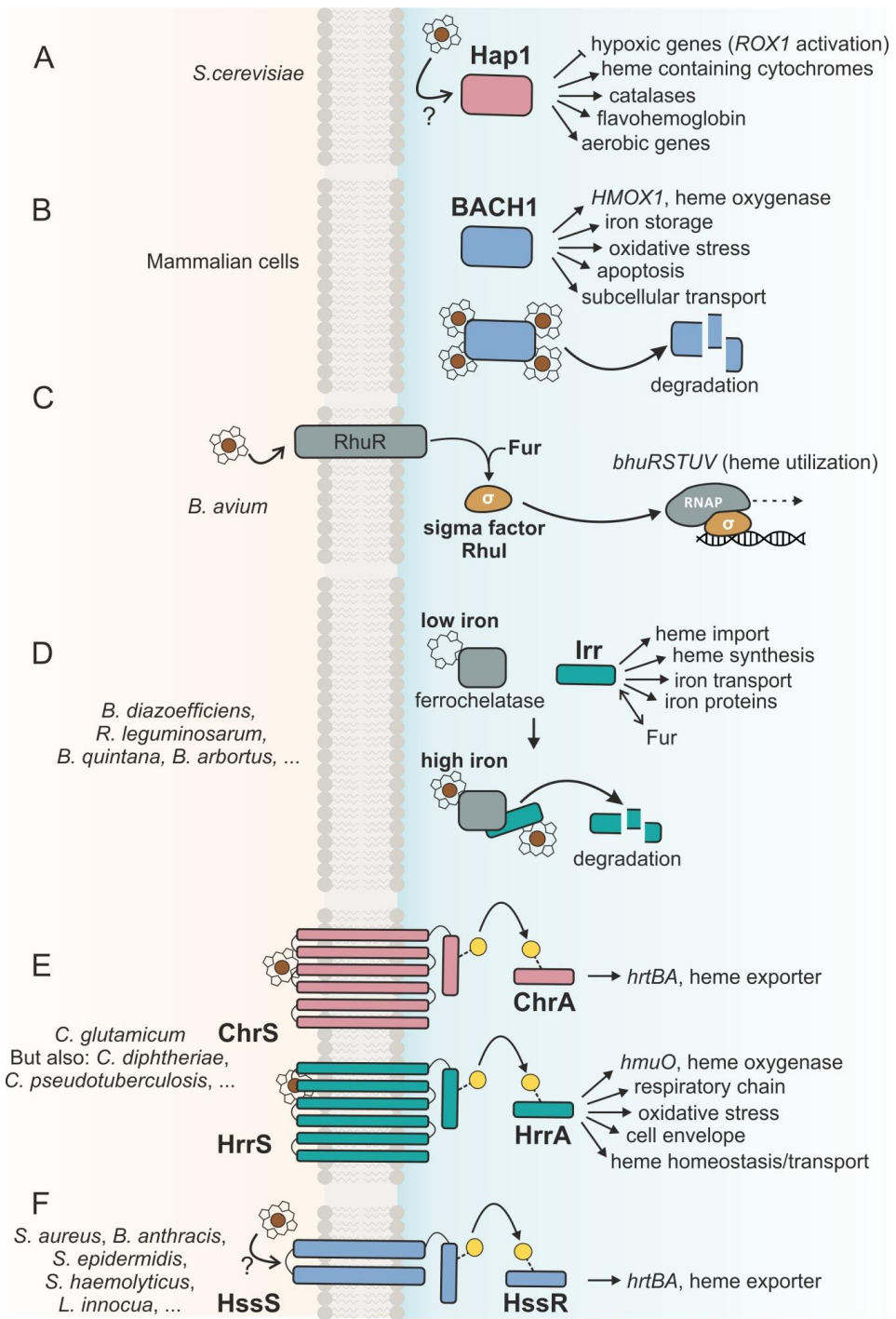


Figure 2: Heme sensor systems. To cope with the multi-faceted stimulus heme, sophisticated heme sensor systems have evolved in both eukaryotes and prokaryotes. Six examples are depicted in this Figure.

A: In *Saccharomyces cerevisiae*, Hap1 regulates heme containing cytochromes, a catalase and flavohemoglobin in a heme-dependent manner in response to hypoxia (Zhang and Hach, 1999).

B: In mammalian cells, BACH1 regulates more than 50 genes, involved in oxidative stress, iron metabolism, heme metabolism, apoptosis and several other cellular mechanisms. Upon heme binding, BACH1 is exported from the nucleus and degraded subsequently (Zenke-Kawasaki *et al.*, 2007).

C: In *Bordetella avium*, RhuR, a membrane anchored heme sensor, interacts with heme and activates the sigma factor Rhul, which are shown to be responsible for heme-dependent activation of $P_{bhuRSTUV}$ (needed for heme utilization, (Kirby *et al.*, 2004)).

D: The rhizobial Irr protein was shown to be involved in the regulation of heme utilization, heme import and heme synthesis in *Bradyrhizobium diazoefficiens* (Qi *et al.*, 1999). In high iron containing environments Irr binds heme and forms a complex with the ferrochelatase, which inserts an iron molecule into protoporphyrin IX. In response to this binding, Irr is degraded. This part of the figure is adapted from (Qi and O'Brian, 2002). Other organisms containing an *irr* gene are e.g., *Rhizobium leguminosarum*, *Bartonella quintana*, and *Brucella abortus*.

E: In *Corynebacterium glutamicum*, two paralogous two-component systems are involved in the regulation of heme homeostasis. While the ChrSA system regulates the detoxification of heme by activating the expression of *hrtBA*, which encodes for a heme exporter, HrrSA orchestrates a homeostatic response, which was unraveled as a part of this thesis (Hentschel *et al.*, 2014; Keppel *et al.*, 2018a). A similar sensor setup can be found in e.g., *Corynebacterium diphtheriae* or *Corynebacterium pseudotuberculosis*.

F: In *Staphylococcus aureus* and *Bacillus anthracis* the HssSR TCS activates the expression of *hrtBA* in a heme-dependent manner. For these systems however, it is unclear whether the kinases interact directly with heme or whether secondary effects are sensed (Stauff and Skaar, 2009a; Stauff and Skaar, 2009b). HssRS homologs are also present in e.g., *Staphylococcus epidermidis*, *Staphylococcus haemolyticus* and *Listeria innocua*.

The Gram-negative bacterium *Bordetella avium* controls the expression of its heme utilization system by adjusting the activity of an ECF sigma factor (Figure 2C). Here, a membrane bound protein named RhuR interacts with extracellular heme and activates the sigma factor Rhul, which then activates the *bhuR* promoter (Kirby *et al.*, 2004). Additional evidences hint to an iron-dependent influence of Fur on Rhul activity.

In the nitrogen-fixating bacterium *Bradyrhizobium diazoefficiens* (former *Bradyrhizobium japonicum*), a regulator named Irr (Figure 2D) was shown to be involved in the regulation of heme utilization, heme import and heme synthesis by repressing, e.g., *hemB*, which encodes a crucial enzyme in the heme biosynthesis pathway or the *hmuVUT* operon, encoding a heme-import system (Hamza *et al.*, 1998; Rudolph *et al.*, 2006). Interestingly, while Irr belongs to the family of Fur-like proteins, it does not bind iron directly, but senses the iron pool indirectly *via* heme interaction with a heme regulatory motif (HRM, (Qi *et al.*, 1999; Qi and O'Brian, 2002)). Additionally, direct interaction of Irr with the ferrochelatase, the enzyme, which catalyzes the terminal step of heme biosynthesis by inserting an iron molecule into protoporphyrin IX, could be shown. The Irr-ferrochelatase complex is only formed under high-iron conditions (if heme is produced) and leads to the degradation of Irr and thereby to the de-repression of its target genes (Qi and O'Brian, 2002). Furthermore, in *Rhodobacter sphaeroides*, Irr was found to be involved in the regulation of specific, iron-induced stress

responses, e.g. response to oxidative stress by repressing the expression of *katE*, which encodes a catalase (Peuser *et al.*, 2012).

Notably, some alpha-proteobacteria rely entirely on *Irr* for their iron-responsive gene regulation, while *Fur* inhibits a rather minor role compared to e.g. *E. coli*, where it represents the global regulator of iron homeostasis (Johnston *et al.*, 2007). This setup is particularly interesting because these bacteria integrate heme and iron homeostasis into one regulon and thereby sense “functional” iron pools (in form of heme) instead of free iron (Johnston *et al.*, 2007).

2.3 The heme-responsive two component systems HrrSA and ChrSA

In Gram-positive bacteria, TCSs appear to be the predominant form of heme sensing. The pathogenic species *B. anthracis* and *S. aureus* deploy a system called HssRS to determine heme concentrations and subsequently activate the expression of a heme exporter, encoded by the *hrtBA* operon (Figure 2F, (Stauff and Skaar, 2009a; Stauff and Skaar, 2009b)). Interestingly, it was suggested that the *S. aureus* kinase HssS might not sense heme molecules directly. The application of several non-iron metalloporphyrins showed that, instead, secondary effects of heme toxicity (e.g., heme-induced cell-wall damage or membrane disruption) might influence the activity of this system (Wakeman *et al.*, 2014). A recent study could demonstrate significant cross-regulation between HssRS and a second system called HssRS interfacing ICS (HitRS), which indeed integrates cell envelope stress into the HssRS regulon (Mike *et al.*, 2014). Homologous TCSs can be found in *Lactococcus lactis* or *Staphylococcus epidermidis* (Stauff and Skaar, 2009a).

A unique sensing mechanism for heme can be found in the *Corynebacteriaceae* family. In the human pathogen *C. diphtheriae* and the biotechnologically relevant soil bacterium *C. glutamicum*, extensive studies established two TCSs, named HrrSA and ChrSA, as critical regulatory systems for the utilization and detoxification of heme (Bibb and Schmitt, 2010; Frunzke *et al.*, 2011; Heyer *et al.*, 2012). While the interaction of TCSs on the level of phosphorylation or target gene activation is known for several regulons (Laub and Goulian, 2007; Mike *et al.*, 2014), this particular setup is remarkable, as it is the first example of two paralogous systems reacting to the same stimulus (Figure 2E). We could show that in *C. glutamicum*, both HKs, HrrS and ChrS, directly interact with heme (Keppel *et al.*, 2018b). After stimulus perception, the kinases not only phosphorylate their cognate RRs, but may also compensate for a loss of the other kinase as significant cross-phosphorylation was observed between these two systems. Previous studies postulated that this cross-talk is proofread by phosphatase activities of HrrS and ChrS. With the specific dephosphorylation of HrrA and ChrA, an unwanted activation of these regulators is prevented and the system is

shut down in absence of the stimulus (Hentschel *et al.*, 2014), allowing both systems to fulfill their designated roles in the heme metabolism of *C. glutamicum*. While HrrSA is responsible for the activation of *hmuO*, which encodes a heme oxygenase and enables the cell to use heme as an alternative iron source, ChrSA positively regulates *hrtBA*, which encodes a heme regulated transporter efflux pump to cope with toxic, intracellular heme concentrations (Frunzke *et al.*, 2011; Hentschel *et al.*, 2014; Heyer *et al.*, 2012). For HrrSA, six additional target genes were postulated (Frunzke *et al.*, 2011). These targets are involved in heme biosynthesis (*hemE*, *hemH* and *hemA*) and encode two heme-containing proteins of the respiratory chain (*ctaD* and *ctaE*). Additionally, binding of HrrA between the *chrSA* operon and its target operon *hrtBA* was observed (Frunzke *et al.*, 2011). As discussed earlier, information on iron availability is fed into the HrrA regulon via DtxR, the master regulator of iron homeostasis, as both *hrrA* and the target gene *hmuO* are repressed in an iron-dependent manner (Wennerhold and Bott, 2006). Besides a significant, positive autoregulation of ChrSA, the only identified binding of ChrA is in the promoter region of *hrrA* and *hrtBA* (Heyer *et al.*, 2012).

Interestingly, despite the identical, genomic setup, the regulatory output of the two systems seemingly differs between *C. diphtheriae* and *C. glutamicum*. While *hrtBA* is exclusively regulated by ChrSA in both species, a coordinated control of *hmuO* was proposed for HrrSA and ChrSA for *C. diphtheriae* (Bibb *et al.*, 2005; Bibb and Schmitt, 2010). In contrast to the regulatory setup in *C. glutamicum*, which utilizes HrrSA as the only activator of *hmuO*, ChrSA is proposed as the predominant regulatory system for the *hmuO* promoter (80 %) in *C. diphtheriae*, while the HrrSA contribution is only minor (20 %). This hypothesis was derived from single RR deletion mutants (Bibb *et al.*, 2007). A similar cooperative control could recently be shown for the regulation of *hemA*, which encodes a glutamyl-tRNA reductase that catalyzes an early step in the biosynthesis of heme (Burgos and Schmitt, 2016). Additionally, the same study proposed that HrrS inhibits a minimal kinase activity and functions primarily as a phosphatase. However, this theory is mainly based on *in-vitro* data. Furthermore, *in-vivo* phosphorylation studies with HrrA indicated that this RR is phosphorylated under virtually all conditions and independently of whether hemoglobin was added as a stimulus, or not. Additionally, no *in-vivo* phosphorylation of ChrA could be determined in this study. For the *in-vivo* phosphorylation experiments, cell samples were taken after 24 h of cultivation in hemoglobin containing medium. In *C. glutamicum*, it could be shown that heme is rapidly taken up by the cells and that the highest stimulus intensity was observed 30 minutes after addition of hemin (Keppel *et al.*, 2018a). In the light of these findings, one could propose an alternative interpretation of the findings in *C. diphtheriae*: after 24 h of cultivation, all exogenous heme/hemoglobin is consumed and the endogenous heme pool, which slightly increases in the stationary phase, compared to exponential phase

(Keppel *et al.*, 2018a), is enough to stimulate HrrA phosphorylation – but not ChrA phosphorylation. Alternative experiments, where the phosphorylation state of HrrA and ChrA in direct response to hemoglobin contact - or even in a time resolved manner - might give further insight into the heme-dependent signal transduction in *C. diphtheriae*.

A comparable organization and high sequence identities with small, but impactful differences in the regulatory processes indicate that these two systems in *C. glutamicum* and *C. diphtheriae* originate from a common ancestor but evolved to adapt to the different environmental conditions that are faced by the different bacterial species.

However, as some aspects of the regulatory interplay between HrrSA and ChrSA remain unclear to date in both bacterial species, further comparative studies are needed to elucidate the aspects in which the regulatory setups truly differ - and where proposed differences stem from not fully understood, regulatory mechanisms.

2.3.1 Heme perception by the histidine kinases HrrS and ChrS

For the modulation of an appropriate, cellular output in response to an extracellular stimulus, a precise, initial signal detection is critical. In the TCSs HrrSA and ChrSA, the two membrane bound kinase proteins are responsible for this stimulus perception. The recognition is enabled by direct interaction with the input molecule heme. The direct HK-heme interactions was first reported in the publication “Membrane Topology and Heme Binding of the Histidine Kinases HrrS and ChrS in *Corynebacterium glutamicum*”, conducted as part of this PhD thesis (Keppel *et al.*, 2018b). In this comparative analysis, the N-terminal sensor domains of HrrS and ChrS were mapped using PhoA and LacZ fusions, which revealed that both HKs are embedded into the membrane *via* six α -helices (transmembrane helices, TMHs). With an N-terminal sequence identity of only 8.5 %, the conservation of the sensory domain is rather minor, making the seemingly conserved structural characteristics of six TMHs even more interesting. In line with our data, the sensor domain of ChrS in *C. diphtheriae* was also predicted to be anchored *via* six TMHs (Bibb and Schmitt, 2010), despite only moderate amino acid sequence conservation to the kinases of *C. glutamicum* (ChrS: 29 % in the whole protein, 23 % in the N-terminus; HrrS: 35 % in the whole protein, 41 % in the N-terminus). This structural conservation, rather than conservation on the level of sequence, hints to a general function of the α -helices beyond anchoring of the proteins in the membrane. It can be speculated that the three cytoplasmatic loops or the six helices are involved in the intramolecular changes that follow heme perception.

In the HssRS system of *S. aureus* and *B. anthracis*, the periplasmic sensing domain of HssS is predicted to be flanked by only two transmembrane helices (Stauff and Skaar, 2009a). Additionally, the authors of this study speculate that the interaction with heme takes place

intracellularly, indicating that the mechanism of heme sensing vastly differs between HssRS and HrrSA/ChrSA.

Another interesting sensing mechanism was proposed for the BceSR system (Fritz *et al.*, 2015). This system is involved in the resistance against bacitracin but does not interact with the antibiotic directly. Instead, the HK BceS interacts with the bacitracin transporter BceAB and the activity of this drug efflux pump acts as the stimulus for the TCS (Fritz *et al.*, 2015). In *C. glutamicum* however, neither deletion of *hrtBA* (heme export, Figure S1) nor *hmuTUV* (heme import, data not shown) led to reduced activation of a P_{hrtBA} target gene reporter. This indicates that, in this case, the act of heme-transport does not directly contribute to the sensing of this molecule.

Instead we found that in the HK HrrS, the exchange of one of the three conserved aromatic amino acid residues Y¹¹², F¹¹⁵, and F¹¹⁸ to alanine led to reduced heme sensitivity of our reporter system. The residues are located in the cytoplasmic membrane and inside TMH number four (Keppel *et al.*, 2018b). In ChrS, the exchange of the same triplet led to an alternative mode of heme interaction as we noticed a red shift of the Soret band from 406 to 418 nm when conducting heme-bound, mutant protein to UV-visual spectroscopy. Unlike in HrrS, the triplet is localized in the extracellular loop between TMH three and four and not in the membrane. This small difference in position might be one explanation for the higher heme sensitivity of the ChrSA system that we reported in the same study. In a $\Delta hrrS$ strain, a P_{hrtBA} -*eyfp* reporter (activated by phosphorylated ChrA) showed measurable output in response to extracellular hemin concentrations as low as 0.5 μ M. In a $\Delta chrS$ strain, on the other hand, a P_{hmuO} -*eyfp* reporter (activated by phosphorylated HrrA) showed increased heme-dependent output only in medium containing at least 4 μ M hemin. However, a high background activity was measured for *hmuO*, which was independent of the addition of external heme and which might be triggered by the endogenous heme pool of the cell. (Keppel *et al.*, 2018b).

The higher sensitivity of the ChrSA detoxification system towards small changes in extracellular heme availability is physiologically reasonable, since it prevents heme export *via* HrtBA under non-toxic conditions. A fast, possibly extracellular sensing by ChrS might contribute to this high sensitivity and allows a rapid adaptation to environmental changes to fine-tune *hrtBA* expression. The sensing by HrrS most likely happens inside the membrane. By this mode of heme-interaction, the kinase probably senses a more stable pool of heme that accumulates in the membrane from both endogenous and exogenous sources. As a result, HrrA activity - and ultimately *hmuO* expression - might get adjusted more conservatively.

An interesting approach for future studies on the heme perception by HrrS and ChrS might be to narrow down the stimulus spectrum of both HKs. In our experiments, both TCS reacted to exogenously added hemin. However, it is possible that, while both HKs generally recognize iron-bound porphyrins, the affinity to certain heme types (e.g., heme *a*, heme *b*, heme *o*) might significantly differ between HrrS and ChrS. As hemin is the only commercially available and easily soluble iron-bound porphyrin, it is not possible to directly test various heme types. In *C. glutamicum*, the membrane bound CtaB catalyzes the reaction from heme *b* to heme *o*, which is subsequently converted to heme *a* by CtaA (Svensson *et al.*, 1993). By overexpression or deletion of one of the corresponding genes (*ctaB* or *ctaA*) the level of one heme type (*b*, *o* or *a*) could be significantly increased. Subsequently, the activity of target gene reporters could be observed in strains with changed heme pools. Changed phosphorylation levels might permit conclusions whether HrrS and ChrS differ in their preference with respect to different heme types.

In conclusion, our publication “Membrane Topology and Heme Binding of the Histidine Kinases HrrS and ChrS in *Corynebacterium glutamicum*” gives novel insight into the unique sensing mechanism of Gram-positive bacteria, which dedicate two independent kinases to sense heme and subsequently adjust their metabolism. Here, we present the example of a transient heme sensor system, which utilizes three aromatic amino acids to sense heme. Interpreting our findings further, a tyrosine (Y¹¹² in HrrS) might act as an axial ligand of the iron atom, while two phenylalanine residues (F¹¹⁵ and F¹¹⁸) might be important to the interface through aromatic stacking interactions with the porphyrin ring of heme. These results are in line with a recent study that analyzed the top five residues with high frequencies in heme-protein interaction sites and which found that cysteine, histidine, methionine as well as tyrosine and phenylalanine are the most prominent amino acids in such binding pockets (Keppel *et al.*, 2018b; Li *et al.*, 2011). In general, our study provides a basis for further analysis on structural and functional design of other important heme sensors and can help with the bioinformatical identification of novel heme binding domains in the future, as the prediction of these domains is, to this date and due to the high diversity in heme-interfaces, not reliably possible.

2.4 Heme-responsive gene regulation in *C. glutamicum*

Signal perception is followed by the modulation of an appropriate output. In *C. glutamicum*, heme perception by HrrS and ChrS is translated to HrrA/ChrA dependent gene regulation *via* phosphotransfer and thereby activation of the RRs. In common with many other characterized, heme-induced regulators, the first identified targets of these two TCSs were

involved in the detoxification (*hrtBA*, regulated by ChrSA), utilization (*hmuO*, regulated by HrrSA) and synthesis (*hemA*, *hemE*, *hemH*) of heme (Frunzke *et al.*, 2011; Heyer *et al.*, 2012).

2.4.1 Heme utilization vs. detoxification – a balancing act

To address the question how HrrSA and ChrSA differ in their signal transduction and the subsequent modulation of a physiological response, the temporal characteristics of the heme-induced detoxification and utilization were investigated (Keppel *et al.*, 2018c). On that account, we performed an extensive profiling of previously published target gene reporters (Hentschel *et al.*, 2014; Heyer *et al.*, 2012). These reporters are fusions of the promoter regions of the genes of interest (e.g., P_{hmuO} , P_{hrtBA}) with the *eyfp* gene, which encodes a yellow fluorescent protein (an expanded dataset can be found in the supplementary Figures S2-6). This reporter setup enables the determination of promoter activity by measuring the fluorescent output in response to a stimulus (in this case: hemin). Here, we screened the P_{hmuO} -*eyfp* and P_{hrtBA} -*eyfp* target gene reporters in the background of the wild type strain, as well as in mutant strains lacking single components of the two TCSs and in minimal medium containing different heme or iron concentrations (Keppel *et al.*, 2018c). The resulting dataset was integrated into a quantitative mathematical model, which was then used to test hypotheses on possible strategies that are applied by the two closely related TCSs to ensure physiologically appropriate target gene activation (Figure 3A).

In some environments, it makes sense for a bacterial cell to prioritize detoxification responses over the acquisition or utilization of nutrients, as toxic molecules can constitute an imminent threat, which demands a prompt reaction to ensure survival. Additionally, essential nutrients can often be toxic in elevated levels as already emphasized by the Swiss physician and founder of modern toxicology, Paracelsus (16th century), who proposed “All things are poison, and nothing is without poison, the dosage alone makes it so a thing is not a poison” (Borzelleca, 2000).

Examination of P_{hrtBA} and P_{hmuO} activity in wild type cells and in response to exogenous heme shows that *C. glutamicum* adheres to the principle of “detoxification first” when shaping its physiological response to heme (Figure 3B). After stimulus addition, we observed a nearly instant, transient, ChrSA-governed P_{hrtBA} response (Figure 3B, red line) while HrrSA-dependent P_{hmuO} activity was significantly delayed (green line). Together with the previous finding, that the threshold for heme-induced *hrtBA* activity is lower than for *hmuO* activity (Keppel *et al.*, 2018b), this establishes the regulation of *C. glutamicum* heme detoxification as fast and highly transient response to changing environmental conditions.

An additional, interesting observation was the steady response time of the P_{hrtBA} reporter in reaction to increasing heme concentrations – only the time of active promoter output increased with higher concentrations. Our model predicted, that this behavior is enabled by a nearly instant promoter saturation by phosphorylated ChrA (ChrA~P), following ChrS-heme interaction. Furthermore, we discovered a contribution of the HrrS kinase activity to the initial ChrA~P pool, as a $\Delta hrrS$ mutant strain showed a slightly delayed P_{hrtBA} reaction to the heme stimulus.

Another aspect, that distinguishes *hrtBA* and *hmuO* activity is the deactivation time. The response curves in Figure 3A clearly show that the promoter of *hrtBA* is shut off nearly instantly after 3-4 h. The following decline is the dilution of fluorescent eYFP protein by cell growth while no new reporter molecule is produced. Here, the model predicted, that this shut off correlates with the time it takes until all exogenous heme is depleted. This is in line with the previously discussed hypothesis, that - in contrast to HrrS, which senses heme in the membrane - ChrS interacts with the stimulus in the periplasm. Therefore, one could speculate that ChrS activity is mostly influenced by the extracellular heme pool while protein-bound heme in the cytoplasm or the membrane contributes to ChrS activation to a lesser extent. Here, further studies on the heme uptake, procession and storage could significantly contribute to our understanding of how the diverse sensing mechanisms of ChrS and HrrS influence the activation of downstream target gene expression.

A screening with phosphatase-OFF mutant strains, as well as previous studies indicate that the phosphatase activity of ChrS has significantly more impact than the HrrS phosphatase activity (Hentschel *et al.*, 2014; Keppel *et al.*, 2018c). This strong phosphatase activity, together with a possible extracellular sensing, might enable the observed, rapid shutoff of the detoxification response when the heme pool drops below a critical threshold.

Taken together, we hypothesize that the detoxification response of *C. glutamicum* is shaped by at least four important factors: i) a nearly instant promoter saturation by ChrA~P allows a rapid response under all tested conditions, ii) HrrS contributes to the initial ChrA~P pool, *via* cross-phosphorylation, iii) the speculated ChrS-heme interface is located closer to the periplasm, compared to the HrrS-heme interface, which might lead to slightly faster adaption to changing environmental conditions and less influence of endogenously produced heme or heme storage, and iv) a strong ChrS phosphatase activity shuts down heme export *via* HrtBA rapidly and effectively after stimulus decline and prevents unwanted cross-phosphorylation by HrrS under non-inducing conditions.

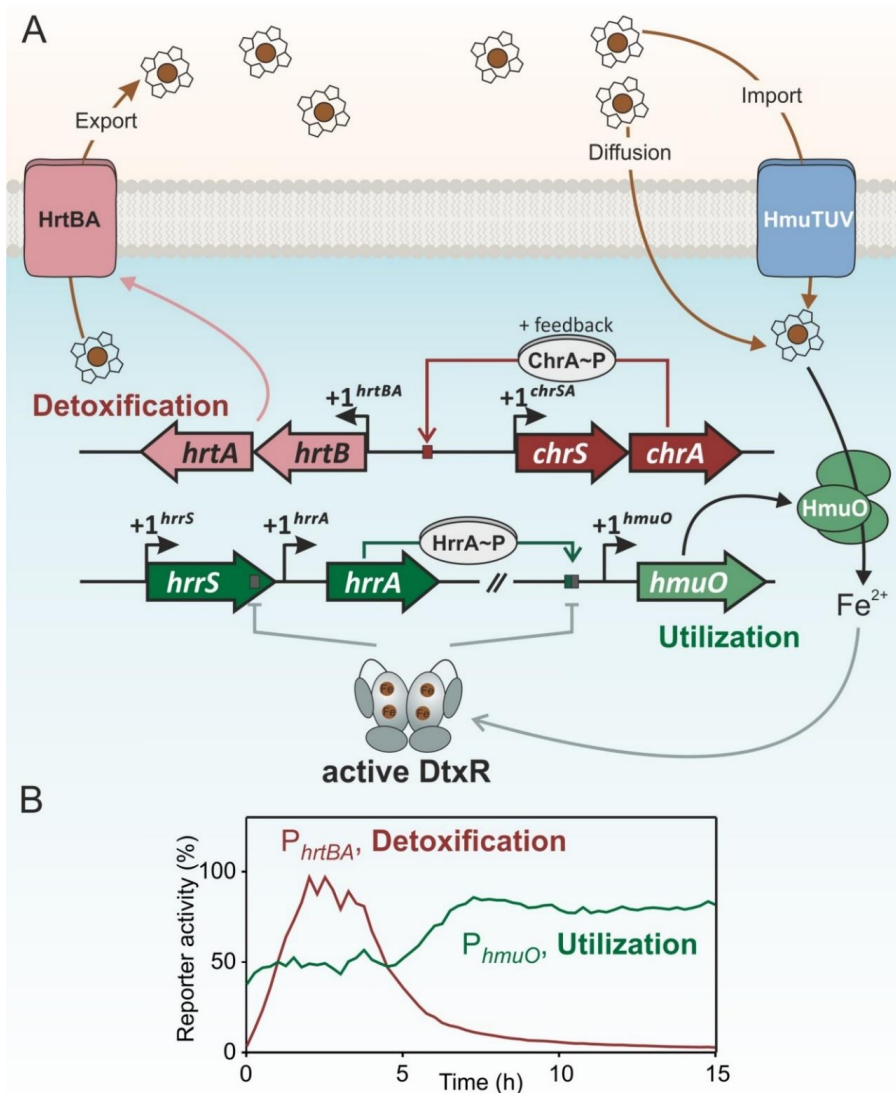


Figure 3: Heme utilization and detoxification is coordinated by the HrrSA and ChrSA TCSs in *C. glutamicum*. **A:** Genetic organization of the two TCS HrrSA and ChrSA and their target genes *hmuO* and *hrtBA*, respectively. Heme can diffuse over the bacterial membrane or is transported into the cell by the HmuTUV uptake system. Inside the cell, the heme oxygenase HmuO (light green) can degrade heme to release iron for important cellular processes. Intracellular Fe^{2+} is sensed by DtxR (grey), which dimerizes and represses not only *hmuO* expression but also the *hrrA* gene itself, which encodes the response regulator HrrA. After phosphorylation by HrrS (heme-dependant), this RR is critical for the activation of *hmuO* expression. The ChrSA TCS not only activates expression of *hrtBA*, which encodes a heme exporter that is responsible for the detoxification of high, intracellular heme concentrations, but also the expression of its own operon (positive feedback). **B:** Heme-induced reporter output of P_{hrtBA} -*eyfp* and P_{hmuO} -*eyfp* in *C. glutamicum* wild type cells (taken from Keppel *et al.*, 2018c). For this experiment, *C. glutamicum* cells were transformed with either pJC1- P_{hrtBA} -*eyfp* or pJC1- P_{hmuO} -*eyfp*. Iron deprived cells were subsequently cultivated in a microbioreactor system (Biolector) in CGXII minimal medium with 2 % (w/v) glucose containing 4 μ M hemin. The eYfp fluorescence was measured as the output of target promoter activation, and backscatter values were recorded to monitor biomass formation. For further information see Keppel *et al.* (2018c).

In contrast to *hrtBA* expression, the *hmuO* reporter revealed a significantly delayed response after addition of heme as a stimulus (Figure 3B). Counterintuitively, the more extracellular heme is added to the medium, the more delayed the *hmuO* expression is. In this context, our mathematical model confirmed that the main factor influencing this particular expression pattern is the iron dependent repression of *hrrA* and *hmuO* by the global iron regulator DtxR (Keppel *et al.*, 2018c; Wennerhold and Bott, 2006). Higher heme concentrations also translate to a higher, intracellular iron pool and thereby a higher, initial DtxR activity, as predicted by our model. Using this regulatory setup, information on Fe^{2+} availability (*via* the co-repressor of DtxR) can directly be integrated at the level of *hmuO* and *hrrA* expression - in contrast to the rapid, iron-independent *chrSA-hrtBA* setup. Additionally, we could show that HrrA does not simply displace DtxR on the promoter of *hmuO* but is in fact an essential activator, even in the absence of DtxR repression (Keppel *et al.*, 2018c).

One aspect, future studies could focus on, is the phosphorylation level of both HrrA and ChrA under changing heme concentrations, to supplement the information we gathered *via* characterization of target gene reporters. A suitable method for this might be the application of Phos-Tag SDS-PAGE (sodium dodecyl sulfate polyacrylamide gel electrophoresis), where phosphorylated proteins are separated from the non-phosphorylated counterparts by interacting with a phosphate-binding tag in the gel matrix (Kinoshita *et al.*, 2006). Examination of the phosphorylation state of HrrA and ChrA following stimulus might give new insight on whether stimulus perception and/or transduction of HrrS and ChrS indeed differ and how much secondary effects - like the aforementioned DtxR repression on *hrrA* - impact the observed, different heme sensitivity. Information on the phosphorylation state under different conditions might reveal how much the different signal perceptions influences downstream processes like target gene activation and how reliable the utilization of target gene reporters as tools for the time resolved investigation of physiological responses really are.

In conclusion, we found that not only differences in signal perception are responsible for the diverse target gene expression patterns in response to heme. The entirety of a tightly balanced interplay between phosphorylation, dephosphorylation and cross-phosphorylation as well as the interference with other regulatory systems (e.g., with the iron-responsive regulator DtxR) shapes the physiological reaction to a multifaceted and complex stimulus such as heme (Figure 3A). The here presented data might be further used as a basis for in-depth systemic analysis of the bacterial heme homeostasis of Gram-positive bacteria that often dedicate at least one TCS to heme-responsive gene regulation. We expect that our findings will be - at least partly - transferable to pathogens, especially to *C. diphtheriae*, due to high sequence identities of the homologous systems. A comparative analysis of the

temporal characteristics of the detoxification and utilization responses might give further insights into what parts of the pathways are essential for the appropriate, physiological reaction to exogenous heme in general and which parts have evolved as a result of the particular, environmental niche (soil in the case of *C. glutamicum* and the upper respiratory system of a host in the case of *C. diphtheriae*).

2.5 Genome-wide profiling of the HrrSA regulon

Previous studies suggest, that the regulon of ChrSA is small and very specific (Hentschel, 2015; Heyer *et al.*, 2012). So far, the only confirmed regulatory roles of this TCS are the activation of its own operon and the *hrtBA* operon as well as a not fully understood involvement in the regulation of the *hrrA* gene. This narrow role fits the purpose of a detoxification system and allows for a specific, fast and transient export of toxic heme levels in times of demand and without secondary effects. However, so far, a genome-wide binding analysis has been only performed for HrrA and in future studies, single genes might be added to the ChrSA regulon.

In contrast to ChrSA, HrrSA seems to coordinate a global, homeostatic response to heme and heme-triggered oxidative stress. Previous studies proposed involvement in the regulation of the utilization and synthesis of heme as well as in the control of expression of heme containing proteins in the respiratory chain (Frunzke *et al.*, 2011).

In the framework of this thesis, we conducted a time-resolved, stimulus-dependent profiling of dynamic DNA-binding of HrrA via chromatin affinity purification combined with sequencing (ChAP-Seq). This extensive analysis resulted in the identification of more than 250 genomic targets of this response regulator. Among others, we found genes that encode proteins associated with heme biosynthesis, the respiratory chain, oxidative stress response and cell envelope remodeling. This dataset of genome-wide HrrA binding sites was combined with time-resolved comparative transcriptome analysis (RNA-Seq) of the wild type strain and a $\Delta hrrA$ mutant strain in response to exogenous heme addition (Keppel *et al.*, 2018a). By this means, we were able to correlate HrrA binding with the subsequent regulatory output and establish HrrSA as a truly global player in the systemic response strategy of *C. glutamicum* to the complex stimulus heme.

In the following sections, the current knowledge on regulatory mechanisms of HrrSA and ChrSA, their target genes, and the function of these targets will be summarized, and novel findings will be highlighted.

2.5.1 Heme degradation and detoxification

The earliest identified targets of HrrSA and ChrSA are involved in a) the degradation (*hmuO*, which encodes a heme oxygenase and is regulated by HrrSA) and b) the transport/export of heme (*hrtBA*, regulated by ChrSA).

The control of heme oxygenase expression is a common theme among many well-characterized, heme-induced regulators in both eukaryotes and prokaryotes. The degradation of free heme by these oxygenases is proposed as the main method of detoxification in eukaryotic cells (Kumar and Bandyopadhyay, 2005). In many bacterial species, these enzymes are furthermore critical for the access to heme as alternative iron source (Wilks and Ikeda-Saito, 2014).

Especially pathogenic bacteria frequently face elevated heme levels and thus evolved various, alternative and oxygenase-independent strategies to prevent toxic intracellular concentrations. The easiest way is the application of exporter proteins, for example HrtBA, found not only in *C. glutamicum* and *C. diphtheriae*, but also in *S. aureus*, *B. anthracis*, and *L. lactis*, as discussed earlier. However, while some studies suggested an increased heme sensitivity of $\Delta hrtBA$ deletion strains (Stauff and Skaar, 2009a), the mechanism of transport remains unknown. Furthermore, it is not known whether these proteins export heme directly or whether metabolites of heme degradation are transported over the membrane (Anzaldi and Skaar, 2010).

Another well characterized detoxification system is the Pef efflux complex of the neonatal pathogen *Streptococcus agalactiae* (Fernandez *et al.*, 2010). In this bacterium, the transcriptional regulator PefR, a MarR-superfamily protein, represses expression of the operons, which encode this efflux system, in a porphyrin-dependent manner.

2.5.2 The regulation of heme biosynthesis in *C. glutamicum*

Due to the importance of heme in central cellular processes, the biosynthesis of this molecule is highly conserved. The early precursor δ -amino levulinic acid (ALA) is essential for heme synthesis in both eukaryotes and prokaryotes. In bacteria ALA is derived from the charged glutamyl-tRNA^{Glu} (Figure 4A) *via* a reaction catalyzed by the glutamyl-tRNA reductase, which is encoded by *hemA* (Choby and Skaar, 2016).

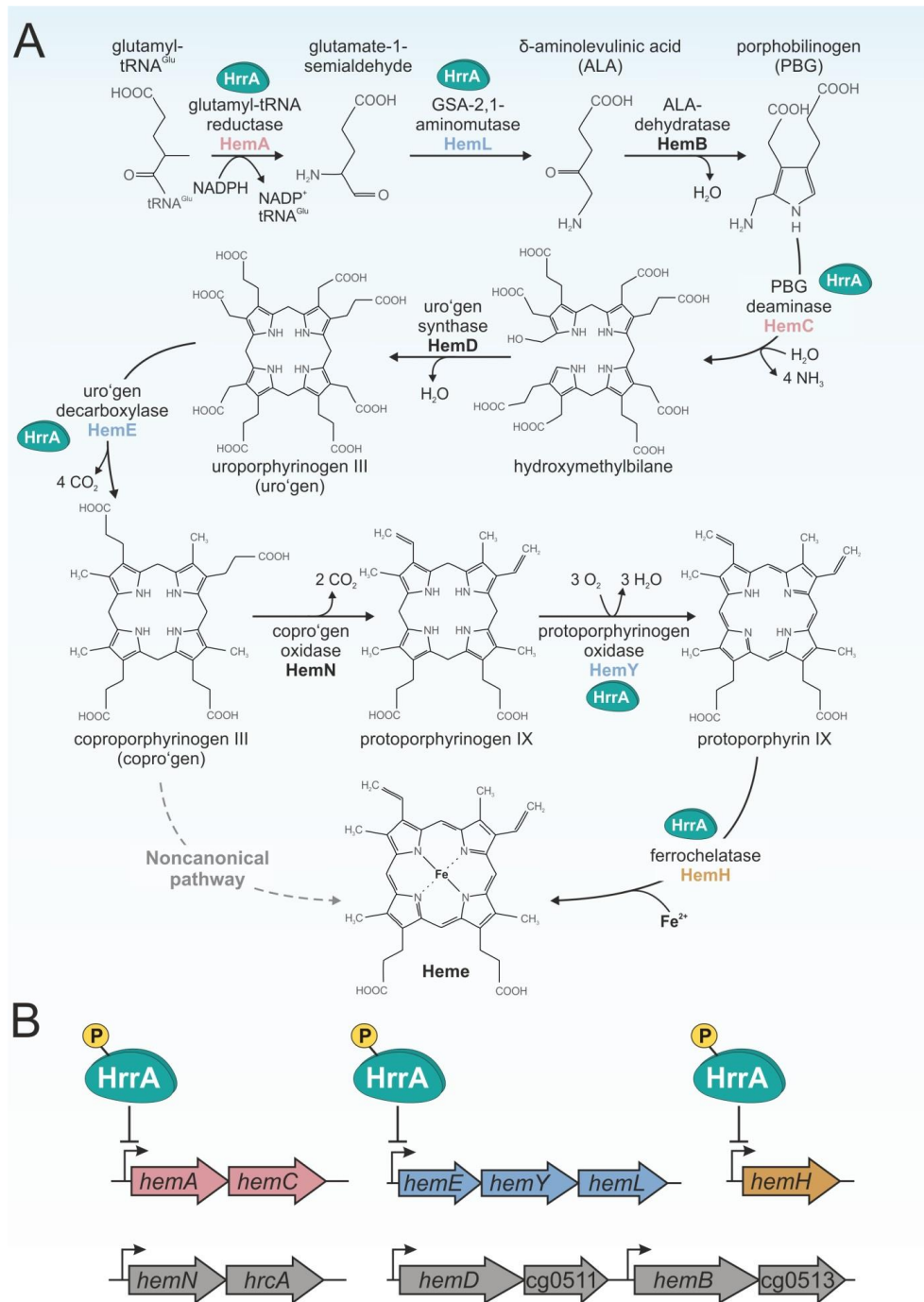


Figure 4: The classical heme biosynthesis pathway in bacteria. **A:** The synthesis of heme in bacteria is highly conserved and starts with the conversion of the charged glutamyl-tRNA^{Glu} to ALA. Several conserved, enzymatic steps lead to the formation of uroporphyrinogen III, which can either be used as precursor for other molecules or subsequently processed in the classical synthesis pathway to coproporphyrinogen III and finally heme. For steps, in which gene expression is repressed by HrrA, the corresponding proteins are colored. The names of the

enzymes are indicated at the arrows and the names of the corresponding proteins in *C. glutamicum* are indicated in bold lettering. Figure adapted from (Heinemann *et al.*, 2008) and (Choby and Skaar, 2016). **B**: Genetic organization of HrrA-controlled heme synthesis genes in *C. glutamicum*.

Two molecules of ALA are subsequently processed to porphyrinogen and, in a series of reactions, converted to the tetrapyrrole molecule uroporphyrinogen III. In various bacteria, this molecule can be used as precursor for several cofactors, including, for example, Vitamin B₁₂ and, in methanogenic Archaea, coenzyme F430 (Choby and Skaar, 2016; Heinemann *et al.*, 2008; Leeper, 1985). The decarboxylation reaction from uroporphyrinogen III to coproporphyrinogen III is catalyzed by a uroporphyrinogen III decarboxylase (HemE). From coproporphyrinogen III, two pathways lead to heme as an end product. In the classical pathway, which is depicted in Figure 4, two additional catalytic steps lead to protoporphyrin IX. Subsequently, the protoporphyrin ferrochelatase (HemH) inserts a ferrous iron into the center of this molecule to form protoheme IX - heme *b* (Camadro and Labbe, 1988; Choby and Skaar, 2016). In the noncanonical pathway, often performed by Gram-positive bacteria, uroporphyrinogen III is first converted to coproporphyrin III and subsequently, the ferrochelatase inserts an iron to form coproheme, which is then decarboxylated by HemQ to form heme *b*. This enzyme is found only in members of the Firmicutes and Actinobacteria (Choby and Skaar, 2016). So far, no experimental data for the biosynthesis of heme in *C. glutamicum* is available. However, genes, which encode for all enzymes of the classical pathway, could be identified in this bacterium (Figure 4B), while the Actinobacteria-typical HemQ, which is critical for the noncanonical pathway, has not been found so far.

Due to its toxicity, the biosynthesis of heme needs to be tightly controlled and adapted in response to intracellular and extracellular heme levels. Previous studies described HrrA as a general repressor of heme biosynthesis in *C. glutamicum* (Frunzke *et al.*, 2011). In *C. diphtheriae*, both HrrA and ChrA are postulated as regulators of *hemA* (Burgos and Schmitt, 2016).

In this PhD thesis, a genome-wide approach was used to analyze the binding and regulatory impact of HrrA targets by combining ChAP-Seq analysis and RNA-Seq (Keppel *et al.*, 2018a). We confirmed significant, heme-induced binding of HrrA in the promoter regions of the *hemEYL* operon (60 base pairs (bp) upstream of the start codon and the transcription start site (TSS) of *hemE*), the *hemAC* operon (26 bp upstream of the start codon, 17 Bp upstream of the TSS of *hemA*), and 16 bp upstream of the *hemH* start codon/TSS (genomic organization of the genes is depicted in Figure 4B).

Additionally, the corresponding mRNA levels of these genes were significantly increased in a $\Delta hrrA$ strain compared to wild type *C. glutamicum*. In case of the uroporphyrinogen decarboxylase (*hemE*), the mRNA level (in transcripts per million (tpm)) was increased 8.3-fold in the $\Delta hrrA$ strain and 0.5 h after heme addition. The mRNA level of *hemH*, encoding the ferrochelatase, increased 15.7-fold, while *hemA* was only slightly increased in the $\Delta hrrA$ deletion strain (1.6-fold 0.5 h after heme addition, 2-fold after 2 h of incubation). These findings once more emphasize the role of HrrA as a heme-dependent repressor of various steps of the heme biosynthesis of *C. glutamicum* (Figure 4). As an early control step, HrrA regulates the production of the early precursor ALA from glutamyl-tRNA^{Glu} by repressing the glutamyl-tRNA reductase (*hemA*). Additionally, HrrA prevents the conversion of uroporphyrinogen III to coproporphyrinogen III and thereby allowing an increased flow from uroporphyrinogen III to other cofactors by strongly repressing *hemE*. Finally, HrrA controls the insertion of the iron atom by repressing the expression of the ferrochelatase *hemH* and thereby balancing the endogenous biosynthesis of heme according to the cellular needs and the availability of external sources. With this regulatory behavior, HrrA shifts the focus of cells in heme-rich environments towards utilization of external heme instead of spending valuable resources for an endogenous synthesis.

2.5.3 The heme-dependent, HrrSA-mediated control of respiratory chain genes

Heme is irreplaceable in most organisms, partly due to its function as protein-bound prosthetic group that enables the sequential electron flow through the respiratory chain complexes of bacterial membranes and eukaryotic mitochondrial membranes (Kim *et al.*, 2012; Schagger, 2002). In its core functionality, the generation of ATP during the oxidative phosphorylation, coupled to respiratory electron transfer, is conserved between most bacteria. In general, the bacterial cell utilizes several donors to transfer an electron to different carriers (e.g. ubiquinone, menaquinone), which is mediated by dehydrogenases. The transfer of electrons itself and the associated transport of protons over the bacterial membrane leads to the establishment of a proton motive force (PMF), which can then be used to generate ATP (Lodish *et al.*, 2000).

The electron transport chain of *C. glutamicum* is branched, and consists of i) a cytochrome *bc*₁-*aa*₃ supercomplex, encoded by *ctaD* and the operons *ctaCF* and *ctaE-qcrCAB* and ii) the cytochrome *bd* oxidase encoded by *cydA* and *cydB*, of the *cydABDC* operon (Bott and Niebisch, 2003). The supercomplex is composed of two parts, the cytochrome *bc*₁ complex (Figure 5A, grey) and the *aa*₃ oxidase (Figure 5A, blue). The *bc*₁ complex consists of cytochrome *b* (QcrB), which contains two heme *b* molecules, the Rieske iron-sulfur protein QcrA, and the non-soluble cytochrome *c*₁ QcrC, which binds two heme *a* molecules (Niebisch and Bott, 2001). The *aa*₃ oxidase has four subunits: CtaF, CtaC, CtaD, which

contains two heme *a* molecules, and CtaE (Niebisch and Bott, 2003). In contrast to that, the alternative menaquinol *bd* oxidase is composed of only two subunits (Figure 5B): CydB, which binds a heme *b* molecule and CydA, harbouring a heme *b* and a heme *d* molecule.

The deletion of critical parts of the *bc₁-aa₃* supercomplex, e.g. in a $\Delta qcrCAB$ or $\Delta ctaD$ strain, leads to a strong growth defect in *C. glutamicum*, indicating that the *bc₁-aa₃* branch is of outstanding importance for the proper establishment of a PMF and that its function cannot be fully substituted by the *bd* branch (Bott and Niebisch, 2003; Niebisch and Bott, 2001; Niebisch and Bott, 2003). The alternative *bd* oxidase was identified in *C. glutamicum* cells that were cultivated in copper-free medium (Bott and Niebisch, 2003; Kusumoto *et al.*, 2000). Under normal conditions, the oxidase seems to be mainly expressed to supplement the respiratory chain in the stationary phase (Kusumoto *et al.*, 2015), possibly due to its high affinity to oxygen.

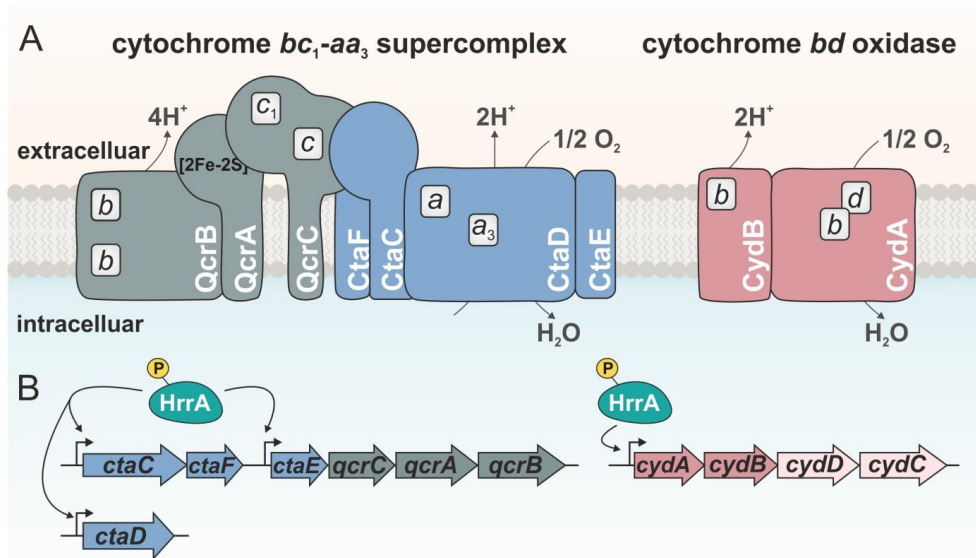


Figure 5: The respiratory chain of *C. glutamicum*. **A:** Schematic illustration of the two branches of the electron transport chain in *C. glutamicum*. Left: the cytochrome *bc₁-aa₃* supercomplex consists of the cytochrome *bc₁* complex (grey), encoded by *qcrCAB*, and the cytochrome *aa₃* oxidase (blue), encoded by *ctaE*, *ctaCF* and *ctaD*. Right: The cytochrome *bd* oxidase (red) is encoded by *cydA* and *cydB*, in the *cydABDC* operon. Boxes indicate heme molecules (heme *b*, heme *c*, heme *a*, heme *d*). Figure modified from Niebisch and Bott (2001). **B:** HrrA control and organization of genes involved in the respiratory chain in *C. glutamicum*.

While several studies concentrated on the function and the structure of the respiratory chain in *C. glutamicum* (Kusumoto *et al.*, 2000; Niebisch and Bott, 2001; Niebisch and Bott, 2003), little is known about the regulation of respiratory chain genes. A recent study could show, that overexpression of the sigma factor SigC (σ^c) leads to strong induction of the *cydABDC*

operon, which encodes for the cytochrome *bd* oxidase (Figure 5A), while expression of the *ctaE-qcrCAB* operon (*bc₁-aa₃* supercomplex) was reduced (Toyoda and Inui, 2016). However, neither the mechanism of how σ^C represses genes of the *bc₁-aa₃* supercomplex, nor the stimulus, which leads to σ^C activity and the subsequent recruitment of the RNA-polymerase to the *cyd* operon, is known to date. Additionally, in this study, the conclusions regarding the regulatory roles of σ^C were drawn from the overexpression of *sigC*. The positive role of a sigma factor can be shown by its overexpression: an increased protein level leads to an increased RNA polymerase recruitment to the target promoter. Negative effects on expression, on the other hand, can either represent a physiological relevant repression, or stem from, for example, unspecific competition between the overrepresented alternative sigma factor and other sigma factors. In this regard, future experiments, like the deletion of *sigC* or binding assays between the *ctaE* promoter and σ^C are needed to verify the role of this sigma factor as a repressor of the *ctaE-qcrCAB* operon. For now, this repressive role should be viewed critically.

In the context of the stimulus, which leads to σ^C activity, the authors of the study speculate, that a defect electron transfer in the *aa₃* oxidase might induce σ^C activity (Toyoda and Inui, 2016). Recently, such an electron transfer defect was studied in copper-deficient *C. glutamicum* cells and - indeed - an activation of the σ^C regulon was observed in these experiments (Morosov *et al.*, 2018).

Additional regulators of respiratory chain genes are HrrA, which was shown to bind and activate the promoter of the *ctaE-qcrCAB* operon (Frunzke *et al.*, 2011), and OxyR, which was described as a repressor of the *cydABCD* operon (Milse *et al.*, 2014; Teramoto *et al.*, 2013).

In our recent study, we described HrrA as a crucial regulator coordinating the expression of all genes constituting the respiratory chain of *C. glutamicum* (Keppel *et al.*, 2018a). We could not only confirm the previously proposed, strong HrrA binding in front of the *ctaE-qcrCAB* operon and in the promoter region of *ctaD* (Frunzke *et al.*, 2011), we also found binding in front of the *ctaCF* operon (Figure 5B). Additionally, in a Δ *hrrA* deletion strain, RNA-Seq data revealed strong decrease in the mRNA levels of all respiratory chain genes, which were bound by HrrA in ChAP-Seq experiments (Keppel *et al.*, 2018a). These findings establish HrrSA as a heme-dependent activator of all genes, which together encode the complete cytochrome *bc₁-aa₃* supercomplex.

Furthermore, we identified a positive regulatory role of HrrSA on *cydABDC*, which encodes the second branch of the respiratory chain. However, in RNA-Seq analysis, the mRNA level of the *cyd* operon seems to slowly increase, even 4 h after hemin addition, in contrast to the

mRNA level of *ctaE-qcrCAB*, which increased instantly after stimulus addition but already slightly declined after 4 h of cultivations (Figure 6A).

These results seem counterintuitive at first, as both operons are regulated by HrrSA in a heme-dependent manner but show diverse transcriptional changes in response to stimulus addition. A possible explanation for this behavior can be found in the HrrSA-mediated regulation of an additional gene: significant binding of HrrA was observed in front of *sigC*, which encodes the earlier discussed sigma factor σ^C , an activator of the *cydABDC* operon and postulated repressor of *ctaE-qcrCAB* expression. The mRNA level of *sigC* was nearly 5-fold increased in a $\Delta hrrA$ deletion strain, suggesting that active HrrA represses this gene. In line with this assumption, *sigC* mRNA levels decreased upon heme addition in wild type cells (Figure 6A).

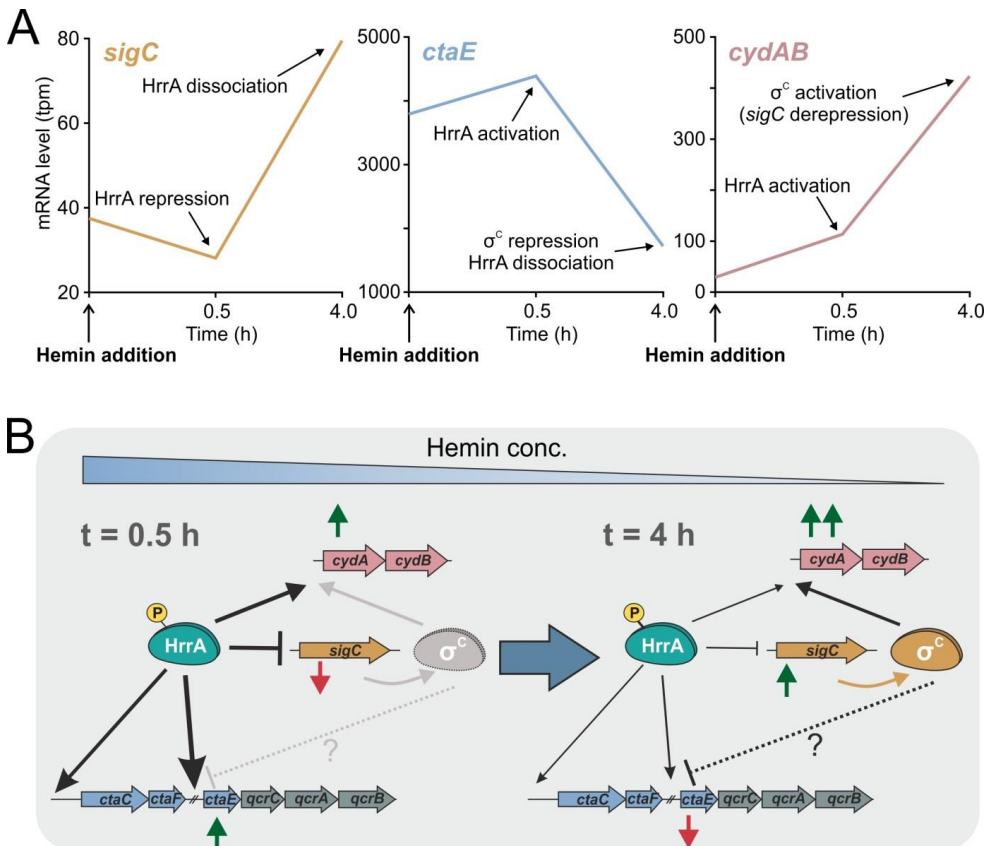


Figure 6: Proposed model of the heme-dependent, regulatory setup of respiratory chain genes in *C. glutamicum*.

A: mRNA levels of *sigC*, *ctaE* and *cydAB* in transcripts per million (tpm). The transcriptome of iron starved *C. glutamicum* wild type cells was determined before ($t=0$ h) and 0.5 h and 4 h after addition of 4 μ M hemin. See

Keppel *et al.* (2018a) for further details.

B: Directly in response to extracellular hemin addition (0.5 h), HrrA gets phosphorylated and activates expression of the *ctaCF* and the *ctaE-qcrCAB* operons as well as *ctaD*, which together encode the full cytochrome *bc₁-aa₃* supercomplex. Additionally, HrrA activates the expression of the *cydABDC* operon, which encodes the cytochrome *bd* oxidase, and represses expression of *sigC*, which encodes the sigma factor σ^C . **B:** With the consumption of heme, after 4 h, the phosphorylation level and activity of HrrA is decreased and subsequently, *sigC* expression is de-repressed. Furthermore, HrrA activation of *ctaCF*, *ctaE-qcrCAB* and *ctaD* as well as the *cyd* operon lessens. σ^C recruits the polymerase to the *cyd* operon and possibly represses the expression of *ctaE-qcrCAB*, leading to a soft switch between the two branches of the respiratory chain.

In this context, we propose the following mechanism of heme-induced regulation of respiratory chain genes, as depicted in Figure 6B: The initial perception of extracellular hemin addition (30 minutes after hemin pulse), leads to phosphorylation of HrrA and subsequently to DNA-binding and activation of genes, which encode for the cytochrome *bc₁-aa₃* supercomplex, especially *ctaE-qcrCAB*. Additionally, HrrA activates the *cydABDC* operon, while at the same time repressing *sigC* expression.

In-vitro determination of the K_d values of HrrA to the promoters of *ctaE*, *cydA* and *sigC* revealed a three-fold higher affinity of HrrA to P_{ctaE} (K_d 0.10 μ M) than to P_{cyd} (K_d 0.26 μ M) or to P_{sigC} (K_d 0.27 μ M). The high affinity to *ctaE* can explain the minor increase of *ctaE* mRNA level in response to hemin addition. It is likely, that even under normal conditions and without addition of exogenous hemin, HrrA is partly phosphorylated, triggered by endogenous synthesis of heme. Therefore, these fractions of HrrA~P might activate high affinity targets, such as *ctaE*.

Over the course of the cultivation, the added heme is degraded and consequently, the HrrA~P level most likely decreases (Figure 6B, 4 h). This leads to de-repression of *sigC*. The following synthesis of the sigma factor σ^C results in even further increase of *cydABDC* mRNA levels (Figure 6A). On the other hand, the expression of the *ctaE-qcrCAB* operon decreases, most likely due to HrrA-dissociation in response to stimulus decline, possibly combined with repression of this operon by σ^C .

Interestingly, we found that genes, which are activated by both HrrA and σ^C , and thereby have a regulatory setup that is comparable with the setup of *cydABDC*, also show the same expression behavior as the *cyd* operon: weak, initial response to a heme stimulus, but increased mRNA levels after 4 h of cultivation. Examples for genes with such a genomic setup are *ctaA* and *ctaB*, which are involved in the conversion of heme *b* to heme *a* and which are activated by both, HrrA and σ^C .

In general, HrrA shows sustained, minor activity even without external stimulus input. This is reflected by significant differences in mRNA levels of target genes (e.g., *ctaE* or *hmuO*)

between a *hrrA* deletion strain and the wild type strain, even in iron-starved, stationary cells in medium without external heme source (Keppel *et al.*, 2018a). While this behavior might be triggered by endogenous synthesized heme, it also represents a major difference to ChrA-mediated target gene activation. In the case of ChrSA, the main target of this TCS, *hrtBA*, is highly inducible but without extracellularly added heme, this gene shows the same, very low output in the $\Delta chrA$ strain and the wild type strain alike. The high background activity of HrrA might also be the reason for the low inducibility of e.g. *ctaE* in response to heme, as discussed previously (Figure 6A). In future studies, this hypothesis could be tested by controlling the endogenous heme synthesis of *C. glutamicum* in a heme-independent manner. For this, one could reintroduce several heme synthesis genes (see Figure 4A) under, e.g., IPTG-inducible promoters and subsequently measure HrrA binding and/or target gene activation in response to different endogenously synthesized heme pools. This experimental setup might help to understand how much HrrA contributes to respiratory chain gene expression under native conditions (e.g., in FeSO₄-containing medium), in which cellular synthesized heme represents the sole stimulus for the HrrSA system. Furthermore, the background level of HrrA could be measured by significantly lowering the heme synthesis and subsequently comparing target gene activation under these conditions to wild type like target gene activation. Testing ChrA-mediated gene regulation in a similar setup might reveal insight into how HrrSA and ChrSA differ in their inducibility and at which point ChrSA turns on the heme detoxification.

In conclusion, the here presented network design (HrrA repressing the expression of another activator (σ^C) of its own target genes) allows the cell to react in two very diverse ways downstream of a single, regulatory pathway. In the presented example it becomes clear that, although HrrSA has a single stimulus, this system is able to prioritize the expression of the more efficient but heavily heme-demanding cytochrome *bc1-aa3* branch over the cytochrome *bd* branch in response to a strong, extracellular heme pulse. This is achieved by a combination of activation (e.g., *ctaE-qcrCAB*, *cydABDC*) and repression (*sigC*) of gene expression as well as altered affinities of the RR to different target genes.

2.5.4 Other targets of HrrSA

Interestingly, although neither the regulator, nor the constitution of the regulon is conserved, *C. glutamicum* cells and eukaryotic (mammalian) cells seem to react with a similar, regulatory logic to heme as a stimulus. Previously unknown genes of the HrrA regulon include, e.g., *katA* (catalase), *trxB* (thioredoxin reductase) or *mpx* (mycothiol peroxidase). Genes, which encode a catalase, a thioredoxin reductase and a mycothiol peroxidase were also identified as part of the mammalian BACH1 regulon - in addition to e.g., *HMOX1*, encoding a heme oxygenase. Furthermore, a heme-dependent, regulatory effect of BACH1 on *TKT*

(transketolase) has been described in the past (Warnatz *et al.*, 2011). Notably, in *C. glutamicum*, significant binding of HrrA was observed in the intergenic region between the divergent genes *ctaB* and *tkt* (also encoding a transketolase), but under the applied conditions, a regulatory effect of HrrA on *tkt* could not be shown so far. However, the transketolase, which is an important enzyme of the nonoxidative part of the pentose phosphate pathway, was recently shown to help cancer cells to meet their high demand for NADPH to counteract the high oxidative stress these cells are facing (Xu *et al.*, 2016). This once more shows, that the link between heme-responsive gene regulation and oxidative stress is omnipresent - not only in form of catalase expression control.

The transketolase seems to be not the only HrrA target in the central carbon metabolism. We identified HrrA binding, as well as a slight regulatory effect, on *gapA* and *gapB*, which encode glyceraldehyde-3-phosphate dehydrogenases (GapDHs). These proteins are involved in glycolysis (GapA) and gluconeogenesis (GapB). In human skin cells it was shown, that oxidative stress may block glycolysis by inhibiting GapDHs (Kuehne *et al.*, 2015) and in *C. diphtheriae*, a GapDH is redox-controlled by S-mycothiolation (Hillion *et al.*, 2017). HrrA might counteract this impaired flux through the glycolysis in response to heme-induced stress by increasing the expression of *C. glutamicum*'s GapDHs (Keppel *et al.*, 2018a). To verify this theory, one could monitor the GapDH activity of both wild type and the $\Delta hrrA$ strain in response to varying heme concentrations, using commercially available GapDH assays.

Heme-induced oxidative stress does not only impact the central carbon metabolism but can also negatively influence the cell envelope. Binding of HrrA was observed in front of *ino1* (synthesis of inositol-derived lipids (Baumgart *et al.*, 2013)), *mepA* (a putative cell wall peptidase (Möker *et al.*, 2004)), and *malR*, which encodes a MarR-type regulator that is possibly involved in stress-responsive cell envelope remodeling (Hünnefeld and Frunzke, manuscript submitted). Interestingly, binding of both, MalR and HrrA, could be identified upstream of *murB*, which encodes a UDP-N-acetylenolpyruvoylglucosamine reductase, involved in synthesis of the cell wall, upstream of *lysC*, which is involved in lysine synthesis and upstream of *oppA*, encoding the subunit of an uncharacterized ABC transporter system. Additionally, both regulators bind to the promoters of the uncharacterized genes cg0431 and cg0439, a putative membrane protein and a putative glycosyltransferase, as well as either upstream (23 base pairs in the case of HrrA) or downstream (90 base pairs in the case of MalR) of the *malR* transcriptional start site. A negative autoregulation is postulated in the case of MalR, and, as the *malR* mRNA levels were increased two-fold in a $\Delta hrrA$ strain, compared to wild type, HrrA seems to repress this gene as well. These findings suggest that HrrA feeds information regarding heme availability or heme stress into the cell envelope regulon in order to prevent or decrease heme-induced cell damage.

Taken together, we found strong evidence for a global regulatory function of HrrSA that integrates a systemic response to heme and is not only restricted to the utilization and biosynthesis of heme. Instead, HrrSA adjusts gene expression of the respiratory chain depending on heme demand. Furthermore, this TCS controls aspects of the oxidative stress response and might counteract heme-induced inhibition of the glycolysis. Finally, HrrSA mediates remodeling of the cell envelope, most likely to prevent or to react to cellular damage caused by heme.

2.5.5 A glimpse into the unknown: HrrSA regulates several uncharacterized, cellular transport processes

Out of over 250 genes, which were identified as HrrA targets in a genome wide binding analysis, more than 120 genes are not characterized and/or are located in the prophage region (approximately 30 genes). Many of these targets are involved in transport processes and selected examples are shown in Table 1. The full dataset can be accessed as supplementary information in Keppel *et al.* (2018a).

An example for such an uncharacterized gene is cg2675. In cells, which were incubated for 30 minutes in hemin containing medium, the region upstream of cg267 (9 to 34 base pairs in front of the start codon) showed the highest peak intensity among all genomic targets. This gene is part of the predicted cg2678-cg2677-cg2676-cg2675-cg2674 operon. While the region in front of cg2675 is bound with the highest intensity in response to heme, another, significantly smaller peak was observed 1800 base pairs upstream of the first gene of the operon (cg2678; Table 1). Despite the significant distance between the secondary peak and the start codon of the first gene in the operon, all genes of this operon were found to be downregulated three to four-fold in a $\Delta hrrA$ strain compared to the wild type strain, indicating that phosphorylated HrrA acts as an activator of this operon in response to extracellular heme.

So far, no studies investigated the function of the gene product of these ORFs in *C. glutamicum*. Bioinformatical analysis predicts that Cg2675 contains an ATP-binding domain and is most likely part of an ATP-binding cassette (ABC) transporter. Prototypical ABC transporter systems consist of two transmembrane domains and two ABC domains (or nucleotide-binding domains) that are located in the cytoplasm. Additionally, a soluble periplasmic substrate-binding protein is often associated with these complexes. Such a system is most likely encoded by the here discussed operon: cg2678 encodes a putative, periplasmic binding protein, cg2677 and cg2676 encode membrane proteins, cg2675 encodes a putative ATP binding subunit and the last gene, cg2674 has no characterized homologs and encodes a soluble protein without highly conserved domains.

The cg2678-2674 operon structure is highly conserved among orthologous genes in e.g. *Corynebacterium efficiens* and *Corynebacterium aurimucosum*, or in *Mycobacterium smegmatis* and *Mycobacterium avium*. In most cases, a domain analysis (Marchler-Bauer *et al.*, 2017) predicted the presence of a DdpA-like dipeptide binding domain in cg2678 orthologs (Olson *et al.*, 1991).

In this context, a study on the *E. coli* dipeptide ABC transporter DppBCDF found, that heme can competitively bind to the dipeptide binding side of the transporter system, both *in vitro* and *in vivo*. Furthermore, deletion of two dipeptide transporters led to the inability of the cells to utilize heme as alternative iron source, while the single deletion mutants were still able to import heme (Létoffé *et al.*, 2006). In *C. glutamicum*, we were able to delete the *hmuTUV* operon, which has been reported to encode the major heme uptake system in *C. diphtheriae* (Drazek *et al.*, 2000), without causing significant growth defects in a medium that contains heme as sole iron source (Frunzke *et al.*, 2011). From these findings, we drew the conclusion that either a) diffusion of heme over the membrane is sufficient for growth in a medium, in which no other bacterial species compete for the iron source, or b) other, uncharacterized transport mechanisms play a role in the heme import of *C. glutamicum*. The identification of a putative ABC transporter with predicted dipeptide/heme binding properties as an important target gene of HrrA suggests a role of this protein in heme uptake. Consequently, future studies might contribute to our understanding of heme import in this bacterium by further characterization of the cg2678-cg2677-cg2676-cg2675-cg2674 operon. After all, it would make sense physiologically, if HrrSA, the system, which also activates heme utilization (*hmuO*), would regulate an alternative heme importer in response to elevated, extracellular heme levels.

Another peptide binding target of HrrA is encoded by *oppA*, which encodes the periplasmic dipeptide-binding protein of an ABC transporter. Under the tested conditions, HrrA binding 270 base pairs upstream of the *oppA* start codon only translated to minor decrease in mRNA levels (Table 1). It is, however, another example of a HrrA bound gene, which is involved in the transport of dipeptides and might be regulated by HrrA under conditions that differ from the tested ones.

Table 1: Overview of genes, which encode putative transporters and are regulated heme-dependently by HrrA. **a:** The distance of HrrA binding to the corresponding gene start site (translational start site, TLS) is predicted by the maximal peak intensity (HrrA binding) in ChAp-Seq experiments (Keppel *et al.*, 2018a). **b:** Changes in mRNA levels (calculated as $\log_2(\text{transcripts per million } (\Delta hrrA)/\text{transcripts per million (wt)})$) are derived from RNA-Seq experiments with a $\Delta hrrA$ and a wild type strain 30 minutes after addition of hemin to the medium (Keppel *et al.*, 2018a). In cases of operons, the changes in mRNA levels of the first genes of each operon are shown. **c:** The putative function was derived from the comparison with homologous proteins and supported by domain prediction tools (Camacho *et al.*, 2009; Marchler-Bauer *et al.*, 2017). **d:** Orthologous proteins were investigated using the "blast" tool (Camacho *et al.*, 2009). Brackets indicate the amino acid sequence identity and the pub med accession number or the gene ID in *C. diphtheriae*. In case of operons, the identities are for the first gene of the operon. Abbreviated names: *C.* = *Corynebacterium*, *R.* = *Rhodococcus*, *M.* = *Mycobacterium*, *S.* = *Streptomyces*. **e:** Known or predicted regulation of the genes. A putative McbR binding site is located in front of cg2678-2674, a predicted AmtR binding site in front cg2181 (*oppA*). cg2181 is additionally downregulated in a $\Delta dtxR$ mutant strain (Wennerhold and Bott, 2006). For cg1280, LexA repression could be shown experimentally (exp.) in response to SOS stress (Jochmann *et al.*, 2009).

Locus/operon	Distance to TLS (bp) ^a	$\log_2(\Delta hrrA/wt)^b$	Putative function ^c	Examples for orthologous proteins (<40 % seq. identity) ^d	Regulation ^e
cg2678-2674	9 (cg2675) 1800 (cg2674)	-1.8	ABC-type transport system, putative dipeptide (heme) binding	<i>C. deserti</i> (88, WP_053546203.1) <i>C. efficiens</i> (75, WP_011075871.1), <i>C. doosanense</i> (75, WP_018020606.1) <i>C. maris</i> (71, WP_020935480.1) and several other <i>Corynebacterineae</i>	McbR (binding site predicted)
cg2181 (<i>oppA</i>)	270	0.4	ABC-type peptide transport system, secreted component	<i>C. diphtheriae</i> (67, DIP0956), <i>C. crudilactis</i> (90, WP_066566268.1), <i>C. pseudotuberculosis</i> (65, WP_013241615.1), <i>M. tuberculosis</i> (52, NP_218183.1) and several other <i>Corynebacterineae</i>	AmtR (binding site predicted) Upregulated $\Delta dtxR$
cg1767-1769	19	3	putative ABC-type multidrug transport system (predicted antibiotic binding domain in cg1767)	<i>C. efficiens</i> (71, WP_011075564.1), <i>C. aurimucosum</i> (61, WP_101736368.1), <i>C. diphtheriae</i> (57, DIP1298), <i>S. coelicolor</i> A3 (44, NP_628256.1) and several other <i>Corynebacteriaceae</i>	GlxR (predicted)
cg1077	17	3.1	putative permease (MFS)	<i>C. efficiens</i> (68, WP_006770020.1), <i>C. diphtheriae</i> (55, WP_014320370.1), <i>C. testudinoris</i> (63, WP_047252666.1) and in several other <i>Corynebacteriaceae</i>	-
cg3101	25	-1.8	putative permease (MFS) AI-2E transporter domain	<i>C. crenatum</i> (98, WP_035096849.1), <i>C. crudilactis</i> (83, WP_066568425.1), several other highly conserved (>70%) orthologs in <i>Corynebacteriaceae</i> , <i>C. diphtheriae</i> (61, DIP2122), <i>C. pseudotuberculosis</i> (59, WP_041481416.1)	-
cg0390	380	0.2	putative permease (MFS)	<i>C. crudilactis</i> (85, WP_066563970.1), <i>C. deserti</i> (77, WP_053543973.1), <i>C. callunae</i> (77, WP_029703718.1), <i>C. efficiens</i> (75, WP_006770182.1), and several other <i>Corynebacteriaceae</i>	-
cg1289	546	-0.4	putative multidrug efflux permease (MFS) DHA2 domain	<i>C. deserti</i> (85, WP_053544600.1), <i>C. efficiens</i> (78, WP_006769833.1), <i>R. rhodochrous</i> (68, WP_059382046.1), and several other <i>Corynebacteriaceae</i>	LexA (exp.)
cg1526	29	0.7	putative multidrug efflux permease (MFS)	<i>C. deserti</i> (66, WP_053546129.1), <i>C. callunae</i> (63, WP_015651121.1)	-
cg3402	13	-1.1	putative copper chaperon CopZ domain	<i>C. deserti</i> (73, WP_053545987.1), <i>C. crudilactis</i> (72, WP_066569203.1), <i>C. efficiens</i> (68, BAC19623.1), <i>C. ulcerans</i> (69, WP_013912599.1), <i>C. diphtheriae</i> (63, DIP2285) and several other <i>Corynebacteriaceae</i>	-
cg3411	18	-0.7	putative copper chaperon CopZ domain	Highly conserved. <i>C. crudilactis</i> (91, WP_066569203.1), <i>C. deserti</i> (85, WP_053545987.1), <i>C. lubricantis</i> (74, WP_018296544.1), <i>C. ammoniagenes</i> (73, WP_040355169.1), several other <i>Corynebacteriaceae</i> . 33% identity to the copper-transporting ATPase 2 isoform a (Homo sapiens, XP_011533420.1)	-

In general, a surprisingly high number of putative transporters with unknown functions are targets of HrrA, including the cg1766-cg1767-cg1768-*ctaA* operon, which partly encodes the subunits of another ABC transport system. HrrA binding in front of the second gene of this operon (cg1767) leads to a nearly ten-fold downregulation of genes two (cg1767) and three (cg1768) only, indicating that HrrA acts as a repressor on these genes. Expression of the first gene in the operon (cg1766, *mptB*), however, does not significantly change in a $\Delta hrrA$ strain and expression of the last gene (*ctaA*), is impacted only slightly (approx. 30 % reduction in mRNA level in a $\Delta hrrA$ strain). This indicates that secondary transcriptional start sites (TSSs) might be present in this operon to allow targeted, HrrA-mediated regulation of cg1767 and cg1768 only. With this, these genes would represent another example of a transporter system that is regulated by HrrA in a heme-dependent manner. Still, the physiological function of the unusual cg1766-cg1767-cg1768-*ctaA* operon structure and its transporter target remain unknown.

Another interesting target is cg1077. HrrA shows significant, heme-induced binding in the region approximately 17 base pairs upstream of the start codon of this gene. For this promoter, the peak intensity is the eleventh highest intensity measured. Additionally, deletion of *hrrA* leads to nearly 9-fold increased mRNA levels of cg1077, establishing HrrA as a strong repressor of this gene. The gene product is predicted to be a transporter of the major facilitator superfamily (MFS) – a membrane transport protein. MFS proteins transport a broad range of targets and are classified into five clusters: 1) drug-resistance proteins, 2) sugar facilitators, 3) facilitators for Krebs cycle intermediates, 4) phosphate ester-phosphate antiporters, and 5) oligosaccharide-H⁺ symporter (Marger and Saier, 1993). In the past, MFS transporters have been shown to be important for antibiotic stress responses, but can also be crucial for the oxidative stress response, as demonstrated in *Campylobacter jejuni*, where the deletion of the *cmeG* gene, which encodes the putative MFS efflux transporter CmeG, led to a higher susceptibility to H₂O₂ induced stress (Jeon *et al.*, 2011). However, as we did not find any characterized, homologous genes to cg1077, the function of the gene product and its role in the HrrA-mediated heme response in *C. glutamicum* can only be speculated upon.

A putative permease, which is highly bound by HrrA and downregulated nearly four-fold in a $\Delta hrrA$ strain, is encoded by cg3101. The gene product of this ORF shows a 30 % sequence identity with the putative transporter YhhT in *E. coli*, which belongs to the Autoinducer-2 Exporter (AI-2E) family and which might be involved in quorum-sensing signaling (Herzberg *et al.*, 2006). Additional membrane anchored transporter proteins, which are bound and/or regulated by HrrA, include cg0390, cg1289 and cg1526, which all encode uncharacterized MFS permeases. In future studies, the characterization of HrrA-regulated transport

processes in *C. glutamicum* might significantly contribute to our understanding of the cellular response to heme and give insight into the range of metabolites and substrates, which are preferably imported and exported by the cell in response to heme as a stimulus.

Such a substrate could be copper, since HrrA seems to play a role in the heme-mediated regulation of copper-dependent processes. HrrA binding was observed 13 base pairs upstream of cg3402 and 18 base pairs upstream of cg3411. Both genes show an approximate two-fold downregulation in a $\Delta hrrA$ strain, indicating that HrrA acts as an activator on these genes. Bioinformatic analysis of the small gene products of these genes revealed that both contain a CopZ-like domain and therefore most likely encode copper chaperones. In context of the proposed role of HrrA in the regulation of respiratory chain genes, an additional regulation of, for example, copper import is not surprising since copper ions are not only crucial for the function but also for the assembly of respiratory chain complexes (Morosov *et al.*, 2018). In *C. glutamicum*, two other systems are involved in the response to copper stress: the TCS CopRS (Schelder *et al.*, 2011) and the regulator CsoR (Teramoto *et al.*, 2015). Here, one could speculate, that HrrSA additionally feeds information on heme availability into the regulons of these two systems. By upregulating the expression of copper chaperons in response to elevated, extracellular heme levels and the subsequent upregulation of the *bc₁-aa₃* supercomplex, HrrA might ensure that the increased copper demand of the super complex can be met by the cell.

In conclusion, the here presented dataset might pave the way for further studies on several, previously uncharacterized genes as the knowledge, that these genes are regulated in a heme-induced and HrrA-mediated manner, might be the greatly needed first hint for the understanding of the physiological role of these genes.

2.5.6 The regulon of HrrSA and other global regulons: A comparison

For the first time, a time-resolved dataset of stimulus-dependent regulator binding and the resulting transcriptional changes permits global insight into the heme-responsive regulon of a bacterial cell. In many studies, the complete description of regulatory networks fostered the functional analysis of previously unknown genes. In 2009, for example, several, previously uncharacterized genes, which are essential for the heme biosynthesis in zebrafish, were identified in a large-scale computational screen as they were consistently co-expressed with the core machinery of heme biosynthesis (Nilsson *et al.*, 2009). Bioinformatical analysis of HrrA-binding, together with the co-expression of characterized and uncharacterized targets under different environmental conditions might narrow down the function of the set of HrrA-bound genes that, so far, have no assigned purpose. An example for this could be the cg2678-cg2677-cg2676-cg2675-cg2674 operon, which was discussed earlier, and which could, based on its regulatory setup and the characteristic gene output in response to heme,

be identified as a dipeptide transporter with the secondary function of heme import in future studies.

In general, the extensive regulon of HrrA with more than 250 putative targets and its involvement in the regulation of many crucial cellular processes (respiratory chain, oxidative stress response, glycolysis, cell envelope, expression of other regulators) bring HrrA on par with other global regulators proteins like Fur, ArcA or Crp in *E. coli*.

The authors of a study from 2014 were able to reconstruct the whole *E. coli* Fur transcriptional regulatory network in response to iron by performing ChIP-Seq experiments and combining the results with RNA-Seq data (Seo *et al.*, 2014). Here, 143 iron-dependent binding peaks were identified for Fur. A recent study on the homologous regulator in *B. subtilis* postulated a comparable regulon with 89 binding sites (unrefereed preprint, (Pi and Helmann, 2018)). For Fur, the expression level of the regulator was sufficient to perform the purification experiments in the native, genomic context. For HrrA, plasmid-based expression of *hrrS* and *hrrA* under native promoters was necessary. Thus, among the 250 binding peaks of HrrA, some of the peaks with low intensity might result from slightly increased *hrrSA* expression and unspecific HrrA binding.

The amount of target genes or binding sites of other, well characterized, global regulators in *E. coli* are close to the regulon of Fur, which directly binds and influences 110 target genes (Seo *et al.*, 2014). For the leucine-responsive protein (Lrp), 138 unique binding regions have been identified (Cho *et al.*, 2008). ArcA, which reprograms the *E. coli* metabolism under anaerobic conditions, binds to 176 sites, some of which are in front of the same genes (Park *et al.*, 2013). In ChIP-seq experiments with FNR, a global regulator of anaerobiosis, this regulator bound to 207 genomic regions (Myers *et al.*, 2013). The same study also provides insight into the binding behavior of other DNA-interacting proteins, like the house keeping sigma factor σ^{70} , which bound to 2,106 different genomic sites under anaerobic conditions, or H-NS, which was found to bind to 722 regions on the genome. Interestingly, several studies report the identification of multiple binding peaks in the binding sites of the respective regulators, e.g. Fur in *E. coli* (Seo *et al.*, 2014). This is in line with observations, made in ChAp-Seq experiments with HrrA. This phenomenon is only found for certain subsets of target genes and possibly hints to an alternative binding behavior on these specific regions. Thus, analysis of “multiple peak” regions across several global regulators might be an interesting target of future studies.

The main aspect, which separates the analysis of HrrA from the studies of most other global regulators, is that information on HrrA binding was acquired before stimulus addition, shortly after stimulus addition (30 min) and with decreasing stimulus intensities (2 h, 4 h, 9 h, 24 h).

This approach revealed a proportional behavior of the HrrA regulon during the first hours after heme addition and also showed the period of time in which the network rewires/overrelaxes as soon as externally supplied heme is depleted. Several other studies performed binding analysis either before and after stimulus addition at single fixed time points, or observed the binding of a regulator to selected target genes over several time points by combining ChIP with qPCR for only a selected number of target genes (Beauchene *et al.*, 2017; Pi and Helmann, 2017).

2.6 Conclusion and outlook

Heme is a molecule, which is essential for nearly all cellular life but is toxic at elevated levels for eukaryotes and prokaryotes alike. Thus, it is not surprising that sophisticated, heme-responsive regulatory mechanisms have evolved in all kingdoms of life. In Gram-positive bacteria, TCSs are the predominant form of heme sensing and, interestingly, some members of the *Corynebacteriaceae* family even utilize two TCSs, HrrSA and ChrSA, to adjust their cellular response to this multifaceted molecule. This PhD thesis contributed to the understanding of the signal perception (Keppel *et al.*, 2018b), the temporal dynamics of the activation of single target genes (Keppel *et al.*, 2018c), and granted a view on the whole regulon of one of the systems (Keppel *et al.*, 2018a). Nevertheless, urgent questions regarding these two interesting TCSs remain.

The more we learn about HrrSA and ChrSA, the more puzzling the small, subtle interactions between these systems become. Previous studies reported, that both HKs, HrrS and ChrS, are able to phosphorylate their cognate and their non-cognate RR, while the dephosphorylation reaction of the cognate RR is highly specific (Hentschel *et al.*, 2014). In this setup, HrrS phosphorylation seems to contribute, at least partly, to the nearly instantaneous activation of the ChrSA target gene and detoxification module *hrtBA* (Keppel *et al.*, 2018c). However, due to a high sequence identity of the RRs (nearly 60 %), drawing conclusion regarding the specificity of RR-DNA interactions becomes immensely difficult. Exemplarily, electrophoretic mobility shift assays with HrrA and ChrA suggested that both regulators bind in the intergenic region between *hrtBA* and *chrSA*. Data from the genome wide HrrA-binding screening confirmed this binding for HrrA, which appears to be significantly heme-dependent, and preliminary data with ChrA support this assumption.

ChrA binding is essential for the activation of both, *hrtBA* and *chrSA*. This is demonstrated by target gene reporters of both operons being completely inactive in a $\Delta chrA$ strain. The effect of HrrA binding on the adjacent genes is less obvious. Shortly after stimulus addition

(30 min), we measured a two-fold decreased mRNA level of *hrtB* in the $\Delta hrrA$ strain, compared to the wild type. However, after 4 h of cultivation, contrary behavior was observed and the mRNA level of *hrtB* was increased four-fold in the deletion strain. While the effect of *hrrA* deletion was less drastic on the *chrSA* operon, the paradox activation pattern of decreased expression shortly after hemin addition and increased expression after 4 h is shared between the divergently located *hrtBA* and *chrSA* operons.

One could think of several theories, which could explain HrrA involvement in the heme detoxification response. The simplest one would be that HrrA acts as a weak activator of *hrtBA* expression. However, for *hrtBA* expression, presence of ChrA is critical. In contrast to the $\Delta hrrA$ strain, which shows a slight reduction of initial *hrtBA* expression, P_{hrtBA} activity is fully repressed in a $\Delta chrA$ strain (Figure S5). This indicates, that the putative role of HrrA as an activator of *hrtBA* must be ChrA dependent and HrrA cannot act as sole regulator of this gene. According to this premise, at least two regulatory mechanisms are possible: i) phosphorylated and dimerized HrrA binds, governed by ChrA, the intergenic region between *hrtBA* and *chrSA* or ii) in the initial phase after stimulus contact HrrA and ChrA form a heterodimer complex which contributes to *hrtBA* activation, which appears to be more likely.

In both cases, shortly after the first contact to heme as a new iron source, DtxR repression inhibits HrrA activation or binding on some of its target promoters, e.g. P_{hmuO} . Consequently, HrrA binds and activates secondary targets, e.g. *hrtBA*, either as homodimer governed by ChrA, or in a heterodimer complex with ChrA. The two-fold decrease of the *hrtBA* mRNA level in the $\Delta hrrA$ strain, 30 minutes after hemin addition, could be a result of the absence of this activation. The absence of HrrA repression on heme biosynthesis genes in the $\Delta hrrA$ strain, however, could also lead to higher, intracellular heme concentrations caused by endogenous production. After 4 h of cultivation, these elevated heme levels trigger ChrS and HrrS activity, which subsequently phosphorylate the only target in a $\Delta hrrA$ strain, ChrA, which activates P_{hrtBA} as a secondary effect. This theory is supported by a second observation: in a $\Delta hrrA$ strain, which is incubated in 4 μM FeSO_4 as iron source, a delayed, but significant *hrtBA* reporter output can be observed. In wild type cells, on the other hand, no *hrtBA* activity can be measured in iron containing medium (Figure S5).

The RR ChrA activates its own operon in a positive feedback loop and thus, the initial concentrations of both ChrS and ChrA appear to be initially low - but strongly increase in response to heme. HrrS and HrrA, on the other hand, seem to be constitutively expressed with only minor changes in expression after heme addition. In this setup, and due to high sequence identities between the two RRs, one could speculate that the formation of ChrA-HrrA heterodimers contributes to the instantaneous saturation of the *hrtBA* promoter upon

stimulus perception of ChrS until the ChrA concentration is sufficiently high for the formation of homodimers.

The physiological relevance of RR heterodimers has been shown for some TCSs, for example in the Rcs phosphorelay system of *E. coli*. In this system, the RR RcsB regulates transcription either as a phosphorylated homodimer or forms, in a partly phosphorylation independent manner, dimers with other proteins such as RcsA, BglJ or GadE (Pannen *et al.*, 2016). In the case of HrrA and ChrA, further studies would have to concentrate on a confirmation of such interactions, for example by simple co-purification experiments. In a second step, the physiological relevance of the heterodimer complexes would have to be demonstrated. For *in-vivo* measurements, the formation of HrrA-ChrA complexes could be shown in two-hybrid experiments under different conditions and at various time points.

Apart from the unknown regulatory effect of HrrA on *hrtBA*, other, similarly pressing questions remain regarding the ChrSA regulon. While some indications speak for a very narrow regulon of this TCS, a genome wide binding analysis could finally unravel the true nature of ChrA regulation. In preliminary experiments, only minor peaks in the intergenic region between *hrtBA* and *chrSA*, as well as upstream of *hrrA*, could be identified so far. This might be attributed to an even lower expression rate of *chrA*, compared to *hrrA*, or to a vastly different time scale on which ChrA binding happens. While these preliminary results once more hint at a very narrow regulon of ChrSA, further experiments are required to test the functionality of the construct and to improve protein yields of ChrA ChAP-Seq experiments.

A third unanswered question revolves around the overlap of the DtxR regulon and the HrrA regulon in *C. glutamicum*. In the past, the regulatory setup appeared to be simple: DtxR adds an additional layer of control on top of the HrrA regulon by not only repressing target genes in an iron-dependent manner (e.g., *hmuO*), but also on the *hrrA* gene itself. However, our recent study suggests, that the setup is more convoluted, since we found a regulatory effect of HrrA on the *dtxR* gene (Keppel *et al.*, 2018a). This indicates that a reciprocal network structure shapes the interference between DtxR-HrrA. While this is in agreement with the more global role of HrrA, which we postulated in this study, it also raises questions regarding the regulatory hierarchy of these two important proteins.

In future studies, the description of all DtxR binding sites in the genome, for example in ChIP-Seq or ChAP-Seq experiments, might allow for the construction of an overarching map of HrrA and DtxR binding and help to identify additional overlaps in - so far unknown - regions of the *C. glutamicum* genome. The regulation of the *hmuO* gene exemplifies the regulatory interference of HrrA and DtxR. Further genome-wide approaches will provide system-level insights into the dynamics and interferences of regulatory networks. These findings will clarify

whether i) the interaction of DtxR with HrrA at the promoter of *hmuO* (DtxR as crucial repressor, HrrA as crucial activator) is an example for the prevalent mechanism of coordinated gene control, or ii) whether other modes of regulatory interferences exist.

Conclusion

In summary, this PhD thesis provides evidence for a direct sensing of heme by the two kinases HrrS and ChrS and reveals possible differences in the heme-protein interfaces of these sensors (Keppel *et al.*, 2018b). Furthermore, the thesis contributes to the understanding of the regulatory interplay between HrrSA and ChrSA by presenting a comprehensive screening of a variety of mutant strains. Moreover, a resulting mathematical model describes the temporal dynamics of some crucial, underlying, regulatory mechanisms (Keppel *et al.*, 2018c).

Lastly, we provide an insight into the systemic response that is governed by the heme-inducible RR HrrA (Keppel *et al.*, 2018a). This dataset does not only reveal the complexity of the response to heme as a stimulus, but will, in future studies, help to foster the functional analysis of previously uncharacterized genes possibly involved in the regulation of the respiratory chain, cellular transport processes, oxidative stress and the remodeling of the cell envelope of *C. glutamicum*.

3. Publications and manuscripts

For the here presented publication and manuscripts, aspects of the “CRediT” taxonomy will be used to describe author contributions (McNutt *et al.*, 2017). The definitions of the contributor roles are declared as following:

Contributor Role	Role Definition
Conceptualization	Ideas; formulation or evolution of overarching research goals and aims.
Formal Analysis	Application of statistical, mathematical, computational, or other formal techniques to analyze or synthesize study data.
Investigation/Experiments	Conducting a research and investigation process, specifically performing the experiments, or data/evidence collection.
Methodology	Development or design of methodology; creation of models
Project Administration	Management and coordination responsibility for the research activity planning and execution.
Software	Programming, software development; designing computer programs; implementation of the computer code and supporting algorithms; testing of existing code components.
Supervision	Oversight and leadership responsibility for the research activity planning and execution, including mentorship external to the core team.
Visualization	Preparation, creation and/or presentation of the published work, specifically visualization/data presentation.
Writing – Original Draft Preparation	Creation and/or presentation of the published work, specifically writing the initial draft (including substantive translation).
Writing – Review & Editing	Preparation, creation and/or presentation of the published work by those from the original research group, specifically critical review, commentary or revision – including pre- or post-publication stages.

3.1 Membrane Topology and Heme Binding of the Histidine Kinases HrrS and ChrS in *Corynebacterium glutamicum*.

Keppel M., Davoudi E., Gätgens C. and Frunzke J.

Published in *Frontiers in Microbiology*

Contributor Role	Contributor
Conceptualization	MK (80 %) JF (20 %)
Formal Analysis	MK (100 %)
Investigation/Experiments	MK (60 %) ED (20 %) CG (20 %)
Methodology	MK (80 %) ED (10 %) CG (10 %)
Project Administration	MK (50 %) JF (50 %)
Software	-
Supervision	ED (20 %) JF (80 %)
Visualization	MK (100 %)
Writing – Original Draft Preparation	MK (80 %) JF (20 %)
Writing – Review & Editing	MK (30 %) ED (20 %) JF (50 %)

Overall contribution MK: 80 %



Membrane Topology and Heme Binding of the Histidine Kinases HrrS and ChrS in *Corynebacterium glutamicum*

Marc Keppel, Eva Davoudi, Cornelia Gätgens and Julia Frunzke*

Institute of Bio- and Geosciences, IBG-1: Biotechnology, Forschungszentrum Jülich, Jülich, Germany

OPEN ACCESS

Edited by:

Marc Bramkamp,
Ludwig-Maximilians-Universität
München, Germany

Reviewed by:

Iain Sutcliffe,
Northumbria University,
United Kingdom
Angela Wilks,
University of Maryland, Baltimore,
United States

*Correspondence:

Julia Frunzke
j.frunzke@fz-juelich.de

Specialty section:

This article was submitted to
Microbial Physiology and Metabolism,
a section of the journal
Frontiers in Microbiology

Received: 11 December 2017

Accepted: 26 January 2018

Published: 09 February 2018

Citation:

Keppel M, Davoudi E, Gätgens C
and Frunzke J (2018) Membrane
Topology and Heme Binding of the
Histidine Kinases HrrS and ChrS
in *Corynebacterium glutamicum*.
Front. Microbiol. 9:183.
doi: 10.3389/fmicb.2018.00183

The HrrSA and the ChrSA two-component systems play a central role in the coordination of heme homeostasis in the Gram-positive soil bacterium *Corynebacterium glutamicum* and the prominent pathogen *Corynebacterium diphtheriae*, both members of the *Corynebacteriaceae*. In this study, we have performed a comparative analysis of the membrane topology and heme-binding characteristics of the histidine kinases HrrS and ChrS of *C. glutamicum*. While the cytoplasmic catalytic domains are highly conserved between HrrS and ChrS, the N-terminal sensing parts share only minor sequence similarity. PhoA and LacZ fusions of the N-terminal sensor domains of HrrS and ChrS revealed that both proteins are embedded into the cytoplasmic membrane via six α -helices. Although the overall membrane topology appeared to be conserved, target gene profiling indicated a higher sensitivity of the ChrS system to low heme levels ($< 1 \mu\text{M}$). *In vitro*, solubilized and purified full-length proteins bound heme in a 1:1 stoichiometry per monomer. Alanine-scanning of conserved amino acid residues in the N-terminal sensor domain revealed three aromatic residues (Y¹¹², F¹¹⁵, and F¹¹⁸), which apparently contribute to heme binding of HrrS. Exchange of either one or all three residues resulted in an almost abolished heme binding of HrrS *in vitro*. In contrast, ChrS mutants only displayed a red shift of the solet band from 406 to 418 nm suggesting an altered set of ligands in the triple mutant. In line with target gene profiling, these *in vitro* studies suggest distinct differences in the heme-protein interface of HrrS and ChrS. Since the membrane topology mapping displayed no extensive loop regions and alanine-scanning revealed potential heme-binding residues in α -helix number four, we propose an intramembrane sensing mechanism for both proteins. Overall, we present a first comparative analysis of the ChrS and HrrS kinases functioning as transient heme sensors in the *Corynebacteriaceae*.

Keywords: *Corynebacterium glutamicum*, two-component systems, heme, heme-binding protein, transient heme sensing, ChrSA, HrrSA

INTRODUCTION

Heme represents a ubiquitous cofactor of proteins and plays a vital role in a variety of cellular processes, including electron transport, oxygen transport, or oxidative stress responses (Poulos, 2007). Ferriprotoporphyrin IX (heme) is also the predominant form of iron in vertebrates and is consequently also exploited as an important iron source for – not only – pathogenic bacteria

(Andrews, 2008; Cornelis et al., 2011). Elevated heme levels, however, cause toxicity by so far not satisfactorily settled mechanisms (Anzaldi and Skaar, 2010). Thus, the intracellular heme pool is typically tightly balanced by a complex and integrative regulatory network.

In bacteria, two-component systems (TCS) represent a ubiquitous principle used by the cells to sense and respond to a variety of different stimuli (Mascher et al., 2006). A prototypical TCS consists of a membrane bound histidine kinase (HK) with a unique sensing domain and a conserved, catalytically active kinase core and a cytoplasmic response regulator (RR) which can be phosphorylated and activated by the HK (Zschiedrich et al., 2016). In response to the stimulus, the HK is autophosphorylated at a conserved histidine residue. The following phosphoryl transfer to the RR typically leads to the activation of this protein, which then drives cellular adaptation, for example, by controlling target gene expression (Stock et al., 2000; Laub and Goulian, 2007).

In the Gram-positive soil bacterium *Corynebacterium glutamicum*, two paralogous TCS, HrrSA and ChrSA, have been reported to play a central role in the control of heme homeostasis (Frunzke et al., 2011; Bott and Brocker, 2012; Heyer et al., 2012). While the HrrSA system is crucial for utilization of heme as an alternative iron source by activating the expression of the heme oxygenase (*hmuO*) under iron limiting conditions (Frunzke et al., 2011), the TCS ChrSA is required to cope with elevated heme levels by activating the expression of a putative heme exporter *hrtBA* (Heyer et al., 2012). Significant cross-phosphorylation between these two systems has been demonstrated in previous studies (Hentschel et al., 2014) reflecting the striking similarity of the HisKA_3 domains of the sensor kinases HrrS and ChrS [pfam07730, ~40% sequence identity (Finn et al., 2010)]. In contrast, the N-terminal, membrane anchored signal perception domains of the sensor kinases share a low sequence identity of only 8.5% (Supplementary Figure S1). Nevertheless, previous studies provided evidence that heme is perceived as a stimulus by both kinases (Frunzke et al., 2011; Heyer et al., 2012).

In nature, the predominant types of heme are heme *b* and heme *c*. While heme *c* is mostly found covalently bound to proteins, heme *b* is often non-covalently bound (Bowman and Bren, 2008; Brewitz et al., 2017). According to a bioinformatical analysis of 125 different heme-binding proteins, the top five residues with high frequencies in close proximity to the binding pocket are cysteine, histidine, phenylalanine, methionine, and tyrosine (Li et al., 2011). Overall, 31 different structural folds were reported for the protein–heme interaction, hinting to a very diverse mode of interaction between proteins and heme as ligand (Li et al., 2011).

In the ChrS homolog of *Corynebacterium diphtheriae*, a single tyrosine residue (Y61) was speculated to be involved in heme binding (Ito et al., 2009; Bibb and Schmitt, 2010). A further example of a heme-responsive TCS is the heme sensor system (HssRS), which has been studied in *Staphylococcus aureus* and *Bacillus anthracis* (Stauff and Skaar, 2009a,b). In this case, several amino acids were speculated to be involved in heme binding. However, the periplasmic loop domain of HssS represents a significant difference to HrrS and ChrS in *Corynebacteria*. In

contrast to ChrS, heme binding and membrane topology of HrrS has not been studied so far.

Here, we performed a comparative sequence and biochemical analysis of the transmembrane domain of *C. glutamicum* HrrS and ChrS. Our data suggested that regardless of the low sequence identity of the sensor domain, both kinases are embedded into the cytoplasmic membrane via six α -helices. *In vitro* analysis of purified full-length proteins revealed that HrrS and ChrS bind heme in a 1:1 stoichiometry per monomer. Furthermore, three conserved aromatic residues (Y¹¹², F¹¹⁵, and F¹¹⁸) were identified, which are of crucial importance for heme binding of HrrS. Conclusively, we provide insights into the organization of the sensor domain of these two closely related HKs and present a model for an intramembrane heme interface for signal perception.

MATERIALS AND METHODS

Bacterial Strains and Growth Conditions

Corynebacterium glutamicum ATCC 13032 was used as wild type strain (Kalinowski et al., 2003) (Supplementary Table S1). For reporter studies, a BHI pre-culture (brain heart infusion, Difco BHI, BD, Heidelberg, Germany) was inoculated with cells from a fresh agar plate and incubated for 8–10 h at 30°C. Subsequently, cells were transferred into a CGXII (Keilhauer et al., 1993) preculture containing 2% (w/v) glucose and 0 μ M FeSO₄. These conditions have been optimized to achieve iron starvation. Protocatechuic acid (PCA) was present in the pre-culture, allowing the uptake of trace amounts of iron. After overnight growth, a CGXII main culture (containing hemin as iron source) was inoculated to an OD₆₀₀ of 1. If necessary, 25 μ g/ml kanamycin or 10 μ g/ml chloramphenicol was added.

Escherichia coli was cultivated in Lysogeny Broth (LB) medium at 37 or 20°C for protein production. If necessary, 50 μ g/ml kanamycin or 34 μ g/ml chloramphenicol was added.

Cloning Techniques and Recombinant DNA Work

Routine molecular biology methods were performed according to standard protocols (Sambrook and Russell, 2001). Chromosomal DNA of *C. glutamicum* ATCC 13032 was used as template for PCR amplification of DNA fragments and prepared as described earlier (Eikmanns et al., 1994). DNA sequencing and synthesis of oligonucleotides was performed by Eurofins Genomics (Ebersberg, Germany).

For the construction of expression plasmids (Supplementary Table S1), DNA fragments were amplified with oligonucleotides given in Supplementary Table S2 and assembled into a vector backbone either by Gibson et al. (2009) or via standard restriction digestion and ligation. For the *phoA/lacZ* assays, pT7-5-*phoA* and pT7-5-*lacZ* were used as vector backbones. Both plasmids were kindly donated by the laboratories of G. Uuden (Bauer et al., 2011).

Wild type and mutant versions of *hrrS* and *chrS* were expressed from the pKW3 plasmid backbone. The mutations were introduced via “QuikChange Lightning” site directed

mutagenesis according to the supplier's manual (Agilent Technologies, Santa Clara, United States). The origin plasmid was digested with *DpnI* (digestion of methylated DNA) and the mutant plasmid was transferred into *E. coli* TOP-10. The introduced mutations were confirmed by sequencing.

Alkaline Phosphatase and β -Galactosidase Assays

For both, the alkaline phosphatase (PhoA) and the β -galactosidase (LacZ) assay, *E. coli* TG-1 was transformed with truncated *hrrS* or *chrS* versions fused to either *phoA* or *lacZ* in the pT7-5 vector and grown overnight in LB medium containing kanamycin (50 μ g/ml). The overnight culture was diluted 1:50 in fresh medium and grown for 1.5 h (\sim OD₆₀₀ = 0.1). Subsequently, expression of the *phoA/lacZ* fusions was induced with 1 mM IPTG for 1 h. The activities of PhoA and LacZ fusions were measured as described as follows: for the PhoA assay, 100 μ l of the *E. coli* cells were harvested and resuspended in 300 μ l of 1 mM Tris-HCl (pH = 8.0). Cells were permeabilized by the addition of 25 μ l 0.1 % (w/v) SDS and 25 μ l chloroform to allow both substrates (*p*-nitrophenyl phosphate and 2-nitrophenyl β -D-galactopyranoside) to enter the cells. Samples were incubated for 20 min at room temperature (Manoil, 1991). Subsequently, 200 μ l of the upper phase was transferred to a microtiter plate and the reaction was started by the addition of 25 μ l of a 5 mg/ml *p*-nitrophenyl phosphate solution (in 1 mM Tris-HCl, 5 mM MgCl₂, pH 8.0). For background measurement and normalization, Abs₆₀₀ and Abs₅₀₀ were measured immediately. The plates were incubated at 28°C for up to 2 h and the yellow color change was determined by measuring the Abs₄₂₀.

For LacZ, the protocol was derived from a protocol published by Miller (1992): 100 μ l of the *E. coli* culture was harvested and resuspended in 300 μ l buffer Z (60 mM Na₂HPO₄·12H₂O, 40 mM NaH₂PO₄·H₂O, 1 mM MgSO₄·7H₂O, 10 mM KCl, and 100 mM freshly added DTT).

The cells were permeabilized and transferred to a microtiter plate. The reactions were started by addition of 25 μ l of a 5 mg/ml 2-nitrophenyl β -D-galactopyranoside solution (in 100 mM K₂HPO₄, pH = 7.0). Measurements were performed as described for PhoA above. Miller units for both enzymes were calculated according to Supplementary Formula S1.

Reporter Assays

For fluorescent reporter assays a 20 ml pre-culture of CGXII minimal medium containing 2% (w/v) glucose was inoculated from a 5 ml BHI culture of *C. glutamicum* carrying the reporter plasmid (e.g., pJC1_P_{hmuO}-*eyfp* or pJC1_P_{hrrBA}-*eyfp*) (Hentschel et al., 2014) and expressing a *hrrS* or *chrS* mutant gene (fused to the *flag*-gene) from the plasmid pKW3 under control of the native promoter. To cause iron starvation, no additional iron source was added to the CGXII medium (PCA was present in the pre-culture, allowing the uptake of trace amounts of iron). The cells were incubated overnight at 30°C in a rotary shaker and grew to an OD₆₀₀ of \sim 10–20. Reporter assays in microtitre scale were performed in the BioLector system (m2p-labs GmbH,

Aachen, Germany). Therefore, 750 μ l CGXII medium containing 2% (w/v) glucose and 2.5 μ M hemin were inoculated from the second pre-culture with iron-starved cells to an OD₆₀₀ of 1 and cultivated in 48-well Flowerplates® (m2p-labs GmbH, Aachen, Germany) at 30°C, 95% humidity, 1200 r.p.m. For the hemin stock solution, hemin (Sigma-Aldrich, Munich, Germany) was dissolved in 20 mM NaOH to a concentration of 2.5 mM and diluted in water to 250 μ M. Biomass production of the growing cells was determined as the backscattered light intensity of sent light with a wavelength of 620 nm (signal gain factor of 12). For the measurement of eYFP fluorescence, the chromophore was excited at 510 nm and emission was measured at 532 nm (signal gain factor of 50). The specific fluorescence corresponds to the total eYFP fluorescence signal in relation to the backscatter signal and is given in arbitrary units (a.u.) (Kensy et al., 2009).

Overproduction and Purification of Full-Length Histidine Kinases

For the overproduction of HrrS-CStrep and ChrS-CStrep, *E. coli* BL21(DE3) was either transformed with the vectors pET24b-*hrrS*-Cstrep, pET24b-*chrS*-Cstrep or a mutated version and cultivated in 500 ml LB medium at 37°C and 100 rpm. At an OD₆₀₀ of \sim 0.7, expression was induced by the addition of 0.5 mM IPTG. After 12–16 h at 20°C, cells were harvested by centrifugation (4000 \times g at 4°C, 10 min). The cell pellet was stored at –20°C. For protein purification, the cell pellet was resuspended in buffer W (100 mM Tris-HCl, pH = 8.0, 250 mM NaCl), containing “complete” protease inhibitor cocktail (Roche, Germany). Cells were disrupted by passing a French pressure cell (SLM Aisco, Spectronic Instruments, Rochester, NY, United States) three times at 207 MPa. The cell debris was removed by centrifugation (6900 \times g, 4°C, 20 min), followed by an ultracentrifugation of the cell-free extract for 1 h (150,000 \times g, 4°C). Pellets containing the membrane fraction were resuspended in 3 ml buffer W containing protease inhibitor. For solubilization of HrrS-CStrep and ChrS-CStrep, the membrane fraction was incubated with 1% n-Dodecyl- β -D-Maltoside (DDM) (Biomol, Germany) at 25°C on a rotary shaker for 1 h. After a second ultracentrifugation step (0.5 h, 150,000 \times g, 4°C), solubilized HrrS-CStrep and ChrS-CStrep present in the supernatant were purified by strep-tactin affinity chromatography (1 ml column volume, CV). Equilibration was performed with 15 CV buffer W containing 0.03% DDM. After washing with 15 CV of buffer W containing 0.03% DDM, CStrep-proteins were eluted with 5 CV of buffer W containing 0.03% DDM and 15 mM desthiobiotin. Fractions containing the desired Strep-tagged proteins were pooled, and the buffer was exchanged against HEPES-buffer (20 mM HEPES, pH 7.5, 20 mM KCl, 20 mM MgCl₂, 200 mM NaCl) using a PD10 desalting column (GE Healthcare, Munich, Germany). The purified proteins were kept at 4°C and immediately used for heme-binding studies. Purity of protein samples was analyzed on a 12% SDS-polyacrylamide gel, which was afterward stained with Coomassie brilliant blue (G250, VWR Chemicals, Pennsylvania, United States). The protein concentration was determined using the extinction coefficients [ϵ (HrrS) = 35535, ϵ (ChrS) = 51575]

with a nano-spectrophotometer at 280 nm. In our elution fractions, the DDM interfered with other assays such as Bradford protein assay or Pierce BCA Protein Assay (Thermo Fisher, Waltham, United States).

Western Blot Analysis

The production of HrrS and ChrS flag-tag variants was verified by western blot analysis. *C. glutamicum* Δ hrrS Δ chrS strains expressing a hrrS or chrS mutant gene (fused to the flag-gene) from the plasmid pKW3 under control of the native promoter were cultivated as described in the Section "Bacterial strains and growth conditions." After 12 h, the cells were harvested and disrupted by passing a French pressure cell. Subsequently, 20 μ g of protein extract were resuspended in SDS sample buffer (124 mM Tris-HCl, pH = 6.8, 20% (v/v) glycerol, 4.6% (w/v) SDS, 1.4 M β -mercaptoethanol, 0.01% (w/v) bromophenol blue) and the proteins separated by SDS-gel electrophoresis (12% separating gel, Bio-Rad Laboratories, Inc., United States). The gel was electroblotted via a Transblot Semi-Dry Transfer Cell (Bio-Rad Laboratories, Inc., United States) to a nitrocellulose membrane (Amersham[®] Hybond-ECL Membranes, GE Healthcare, Germany) in Towbin-Blotpuffer (25 mM Tris, 192 mM Glycine, 20% (v/v) Methanol). Transfer was carried out for 45 min (15 V). The membrane was blocked for 1 h in TBST (20 mM Tris-HCl pH = 7.5, 500 mM NaCl, 0.05% (v/v) Tween 20) with 5% (w/v) skim milk powder and subsequently washed in TBST and for the specific detection of FLAG-tagged proteins. Membranes were incubated for 1 h in ANTI-FLAG[®]-antibody (produced in mouse, 5 μ g/ml, Sigma-Aldrich, Munich, Germany). After washing in TBST (3 \times) the membrane was incubated in a 1:10000 dilution of peroxidase-coupled anti-mouse secondary antibody for 1 h (GE Healthcare, Germany). For the detection of peroxidase activity, the "Amersham ECL-Select Western Blotting Detection" reagent was used (GE Healthcare, Germany) and analyzed with the LAS-3000 mini (Fuji Photo Film Co., Tokyo, Japan).

Heme-Binding Assays with Purified Protein

To assess the heme binding of purified kinases, we proceeded as following: after cell disruption and removal of cell debris by centrifugation, the cleared lysate of *E. coli*, overproducing HrrS or ChrS, was incubated with 50 μ M hemin for 1 h at 4°C prior to ultracentrifugation of the cell-free extract for 1 h (150,000 \times g, 4°C). Subsequently, the proteins were purified as described above. The purified protein was then analyzed via UV-visual spectroscopy: The absorption from 280 to 600 nm was determined using the UV/Visible double beam spectrophotometer UV-1601 PC (Shimadzu, Kyoto, Japan). For *in vitro* binding assays, purified protein (no pre-incubation with hemin) was added to buffer containing hemin concentrations from 0.5 to 36 μ M and incubated for 5 min at room temperature. Subsequently, the absorption from 280 to 600 nm was determined. The samples were then referenced to respective hemin concentrations in buffer without protein.

In Vitro Phosphorylation Assays

The autophosphorylation of both full-length HKs was determined as follows: immediately after purification, both kinases were incubated with 0.25 μ M [γ -³³P]-ATP (10 mCi/ml; PerkinElmer, United States) mixed with 80 μ M non-radioactive ATP. The mixture was incubated for up to 30 min and at different time points 7 μ l aliquots were removed, mixed with an equal volume of 2 \times SDS loading buffer (124 mM Tris-HCl, pH = 6.8, 20% (v/v) glycerol, 4.6% (w/v) SDS, 1.4 M β -mercaptoethanol, 0.01% (w/v) bromophenol blue) and kept on ice. Without prior heating, the samples were subjected to an SDS-PAGE (12% separating gel, Bio-Rad Laboratories, Inc., United States). Dried, gels were exposed on storage phosphor imaging films (Fuji Photo Film Co., Tokyo, Japan) and analyzed with a Typhoon Trio Scanner (GE Healthcare, Germany) after 24 h.

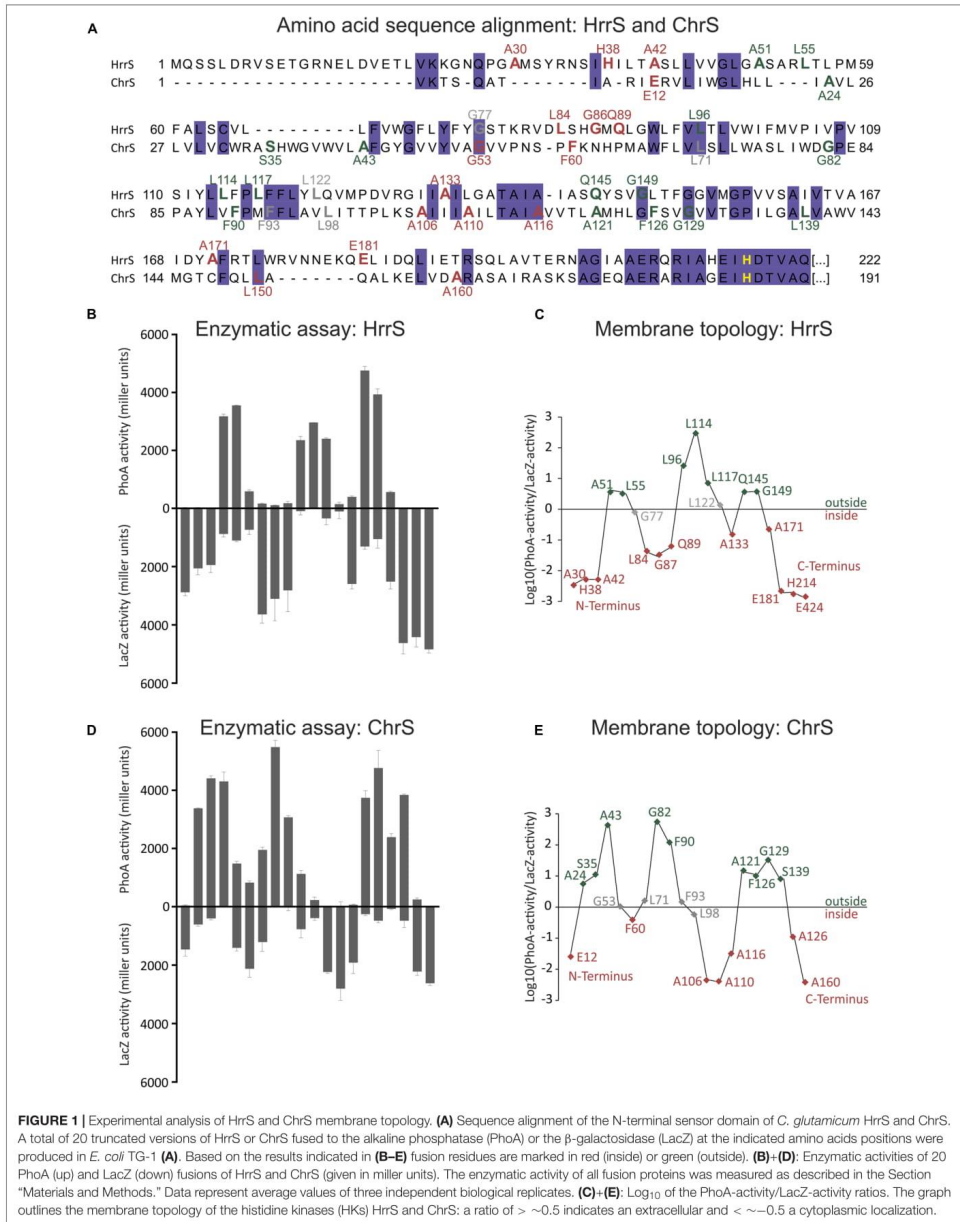
RESULTS

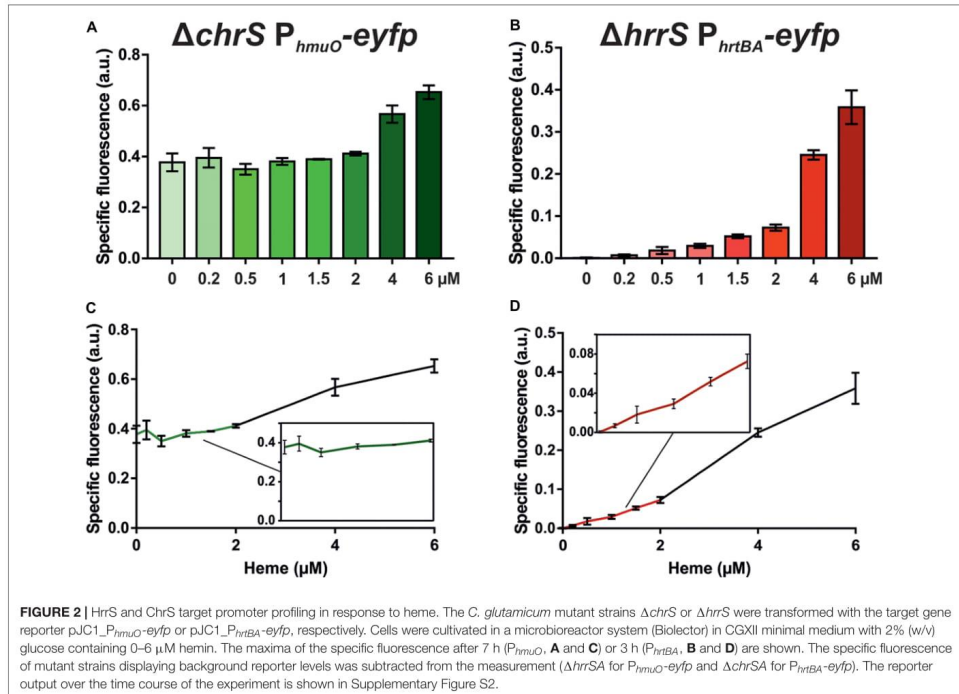
Transmembrane Organization of HrrS and ChrS Is Highly Conserved

The HrrSA and ChrSA systems represent two homologous TCS involved in heme-responsive gene regulation in *C. glutamicum*. Whereas the cytoplasmic domains of the HrrS and ChrS kinases show a high sequence identity (39.4% in the HisKA_3 domains), the N-terminal sensor domains share only minor conservation at the sequence level (8.5%, Supplementary Figure S1). In order to unravel mechanistic differences or similarities in signal perception, we analyzed the transmembrane topology of both N-terminal sensor domains. For this purpose, we used online prediction tools in combination with an experimental approach based on PhoA/LacZ fusions. For the prediction of membrane spanning α -helices different analysis tools were applied, including TopPredII (Claros and von Heijne, 1994), TMPred (Hofman and Stoffel, 1993), Hmmtop (Tusnady and Simon, 2001), Minnow polyview (Porollo et al., 2004), CBS TMHMM (Krogh et al., 2001), DAS (Cserzo et al., 1997) Mpx (Snider et al., 2009), TOPCONS (Tsirigos et al., 2015), and Phobius (Kall et al., 2007).

As indicated in Supplementary Table S3, five out of nine programs suggested five transmembrane helices (TMHs) for ChrS, whereas three tools predicted six TMHs. The outcome of this analysis was even more diverse in the case of HrrS, where predictions ranged from 3 to 7 TMHs for the HrrS sensor domain – highlighting the importance of experimental verification.

For each kinase gene, hrrS and chrS, several truncated versions were fused to the phoA and lacZ genes at their 3'-end, encoding the alkaline phosphatase (PhoA) or the β -galactosidase (LacZ), respectively (Figure 1A). By expressing these fusion genes in *E. coli* TG-1, C-terminally truncated forms of HrrS and ChrS were obtained, that are linked to intact PhoA or LacZ enzymes. While PhoA displays high enzymatic activity if located in the periplasm, LacZ is only active if the enzymatic part of the protein is accessible in the cytosol (Manoil, 1991). Positions of the fusion constructs were distributed over the N-terminal sensor domain while focusing on residues close to predicted TMHs. Remarkably,





this analysis revealed that both kinases, HrrS (Figures 1B,D) and ChrS (Figures 1C,E), are embedded into the cytoplasmic membrane via six TMHs. Thus, despite their minor sequence similarity, HrrS and ChrS share a conserved membrane topology. Referring to the results of the topology prediction tools, only TOPCONS (Tórisirion et al., 2015) and HMMTOP (Tusnady and Simon, 2001) were in line with our experimental data for both HrrS and ChrS.

Target Gene Profiling Revealed a Higher Sensitivity of ChrS toward Heme in Comparison to HrrS

As a next step in the comparative analysis of HrrS and ChrS, we performed a profiling of target gene activation in response to heme as a stimulus. To avoid cross-phosphorylation between the systems and to focus on pathway activation mediated by only one of the two HKs, the deletion strains $\Delta chrS$ and $\Delta hrrS$ were transformed with the respective target gene reporter constructs (pJC1_ P_{hmuO} -*eyfp* and pJC1_ P_{hrtBA} -*eyfp*, respectively) (Hentschel et al., 2014). In the case of HrrS, the respective target promoter P_{hmuO} already revealed a high background output caused by the iron limiting conditions leading to DtxR

derepression (Wennerhold and Bott, 2006) (Figure 2, full spectra in Supplementary Figure S2). Heme-dependent activation via HrrS was only observed for heme concentrations above 4 μ M resulting in a 1.5- to 1.7-fold induction ($\pm 0.08/\pm 0.13$) of the reporter (Figure 2A). In contrast to that the ChrS target gene reporter P_{hrtBA} -*eyfp* (heme detoxification) showed almost no background activity and displayed a sensitive induction profile already at low (< 1.5 μ M) heme concentrations, with a fold change of about 8 in the lower micromolar range ($\pm 2.2, 0.2$ –1.5 μ M) (Figure 2B). These findings are in agreement with previous data (Hentschel et al., 2014), suggesting a very sensitive response of the ChrSA system toward low heme levels, in contrast to the HrrSA system which facilitates heme utilization as an iron source, but only under iron limiting conditions (Figures 2C,D). Taken together, these results confirmed the heme-responsive activation of the HKs, but also provided evidence for differences in signal perception and ligand-binding affinity.

HrrS and ChrS Are Heme-Binding Proteins

In the following, we performed *in vitro* studies to test whether both kinases bind heme via their N-terminal sensor domain. Therefore, both proteins were purified from *E. coli* BL21

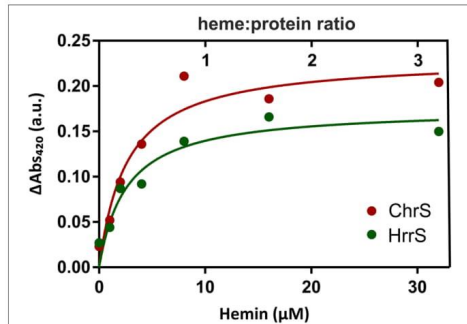


FIGURE 3 | UV-Vis analysis of the heme-binding properties of HrrS and ChrS. For heme-binding assays, different amounts of heme were titrated to 10 μM purified HrrS or ChrS to a final concentration of 0, 2, 4, 8, 16, and 32 μM . The mixture was incubated for 5 min at RT and then analyzed by UV-visual spectroscopy. The resulting absorbance was referenced against the absorption of buffer containing only DDM micelles but no protein. The graph shows the maxima of the solet peaks at 420 nm.

(DE3) by the means of an N-terminal Streptactin tag (see the section “Materials and Methods”). Subsequently, 10 μM of solubilized and purified protein was mixed with different concentrations of heme and analyzed by ultraviolet-visible spectroscopy (UV-Vis). Resulting spectra with the characteristic solet-peak at 406–420 nm were referenced against a buffer control, containing only the DDM micelles, in the absence of protein. The maximum values of the characteristic solet-peaks of heme/protein interaction at 420 nm are shown in Figure 3.

In our assay, both HrrS and ChrS showed heme-binding properties and the absorbance ΔAbs_{420} saturated slightly above 8 μM suggesting that both kinases bind heme in a 1:1 ratio (see full spectra in Supplementary Figure S3). These data, thus, emphasize that ChrS and HrrS contain a single heme-binding site per monomer.

Identification of Putative Heme-Binding Residues by Alanine Scanning of HrrS

Subsequently, we aimed at the identification of amino acid residues potentially involved in heme binding. Therefore, several conserved residues in the transmembrane domain of HrrS were exchanged against alanine to disrupt the heme-protein interface. The chosen amino acid residues are conserved among HrrS orthologs of several *Corynebacteriaceae* species (Supplementary Figure S4) and located within the N-terminal sensor domain of the kinase. Proper synthesis of most resulting proteins in *C. glutamicum* was confirmed by western blot analysis (Figure 4B). The heme-responsive activation of HrrS was monitored by using the P_{hmuO} -*eyfp* target gene reporter described earlier (Hentschel et al., 2014).

Proteins were produced in a *C. glutamicum* $\Delta\text{hrrS}\Delta\text{chrS}$ mutant strain to avoid cross-activation by the respective non-cognate kinase (Hentschel et al., 2014). The *C. glutamicum*

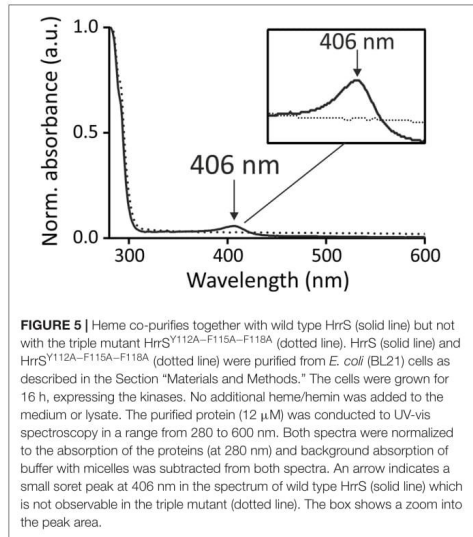
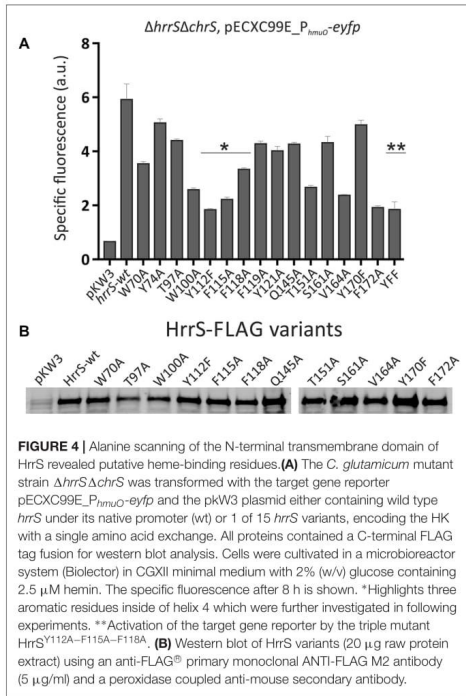
$\Delta\text{hrrS}\Delta\text{chrS}$ strain was transformed with the reporter plasmid pECCX99E- P_{hmuO} -*eyfp* (chloramphenicol resistance) and complemented with pKW3 (kanamycin resistance) carrying either wild type *hrrS* under the control of its own promoter (P_{hrrS} -*hrrS*) or one of the 15 *hrrS* single residue exchange variants. Whereas the empty vector control only displayed background levels of fluorescence, a significant reporter output could be restored by complementation with wild type *hrrS* (Figure 4A, full spectra shown in Supplementary Figure S5).

With this approach several residues were identified, that, upon exchange against alanine, led to a significantly reduced reporter output [up to 66 % reduction (Y112) compared to wild type HrrS]. Particularly interesting is a cluster of four aromatic amino acids inside or in close proximity of α -helix 4: W¹⁰⁰-Y¹¹²-F¹¹⁵-F¹¹⁸. Indeed, previous studies revealed that tyrosine and phenylalanine residues are prime candidates for heme-interaction (Li et al., 2011). However, the tryptophan W¹⁰⁰ appeared to be of structural importance for HrrS. This residue is located in the middle of α -helix three and purification of this variant led to a highly unstable and aggregated eluate, while HrrS-wt or other variants were purified as stable protein. Furthermore, HrrSW100A and HrrST97A show slightly reduced protein amounts in our western blot analysis (Figure 4B). Consequently, we concentrated on the triple residue, intermembrane motive Y¹¹²-F¹¹⁵-F¹¹⁸ (marked as * in Figure 4). Exchange of the residue Y112 to alanine (HrrSY112A) resulted in reduced proteins levels (data not shown), and thus, HrrSY112F was used for further analysis (Figure 4B). In comparison with the single mutants, a simultaneous exchange of all three conserved residues (Y¹¹²-F¹¹⁵-F¹¹⁸), however, led to no further decrease in target promoter activation (Figure 4, marked as **). We speculate that even after complete loss of signal perception, HrrS will still exhibit background kinase activity resulting in the activation of *hmuO* transcription.

Based on the finding for HrrS, we also investigated the second kinase, ChrS, in an analogous experiment. However, here, the plasmid-based overexpression of *chrS* variants was hampered by the fact that ChrS appeared to exhibit a very strong phosphatase activity resulting in weak target promoter activation ($p\text{JCl}_1$ - P_{hrrBA} -*eyfp*) upon overproduction. Even for an expression of *chrS* on the same plasmid ($p\text{JCl}_1$ - P_{hrrBA} -*eyfp*- P_{chrS} -*chrS*), only minor activities could be measured for the reporter (Supplementary Figure S6). Nevertheless, again the exchange of the three residues Y⁸⁷, F⁹⁰, and F⁹⁴ resulted in a significantly lower reporter output. These residues are conserved in the sensor domains of HrrS and ChrS in *C. glutamicum*. However, because of the very low reporter output, the findings for ChrS must be viewed critically.

HrrSY112A–F115A–F118A Shows Impaired Heme-Binding Properties

In the following, the role of the three aromatic amino acids, as putative heme-binding residues in HrrS, was further investigated in *in vitro* heme-binding assays. For this purpose, wild type protein as well as the triple mutant HrrSY112A–F115A–F118A were overproduced in *E. coli* BL21 and subsequently solubilized and



purified as described in the Section “Materials and Methods.” Upon analysis of 12 μ M of both proteins (no addition of heme) via UV-vis spectroscopy (280–600 nm) and normalization to the protein absorption (Abs₂₈₀), HrrS consistently showed a sorset band at 406 nm which was lacking for the triple mutant (Figure 5). This peak corresponds to small amounts of heme co-purified from the *E. coli* extracts. Remarkably, this peak was not observed for the HrrS^{Y112A-F115A-F118A} triple mutant protein providing first evidence that heme binding of HrrS was impaired by the exchange of these residues (Figure 5). Also for the single HrrS mutants (HrrS^{Y112A}, HrrS^{F115A}, and HrrS^{F118A}), ChrS, and the ChrS^{Y87A-F90A-F94A} variant, no co-purification was observed either (Supplementary Figure S7).

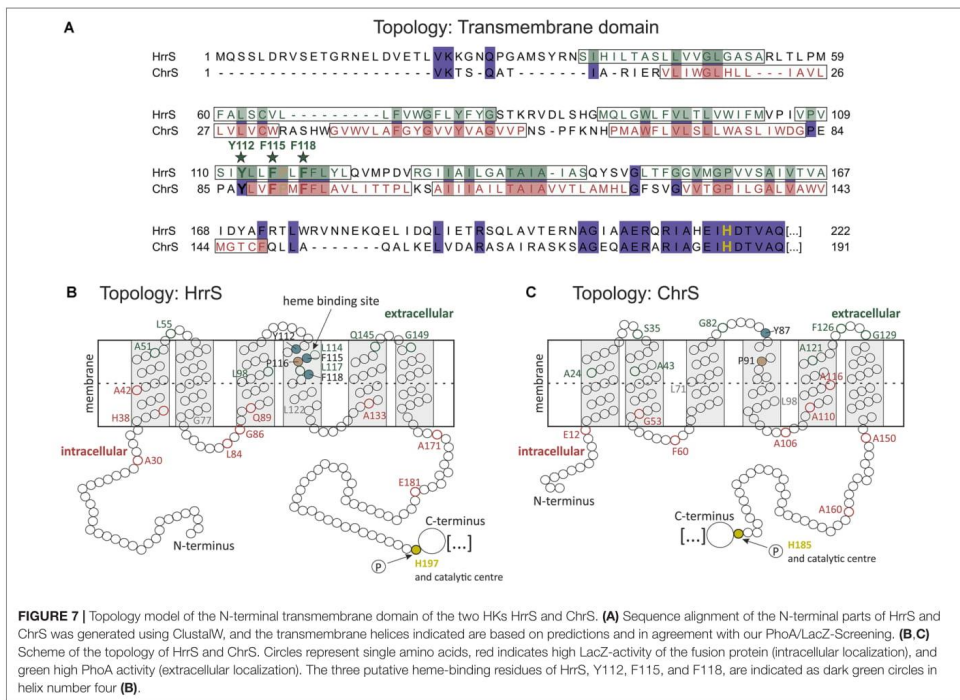
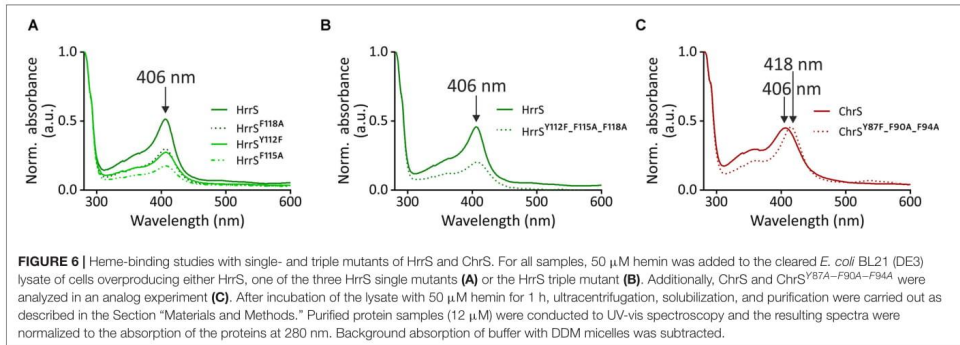
However, only a small fraction of the purified HrrS appeared to be in the heme-bound state. To enhance this effect, 50 μ M hemin was added to the cleared *E. coli* lysate prior to protein purification. The lysate was incubated for 1 h at 4°C and subsequently, purification was carried out as described above. After this reconstitution, a significantly increased peak was observed for wild type HrrS after the purification, and now, even the single mutants or the triple mutant HrrS^{Y112A-F115A-F118A} were co-purified with small amounts of heme/hemin (Figure 6). In contrast to the wild type protein, however, the binding was

strongly reduced. Similar to the alanine scanning, no clear difference between the single (Figure 6A) and the triple mutants (Figure 6B) was noticeable, suggesting that all three residues are equally important for the formation of the heme-protein interface. *In vitro* autophosphorylation of HrrS and the triple mutant HrrS^{Y112A-F115A-F118A} indicated that both proteins are correctly folded and enzymatically active (Supplementary Figure S8).

Analogous experiments were performed for ChrS and the triple mutant ChrS^{Y87A-F90A-F94A}. Both proteins were not purified with bound heme from *E. coli* membranes (Supplementary Figure S7). However, upon addition of hemin to the cleared lysate prior to purification a significant sorset band at 406 nm emerged for ChrS demonstrating the ability of this protein to bind *in vitro* (Figure 6C). Interestingly, for ChrS^{Y87A-F90A-F94A}, the peak volume was not reduced but showed a significant red shift from 406 to 418 nm. Thus, heme binding of ChrS^{Y87A-F90A-F94A} is somehow affected but obviously, the heme-protein interface differs from HrrS where exchange of the same conserved triplet (HrrS^{Y112A-F115A-F118A}) almost abolished heme binding in the homologous HK.

DISCUSSION

Bacterial heme homeostasis relies on complex regulatory networks integrating iron- and heme availability to harmonize intracellular processes involved in heme degradation (e.g., HmuO), export (HrtBA), biosynthesis, and heme-containing proteins (Andrews et al., 2003; Yasmin et al., 2011). The Gram-positive soil bacterium *C. glutamicum*, remarkably, invests 2



out of 13 TCS for the maintenance of heme homeostasis (Frunzke et al., 2011; Bott and Brocker, 2012; Heyer et al., 2012). Information on iron availability is integrated into the network via the global iron-dependent regulator DtxR, which represses both the *hmuO* gene as well as *hrrA* encoding the RR of the HrrSA “heme utilization system” (Wennerhold

and Bott, 2006). This overall network topology is conserved between the non-pathogenic soil bacterium *C. glutamicum* and the prominent pathogen *C. diphtheriae* highlighting that heme regulatory processes are not restricted to pathogens of vertebrates but represent a significant fitness trait of many bacterial species in the battle for iron.

In this study, we demonstrated that the two HKs of the TCS, HrrSA, and ChrSA, bind heme in a 1:1 stoichiometry per HK monomer. This is in agreement with previous studies reporting the activation of HrrSA and ChrSA target gene expression (e.g., *hmuO* and *hrtBA*, respectively) in response to heme availability (Bibb et al., 2007; Bibb and Schmitt, 2010; Frunzke et al., 2011; Heyer et al., 2012; Hentschel et al., 2014; Burgos and Schmitt, 2016).

For both kinases, heme binding occurs at an N-terminal sensing domain which is embedded in the cytoplasmic membrane via six TMHs connected by only small loop regions (Figure 7A). Although our studies revealed a similar membrane topology, the sequence conservation of the sensor domain is rather minor (8.5% sequence identity). This is in line with the finding that heme recognition differs between the systems. Whereas exchange of three conserved aromatic residues (tyrosine 112 and the phenylalanine residues 115 and 118) almost abolished heme binding of HrrS, exchange of these amino acids in the sensor domain of ChrS only resulted in a red shift of the solet band toward an absorption maximum at 418 nm. Differences in heme perception are also reflected by the profiling assay demonstrating a much more sensitive response of the ChrS kinase to heme as a stimulus (Figure 2). The central iron atom of heme can either be bound in a penta- or hexa-coordinated manner (Brewitz et al., 2017). The position of the solet band of heme-binding proteins is significantly influenced by the chemical nature of the amino acid ligands (Vickery et al., 1976). Because of this, one can speculate that an altered set of ligands with different chemical properties participates in heme binding of the triple mutant ChrS^{Y87A-F90A-F94A}, resulting in a red shift of the solet band. This set of alternative ligands seems not to be present in HrrS, however. Based on these findings, we cannot exclude that the triplet of conserved aromatic residues is involved in ChrS heme binding as well.

Sequence analysis of ChrS/HrrS paralogs revealed that the three aromatic residues are highly conserved in different *Corynebacteriaceae* species (Supplementary Figure S3). In their recent study, Li et al. (2011) analyzed the top five amino acids with high frequencies in heme-binding pockets and concluded that cysteine, histidine, methionine as well as tyrosine and phenylalanine are the most prominent residues in such interaction centers. Attributed to the chemical versatility of the heme molecule, different heme-protein interactions are possible (Brewitz et al., 2017). Whereas amino acids may act as axial ligands of the central iron atom via sulfur, nitrogen or oxygen donor atoms (cysteine, histidine, lysine, and tyrosine, respectively), π -stacking interactions via aromatic residues (phenylalanine, tyrosine, or tryptophan) may also contribute to the heme interface. For HrrS, we identified three aromatic residues (Y¹¹², F¹¹⁵, and F¹¹⁸), which upon exchange, led to a reduced reporter output in response to heme. Remarkably, an exchange of Y112 to phenylalanine (lacking the hydroxyl group of tyrosine) led to a drastically reduced heme binding (Figures 5, 6). We therefore speculate that the tyrosine 112 may act as an axial ligand of the

central iron atom. Also in NEAT (NEAr Transporter) proteins, several well-studied cases confirmed single tyrosine residues coordinating the central metal ion of the heme molecule (Grigg et al., 2007; Sharp et al., 2007; Villareal et al., 2008).

While Y¹¹² is concluded to be crucial for the interaction with the iron atom, the phenylalanine residues F¹¹⁵ and F¹¹⁸ might be important for the interface through aromatic stacking interactions with the porphyrin ring of heme (Schneider et al., 2007; Smith et al., 2010; Li et al., 2011). Interestingly, a single proline residue (P¹¹⁶) is located between the two phenylalanine residues and is, together with the YFF motif, conserved between HrrS and ChrS (Figure 6A). This amino acid might be involved in shaping the heme interface by kinking the α -helix number four (von Heijne, 1991) thereby creating a heme-binding pocket consisting of the three residues Y¹¹²-F¹¹⁵-Y¹¹⁸ (Figure 7B). This effect has been demonstrated for the cysteine-proline (CP) dipeptide motif representing a prominent heme-regulatory motif (Lathrop and Timko, 1993).

In *C. diphtheriae*, the ChrS membrane topology was predicted using the two tools TMpred and DAS and experimentally analyzed via six PhoA/LacZ fusions (Bibb and Schmitt, 2010). Comparable to HrrS and ChrS in *C. glutamicum*, six TMHs were postulated (Figures 7B,C). In this study, alanine scanning of the N-terminus of this homologous protein revealed several kinase mutants with inability to activate the target operon *hrtBA*. A conserved tyrosine residue in TMH number two (Y⁶¹) was postulated as a prime candidate for heme binding (Bibb and Schmitt, 2010). This amino acid Y⁶¹ in ChrS (*C. diphtheriae*) corresponds to Y⁷⁴ in HrrS (*C. glutamicum*, see Supplementary Figure S3). However, in our study the exchange of this residue to alanine had no significant effect (Figure 4). In contrast, the exchange of phenylalanine residue 114 to alanine in *C. diphtheriae* ChrS (TMH number four) led to a 40% decreased P_{hrtBA} activity. Interestingly, this residue is conserved between most *Corynebacteriaceae* and as supporting evidence phenylalanine F¹¹⁸ is part of our postulated Y¹¹²-F¹¹⁵-F¹¹⁸ heme-protein interface in HrrS, suggesting a conserved function and mode of interaction.

As a further heme-responsive TCS, Stauff and Skaar (2009a,b) characterized the conserved HssRS of *Staphylococcus aureus* and *Bacillus anthracis* and predicted an N-terminal periplasmic sensing domain flanked by two transmembrane helices. Their findings indicate that the mode of signal perception of HssS (*S. aureus* and *B. anthracis*) vastly differs from HrrS/ChrS from *Corynebacterium* species. Exchange of several residues in the extracellular part of *B. anthracis* HssS did not lead to the identification of the heme-binding site, but the fact, that the sensing domain is flanked by two helices led to the prediction, that this protein detects a signal located either in the periplasm or within the membrane itself, similar to HrrS (Stauff and Skaar, 2009a). As in our study, the exchange of residues likely not involved in heme binding (such as arginine or lysine) showed reduced phenotype complementation and led to the speculation that this

domain might be more involved in signal transduction than previously expected.

In summary, this study provides evidence for a direct sensing of heme via the N-terminal sensor domain of the HKs ChrS and HrrS in *C. glutamicum*. Although the particular binding pocket may differ between the proteins, they represent two further examples of proteins involved in transient heme-sensing of bacteria. Considering the versatile composition of heme-protein interfaces in nature, the molecular and structural analysis of heme proteins provides an important basis for the prediction of novel domains potentially involved in heme sensing.

AUTHOR CONTRIBUTIONS

MK, ED, and JF conceived the study; MK, ED, and CG performed the experiments; MK and ED analyzed the data; and MK and JF wrote the manuscript.

REFERENCES

- Andrews, N. C. (2008). Forging a field: the golden age of iron biology. *Blood* 112, 219–230. doi: 10.1182/blood-2007-12-077388
- Andrews, S. C., Robinson, A. K., and Rodriguez-Quinones, F. (2003). Bacterial iron homeostasis. *FEMS Microbiol. Rev.* 27, 215–237. doi: 10.1016/S0168-6445(03)00055-X
- Anzaldi, L. L., and Skaar, E. P. (2010). Overcoming the heme paradox: heme toxicity and tolerance in bacterial pathogens. *Infect. Immun.* 78, 4977–4989. doi: 10.1128/IAI.00613-10
- Bauer, J., Fritsch, M. J., Palmer, T., and Unden, G. (2011). Topology and accessibility of the transmembrane helices and the sensory site in the bifunctional transporter DcuB of *Escherichia coli*. *Biochemistry* 50, 5925–5938. doi: 10.1021/bi1019995
- Bibb, L. A., Kunkle, C. A., and Schmitt, M. P. (2007). The ChrA-ChrS and HrrA-HrrS signal transduction systems are required for activation of the *hemO* promoter and repression of the *hemA* promoter in *Corynebacterium diphtheriae*. *Infect. Immun.* 75, 2421–2431. doi: 10.1128/IAI.01821-06
- Bibb, L. A., and Schmitt, M. P. (2010). The ABC transporter HrtAB confers resistance to hemin toxicity and is regulated in a hemin-dependent manner by the ChrAS two-component system in *Corynebacterium diphtheriae*. *J. Bacteriol.* 192, 4606–4617. doi: 10.1128/JB.00525-10
- Bott, M., and Brocker, M. (2012). Two-component signal transduction in *Corynebacterium glutamicum* and other *corynebacteria*: on the way towards stimuli and targets. *Appl. Microbiol. Biotechnol.* 94, 1131–1150. doi: 10.1007/s00253-012-4060-x
- Bowman, S. E., and Bren, K. L. (2008). The chemistry and biochemistry of heme c: functional bases for covalent attachment. *Nat. Prod. Rep.* 25, 1118–1130. doi: 10.1039/b717196j
- Brewitz, H. H., Hagelueken, G., and Imhof, D. (2017). Structural and functional diversity of transient heme binding to bacterial proteins. *Biochim. Biophys. Acta* 1861, 683–697. doi: 10.1016/j.bbagen.2016.12.021
- Burgos, J. M., and Schmitt, M. P. (2016). The ChrSA and HrrSA two-component systems are required for transcriptional regulation of the *hemA* promoter in *Corynebacterium diphtheriae*. *J. Bacteriol.* 198, 2419–2430. doi: 10.1128/JB.00339-16
- Claros, M. G., and von Heijne, G. (1994). TopPred II: an improved software for membrane protein structure predictions. *Comput. Appl. Biosci.* 10, 685–686. doi: 10.1093/bioinformatics/10.6.685
- Cornelis, P., Wei, Q., Andrews, S. C., and Vinckx, T. (2011). Iron homeostasis and management of oxidative stress response in bacteria. *Metallomics* 3, 540–549. doi: 10.1039/c1mt00022e
- Cserzo, M., Wallin, E., Simon, I., von Heijne, G., and Elofsson, A. (1997). Prediction of transmembrane alpha-helices in prokaryotic membrane proteins: the dense

FUNDING

The authors acknowledge financial support by the Deutsche Forschungsgemeinschaft (FR 2759/4-1) and by the Helmholtz Association (W2/W3-096).

ACKNOWLEDGMENTS

We thank Jacqueline Fuchs and Simon Lemm for their help with the cloning of several constructs.

SUPPLEMENTARY MATERIAL

The Supplementary Material for this article can be found online at: <https://www.frontiersin.org/articles/10.3389/fmicb.2018.00183/full#supplementary-material>

- alignment surface method. *Protein Eng.* 10, 673–676. doi: 10.1093/protein/10.6.673
- Eikmanns, B. J., Thum-Schmitz, N., Eggeling, L., Ludtke, K. U., and Sahn, H. (1994). Nucleotide sequence, expression and transcriptional analysis of the *Corynebacterium glutamicum* *gltA* gene encoding citrate synthase. *Microbiology* 140(Pt 8), 1817–1828. doi: 10.1099/13500872-140-8-1817
- Finn, R. D., Mistry, J., Tate, J., Coggill, P., Heger, A., Pollington, J. E., et al. (2010). The Pfam protein families database. *Nucleic Acids Res.* 38, D211–D222. doi: 10.1093/nar/gkp995
- Frunzke, J., Gätgens, C., Brocker, M., and Bott, M. (2011). Control of heme homeostasis in *Corynebacterium glutamicum* by the two-component system HrrSA. *J. Bacteriol.* 193, 1212–1221. doi: 10.1128/JB.01130-10
- Gibson, D. G., Young, L., Chuang, R. Y., Venter, J. C., Hutchison, C. A. III, and Smith, H. O. (2009). Enzymatic assembly of DNA molecules up to several hundred kilobases. *Nat. Methods* 6, 343–345. doi: 10.1038/nmeth.1318
- Grigg, J. C., Vermeiren, C. L., Heinrichs, D. E., and Murphy, M. E. (2007). Haem recognition by a *Staphylococcus aureus* NEAT domain. *Mol. Microbiol.* 63, 139–149. doi: 10.1111/j.1365-2958.2006.05502.x
- Hentschel, E., Mack, C., Gätgens, C., Bott, M., Brocker, M., and Frunzke, J. (2014). Phosphatase activity of the histidine kinases ensures pathway specificity of the ChrSA and HrrSA two-component systems in *Corynebacterium glutamicum*. *Mol. Microbiol.* 92, 1326–1342. doi: 10.1111/mmi.12633
- Heyer, A., Gätgens, C., Hentschel, E., Kalinowski, J., Bott, M., and Frunzke, J. (2012). The two-component system ChrSA is crucial for haem tolerance and interferes with HrrSA in haem-dependent gene regulation in *Corynebacterium glutamicum*. *Microbiology* 158, 3020–3031. doi: 10.1099/mic.0.062638-0
- Hofman, K., and Stoffel, W. (1993). A database of membrane spanning proteins segments. *J. Biol. Chem.* 374:166.
- Ito, Y., Nakagawa, S., Komagata, A., Ikeda-Saito, M., Shiro, Y., and Nakamura, H. (2009). Heme-dependent autophosphorylation of a heme sensor kinase, ChrS, from *Corynebacterium diphtheriae* reconstituted in proteoliposomes. *FEBS Lett.* 583, 2244–2248. doi: 10.1016/j.febslet.2009.06.001
- Kalinowski, J., Bathe, B., Bartels, D., Bischoff, N., Bott, M., Burkovski, A., et al. (2003). The complete *Corynebacterium glutamicum* ATCC 13032 genome sequence and its impact on the production of L-aspartate-derived amino acids and vitamins. *J. Biotechnol.* 104, 5–25. doi: 10.1016/S0168-1656(03)00154-8
- Kall, L., Krogh, A., and Sonnhammer, E. L. (2007). Advantages of combined transmembrane topology and signal peptide prediction—the Phobius web server. *Nucleic Acids Res.* 35, W429–W432. doi: 10.1093/nar/gkm256
- Keilhauer, C., Eggeling, L., and Sahn, H. (1993). Isoleucine synthesis in *Corynebacterium glutamicum*: molecular analysis of the *ilvB-ilvN-ilvC* operon. *J. Bacteriol.* 175, 5595–5603. doi: 10.1128/jb.175.17.5595-5603.1993
- Kensy, F., Zang, E., Faulhammer, C., Tan, R. K., and Buchs, J. (2009). Validation of a high-throughput fermentation system based on online monitoring of biomass

- and fluorescence in continuously shaken microtiter plates. *Microb. Cell Fact.* 8:31. doi: 10.1186/1475-2859-8-31
- Krogh, A., Larsson, B., von Heijne, G., and Sonnhammer, E. L. (2001). Predicting transmembrane protein topology with a hidden Markov model: application to complete genomes. *J. Mol. Biol.* 305, 567–580. doi: 10.1006/jmbi.2000.4315
- Lathrop, J. T., and Timko, M. P. (1993). Regulation by heme of mitochondrial protein transport through a conserved amino acid motif. *Science* 259, 522–525. doi: 10.1126/science.8424176
- Laub, M. T., and Goulian, M. (2007). Specificity in two-component signal transduction pathways. *Annu. Rev. Genet.* 41, 121–145. doi: 10.1146/annurev.genet.41.042007.170548
- Li, T., Bonkovsky, H. L., and Guo, J.-T. (2011). Structural analysis of heme proteins: implications for design and prediction. *BMC Struct. Biol.* 11:13. doi: 10.1186/1472-6807-11-13
- Manoil, C. (1991). Analysis of membrane protein topology using alkaline phosphatase and beta-galactosidase gene fusions. *Methods Cell Biol.* 34, 61–75. doi: 10.1016/S0091-679X(08)61676-3
- Mascher, T., Helmann, J. D., and Unden, G. (2006). Stimulus perception in bacterial signal-transducing histidine kinases. *Microbiol. Mol. Biol. Rev.* 70, 910–938. doi: 10.1128/MMBR.00020-06
- Miller, J. H. (1992). *A Short Course in Bacterial Genetics: A Laboratory Manual and Handbook for Escherichia coli and Related Bacteria*. Plainview, NY: Cold Spring Harbor Laboratory Press.
- Porollo, A. A., Adamczak, R., and Meller, J. (2004). POLYVIEW: a flexible visualization tool for structural and functional annotations of proteins. *Bioinformatics* 20, 2460–2462. doi: 10.1093/bioinformatics/bth248
- Poulos, T. L. (2007). The Janus nature of heme. *Nat. Prod. Rep.* 24, 504–510. doi: 10.1039/b604195g
- Sambrook, J., and Russell, D. W. (2001). *Molecular Cloning: A Laboratory Manual*, 3rd Edn. Cold Spring Harbor, NY: Cold Spring Harbor Laboratory Press.
- Schneider, S., Marles-Wright, J., Sharp, K. H., and Paoli, M. (2007). Diversity and conservation of interactions for binding heme in b-type heme proteins. *Nat. Prod. Rep.* 24, 621–630. doi: 10.1039/b604186h
- Sharp, K. H., Schneider, S., Cockayne, A., and Paoli, M. (2007). Crystal structure of the heme-IsdC complex, the central conduit of the Isd iron/heme uptake system in *Staphylococcus aureus*. *J. Biol. Chem.* 282, 10625–10631. doi: 10.1074/jbc.M700234200
- Smith, L. J., Kahraman, A., and Thornton, J. M. (2010). Heme proteins—diversity in structural characteristics, function, and folding. *Proteins* 78, 2349–2368. doi: 10.1002/prot.22747
- Snider, C., Jayasinghe, S., Hristova, K., and White, S. H. (2009). MPEx: a tool for exploring membrane proteins. *Protein Sci.* 18, 2624–2628. doi: 10.1002/pro.256
- Stauff, D. L., and Skaar, E. P. (2009a). *Bacillus anthracis* HrrS signalling to HrtAB regulates haem resistance during infection. *Mol. Microbiol.* 72, 763–778. doi: 10.1111/j.1365-2958.2009.06684.x
- Stauff, D. L., and Skaar, E. P. (2009b). The heme sensor system of *Staphylococcus aureus*. *Contrib. Microbiol.* 16, 120–135. doi: 10.1159/000219376
- Stock, A. M., Robinson, V. L., and Goudreau, P. N. (2000). Two-component signal transduction. *Annu. Rev. Biochem.* 69, 183–215. doi: 10.1146/annurev.biochem.69.1.183
- Tsirigos, K. D., Peters, C., Shu, N., Kall, L., and Elofsson, A. (2015). The TOPCONS web server for consensus prediction of membrane protein topology and signal peptides. *Nucleic Acids Res.* 43, W401–W407. doi: 10.1093/nar/gkv485
- Tusnady, G. E., and Simon, I. (2001). The HMMTOP transmembrane topology prediction server. *Bioinformatics* 17, 849–850. doi: 10.1093/bioinformatics/17.9.849
- Vickery, L., Nozawa, T., and Sauer, K. (1976). Magnetic circular dichroism studies of myoglobin complexes. Correlations with heme spin state and axial ligation. *J. Am. Chem. Soc.* 98, 343–350. doi: 10.1021/ja00418a005
- Villareal, V. A., Pilpa, R. M., Robson, S. A., Fadeev, E. A., and Clubb, R. T. (2008). The IsdC protein from *Staphylococcus aureus* uses a flexible binding pocket to capture heme. *J. Biol. Chem.* 283, 31591–31600. doi: 10.1074/jbc.M801126200
- von Heijne, G. (1991). Proline kinks in transmembrane alpha-helices. *J. Mol. Biol.* 218, 499–503. doi: 10.1016/0022-2836(91)90695-3
- Wennerhold, J., and Bott, M. (2006). The DtxR regulon of *Corynebacterium glutamicum*. *J. Bacteriol.* 188, 2907–2918. doi: 10.1128/JB.188.8.2907-2918.2006
- Yasmin, S., Andrews, S. C., Moore, G. R., and Le Brun, N. E. (2011). A new role for heme, facilitating release of iron from the bacterioferritin iron biomineral. *J. Biol. Chem.* 286, 3473–3483. doi: 10.1074/jbc.M110.175034
- Zschiedrich, C. P., Keidel, V., and Szurmant, H. (2016). Molecular mechanisms of two-component signal transduction. *J. Mol. Biol.* 428, 3752–3775. doi: 10.1016/j.jmb.2016.08.003

Conflict of Interest Statement: The authors declare that the research was conducted in the absence of any commercial or financial relationships that could be construed as a potential conflict of interest.

Copyright © 2018 Keppel, Davoudi, Gütenas and Frunzke. This is an open-access article distributed under the terms of the Creative Commons Attribution License (CC BY). The use, distribution or reproduction in other forums is permitted, provided the original author(s) and the copyright owner are credited and that the original publication in this journal is cited, in accordance with accepted academic practice. No use, distribution or reproduction is permitted which does not comply with these terms.

3.2 Toxic but Tasty - Temporal Dynamics and Network Architecture of Heme-Responsive Two-Component Signalling in *Corynebacterium glutamicum*.

Keppel M.*, Piepenbreier H.*, Gätgens C., Fritz G. and Frunzke F.

*contributed equally

In revision: *Molecular Microbiology*

Contributor Role	Contributor
Conceptualization	MK (25 %)
	HP (25 %)
	GF (25 %)
	JF (25 %)
Formal Analysis	MK (40 %)
	HP (40 %)
	GF (10 %)
Investigation/Experiments	MK (40 %)
	CG (60 %)
Methodology	MK (50 %)
	HP (50 %)
Project Administration	MK (40 %)
	HP (20 %)
	GF (20 %)
	JF (20%)
Software	HP (60 %)
	GF (40 %)
Supervision	GF (50 %)
	JF (50 %)
Visualization	MK (80 %)
	HP (20 %)
Writing – Original Draft Preparation	MK (64 %)
	HP (12 %)
	GF (12 %)
	JF (12 %)
Writing – Review & Editing	MK (25 %)
	HP (25 %)
	GF (25 %)
	JF (25 %)

Overall contribution MK: 60 %

Toxic but tasty - Temporal dynamics and network architecture of heme-responsive two-component signalling in *Corynebacterium glutamicum*

Marc Keppel^{1#}, Hannah Piepenbreier^{2#}, Cornelia Gätgens¹, Georg Fritz^{2*} and Julia Frunzke^{1*}

* Corresponding authors:

Georg Fritz; Email: georg.fritz@synmikro.uni-marburg.de; Phone: +49 6421 28 22582

Julia Frunzke; Email: j.frunzke@fz-juelich.de; Phone: +49 2461 615430

¹ Institute of Bio- und Geosciences, IBG-1: Biotechnology, Forschungszentrum Jülich GmbH, 52425 Jülich, Germany

² LOEWE-Zentrum für Synthetische Mikrobiologie, Philipps-Universität Marburg, 35032 Marburg, Germany

These authors contributed equally to this work.

Heme is an essential cofactor and alternative iron source for almost all bacterial species but may cause severe toxicity upon elevated levels and consequently, regulatory mechanisms coordinating heme homeostasis represent an important fitness trait. A remarkable scenario is found in several corynebacterial species, e.g. *Corynebacterium glutamicum* and *Corynebacterium diphtheriae*, which dedicate two paralogous, heme-responsive two-component systems, HrrSA and ChrSA, to cope with the Janus nature of heme. Here, we combined experimental reporter profiling with a quantitative mathematical model to understand how this particular regulatory network architecture shape the dynamic response to heme. Our data revealed an instantaneous activation of the detoxification response (*hrtBA*) upon stimulus perception and we found that kinase activity of both kinases contribute to this fast onset. Furthermore, instant deactivation of the P_{hrtBA} promoter is achieved by a strong ChrS phosphatase activity upon stimulus decline.

While the activation of detoxification response is uncoupled from further factors, heme utilization is additionally governed by the global iron regulator DtxR integrating information on iron availability into the regulatory network. Altogether, our data provide comprehensive insights how TCS cross-regulation and network hierarchy shape the temporal dynamics of detoxification (*hrtBA*) and utilization (*hmuO*) as part of a global homeostatic response to heme.

"All things are poison, and nothing is without poison, the dosage alone makes it so a thing is not a poison"
Paracelsus, 1493-1541

Heme represents an important iron source for almost all bacterial species (1) and is a ubiquitous cofactor of a variety of enzymes (2). Elevated cellular concentrations of heme can however, cause severe toxicity. But this is basically true for all nutrients as already emphasized by the Swiss physician and founder of modern toxicology, Paracelsus (3, 4). Consequently, a robust regulation of homeostasis is key to the cell's survival and typically, sophisticated regulatory mechanisms are engaged in maintaining optimal intracellular conditions and tolerance to environmental fluctuations. Once inside the cell, most bacteria rely on heme oxygenases to catalyse the conversion of heme to biliverdin, thereby salvaging the

central iron atom with the concomitant release of carbon monoxide (5). One early-characterized example for this class of enzymes is HmuO, a heme oxygenase of *Corynebacterium diphtheriae* that was found to be essential for the utilization of free and hemoglobin-bound heme (6, 7). An ortholog of HmuO was also identified in *Corynebacterium glutamicum*, where the deletion of the corresponding gene led to reduced growth on hemin as sole iron source (8). In Gram-negative pathogens, including *Neisseria* spp. and *Pseudomonas aeruginosa*, proteins of the HemO/PigA family were found to catalyse the cleavage of the porphyrin ring structure, but do not share significant sequence similarity with HmuO of

Gram-positive species (9, 10). The cost and benefit of using heme as an alternative iron source, however, needs to be carefully considered by the cell. Corynebacterial species, for example, employ the master regulator of iron homeostasis, DtxR, to feed information on iron availability into the network controlling heme homeostasis. DtxR was shown to repress *hmuO* under iron-replete conditions and thereby adds an additional layer of regulation to the physiological response to heme (6, 11).

While the cause of heme toxicity is not conclusively unravelled (12), organisms have evolved a variety of mechanisms to minimize toxic effects. Whereas some bacteria rely mostly on their oxygenase to degrade excess heme, such as *Neisseria gonorrhoeae* (13) or *Clostridium perfringens* (14), an alternative strategy can be found in the eukaryotic parasite *Plasmodium* spp. which is capable to sequester excess heme in an insoluble substance called hemozoin (12, 15, 16). While in bacteria, ferritin-like proteins can store excess heme, other forms of sequestration are not well described so far (12). A third class of detoxification systems are heme exporters, such as HrtBA which have been described for several Gram-positive species including *Staphylococcus aureus* (17, 18), *Bacillus anthracis* (17), *Streptococcus agalactiae* (19) and can also be found in corynebacterial species (20, 21).

Bacterial two-component systems (TCS), consisting of a membrane bound histidine kinase (HK) and a cytoplasmatic response regulator (RR) (22, 23), play a central role as transient heme sensor systems in Gram-positive species (24). This is known from bacteria such as *Staphylococcus aureus* and *Bacillus anthracis*, both utilizing the heme sensor system HssRS to react to heme as extracellular stimulus (17, 24). A common theme among *Corynebacteriaceae* appears to be the dedication of two paralogous TCS for the regulation of heme homeostasis (8, 21, 25-27). Here, the HrrSA and ChrSA systems coordinate the expression of genes involved in heme biosynthesis, heme detoxification (*hrtBA*), respiratory chain and the heme oxygenase (*hmuO*). While it was suggested that both TCS have partially overlapping regulons, HrrSA was shown to play an important role in the utilization of heme as an alternative iron source by activating expression of *hmuO*, whereas ChrSA is crucial for the activation of the *hrtBA* operon encoding a heme exporter (8, 21). Furthermore, previous studies of our group revealed significant cross-phosphorylation between these TCS but a highly

specific phosphatase activity of the HKs towards their cognate RR (28). Previous studies focused mostly on the identification of target genes, which were confirmed by different *in vivo* and *in vitro* assays. However, the systemic understanding of this homeostatic network, maintaining balance between heme detoxification and utilization, demands the analysis of temporal dynamics and requires comprehensive insights in the particular network architecture.

In this study, we have conducted an analysis of reporter assays of HrrSA and ChrSA target promoters in the background of the wild type strain, as well as in mutant strains lacking single components of the two TCSs. These data were integrated in a quantitative mathematical model, which was used to test functional hypotheses and to simulate distinct differences in autoregulation and ON/OFF kinetics of target promoters. Finally, by studying the impact of the iron regulator DtxR on *hrrA* and *hmuO* expression at temporal resolution our data as well as the model revealed that DtxR adds a superior regulatory level ensuring the appropriate timing of the heme utilization response.

MATERIALS AND METHODS

Bacterial strains and growth conditions

Bacterial strains used in this study are listed in Table S1. *C. glutamicum* strain ATCC 13032 was used as wild type (29) and either cultivated in BHI (brain heart infusion, Difco BHI, BD, Heidelberg, Germany) as complex medium or CGXII (30) containing 2% (w/v) glucose as minimal medium. All cultivations were performed at 30°C and, if necessary, 25 µg/ml kanamycin was added to the medium for selection. For standard cloning applications, *E. coli* DH5α was cultivated in Lysogeny Broth (Difco LB, BD, Heidelberg, Germany) medium at 37°C in a rotary shaker and for selection, 50 µg/ml kanamycin was added to the medium.

Recombinant DNA work and cloning techniques

Standard cloning and other molecular methods were performed according to standard protocols (31). For most applications, chromosomal DNA of *C. glutamicum* ATCC 13032 was used as template for PCR amplification of DNA fragments and was prepared as described previously (32). All sequencing and synthesis of oligonucleotides was performed by

Eurofins Genomics (Ebersberg, Germany). For the construction of plasmids, the DNA regions of interest were amplified from chromosomal *C. glutamicum* DNA with oligonucleotides listed in Table S2 and ligated into the plasmid backbone (see Table S3) via restriction sites indicated in the same table. Genomic integrations and/or deletions were performed using the pK19*mobsacB* plasmid and the two-step homologues recombination method described earlier (33). Point mutations for the integration of kinase mutants or construction of a mutated reporter plasmid were introduced via "QuickChange Lightning" site directed mutagenesis according to the supplier's manual (Agilent Technologies, Inc., Santa Clara, USA).

Reporter assays

For reporter studies, *C. glutamicum* wild type or one of the mutant strains were transformed with a reporter plasmid (Table S3). A preculture in BHI medium (25 µg/ml kanamycin) was inoculated from a fresh BHI agar plate and incubated for 8-10 h at 30°C in a rotary shaker. After that, cells were transferred into a second preculture in CGXII medium (30) containing 2% (w/v) glucose and 0 µM FeSO₄ to starve the cells from iron. However, protocatechuic acid (PCA) was present in the preculture, allowing the uptake of trace amounts of iron. After growth overnight, the main culture was inoculated to an OD₆₀₀ of 1 in CGXII medium and cultivated in 48-well Flowerplates (m2p-labs GmbH, Aachen, Germany) at 30°C, 95% humidity, 1200 rpm. For the hemin stock solution, hemin (Sigma Aldrich, Munich, Germany) was dissolved in 20 mM NaOH to a concentration of 2.5 mM and, as an iron source, added to the medium in the desired concentrations. Growth of the cells (biomass production) was recorded as the backscattered light intensity of sent light with a wavelength of 620 nm (signal gain factor of 12). For the measurement of eYFP fluorescence, the culture was excited at 510 nm and emission was measured at 532 nm (signal gain factor of 50).

Electrophoretic mobility shift assays (EMSA)

To characterize the operator sequence of HrrA, the protein was produced in *E. coli* BL21 and purified as His₆-tagged variant from cells as described previously (8). As ligand, 30 bp DNA fragments with triplet mutations were amplified and subsequently, 100 ng of the fragments were incubated with 0x, 10x and 30x excess of HrrA in in EMSA buffer (250 mM Tris-HCl pH 7.5, 25 mM MgCl₂, 200 mM KCl, 25% (v/v)

glycerol). After 30 min at room temperature, the samples were loaded to a native 12% polyacrylamide gel (TBE-based, TBE (89 mM Tris base, 89 mM boric acid, 2 mM Na₂EDTA, loading dye: 0.01% (w/v) xylene cyanol dye, 0.01% (w/v) bromophenol blue dye, 20% (v/v) glycerol, 1 x TBE). Electrophoresis was carried out for 60 min at 160 V. DNA was subsequently stained with SYBR Green I (Sigma Aldrich, Munich, Germany).

Mathematical models and mutant simulation

Two mathematical models were developed to assess the determining factors of the dynamics of the heme detoxification and utilization modules (see Supplementary Text; Model equations M1 and M2). A set of ordinary differential equations (ODEs) describes the time-dependent changes in the different components of the two networks under varying heme concentrations as stimulus of both systems. The interactions between the kinases and the response regulators of the two TCSs were described based on the modelling approach by Groban and co-workers (34), while thermodynamic modelling (35) was used to describe the target gene regulation in both systems. The dynamics of the individual components were simulated for wild type conditions as well as different mutant strains. The numerical solution of the ODEs as well as the individual simulations were performed with MATLAB™ software (The MathWorks, Inc.).

RESULTS

Temporal hierarchy in the heme utilization and detoxification response.

Under iron limiting conditions the growth of *C. glutamicum* is significantly impaired, but can be restored by the presence of heme in the medium. Provided that excess heme is toxic to the cells, we wondered which strategy *C. glutamicum* uses to regulate the balance between its heme utilization and detoxification modules. To this end, we studied the expression dynamics of the two major components responsible for heme utilization (*hmuO*) and detoxification (*hrtBA*) in response to an extracellular heme stimulus, by monitoring promoter-reporter fusions for the two systems (28). Interestingly, a wild type strain of *C. glutamicum* transformed with plasmids carrying the reporter constructs (pJC1_P_{hmuO}-*eyfp* or pJC1_P_{hrtBA}-*eyfp*) revealed highly distinct response profiles and a temporal hierarchy in reporter output of the P_{hmuO} and P_{hrtBA} promoters (Fig.

1): While we observed a nearly instant but transient response for the heme detoxification module *hrtBA* to 4 μ M extracellular heme (Fig. 1, red line), the heme utilization module *hmuO* displayed higher initial expression levels compared to *hrtBA*, and experienced an expression boost after a delay of about 5 hours (Fig. 1, green line). This increase in *hmuO* expression temporally coincides with a declining *hrtBA* expression. From a physiological perspective, these antagonistic expression profiles seem plausible and impressively demonstrate the urgency of detoxification over utilization after first contact with the stimulus.

How does *C. glutamicum* implement appropriate timing of detoxification and utilization by using two paralogous TCS responsive to the same stimulus? In this study, we formulated three distinct questions and addressed those by experiments described in following:

- 1) How does cross-regulation between ChrSA and HrrSA affect *hrtBA* and *hmuO* expression, respectively?
- 2) Does the differential interpretation of their common stimulus, i.e. the external heme concentration, impact the response?
- 3) How does regulatory hierarchy and network architecture affect the response profile?

To test the first hypothesis we tested two mutant strains deleted for either one of the HKs (Δ *chrS* and Δ *hrrS*) and transformed them with a reporter plasmid carrying the non-cognate target promoter (Δ *chrS*:pJC1_*P_{hmuO}*-*eyfp* and Δ *hrrS*:pJC1_*P_{hrtBA}*-*eyfp*).

Strikingly, despite some quantitative differences (as discussed below), neither of the deletions changed the qualitative response of the non-cognate target promoter towards heme (Fig. 1B), i.e. the *P_{hrtBA}*-*eyfp* response was still transient in a Δ *hrrS* mutant and the *P_{hmuO}*-*eyfp* response was still delayed in a Δ *chrS* mutant, indicating that cross-regulation between the TCS cannot explain the antagonistic regulation strategy in *C. glutamicum*.

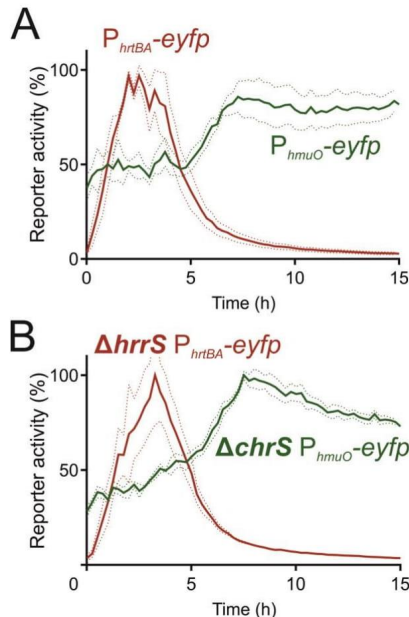


Figure 1: Activation of P_{hmuO} and P_{hrtBA} in response to extracellular heme addition.

(A) The *C. glutamicum* wild type strain was transformed with one of the target gene reporters pJC1_*P_{hmuO}*-*eyfp* or pJC1_*P_{hrtBA}*-*eyfp*. Iron deprived cells were subsequently cultivated in a microreactor system (Biolector) in CGXII minimal medium with 2% (w/v) glucose containing 4 μ M hemin. The eYFP fluorescence was measured as the output of target promoter activation, and backscatter values were recorded to monitor biomass formation. The specific fluorescence (fluorescence/backscatter) was normalized according to material and methods and the reporter activity (%) was calculated with the maximum reporter output. (B) *C. glutamicum* Δ *chrS*:pJC1_*P_{hmuO}*-*eyfp* and Δ *hrrS*:pJC1_*P_{hrtBA}*-*eyfp* grown as described in (A). Non-cognate sensor kinases do not significantly affect the response profile.

Modelling of heme uptake and consumption

Therefore we wanted to test whether the depletion of external heme could serve as a joint trigger to cause opposing regulation of heme utilization and detoxification systems. However, before turning to this question we first asked how long it would take to deplete heme in our experiments? To this end, we considered a simple mathematical model describing

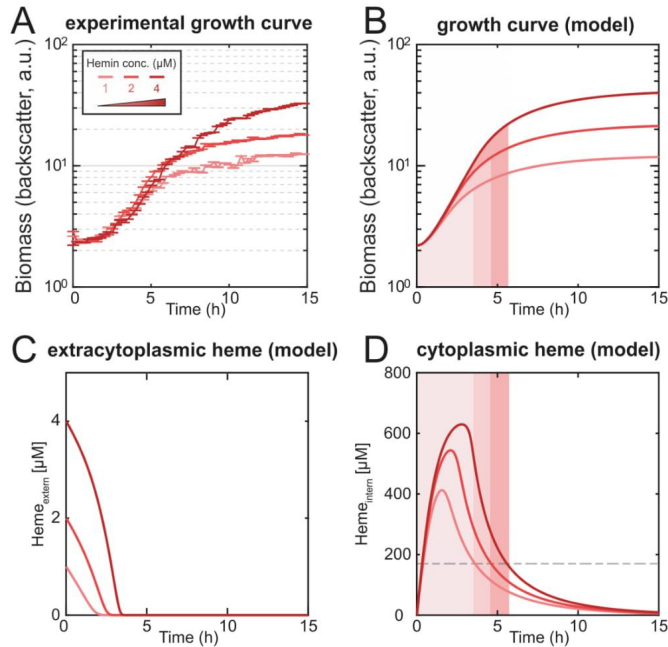


Figure 2: The mathematical model reproduces the experimental growth curves quantitatively.

(A) Growth curves of the *C. glutamicum* wild type strain under increasing hemin concentrations (1 μM , 2 μM and 4 μM). (B) The mathematical model can reproduce the the average growth behaviour (left). (C) The mathematical model predicts the consumption of extracytoplasmic heme and (D) the consumption of the internal heme pool that contributes to growth.

the uptake and consumption of heme, assuming that the reproduction of *C. glutamicum* requires $\sim 5 \times 10^6$ Fe^{2+} molecules per single cell (see Supplementary Text for details). Interestingly, at the given final biomass and at the experimentally determined growth rate in our medium (Fig. 2A) the model predicts a depletion of 4 μM initial heme approx. 3.5 hours after the start of the experiment (Fig. 2C). Within the model, after depletion of extracytoplasmic heme (defined as extracellular and membrane associated heme), there is a time delay of approx. 2 hours until the cytoplasmic heme pool is also depleted below a threshold required for cell growth (Fig. 2D). When comparing the experimental growth curves (Fig. 2A) with the theoretical predictions, the time points of internal

heme exhaustion (Fig. 2D) in fact correlate with the cease of growth of the cultures in experiment and theory (Figs. 2A, B). Also the time point of growth cessation can be tuned by adding different initial heme concentrations (1-4 μM) to the medium (Fig. 2A), as predicted by our model (Fig. 2B).

Transient expression of the *C. glutamicum* *hrtBA* detoxification module

Next, we asked whether the depletion of heme could also explain the transient activity of the *hrtBA* promoter. To this end we extended our mathematical model to also describe stimulus perception and regulation within the two TCSSs, as well as the

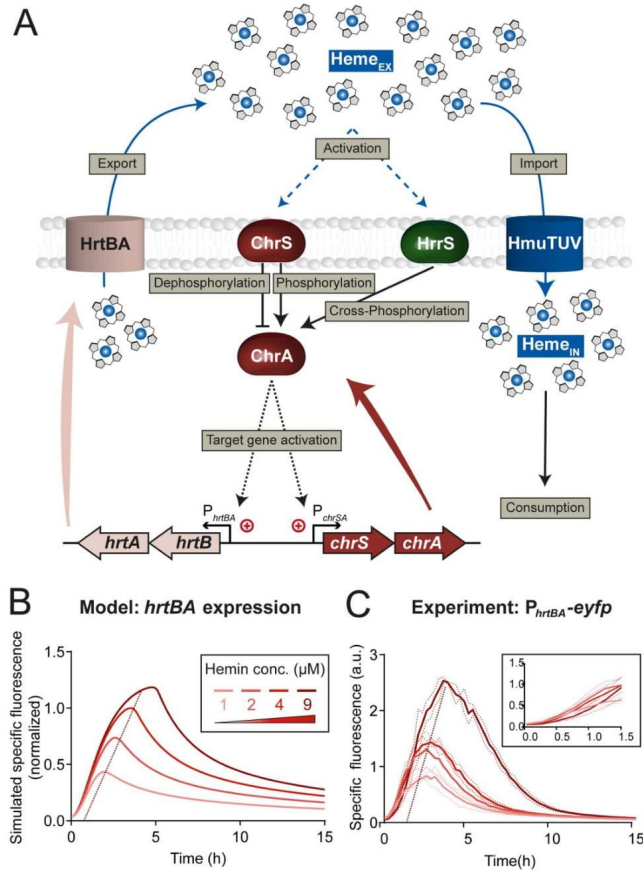


Figure 3: Regulatory scheme and dynamic response of the *C. glutamicum* heme detoxification module.

(A) Scheme of the regulatory interactions considered in the mathematical model for the heme detoxification module. Uptake of external heme molecules via HmuTUV and subsequent consumption/incorporation via diverse enzymes is crucial for bacterial growth under iron starvation. The fine-tuned response to heme in order to avoid intoxication is mainly based on the two TCSs ChrSA and HrrSA. The two kinases ChrS and HrrS are autophosphorylated in response to external hemin. After activation, they (cross-) phosphorylate the response regulator ChrA. In addition, the non-phosphorylated form of ChrS functions as a phosphatase on the phosphorylated response regulator ChrA. The phosphorylated response regulator activates expression of its target genes *hrtBA* and *chrSA*. The gene product of *hrtBA* is a heme exporter that transports internal heme to the extracellular space. (B) Dynamical response of our computational model for the detoxification module (Supplementary Text; Model equations M1) towards different external heme levels, as given by the simulation of specific fluorescence of a P_{hrtBA} -*eyfp* reporter, normalized to the maximal specific fluorescence at 4 μ M heme. (C) Experimental dynamical response of a P_{hrtBA} -*eyfp* reporter in wild type *C. glutamicum* cells towards different heme concentrations supplied in the medium at $t = 0$ h.

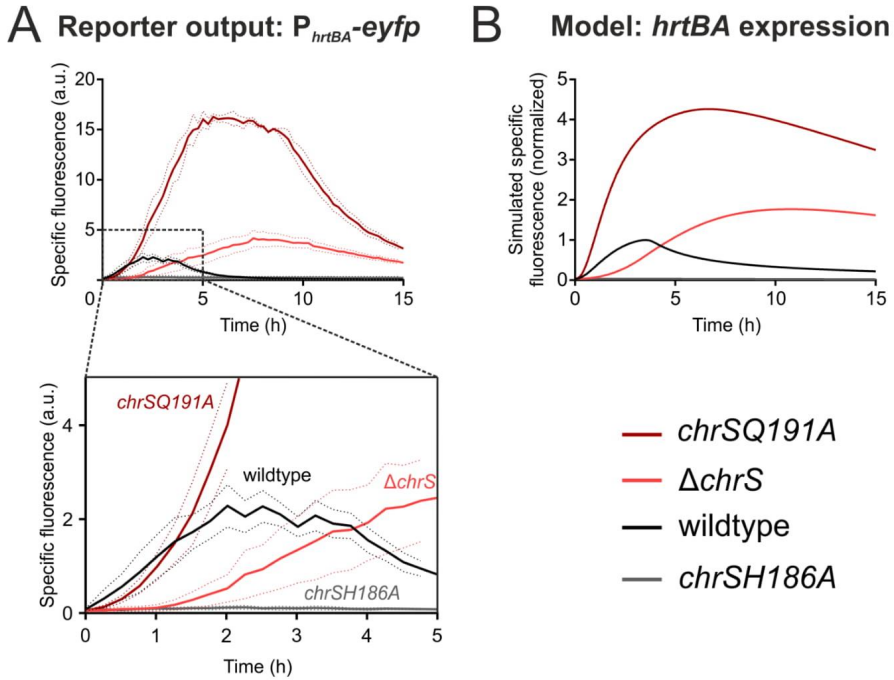


Figure 4: Kinase and phosphatase activity of ChrS shape the *hrtBA* response.

(A) Reporter output of *C. glutamicum* wild type and mutant strains carrying the vector pJC1_ P_{hrtBA} -*eyfp*. Cells were inoculated in CGXII minimal medium with 2% (w/v) glucose containing 4 μ M hemin as iron source. **(B)** Simulated specific fluorescence of the *C. glutamicum* wild type strain and in the mutant strains *chrSQ191A* (phosphatase=off), *chrSH186A* (kinase=off) and Δ *chrS*.

dynamical response of the *chrSA* and *hrtBA* operons (for details the reader is referred to the Supplementary text). Briefly, the model considers sensing of externally added heme and subsequent autophosphorylation of ChrS and HrrS (36), (cross-) phosphorylation of ChrA by phosphorylated HKs (ChrS~P and HrrS~P) and promoter activation of P_{chrSA} and P_{hrtBA} by phosphorylated response regulator ChrA~P (Fig. 3A). Simulations of the model predict that the depletion of external heme dictates the time point of deactivation of P_{hrtBA} , leading to a prolonged promoter activity and higher overall HrtBA production at higher initial heme concentrations (Fig. 3B). In fact,

when experimentally supplying different heme concentrations (1-9 μ M) to the medium, we found that both the strength as well as the duration of P_{hrtBA} -*eyfp* expression increased with increasing amounts of supplied heme (Fig. 3C). In the light of a bifunctional ChrS kinase/phosphatase, exhaustion of external heme is sufficient to explain the transient response dynamics of P_{hrtBA} -*eyfp* expression.

Interestingly, our experimental data also showed that for all heme concentrations the initial promoter activity was almost identical (Fig. 3C) and that the overall peak height is only modulated by the time point of

stimulus decline. This suggests that either (i) despite varying levels of ChrA~P the P_{hrtBA} promoter is nearly fully saturated or (ii) the applied heme concentrations lead to saturation of the sensor kinase and thus to similar phosphorylation levels of ChrA. In order to discriminate between these scenarios, we sought to increase ChrA~P levels in the cell and test whether the P_{hrtBA} will be more active than in the wild type. To this end, we analysed a *chrS* phosphatase-OFF mutant (*chrSQ191A*) still harbouring its kinase activity (28), supposedly leading to higher ChrA~P levels. Interestingly, the *chrSQ191A* phosphatase mutant strain displayed a 7-fold increased P_{hrtBA} -*eyfp* output (Fig. 4A), as incurred by a higher and more sustained promoter activity within the first 4 hours of incubation when compared to the wild type (Fig. 4A inset). A similar behaviour can also be observed in our computational models, in which the maximal phosphorylation level of ChrA is 25% in the wild type as compared to 100% in the phosphatase mutant, leading in our model to a stronger initial promoter activity in the latter case (Fig. 4B). The predicted increase of initial promoter activity is, however, more prominent in the model than in our experimental data, in which the kinase mutant showed a wild type-like behaviour for around 1 h before reaching a stronger promoter activity (Fig. 4A inset). This discrepancy emphasized that saturation of kinase activity is not sufficient to explain the experimental data and that instantaneous promoter occupancy by phosphorylated response regulator may contribute to the fast onset of the detoxification response (see "Memoryless activation of the *hrtBA* detoxification module").

Another interesting feature of the model is that the depletion of external heme leads to a quick dephosphorylation of ChrA~P and promoter shut-off in the wild type. In contrast, in the phosphatase mutant ChrA~P is only slowly diluted and/or degraded by growth or spontaneous dephosphorylation, leading to a significantly delayed promoter shut-off about 1 h after external heme depletion. Thus, the strong phosphatase activity of ChrS is important in wild type cells in order to quickly turn off *hrtBA* expression once external heme is depleted.

Both kinases, ChrS and HrrS, contribute to a fast onset of the P_{hrtBA} promoter

Next, we wanted to study the response of the heme detoxification module in a strain featuring reduced ChrA~P levels. However, a *chrS* mutant deficient in its kinase activity (*chrSH186A*) was unable to activate the

P_{hrtBA} promoter altogether (Fig. 4A; grey line), suggesting that ChrSH186A retains its strong phosphatase activity and likely reduces ChrA~P below a level required to activate P_{hrtBA} .

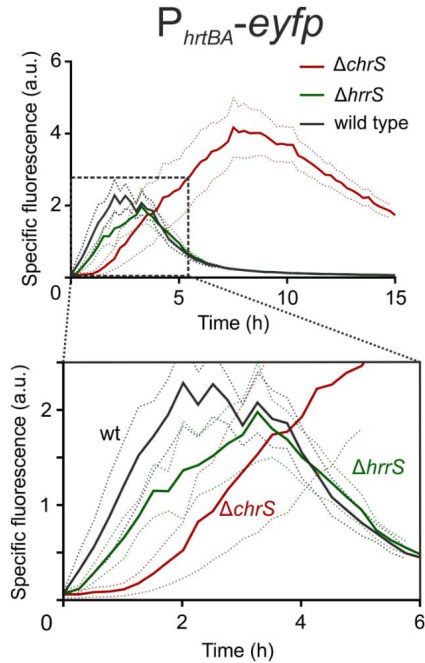


Figure 5: HrrS mediated cross-phosphorylation of ChrA might act as a kick-start impulse contributing to a fast ON-set of the P_{hrtBA} response.

Reporter output of *C. glutamicum* wild type cells and the mutant strains $\Delta hrrS$ and $\Delta chrS$, carrying the vector pJC1- P_{hrtBA} -*eyfp* and cultivated in CGXII minimal medium with 2% (w/v) glucose containing 4 μ M hemin as iron source.

Instead, our model predicted that in a $\Delta chrS$ mutant, which lacks both kinase and phosphatase activity from ChrS, the non-cognate HrrS sensor kinase should be able to slowly, but gradually phosphorylate ChrA~P (28) and thus activate P_{hrtBA} (Fig. 4B; light red). Indeed, the experimental kinetics of the P_{hrtBA} -*eyfp* reporter showed a weaker activation during the first 2 hours, but also displayed a more sustained and eventually a stronger expression peak compared to the wild type (Fig. 4A). Within our computational model this sustained response is again caused by the

slow rate of dilution and/or dephosphorylation of ChrA-P after heme depletion, given the lack of phosphatase activity in the $\Delta chrS$ mutant (Fig. 4B). Taken together, these data show that in the absence of ChrS, the non-cognate kinase HrrS is sufficient to activate the promoter of the detoxification module, P_{hrtBA} .

This provoked the question as to whether the non-cognate kinase HrrS also has an effect on the induction kinetics of P_{hrtBA} in wild type cells. Interestingly, when measuring the P_{hrtBA} -*eyfp* reporter activity in a $\Delta hrrS$ mutant, the mutant indeed showed delayed promoter activation and was about 20-30 min slower than the wild type (Fig. 5). This suggests that HrrS acts as a “kick-starter” in order to speed up the induction of the detoxification system. The additional kinase activity conferred by HrrS might in fact be needed as a support for ChrS to achieve higher ChrA phosphorylation levels, given that our analysis above

suggested that ChrS is already fully in its kinase state for all heme concentrations applied here.

Memoryless activation of the *hrtBA* detoxification module

Above described results suggested that a high promoter occupancy by ChrA-P may contribute to the fast onset of the detoxification response. Considering this scenario, we would not expect memory in the P_{hrtBA} response if two heme pulses were applied at subsequent times. Theoretically, our model predicted nearly identical levels of promoter saturation for different heme levels, suggesting that the application of a second heme pulse should not lead to a faster response and no priming effect on the output should be observable.

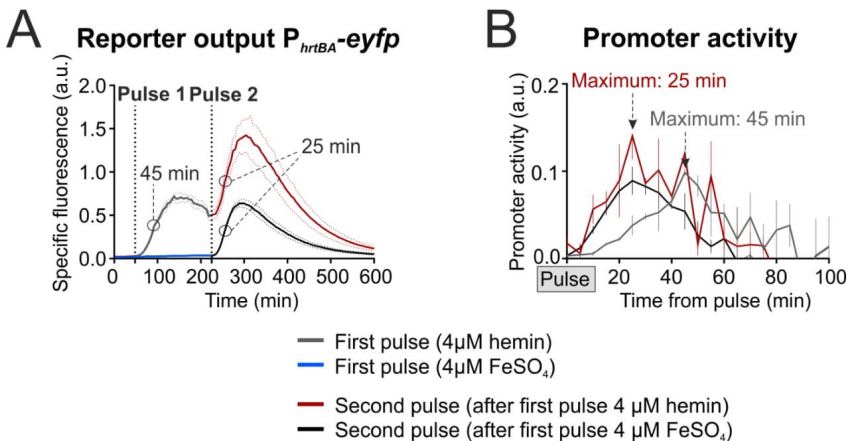


Figure 6: Additional heme pulses do not “prime” the P_{hrtBA} output.

(A) *C. glutamicum* wild type cells were transformed with the target gene reporter $pJC1_{P_{hrtBA}}-eyfp$ and starved from iron overnight as described in material and methods. Subsequently, the cells were inoculated in CGXII minimal medium without iron source and eYFP fluorescence (=reporter output) and backscatter (biomass) was measured every 5 minutes. After 45 min, hemin (A, grey line) or $FeSO_4$ (A, black line) was added to a final concentration of 4 μ M. A second pulse of 4 μ M hemin was applied to both conditions after 225 min. (B) Promoter activities (calculated as derivation of the specific fluorescence over time) of (A) in relation to the first or second pulse.

While lag phase cells (growth depicted in Fig. S1) needed up to 45 minutes to reach maximum promoter

activity following a heme pulse, promoter activity was nearly instantaneously observable after an additional

heme pulse in the early exponential phase (Fig. 6A). This finding was irrespective of whether the cells were primed with a first heme pulse (Fig. 6A, *red line*) or with an iron pulse (Fig. 6A, *black line*). Furthermore, the time point of the second heme pulses did not affect the onset of the P_{hrtBA} response (Fig. S2). These data support the hypothesis, that promoter saturation by phosphorylated response regulator contributes as a significant determinant of response kinetics.

Heme utilization is co-regulated by DtxR integrating information on iron availability.

While a detoxification response must be fast and rather uncoupled from other regulatory interference, utilization of a particular nutrient has to be carefully considered in the light of the current physiological status of the cell: As shown above, the activation of the detoxification module *hrtBA* is solely influenced by the amount of heme in the medium. In contrast, for a decision on heme utilization as an alternative iron source, information on general iron availability needs to be incorporated into the network controlling *hmuO* expression. In this context, it was already revealed by previous studies that both *hrrA* and *hmuO* are repressed by the iron regulator DtxR in response to iron availability (11).

Given that DtxR repression and HrrA activation seem to have opposing effects on the timing of *hmuO* expression, we asked how these signals are prioritized at the P_{hmuO} promoter. To investigate the impact of both regulators on the activation of the heme utilization system, we developed a second mathematical model that focuses on HrrSA and DtxR as main regulators of the P_{hmuO} and P_{hrrA} activity (Fig. 7A). Like before, in this model the description of the non-cognate two-component system (ChrSA) was limited to the cross-phosphorylation of ChrS on HrrA. In addition, we made the simplifying assumption that the activation of DtxR is proportional to the internal heme levels, based on the fact that the iron availability is proportional to the conversion of the internal heme pool under our experimental (iron-limiting) conditions. Activated DtxR and phosphorylated HrrA bind to both P_{hmuO} and P_{hrrA} promoters, where they repress and activate gene expression, respectively. Ultimately, increased production of the heme oxygenase HmuO contributes to heme consumption (8) (see Supplementary Text; Model equations M2 for all details).

Simulations of this computational model revealed a biphasic induction pattern of the P_{hmuO} promoter with a quick activation within the first hour after heme addition, followed by a significantly delayed expression boost at approx. 4-5 hours (for 4 μ M heme) (Fig. 7B), very similar to the experimental dynamics observed before (Fig. 1). Interestingly, when lowering the initial heme concentration, the model predicts an earlier onset of P_{hmuO} activation. Strikingly, when experimentally tuning the initial heme levels, we found this exact hierarchy in the activation of the heme utilization module (Fig 7C): A short delay of 3 hours at 1 μ M heme and a longer delay of 5 hours at 4 μ M heme. As such, this biphasic induction of *hmuO* strikingly differs from *hrtBA* activation by ChrSA and is governed by the influence of the iron repressor DtxR on *hmuO* expression (Fig. 8). Upon depletion of internal heme (and thus iron-levels) below a critical threshold, DtxR dissociates from its target promoters and allows their activation (Fig. 7B, D). Accordingly, lower initial heme concentrations within the medium do also shift the time-point of heme exhaustion to earlier times, thereby rationalizing the earlier induction of gene expression in the heme utilization module. From a physiological perspective this again seems very plausible, suggesting that high levels of the heme utilization system are only required under iron limitation when external heme sources are available.

Regarding the regulatory hierarchy of HrrA and DtxR on P_{hmuO} activity, one can think of two potential scenarios: either (i) HrrA is a *bona fide* activator of *hmuO* expression or (ii) HrrA-binding competes with the binding of the repressor DtxR thereby acting as an activator by derepressing *hmuO*, as might be suggested by the close proximity of their binding sites within the P_{hmuO} promoter (Fig. 8A). Altogether, our experimental data are clearly in favour for HrrA acting as a *bona fide* activator. While P_{hmuO} activity is completely abolished in a $\Delta hrrA$ mutant, it is strongly increased in mutant lacking the *dtxR* gene (Fig. 8B). Furthermore, we tested different triplet mutations in the HrrA binding site in their ability to disrupt HrrA binding. In EMSA-studies, an AAC::TTG mutation in the middle of the HrrA operator completely abolished *in vitro* binding of HrrA to P_{hmuO} (Fig. S3). Subsequently, this mutation was inserted to the $\text{pJC1}_{P_{hmuO}}\text{-eyfp}$ reporter, resulting in the

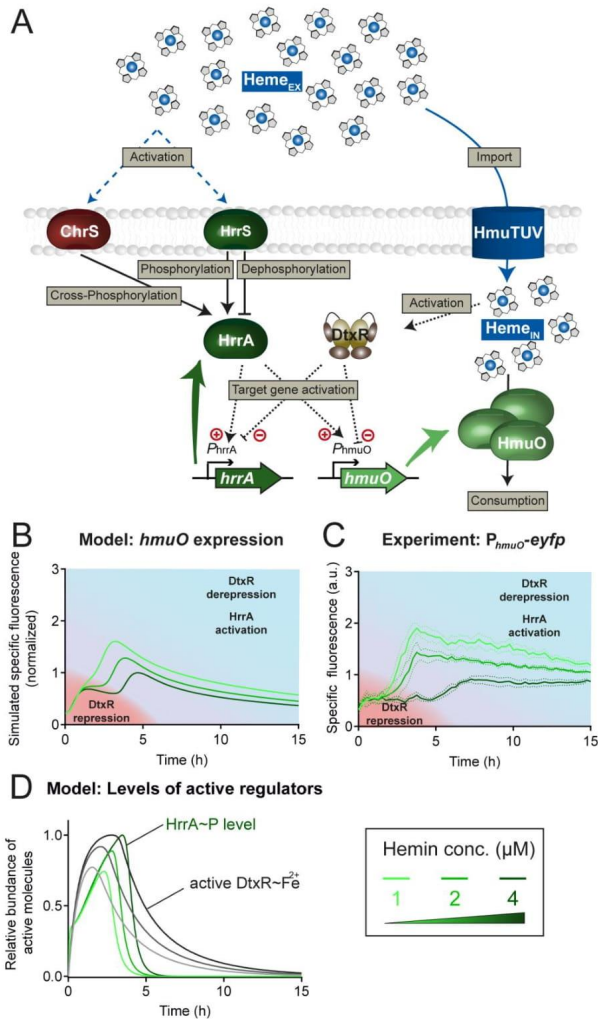


Figure 7: Information on iron availability is integrated into the HrrSA regulated utilization module *hmuO* via DtxR.

(A) The mathematical model of the heme utilization module in *C. glutamicum* shares many basic assumptions with the model of heme detoxification (for description see Fig. 3). Here, heme consumption is assumed to be supported by the heme oxygenase HmuO, whose production is regulated by the phosphorylated response regulator HrrA~P and the iron repressor DtxR. The activation of DtxR is expected to be influenced by internal heme levels. DtxR repression and HrrA activation shape the delayed response of the heme utilization module *hmuO*. (B) The P_{*hmuO*} promoter is activated by the phosphorylated response regulator HrrA~P after a significant

time delay of 3 to 5 hours. Higher heme concentrations lead to a prolonged delay and a lower *hmuO* expression in general. (C) The mathematical model of the heme utilization network in *C. glutamicum* could reproduce this behaviour and gave an explanation regarding (D) the temporal dynamics of both regulators on P_{hmuO} . Levels of the activated iron repressor DtxR increase immediately after addition of heme and repress the promoter activation of P_{hmuO} , proportional to stimulus strength. However, HrrA-P levels increase with a short time delay in response to the stimulus and activate the promoter to a certain extent at the beginning and with increasing intensity upon DtxR dissociation.

pJC1_ P_{hmuO} -*eyfp*^{AAC::TTG} plasmid (Fig. 8A). Irrespective of whether it was introduced to the wild type strain or the $\Delta dtxR$ strain, disruption of HrrA binding decreased the activity of the P_{hmuO} reporter to background levels

(Figs. 8B and S5). These findings clearly indicate that HrrA is does not compete with DtxR for the binding of the P_{hmuO} promoter but is indeed a crucial activator of *hmuO* expression.

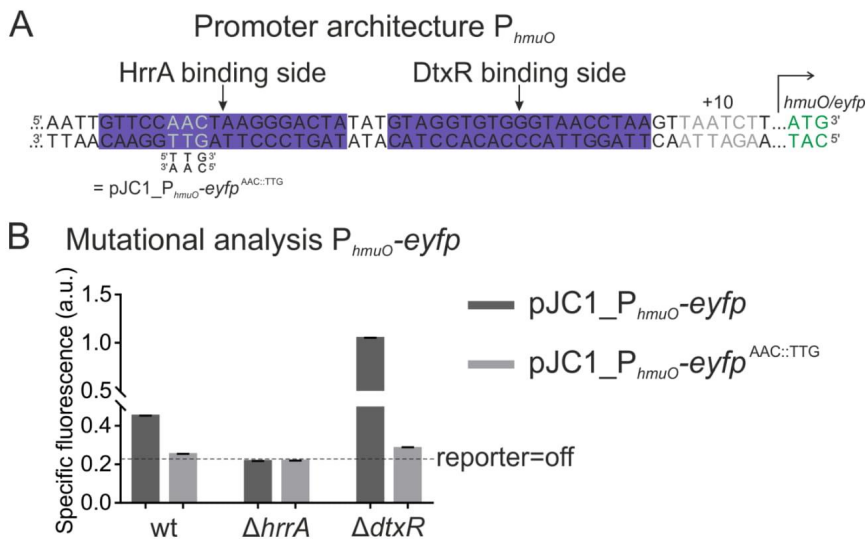


Figure 8: HrrA and DtxR cooperate to control *hmuO* expression in response to iron and heme availability. (A) Promoter architecture of *hmuO*. The DtxR binding site was published previously (11). The AAC::TTG mutation (grey letters) was shown to disrupt HrrA binding to P_{hmuO} in vitro (Fig. S3). (B) Mutational analysis of P_{hmuO} . HrrA binding was abolished by introducing the AAC::TTG mutation into the P_{hmuO} -*eyfp* reporter. All strains were grown in BHI complex medium supplemented with 4 μ M hemin as the $\Delta dtxR$ strain grows poorly in CGXII medium. After iron starvation overnight, the three strains (wild type, $\Delta hrrA$ and $\Delta dtxR$) were inoculated in BHI and the specific fluorescence (eYFP-fluorescence/backscatter) was recorded in 15 minutes intervals. The graph shows the specific fluorescence after 20 h. Full reporter outputs are shown in the supplementary Fig. S4.

DISCUSSION

Orchestration of heme homeostasis and detoxification of excess heme appears to be of utmost importance for *Corynebacteriaceae*, as remarkably, several species dedicate two paralogous TCS to this regulatory task (25). Here, we provide comprehensive insights into the temporal dynamics of *hmuO* and *hrtBA* expression modulated by HrrSA and ChrSA in *C. glutamicum*. Similar regulatory setups, with two paralogous, exclusively heme-dedicated systems are for example found in *C. diphtheria*, *Corynebacterium pseudotuberculosis*, and *Corynebacterium lipophiloflavum* (25, 37), where the corresponding sequence identities and a conserved genomic synteny suggest a similar role of these systems in the coordinated control of heme detoxification and utilization (20, 26). To our knowledge, these systems represent the first example studied in detail, where two paralogous systems coordinate a complex physiological response by perceiving the same stimulus: heme.

As a general principle, the integrative signalling pathway design appears to be especially beneficial if a multifaceted stimulus requires different regulatory and appropriately timed outputs. The response of *C. glutamicum* to extracellular heme sets an interesting example for this, as the physiological adaption is shaped by a fast-reacting ChrSA system regulating expression of the detoxification module and the HrrSA system contributing to a layered dynamic regulation of heme utilization. In a recent study, we could show that the HKs of both TCS, HrrS and ChrS, slightly differ regarding their responsiveness and their general mode of heme-protein interaction (36). However, kinase activity is not the only factor influencing differential target gene activation. While the P_{chrSA} promoter and the divergently located P_{hrtBA} promoter are positively autoregulated from one centred ChrA binding site (Fig. 3A), *hrrS* and *hrrA* are controlled from two distinct promoters. For *hrrA* as well as *hmuO*, the global iron regulator DtxR adds an additional regulatory layer, thereby integrating information on general iron availability in the cell (8, 11). Here, we could show that HrrA does not simply displace DtxR on the promoter of *hmuO* but is in fact an essential activator, also in the absence of DtxR repression (Fig. 8B). By this means, information on heme (stimulus of HrrS) and Fe^{2+} (co-repressor of DtxR) is directly integrated at the level of *hmuO* expression and RR (*hrrA*) synthesis.

In contrast, ChrSA-mediated activation of *hrtBA* expression is solely influenced by heme availability, as expected for a detoxification system. Here, our data suggested an instantaneous saturation of the ChrS kinase and strong activation of P_{hrtBA} in response to exogenous heme - independent of the applied heme concentrations tested in our setup (Fig. 3). Our model and experiments revealed that the overall strength of *hrtBA* expression was determined solely by the duration of the response, as governed by the timescale of heme exhaustion in the medium. Thus, it seems that the comparable levels of P_{hrtBA} promoter occupancy independent from stimulus strength ensure an effective detoxification response even for low toxic heme concentrations, as claimed for a detoxification module.

Another important factor in the maintenance of intracellular heme homeostasis is the previously reported cross-phosphorylation between HrrSA and ChrSA (28). While deletion of *chrS* did not significantly influence the P_{hmuO} activation pattern in our reporter studies (Fig. 1B), deletion of *hrrS* resulted in a delayed P_{hrtBA} activation in response to heme (Fig. 5). These findings suggest a role of HrrSA as a "kick-start" system of *chrSA*, thereby giving *C. glutamicum* a competitive edge by shortening the reaction time to mount the detoxification response. Furthermore, the bifunctionality of ChrS ensures efficient proof-reading of ChrA~P counteracting cross-phosphorylation by HrrS under non-inducing conditions where ChrS is dominantly in its phosphatase state.

Physiologically relevant cross phosphorylation between TCSs was, for example, shown in *Bacillus anthracis* (38). In this case the heme responsive HssRS system was shown to cross interact with HitRS, which is activated by cell envelope stress. Cross-regulation between HssRS and HitRS thereby enables an integrated response of *B. anthracis* to heme and to heme-induced cell envelope damage (39). Interestingly, HrrSA and ChrSA as well as HssRS and HitRS are among the closest related TCS in the particular species reflecting that duplication and subsequent specialization represents an evolutionary driver of TCS signalling towards the integration of multiple signals and the creation of a multifaceted response to complex stimuli. A similar scenario is found with the NarPQ and NarXL systems regulating the response to nitrate and nitrite in *Escherichia coli* (40). For these closely related

systems, significant cross phosphorylation appears to play a role in the modulation of target gene activation and maintenance of nitrogen homeostasis (41).

The regulatory setup shaping the response to heme may also have considerable impact on heme tolerance of the particular species. Already decades ago, van Heyningen reported on the differential sensitivity of *Bacillus* species to heme (42). Mike and coworkers correlated an increased tolerance, as observed for *B. anthracis*, with the employment of two cross-regulating TCS coordinating heme export (HssRS) and cell envelope stress (HitRS) (39). Therefore, it might be conceivable that the employment of two heme-responsive TCSs by some corynebacterial species enables a more robust control of heme homeostasis compared to the regulation by a single system. Remarkably, while the HrrBA exporter is conserved among many Gram-positive species, the TCS systems 'in charge' do not share significant sequence similarity – especially not in their membrane-embedded sensor domains (24, 36). This overall scenario of two cross-regulating TCSs modulating heme homeostasis and detoxification underlines a favorable concept nature employs to respond to the multifaceted stimulus heme.

In summary, we have approached the regulatory interplay between the heme-responsive HrrSA and ChrSA TCSs of *C. glutamicum* by a comprehensive screening of various mutant strains carrying different target promoters. Generation of a mathematical model based on this dataset revealed the underlying mechanisms triggering the antagonistic temporal dynamics in TCS signaling, which shape the cellular response towards the "toxic, but tasty" heme molecule. In the future, we expect that similar work – combining time-resolved monitoring of gene expression and systems-level modeling of the underlying regulatory networks – will help to unravel the logic behind further homeostatic responses.

Acknowledgments

We would like to thank Ulrike Viets for excellent technical support, Eva Davoudi for critical proof-reading and discussion and Dominik Wolf for his help with the EMSA experiments.

This work was financially supported by the Deutsche Forschungsgemeinschaft (DFG SPP 1617; grant FR3673/1-2 and grant FR 2759/4-1) and the Helmholtz Association (W2/W3-096).

Conflict of interest

The authors declare that the research was conducted in the absence of any commercial or financial relationships that could be construed as a potential conflict of interest.

Author contributions

MK, HP, GF and JF conceived the study; MK and CG performed the experiments; MK and HP analyzed the data; HP and GF generated the models; MK, HP, GF and JF wrote the manuscript.

REFERENCES

- Andrews SC, Robinson AK, Rodriguez-Quinones F. 2003. Bacterial iron homeostasis. *FEMS Microbiol Rev* 27:215-37.
- Poulos TL. 2007. The Janus nature of heme. *Natural product reports* 24:504-10.
- Borzelleca JF. 2000. Paracelsus: herald of modern toxicology. *Toxicol Sci* 53:2-4.
- Paracelsus. 1965. "Die dritte Defension wegen des Schreibens der neuen Rezepte" p508-513, *Septem Defensiones* 1538, vol Bd. 2.
- Wilks A. 2002. Heme oxygenase: evolution, structure, and mechanism. *Antioxid Redox Signal* 4:603-14.
- Schmitt MP. 1997. Transcription of the *Corynebacterium diphtheriae hmuO* gene is regulated by iron and heme. *Infect Immun* 65:4634-41.
- Wilks A, Schmitt MP. 1998. Expression and characterization of a heme oxygenase (HmuO) from *Corynebacterium diphtheriae*. Iron acquisition requires oxidative cleavage of the heme macrocycle. *J Biol Chem* 273:837-41.
- Frunzke J, Gatgens C, Brocker M, Bott M. 2011. Control of heme homeostasis in *Corynebacterium glutamicum* by the two-component system HrrSA. *J Bacteriol* 193:1212-21.
- Zhu W, Wilks A, Stojiljkovic I. 2000. Degradation of heme in gram-negative bacteria: the product of the *hemO* gene of *Neisseria* is a heme oxygenase. *J Bacteriol* 182:6783-90.
- Ratliff M, Zhu W, Deshmukh R, Wilks A, Stojiljkovic I. 2001. Homologues of neisserial heme oxygenase in gram-negative bacteria: degradation of heme by the product of the *pigA* gene of *Pseudomonas aeruginosa*. *J Bacteriol* 183:6394-403.
- Wennerhold J, Bott M. 2006. The DtxR regulon of *Corynebacterium glutamicum*. *J Bacteriol* 188:2907-18.
- Anzaldi LL, Skaar EP. 2010. Overcoming the heme paradox: heme toxicity and tolerance in bacterial pathogens. *Infect Immun* 78:4977-89.
- Zhu W, Hunt DJ, Richardson AR, Stojiljkovic I. 2000. Use of Heme Compounds as Iron Sources by Pathogenic *Neisseriae* Requires the Product of the *hemO* Gene. *J Bacteriol* 182:439-447.
- Hassan S, Ohtani K, Wang R, Yuan Y, Wang Y, Yamaguchi Y, Shimizu T. 2010. Transcriptional regulation of hemO encoding heme oxygenase in *Clostridium perfringens*. *J Microbiol* 48:96-101.
- Jani D, Nagarkatti R, Beatty W, Angel R, Slobodnick C, Andersen J, Kumar S, Rathore D. 2008. HDP-a novel heme detoxification protein from the malaria parasite. *PLoS Pathog* 4:e1000053.

16. Fitch CD. 1998. Involvement of heme in the antimalarial action of chloroquine. *Transactions of the American Clinical and Climatological Association* 109:97-106.
17. Stauff DL, Skaar EP. 2009. *Bacillus anthracis* HssRS signalling to HrtAB regulates haem resistance during infection. *Mol Microbiol* 72:763-78.
18. Torres VJ, Stauff DL, Pishchany G, Bezbradica JS, Gordy LE, Iturregui J, Anderson KL, Dunman PM, Joyce S, Skaar EP. 2007. A *Staphylococcus aureus* regulatory system that responds to host heme and modulates virulence. *Cell Host Microbe* 1:109-19.
19. Fernandez A, Lechardeur D, Derre-Bobillot A, Couve E, Gaudu P, Gruss A. 2010. Two coregulated efflux transporters modulate intracellular heme and protoporphyrin IX availability in *Streptococcus agalactiae*. *PLoS Pathog* 6:e1000860.
20. Bibb LA, Schmitt MP. 2010. The ABC transporter HrtAB confers resistance to hemin toxicity and is regulated in a hemin-dependent manner by the ChrAS two-component system in *Corynebacterium diphtheriae*. *J Bacteriol* 192:4606-17.
21. Heyer A, Gatgens C, Hentschel E, Kalinowski J, Bott M, Frunzke J. 2012. The two-component system ChrSA is crucial for haem tolerance and interferes with HrrSA in haem-dependent gene regulation in *Corynebacterium glutamicum*. *Microbiology* 158:3020-31.
22. Zschiedrich CP, Keidel V, Szurmant H. 2016. Molecular Mechanisms of Two-Component Signal Transduction. *J Mol Biol* 428:3752-75.
23. Mascher T, Helmann JD, Uden G. 2006. Stimulus perception in bacterial signal-transducing histidine kinases. *Microbiol Mol Biol Rev* 70:910-38.
24. Stauff DL, Skaar EP. 2009. The heme sensor system of *Staphylococcus aureus*. *Contrib Microbiol* 16:120-35.
25. Bott M, Brocker M. 2012. Two-component signal transduction in *Corynebacterium glutamicum* and other *corynebacteria*: on the way towards stimuli and targets. *Appl Microbiol Biotechnol* 94:1131-50.
26. Bibb LA, Kunkle CA, Schmitt MP. 2007. The ChrA-ChrS and HrrA-HrrS signal transduction systems are required for activation of the *hmuO* promoter and repression of the *hemA* promoter in *Corynebacterium diphtheriae*. *Infect Immun* 75:2421-31.
27. Burgos JM, Schmitt MP. 2016. The ChrSA and HrrSA Two-Component Systems Are Required for Transcriptional Regulation of the *hemA* Promoter in *Corynebacterium diphtheriae*. *J Bacteriol* 198:2419-30.
28. Hentschel E, Mack C, Gatgens C, Bott M, Brocker M, Frunzke J. 2014. Phosphatase activity of the histidine kinases ensures pathway specificity of the ChrSA and HrrSA two-component systems in *Corynebacterium glutamicum*. *Mol Microbiol* 92:1326-42.
29. Kalinowski J, Bathe B, Bartels D, Bischoff N, Bott M, Burkovski A, Dusch N, Eggeling L, Eikmanns BJ, Gaigalat L, Goesmann A, Hartmann M, Huthmacher K, Kramer R, Linke B, McHardy AC, Meyer F, Mockel B, Pfeiferle W, Puhler A, Rey DA, Ruckert C, Rupp O, Sahn H, Wendisch VF, Wiegand I, Tauch A. 2003. The complete *Corynebacterium glutamicum* ATCC 13032 genome sequence and its impact on the production of L-aspartate-derived amino acids and vitamins. *J Biotechnol* 104:5-25.
30. Keilhauer C, Eggeling L, Sahn H. 1993. Isoleucine synthesis in *Corynebacterium glutamicum*: molecular analysis of the *ilvB-ilvN-ilvC* operon. *Journal of Bacteriology* 175:5595-5603.
31. Sambrook J. RD. 2001. *Molecular Cloning: A Laboratory Manual*, 3rd edn. . NY: Cold Spring Harbor Laboratory Press.
32. Eikmanns BJ, Thum-Schmitz N, Eggeling L, Ludtke KU, Sahn H. 1994. Nucleotide sequence, expression and transcriptional analysis of the *Corynebacterium glutamicum gltA* gene encoding citrate synthase. *Microbiology* 140 (Pt 8):1817-28.
33. Niebisch A, Bott M. 2001. Molecular analysis of the cytochrome *bc₁-aa₃* branch of the *Corynebacterium glutamicum* respiratory chain containing an unusual diheme cytochrome *c₁*. *Arch Microbiol* 175:282-94.
34. Groban ES, Clarke EJ, Salis HM, Miller SM, Voigt CA. 2009. Kinetic buffering of cross talk between bacterial two-component sensors. *J Mol Biol* 390:380-93.
35. Bintu L, Buchler NE, Garcia HG, Gerland U, Hwa T, Kondev J, Phillips R. 2005. Transcriptional regulation by the numbers: models. *Curr Opin Genet Dev* 15:116-24.
36. Keppel M, Davoudi E, Gatgens C, Frunzke J. 2018. Membrane Topology and Heme Binding of the Histidine Kinases HrrS and ChrS in *Corynebacterium glutamicum*. *Frontiers in Microbiology* 9.
37. Trost E, Ott L, Schneider J, Schroder J, Jaenicke S, Goesmann A, Husemann P, Stoye J, Dorella FA, Rocha FS, Soares Sde C, D'Afonseca V, Miyoshi A, Ruiz J, Silva A, Azevedo V, Burkovski A, Guiso N, Join-Lambert OF, Kayal S, Tauch A. 2010. The complete genome sequence of *Corynebacterium pseudotuberculosis* FRC41 isolated from a 12-year-old girl with necrotizing lymphadenitis reveals insights into gene-regulatory networks contributing to virulence. *BMC Genomics* 11:728.
38. Laub MT, Goulian M. 2007. Specificity in two-component signal transduction pathways. *Annu Rev Genet* 41:121-45.
39. Mike LA, Choby JE, Brinkman PR, Olive LQ, Dutter BF, Ivan SJ, Gibbs CM, Sulikowski GA, Stauff DL, Skaar EP. 2014. Two-component system cross-regulation integrates *Bacillus anthracis* response to heme and cell envelope stress. *PLoS Pathog* 10:e1004044.
40. Rabin RS, Stewart V. 1993. Dual response regulators (NarL and NarP) interact with dual sensors (NarX and NarQ) to control nitrate- and nitrite-regulated gene expression in *Escherichia coli* K-12. *J Bacteriol* 175:3259-68.
41. Noriega CE, Lin HY, Chen LL, Williams SB, Stewart V. 2010. Asymmetric cross-regulation between the nitrate-responsive NarX-NarL and NarQ-NarP two-component regulatory systems from *Escherichia coli* K-12. *Mol Microbiol* 75:394-412.
42. Van Heyningen WE. 1948. Inhibition of aerobic sporing bacilli by haematin. *Nature* 162:114.

3.3 HrrSA Orchestrates a Systemic Response to Heme and Determines Prioritization of Terminal Cytochrome Oxidase Expression.

Keppel M.*, Davoudi C-F.*, Filipchyk A.*, Viets U., Pfeifer E., Polen T., Baumgart M., Bott M., and Frunzke J.

*contributed equally

Manuscript submitted.

Contributor Role	Contributor
Conceptualization	MK (70 %)
	JF (30%)
Formal Analysis	MK (35%)
	CFD (15 %)
	AF (40 %)
	EP (5 %)
	TP (5 %)
Investigation/Experiments	MK (30 %)
	CFD (15 %)
	UV (45 %)
	EP (10 %)
Methodology	MK (50 %)
	CFD (15 %)
	EP (5 %)
	AF (30 %)
Project Administration	MK (50 %)
	JF (50 %)
Software	AF (80 %)
	EP (10 %)
	TP (10 %)
Supervision	MBA (10 %)
	MBO (20 %)
	JF (70 %)
Visualization	MK (70 %)
	CFD (15 %)
	AF (15 %)
Writing – Original Draft Preparation	MK (80 %)
	JF (20 %)
Writing – Review & Editing	MK (18 %)
	CFD (10 %)
	AF (7 %)
	UV (7 %)
	EP (7 %)
	TP (7 %)
	MBA (7 %)
	MBO (7 %)
	JF (30 %)

Overall contribution MK: 60 %

HrrSA orchestrates a systemic response to heme and determines prioritization of terminal cytochrome oxidase expression

Marc Keppel^{1#}, Cedric-Farhad Davoudi^{1#}, Andrei Filipchuk^{1#}, Ulrike Viets¹, Eugen Pfeifer¹, Tino Polen¹, Meike Baumgart¹, Michael Bott¹, and Julia Frunzke^{1*}

* Corresponding author: Julia Frunzke; Email: j.frunzke@fz-juelich.de; Phone: +49 2461 615430

¹ Institute of Bio- und Geosciences, IBG-1: Biotechnology, Forschungszentrum Jülich GmbH, 52425 Jülich, Germany

[#] These authors contributed equally to this work.

Heme is a multifaceted molecule. While serving as a prosthetic group for many important proteins, elevated levels are toxic to cells. The complexity of this stimulus has shaped bacterial network evolution. However, only a small number of targets controlled by heme-responsive regulators have been described to date. Here, we used a genome-wide approach to monitor the *in vivo* promoter occupancy of HrrA, the response regulator of the heme-regulated two-component system HrrSA of *Corynebacterium glutamicum*. Time-resolved profiling revealed dynamic binding of HrrA to more than 250 different genomic targets encoding proteins associated with heme biosynthesis, the respiratory chain, oxidative stress response and cell envelope remodeling. By repression of *sigC*, which encodes an activator of the *cydABCD* operon, HrrA prioritizes the expression of genes encoding the cytochrome *bc₁-aa₃* supercomplex. These data describe for the first time the systemic response strategy that bacteria have evolved to respond to the versatile signaling molecule heme.

Heme (iron bound protoporphyrin IX) is a versatile molecule that is synthesized and used by virtually all aerobic eukaryotic and prokaryotic cells (1) because it serves as the prosthetic group of hemoglobins, hydroxylases, catalases, peroxidases, and cytochromes (2) and is thereby essential for many cellular processes, such as electron transfer, respiration and oxygen metabolism (3). Furthermore, salvaged heme represents the most important iron source for a variety of pathogenic bacteria (4, 5), and also non-pathogenic bacteria can meet their iron demand by degradation of environmental heme. This becomes evident from the diverse set of heme uptake systems and heme oxygenases that catalyze the degradation of the protoporphyrin ring to biliverdin and the concomitant release of carbon monoxide and iron (6).

While heme represents an essential cofactor for a variety of proteins, this molecule also exhibits severe toxicity at high concentrations. Therefore, organisms have evolved sophisticated regulatory networks to tightly control heme uptake, detoxification, synthesis and degradation (4). Several heme-regulated transcription factors have been described, including the heme activator protein (Hap) 1, which is an activator of genes required for aerobic growth of the

yeast *Saccharomyces cerevisiae* (7); the transcription factor BACH1 (BTB and CNC homology 1), which is conserved in mammalian cells (8, 9); and the rhizobial Irr protein, which is a heme-regulated member of the Fur family of transcriptional regulators (10-12).

In Gram-positive bacteria, two-component systems (TCSs) appear to play a prevalent role in heme-responsive signaling (13, 14), as exemplified by the heme sensor system HssRS of *Staphylococcus aureus* and *Bacillus anthracis*, which controls the expression of the *hrtBA* operon, encoding a heme efflux system in both species (15, 16).

Remarkably, several members of the *Corynebacteriaceae* family, including the human pathogen *Corynebacterium diphtheriae* and the biotechnological platform strain *Corynebacterium glutamicum*, have two paralogous TCSs, namely, HrrSA and ChrSA, dedicated to heme-responsive control of gene expression (17-20). The kinases HrrS and ChrS were recently shown to perceive transient changes in heme availability by direct intramembrane interactions with heme (21, 22). Heme binding triggers autophosphorylation of the sensor kinase, followed by transfer of the phosphoryl group to the cognate response regulators HrrA and ChrA. In *C. glutamicum*,

significant cross-phosphorylation was observed between the closely related systems; however, this crosstalk is proofread by a highly specific phosphatase activity of the kinases toward the cognate response regulators under non-inducing conditions (23). While the ChrSA system appears to be mainly involved in rapid activation of the HrtBA detoxification system (19), previous data suggest that HrrSA coordinates a homeostatic response to heme (18). In recent studies, six direct targets have been described for HrrA, including genes encoding enzymes involved in heme synthesis (*hemE*, *hemA* and *hemH*) and heme utilization (*hmuO*, encoding a heme oxygenase) and the *ctaE-qcrCAB* operon, encoding the heme-containing cytochrome *bc₁-aa₃* supercomplex of the respiratory chain (18).

C. glutamicum possesses a branched electron transport chain comprising the cytochrome *bc₁-aa₃* supercomplex (encoded by *ctaD*, the *ctaCF* operon, and *ctaE-qcrCAB*) and the cytochrome *bd* oxidase, encoded by the first two genes of the *cydABDC* operon (24). Although both the cytochrome *aa₃* oxidase and *bd* oxidase are involved in the establishment of a proton-motive force (PMF), the *aa₃* oxidase is an active proton pump that is responsible for the increased proton translocation number ($6 \text{ H}^+ / 2 \text{ e}^-$) of the cytochrome *bc₁-aa₃* supercomplex compared to that of the *bd* oxidase ($2 \text{ H}^+ / 2 \text{ e}^-$) (24). The presence of the cytochrome *bc₁-aa₃* supercomplex was previously shown to be a characteristic feature of almost all Actinobacteria because members of this phylum lack a soluble cytochrome *c*, instead harboring a diheme cytochrome *c₁* that directly shuttles electrons from the *bc₁* complex to the *aa₃* oxidase (25-29). Furthermore, both terminal oxidases differ in heme content, as the *bc₁-aa₃* supercomplex harbors six heme molecules, while the *bd* oxidase harbors only three. Surprisingly, not much is known about the regulation of terminal oxidases in *C. glutamicum*. In addition to the described activation of the *ctaE-qcr* operon by HrrA, the hydrogen peroxide-sensitive regulator OxyR was described as a repressor of the *cydABDC* operon (30, 31). Furthermore, the extracytoplasmic function (ECF) sigma factor SigC (σ^C) was shown to activate expression of the *cydABDC* operon (30, 32). For σ^C , a speculated stimulus is the defect electron transfer in the *aa₃* oxidase (32) and such a defect was observed under copper-deprivation, which resulted in activation of the σ^C regulon (33).

Interestingly, the regulons of prokaryotic heme regulators described thus far comprise only a low number of direct target genes, most of which are involved in heme export (e.g., *hrtBA*) or degradation (*hmuO*). This picture of prokaryotic heme signaling, however, does not match the complexity of the stimulus. In this study, we performed a time-resolved and genome-wide binding profiling (ChAP-Seq) of HrrA in *C. glutamicum* describing the transient HrrA promoter occupancy of more than 250 genomic targets in response to heme. The obtained results emphasize that HrrSA is a truly global regulator of heme homeostasis, which also integrates the response to oxidative stress and cell envelope remodeling. Transcriptome analysis (RNA-Seq) at different time points after heme induction revealed HrrA to be an important regulator of the respiratory chain, which coordinates the expression of components of both quinol oxidation branches as well as menaquinol synthesis and reduction. Remarkably, HrrA was found to prioritize the expression of operons encoding the cytochrome *bc₁-aa₃* supercomplex by repressing *sigC* expression.

RESULTS

Genome-wide profiling of HrrA promoter occupancy

In previous studies, a number of direct target operons were described in *C. glutamicum* and *C. diphtheriae*, emphasizing the important role of the HrrSA TCS in the control of heme homeostasis (17-20). In this study, we investigated the genome-wide binding profile of HrrA by chromatin affinity purification of twin-Strep-tagged HrrA combined with DNA sequencing (ChAP-Seq). A series of preceding experiments revealed that plasmid-based expression of *hrrA* is required for the envisaged analysis, as, for instance, several known HrrA targets were obscured when *hrrA* was expressed only from one genomic copy. For this purpose, *C. glutamicum* ATCC 13032 lacking both heme-dependent TCSs ($\Delta hrrSA \Delta chrSA$) was transformed with a plasmid encoding the particular systems under the control of their native promoters (pJC1_ *P_{hrrSA}-hrrSA-twin-strep_P_{chrSA}-chrSA-his*). To obtain insights into the stimulus-dependent DNA association and dissociation, *C. glutamicum* cells starved of iron (see Material and Methods) were grown in iron-depleted glucose minimal medium, and samples were obtained before (T_0) and 0.5, 2, 4, 9 and 24 h after the addition of 4 μM hemin. HrrA was purified, and the bound DNA fragments were sequenced (Figure 1A).

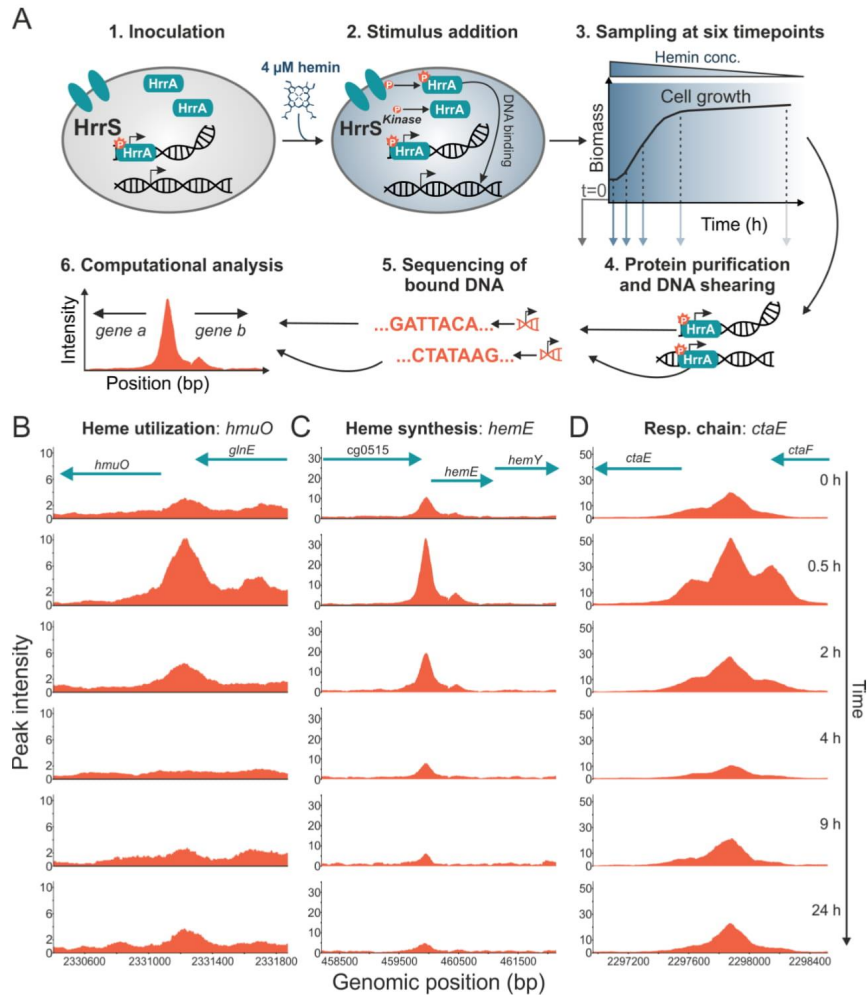


Figure 1: Genome-wide profiling of HrrA binding in response to addition of external heme. (A) ChAP-Seq analysis on the *C. glutamicum* strain $\Delta hrrSA\Delta chrSA$ (pJC1- P_{hrrSA} -*hrrSA*-*twin-strep*- P_{chrSA} -*chrSA*-*his*) grown in iron-depleted glucose minimal medium before and after addition of 4 μ M hemin. The experimental approach is briefly depicted: Cells were harvested at different time points, twin-Strep tagged HrrA was purified and co-purified DNA was sequenced to identify HrrA genomic targets. This approach resulted in the identification of more than 250 genomic regions bound by HrrA upon addition of hemin after 30 minutes. Exemplarily shown is the HrrA binding to regions upstream of operons involved in (B) heme degradation (*hmuO*), (C) heme biosynthesis (*hemE*) and (D) the respiratory chain (*ctaE*).

We obtained substantial enrichment of known HrrA targets in response to heme (e.g., 10-fold *hmuO*, 33-fold *hemE*, 52-fold *ctaE*; Figure 1B, C, D, respectively) and identified more than 250 previously unknown HrrA-binding sites in the *C. glutamicum* genome (Table S3).

As expected, the highest number of peaks was identified at the first time point after the heme pulse (0.5 h), with 272 peaks meeting our applied threshold (peak maximal coverage >3-fold average genomic coverage and a distance of <700 bp to the next translational start site). In comparison, 79 peaks were identified before hemin addition (T_0). These data illustrate the fast and transient DNA binding by HrrA in response to heme. It has to be noted, that the membrane embedded HrrS sensor kinase is also activated by endogenously synthesized heme (Figure S1 and (21)) and that the addition of external heme led to a boost of the HrrSA response. In general, the majority of the discovered HrrA binding sites were close to gene start sites (Figure S2). The binding of HrrA to 11 selected targets was confirmed by electrophoretic mobility shift assays (Figure S3), and a weak palindromic binding motif was deduced from the tested DNA fragments (Figure S4).

The HrrA binding patterns depicted in Figure 1B-D are representative of many bound regions. Thirty minutes after the heme pulse, the average peak intensities increased approximately 4.5-fold in comparison to those at T_0 (Figure 2A). After 2 h of cultivation in hemin, the average peak intensity dropped 2.6-fold in comparison to that of the sample taken after 30 minutes, further decreasing for the sample taken after 4 h (7.1-fold decrease). In our approach, the HrrA peaks reached a minimum after 9 h of cultivation (Figure 2). This dissociation of HrrA from its target promoters is caused by rapid depletion of heme, which was confirmed by spectroscopy of *C. glutamicum* cells (Figure 2A, dashed line) and was also obvious upon visual inspection (Figure S5). However, a slight increase in HrrA DNA binding was noted for cells in the stationary phase, which was likely triggered by the intrinsic heme pool and DtxR derepression of the *hrrA* gene when iron sources become limiting (34) (Figure 2A and D). Of all peaks, that passed our threshold, 128 were upstream of uncharacterized genes, while 144 could be assigned to genes with known or predicted function (Figure 2B).

A relatively high correlation between peak intensities for the time points 0, 0.5, 2 and 4 h (Figure 2C) showed that, while the strength of HrrA binding changed in response to heme availability, the system reacted proportionally for a majority of the binding sites. As expected, the binding at 9 h exhibited the lowest correlation to other time points (Figure 2C). This sample was obtained during the early stationary phase and the low correlation of HrrA peak intensities demonstrated overrelaxation and rewiring of the regulatory network. Here, interference with other regulators likely contributed to the significant changes in the HrrA binding pattern.

The HrrSA TCS shapes heme homeostasis by integrating the response to oxidative stress and cell envelope remodeling

Our dataset confirmed the binding of HrrA to all the targets identified thus far. HrrA was found to bind to the upstream promoter region of genes encoding components of heme biosynthesis (*hemE*, *hemH* and *hemA*), degradation (*hmuO*), and export (*hrtBA*) pathways and heme-containing complexes of the respiratory chain (*ctaE-qcrCAB* operon and *ctaD*). A comprehensive overview of all identified HrrA targets is presented in a separate, supplementary file (Table S3); selected target genes are listed in Table 1. Among the more than 250 novel targets identified in this study, we observed HrrA binding upstream of *ctaB*, which encodes a protoheme IX farnesyltransferase that catalyzes the conversion of heme *b* to heme *o* (24) and upstream of *ctaC*, which encodes subunit 2 of the cytochrome aa_3 oxidase. Remarkably, HrrA binding was also observed upstream of the *cydABDC* operon, which encodes the cytochrome *bd* oxidase of the respiratory chain. Altogether, this set of target genes highlights the global role of the HrrSA system in heme-dependent coordination of both branches of the respiratory chain. The HrrA regulon appeared to cover also the aspect of cofactor supply for the respiratory chain, as several HrrA targets encode enzymes involved in menaquinone biosynthesis (*menA*, *menD*, and *menG*) and reduction (*sdhCD*, *lldD* and *lld*).

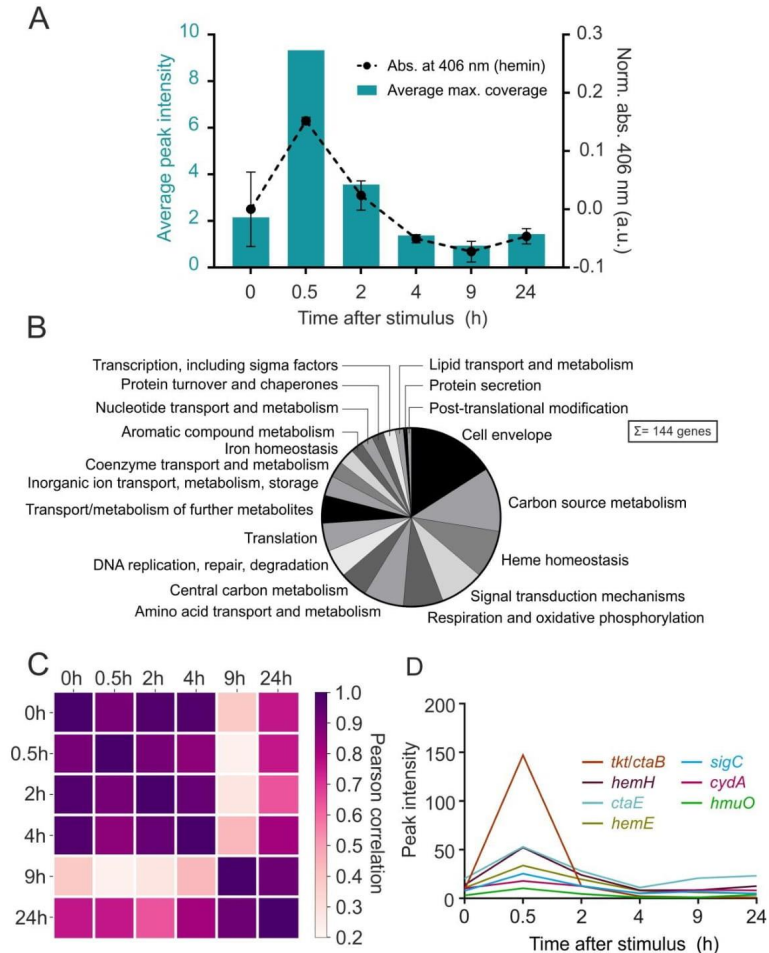


Figure 2: ChAP-Seq analysis revealed HrrA to be a global regulator of heme homeostasis in *C. glutamicum*. (A) HrrA binding in response to the addition of hemin. The bar plot reflects the average peak intensities among detected peaks in ChAP-Seq experiments (peak maximal coverage > 3-fold average genomic coverage and a distance of < 700 bp to the next gene start site). The binding was correlated with the amount of cell-associated hemin (dashed line), measured at corresponding time points by spectroscopy as described in *Material and Methods*. (B) Pie chart presenting the functional categories of HrrA targets (total of 272 genes, among which, 128 encode proteins of unknown function, e.g., several genes of the CGP3 prophage). For a complete overview of HrrA targets, see Table S3. (C) For each peak that passed the threshold (peak maximal coverage > 3-fold average genomic coverage and a distance of < 700 bp to the next ORF start site (TLS)) at time point A, the highest peak in the same region (± 50 nucleotides from the center of the peak) was selected for time point B and *vice versa*. Thus 'paired' peaks for these two time points were obtained, and the Pearson correlation of the intensities of all paired peaks was calculated for all six time points. (D) Peak intensities of selected HrrA targets over time, as identified by ChAP-Seq.

Table 1: Selected target genes of HrrA. Shown are the locus tag (cg number), the gene name and annotation together with a) the distance of the HrrA binding peak, identified via ChAP-Seq, to the start codon (translational start site, TLS) and b) the corresponding peak intensity (*indicate regions on the pJC1_P_{hrrSA}-hrrSA-twin-strep_P_{chrSA}-chrSA-his plasmid), c) relative ratios of the transcript levels in the Δ hrrA deletion mutant compared to wild type (\log_2 fold change). The values are derived from a comparison between the two strains 0.5 h after hemin addition (in brackets are fold change values after 4 h for Δ hrrA/wt). The $\log_2(\Delta$ hrrA/wt) value was not determined for the *hrrA* gene (n.d.).

Locus tag	Gene name	Annotation	Dist. TLS ^a	Peak intensity ^b	$\log_2(\Delta$ hrrA/wt) ^c RNA-Seq
Heme homeostasis/metabolism					
cg2445	<i>hmuO</i>	heme oxygenase	150	10.4	-3.1
cg0516	<i>hemE</i>	uroporphyrinogen decarboxylase	60	33.7	3.1
cg0497	<i>hemA</i>	glutamyl-tRNA reductase	26	25.8	0.6 (1.0)
cg0517	<i>hemY</i>	protoporphyrinogen oxidase	642	6.4	2.8
cg3156	<i>htaD</i>	secreted heme transport-associated protein	151	17.3	-0.3
cg3118	<i>cysl</i>	sulfite reductase hemoprotein	498	3.7	-0.7 (3.1)
cg1734	<i>hemH</i>	ferrochelatase	16	52.9	4.0
cg3247	<i>hrrA</i>	Heme-dependent response regulator	108	*	n.d.
cg2201	<i>chrS</i>	heme-dependent histidine kinase (<i>chrSA</i> operon)	32	*	-0.4
cg2202	<i>hrtB</i>	heme exporter (<i>hrtBA</i> operon)	78	*	-1.0
Respiratory chain					
cg2406	<i>ctaE</i>	cytochrome aa ₃ oxidase, subunit 3	324	52.9	-1.7
cg2780	<i>ctaD</i>	cytochrome aa ₃ oxidase, subunit 1	314	21.8	-1.1
cg1301	<i>cydA</i>	cytochrome bd oxidase	177	17.9	-0.7 (-2.6)
cg2409	<i>ctaC</i>	cytochrome aa ₃ oxidase, subunit 2	259	16.1	-1.4
cg0645	<i>creJ</i>	part of a putative cytochrome P450 system	678	5.1	-0.1 (-1.3)
cg1773	<i>ctaB</i> (<i>tkf</i>)	protoheme IX farnesyltransferase	204	147.0	0.4 (-1.4)
cg2403	<i>qcrB</i>	cytochrome bc ₁ complex, cytochrome b subunit	221	4.8	-1.8
cg3226		L-lactate permease, operon with <i>lldD</i>	622	5.5	-1.7
cg0309	<i>sigC</i> (<i>katA</i>)	RNA polymerase σ factor	38	25.4	2.1
Signal transduction					
cg3315	<i>malR</i>	transcriptional regulator, MarR-family	91	5.2	1.1
cg0444	<i>ramB</i>	transcriptional regulator, involved in acetate metabolism	224	26.7	-0.7
cg2831	<i>ramA</i>	transcriptional regulator, acetate metabolism, LuxR-family	42	5.0	-0.5
cg2103	<i>dtxR</i>	master regulator of iron-dependent gene expression	579	3.3	-0.4
Oxidative stress					
cg3422	<i>trxB</i>	thioredoxin reductase	5	5.8	-0.8
cg2078	<i>msrB</i>	peptide methionine sulfoxide reductase-related protein	282	3.0	-0.7
cg2867	<i>mpx</i>	mycothiol peroxidase, GSH peroxidase-family	56	5.6	-1.5

cg0310	<i>katA</i> (<i>sigC</i>)	catalase	???	25.4	-0.7 (-1.2)
cg1774	<i>tkt</i> (<i>ctaB</i>)	transketolase	16	147.0	0.0
cg1791	<i>gapA</i>	glyceraldehyde-3-phos. dehydrogenase,	287	4.4	-0.3
cg1069	<i>gapB</i>	glycolysis glyceraldehyde-3-phos. dehydrogenase, gluconeogenesis	284	3.5	1.6
Cell envelope					
cg3323	<i>ino1</i>	D-myo-inositol-1-phosphate synthase	156	7.6	1.7
cg0337	<i>whcA</i>	negative role in SigH-mediated oxidative stress response	125	6.4	-0.5
cg2747	<i>mepA</i>	putative cell wall peptidase	69	4.1	-0.2 (-1.4)
cg0061	<i>rodA</i>	putative FTSW/RODA/SPOVE-family cell cycle protein	389	8.7	-1.1
cg0306	<i>lysC</i>	aspartate kinase	40	12.2	0.7
cg2373	<i>murF</i>	D-alanine:D-alanine-adding enzyme	133	23.1	-0.2
cg0423	<i>murB</i>	UDP-N-acetylenolpyruvoylglucosamine reductase	2	18.7	-0.3

Remarkably, HrrA binding was also observed upstream of *gapA* (glyceraldehyde-3-phosphate dehydrogenase) and *tkt* (transketolase), encoding enzymes involved in the central metabolism and previously described as important hubs in the cellular response to oxidative stress (35). However, due to the binding of HrrA in the intergenic region of *tkt* and the divergently encoded *ctaB*, as described earlier, no further regulatory function could be ascertained (Figure S6). Additional genes involved in the oxidative stress response were identified, including *trxB* (thioredoxin reductase (36)), *mpx* (mycothiol peroxidase), *tusG* (trehalose uptake system (37)) and *msrB* (methionine sulfoxide reductase (38)). These findings suggest that the HrrSA system not only controls heme biosynthesis and degradation but also integrates the response to heme-induced oxidative stress.

A further important class of HrrA targets is represented by genes associated with the regulation or maintenance of the *C. glutamicum* cell envelope. The gene products of these previously unknown HrrA targets are, for instance, involved in the synthesis of peptidoglycan (*murA*, *murB*, *murF*), lysine (*lysI*, *lysA*, *lysC*), the peptidoglycan precursor meso-2,6-diaminopimelate (mDAP), inositol-derived lipids (*ino1*) and arabinogalactan (*aftC*). HrrA also exhibited binding to the promoter region of *malR*, which encodes a global regulator involved in stress-responsive cell envelope remodeling (Hünnefeld & Frunzke, manuscript submitted). In addition to *malR*, other genes encoding global transcriptional regulators

(e.g., *ramA*, *ramB*, *amtR* and *dtxR*) were identified as direct HrrA targets, adding a further level of complexity to this systemic response to heme.

Temporal dynamics of promoter occupancy reveal hierarchy in the HrrA regulon

With this time-resolved and genome-wide analysis of HrrA binding, we were also able to visualize distinct binding patterns of HrrA in response to addition and depletion of stimulus. Consequently, we asked whether the binding patterns (ChAP-Seq coverage) could provide information regarding the dissociation constant (K_d) of HrrA to specific genomic targets. We compared the *in vivo* binding patterns of *ctaE*, *cydAB* and *hmuO* (Figure 1). While a constitutively high peak was observed upstream of the *ctaE* promoter, the relative increase upon the addition of exogenous heme was smaller than that observed for other targets (Figure 1D). In contrast, binding to the promoter of *hmuO* occurred with apparently high stimulus dependency and appeared to be very transient, as HrrA was fully dissociated from this promoter 4 h after the addition of hemin (Figure 1B). The addition of heme also resulted in the appearance of secondary binding sites in the *ctaE*, *cydAB* and *hmuO* upstream promoter regions, providing evidence for cooperative binding and/or DNA loop formation in response to high heme levels. In general, we found that genes that were not bound or only moderately bound before the addition of a stimulus generally exhibited higher fold increases in coverage than constitutively bound targets (Figure S7).

Subsequently, we determined the *in vitro* affinity of phosphorylated HrrA to the promoter regions of *ctaE*, *cydAB* and *hmuO* (Table 2, Figure S8). Consistent with the ChAP-Seq data, we measured the highest affinity of HrrA to P_{ctaE} with an apparent K_d of 0.10 μ M (\pm 0.003). We therefore hypothesize that the *ctaE* promoter is a prime target that is constitutively activated by HrrA to maintain high gene expression of the operon encoding the *bc₁-aa₃* supercomplex. In contrast, we measured an almost 3-fold lower apparent K_d for P_{cydAB} , which was consistent with the relatively transient binding pattern observed for this target. With an apparent K_d of 0.19 μ M, the *in vitro* binding affinity of HrrA to the *hmuO* promoter was rather high considering the genomic coverage measured in the ChAP-Seq analysis. However, *in vitro* analysis does not account for the widespread

interference among regulatory networks *in vivo*. In the particular example of *hmuO*, the pattern of HrrA binding was likely the result of interference with the global regulator of iron homeostasis, DtxR, which has been previously described to repress *hmuO* expression by binding to adjacent sites (34). Taken together, these results show that *in vivo* promoter occupancy is not only influenced by the binding affinity of the regulator to the particular target, but also significantly shaped by internetwork interference. Consequently, high *in vivo* promoter occupancy indicates high binding affinity, but conclusions based on weakly bound regions may be confounded by competition with other binding factors.

Table 2: Apparent K_d values of HrrA to the promoters of *hmuO*, *ctaE*, *sigC* and *cydA*. The affinity of phosphorylated HrrA to the indicated regions was measured using purified protein in increasing concentrations and its ability to shift 15 nM DNA fragments covering 250 bp up- and downstream of the maximal ChAP-Seq peak height (for detailed information, see Figure S8).

Promoter	Function	Apparent K_d (μ M)	Peak intensity after hemin addition (ChAP-Seq)
P_{hmuO}	Heme oxygenase	0.19 \pm 0.013	10.4
P_{ctaE}	Cytochrome <i>aa₃</i> oxidase	0.10 \pm 0.003	52.9
P_{sigC}	ECF sigma factor σ^C	0.27 \pm 0.012	25.4
P_{cydA}	Cytochrome <i>bd</i> oxidase	0.26 \pm 0.007	17.9

Subsequently, we determined the *in vitro* affinity of phosphorylated HrrA to the promoter regions of *ctaE*, *cydAB* and *hmuO* (Table 2, Figure S8). Consistent with the ChAP-Seq data, we measured the highest affinity of HrrA to P_{ctaE} with an apparent K_d of 0.10 μ M (\pm 0.003). We therefore hypothesize that the *ctaE* promoter is a prime target that is constitutively activated by HrrA to maintain high gene expression of the operon encoding the *bc₁-aa₃* supercomplex. In contrast, we measured an almost 3-fold lower apparent K_d for P_{cydAB} , which was consistent with the relatively transient binding pattern observed for this target. With an apparent K_d of 0.19 μ M, the *in vitro* binding affinity of HrrA to the *hmuO* promoter was rather high considering the genomic coverage measured in the ChAP-Seq analysis. However, *in vitro* analysis does not account for the widespread

interference among regulatory networks *in vivo*. In the particular example of *hmuO*, the pattern of HrrA binding was likely the result of interference with the global regulator of iron homeostasis, DtxR, which has been previously described to repress *hmuO* expression by binding to adjacent sites (34). Taken together, these results show that *in vivo* promoter occupancy is not only influenced by the binding affinity of the regulator to the particular target, but also significantly shaped by internetwork interference. Consequently, high *in vivo* promoter occupancy indicates high binding affinity, but conclusions based on weakly bound regions may be confounded by competition with other binding factors.

HrrA activates the expression of genes encoding components of both branches of the quinol oxidation pathway

To evaluate how HrrA binding impacts the expression of individual target genes, we analyzed the transcriptome (RNA-Seq) of the *C. glutamicum* wild type strain (ATCC 13032) as well as a Δ *hrrA* mutant.

Analogous to the ChAP-Seq experiments, RNA-Seq analysis was performed prior to the addition of heme (T_0) and 0.5 and 4 h after the heme pulse (in medium containing no other iron source).

At T_0 , before the addition of heme, already 158 genes showed a more than 2-fold altered expression level in wild type cells compared to $\Delta hrrA$ cells ($\Delta hrrA/wt$). In contrast, directly after the addition of stimulus, the expression of 274 of the significantly affected genes (Figure 3A, orange dots) changed more than 2-fold. Of these genes, 120 were upregulated and 154 were downregulated in the $hrrA$ deletion strain. 4 h after addition of heme, only 118 genes exhibited a greater than 2-fold increase or decrease (scatter plots for additional time points are presented in Figure S9).

The $hrrA$ expression decreased after 0.5 h upon the addition of heme, which was likely caused by DtxR repression in response to increased intracellular iron levels (Figure 3B). In contrast, after 4 h of cultivation, $hrrA$ levels significantly increased, reflecting the depletion of heme as an alternative iron source and dissociation of DtxR. Furthermore, differential gene expression analysis revealed HrrA to be an activator of all genes encoding components of the respiratory chain ($ctaE$, $ctaD$, $ctaF$ and $cydA$) and as a repressor of heme biosynthesis ($hemA$, $hemE$ and $hemH$) (Figure 3C)

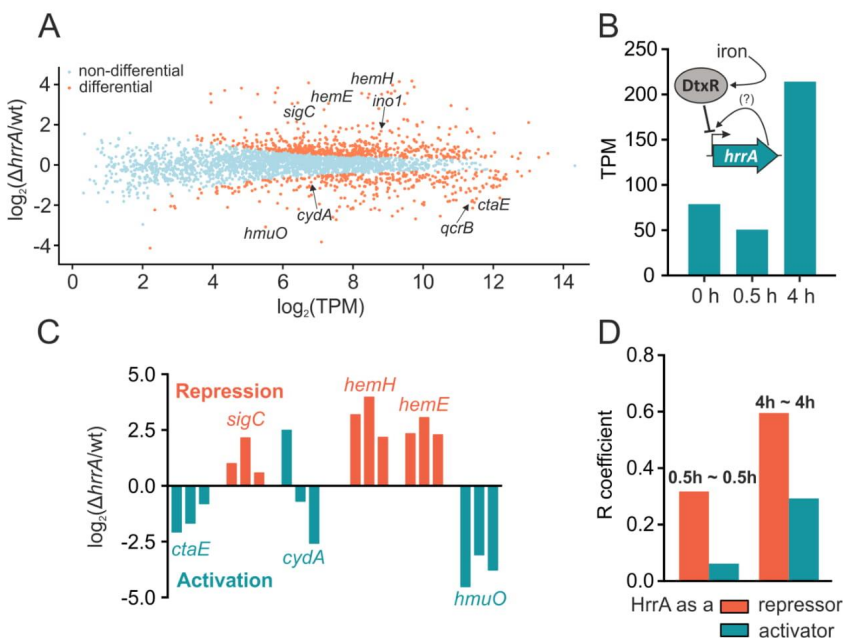


Figure 3: Differential gene expression analysis of wild type *C. glutamicum* and a $\Delta hrrA$ mutant.

(A) Differential gene expression analysis (RNA-Seq) revealed 120 upregulated and 154 downregulated genes in the $hrrA$ deletion strain compared to the wild type (in transcripts per million, TPM) after 30 minutes of cultivation in iron-depleted glucose minimal medium containing 4 μM heme. (B) Expression levels of $hrrA$ (TPM) 0, 0.5 and 4 h after the addition of hemin. A scheme depicts HrrA autoregulation and iron-dependent DtxR repression. (C) Impact of $hrrA$ deletion on the transcript levels of six selected target genes at three different time points (0 h, 0.5 h, 4 h); orange: HrrA acts as a repressor, turquoise: HrrA acts as an activator. (D) ChAP-Seq and RNA-Seq experiments demonstrate higher correlation of ChAP-Seq peak intensities and impact on gene expression (RNA-Seq, $\Delta hrrA/wt$) for targets where HrrA functions as a repressor instead of an activator.

Additionally, *lldD*, encoding a lactate dehydrogenase contributing to the reduced menaquinone pool, was downregulated more than three-fold upon deletion of *hrrA*. Remarkably, we identified HrrA as a repressor of *sigC*, encoding an ECF involved in the control of the branched respiratory chain in response to cytochrome *aa₃* deficiency (32). In addition to the considerable differences between the wild type and the $\Delta hrrA$ mutant, we also observed slightly decreased mRNA levels of genes involved in the oxidative stress response (e.g., *mpx*, mycothiol peroxidase) or cell envelope remodeling (e.g., *malR*, *murB*) in the $\Delta hrrA$ mutant, suggesting HrrA to be an activator of these targets. In many cases, promoter occupancy by HrrA did not result in altered expression levels of the particular target gene (e.g., genes involved in peptidoglycan biosynthesis or the transketolase *tkf*) in a $\Delta hrrA$ mutant under the tested conditions (Table 1). This finding is, however, not surprising considering the multiplicity of signals and regulators affecting gene expression under changing environmental conditions.

Correlation between promoter occupancy and differential gene expression is higher for repressed targets

In nature, all relevant stimuli for a specific gene act as inputs, and therefore, the output and adaptation of gene expression is affected by a multitude of parameters. We examined how HrrA binding (ChAP-Seq) translates to changes in expression of target genes (RNA-Seq) and found that binding and differential gene expression exhibit significantly higher correlation for repressed targets than for genes activated by HrrA (Figure 3B). This phenomenon can be attributed to a generally high hierarchical position of repressors and can be demonstrated for the transcriptional control of the heme oxygenase HmuO. While HrrA binds to P_{hmuO} directly after addition of the stimulus, the iron-dependent regulator DtxR also binds to this promoter and represses *hmuO*. As a result, HrrA binding does not instantly translate to increased expression but is delayed until DtxR dissociates (see Figure S10 for mRNA levels of *hmuO* in wild type and $\Delta hrrA$ cells). In cases where HrrA represses expression, such as of *hemE/hemY*, binding is apparently enough for heme-dependent inhibition, just as DtxR-mediated repression of *hmuO* overwrites the activation of this gene by HrrA.

HrrA determines the prioritization of terminal cytochrome oxidases by repression of *sigC*

The results from ChAP-Seq and RNA-Seq experiments highlight the important role of HrrA in the control of the respiratory chain, including cofactor supply. Our data revealed that HrrA activates the expression of genes encoding the cytochrome *bc₁-aa₃* supercomplex (*ctaE-qcrCAB*, *ctaD*, *ctaFC*, Figure 4) and of *cydAB*, encoding the cytochrome *bd* branch of the respiratory chain. In both cases, multiple HrrA peaks were identified in ChAP-Seq experiments; however, the association of these multiple peaks with the control of particular target operons remains to be studied. Remarkably, the mRNA profiles of the corresponding operons exhibited significantly delayed activation of *cydAB* in response to heme, which was abolished in the $\Delta hrrA$ mutant (Figure 4). In contrast, *ctaE* expression was significantly higher in wild type cells, even before heme addition (T_0), and reaches a plateau 30 minutes after stimulus addition. In this context, notably, we also observed binding of HrrA upstream of *sigC*, which encodes an extracytoplasmic sigma factor that was shown to be involved in the activation of the *cydAB* operon (32). The mRNA level of *sigC* increased more than two-fold in the $\Delta hrrA$ mutant, indicating HrrA to be a repressor of this gene (Figure 4). Consistent with this hypothesis, *sigC* expression was slightly decreased in response to the addition of heme, which correlated with increased HrrA peak intensity (Figure 4E). Additionally, the higher *cydAB* expression, observed in the $\Delta hrrA$ strain before addition of stimulus (Figure 4C) is likely a byproduct of increased *sigC* expression (Figure 4B) and the subsequent σ^C activation of the *cydAB* operon in the same strain. Dissociation of HrrA from P_{sigC} at a later time point (4 h after heme pulse) led to derepression of *sigC* and concomitantly increased expression of *cydAB* in the wild type. Because *cydAB* levels were constitutively low in the $\Delta hrrA$ mutant in response to heme, we hypothesized that activation by HrrA together with an additional boost by SigC (Figure 5) leads to delayed activation of *cydAB* after the heme pulse. Thus, the cells were able to channel most of the available heme pool into the more efficient cytochrome *bc₁-aa₃* supercomplex. The lower apparent K_d of HrrA for the *ctaE* promoter (0.1 μ M) than for P_{cydAB} (0.26 μ M) or P_{sigC} (0.27 μ M) also reflects this prioritization of HrrA targets. Consequently, this almost 3-fold decrease in affinity (apparent K_d) increases the threshold for HrrSA activity to control these targets.

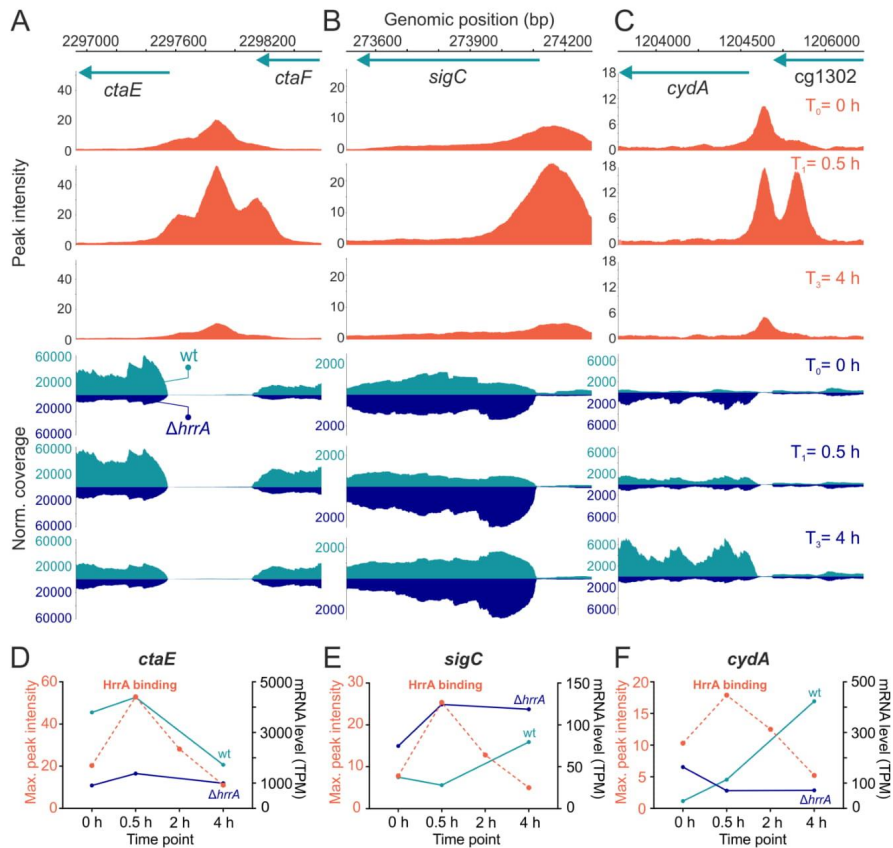


Figure 4: HrrA prioritizes the expression of genes encoding components of the bc_1 - a_3 supercomplex. Depicted are HrrA binding peaks as identified by ChAP-Seq analysis (Figure 1 and 2) in comparison to the normalized coverage of RNA-Seq results (wild type and the $\Delta hrrA$ mutant) for the genomic loci of *ctaE* (A, D), *sigC* (B, E) and *cydA* (C, F). D-F: HrrA binding (max. peak intensities measured by ChAP-Seq experiments) and the mRNA levels (in transcripts per million, TPM) of the respective genes in the $\Delta hrrA$ strain as well as in wild type *C. glutamicum* cells 0, 0.5 and 4 h after the addition of hemin.

DISCUSSION

In this study, we used a genome-wide approach to identify more than 250 genomic target regions of the “heme-responsive regulator” HrrA in *C. glutamicum*. This intriguingly diverse set of target genes, encoding

enzymes involved in heme biosynthesis, heme-containing proteins, components of the respiratory chain, oxidative stress response proteins and proteins involved in cell envelope remodeling, provided unprecedented insight into the systemic response to heme coordinated by the TCS HrrSA.

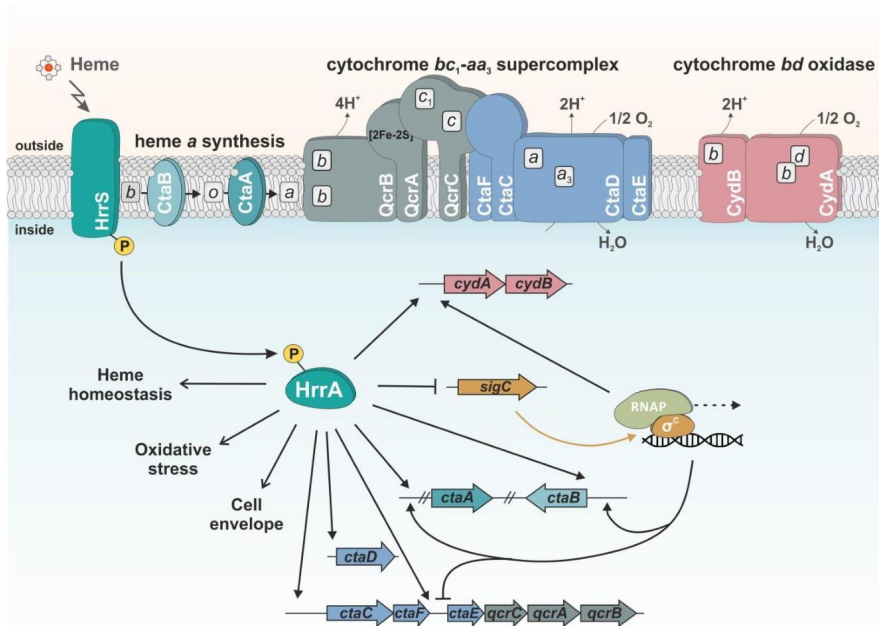


Figure 5: Model of heme-responsive control of components of the respiratory chain by HrrSA. The results of this study reveal HrrSA as a global regulator of heme homeostasis coordinating the expression of genes involved in heme biosynthesis, oxidative stress responses and cell envelope remodeling. An important part of the HrrA regulon is comprised by genes encoding the components of the branched respiratory chain of *C. glutamicum*. While HrrA acts as an activator of all components (*ctaE-qcrCAB*, *ctaA*, *ctaB*, *cydAB*), it represses transcription of the *sigC* gene encoding an important sigma factor required for *cydAB* expression. This regulatory network architecture consequently confers prioritization to the synthesis of the more efficient proton pump, the cytochrome bc₁-aa₃ supercomplex. Bordered boxes, b, c, a, d: heme b, heme c, heme a, heme d.

In Gram-positive bacteria, TCSs appear to play a central role in transient heme sensing, and heme-responsive systems have been described in several prominent pathogens, including *C. diphtheriae*, *S. aureus* and *B. anthracis* (15-18). For all prokaryotic heme regulatory systems, however, only a small number of target genes have been described to date, focusing on targets involved in degradation (*hmuO* (18, 39)), heme export (*hrtBA* (19, 40)) or heme biosynthesis (*hema* (18, 20)). Systems orthologous to HrrSA are found in almost all corynebacterial species, and the high amino acid sequence identity shared by response regulators (87 %, between *C. glutamicum* and *C. diphtheriae* HrrA, Figure S11) suggests that

the important role of HrrSA in the control of heme homeostasis is conserved.

Coping with heme stress

While being an essential cofactor for many proteins, heme causes severe toxicity to cells at high levels (4). In mammalian cells, the BACH1 regulator is inactivated by heme binding and plays a key role in maintaining the balance of the cellular heme pool (8, 41). Heme oxygenases are targets of various heme-dependent regulators (18, 42, 43), and consistent with this principle, the mammalian *HMOX1* gene, encoding an NADPH-dependent oxygenase, is regulated by BACH1 (41). Other identified BACH1 targets are involved in redox regulation, the cell cycle, and

apoptosis as well as subcellular transport processes (9), and the regulon includes genes encoding thioredoxin reductase 1, the iron storage protein ferritin (44) and NAD(P)H menadione oxidoreductase 1 (45).

Although neither the regulator nor the constitution of the regulon is conserved, the responses of BACH1 and HrrSA share a similar logic. Analogous to eukaryotic BACH1, we observed HrrA-mediated activation of *trxB* (thioredoxin reductase), *mpx* (mycothiol peroxidase), and *katA* (catalase), which appear to be required to counteract oxidative stress caused by elevated heme levels. Additionally, HrrA binds to the intergenic region between the divergent genes *ctaB* and *tkt*, the latter encoding a transketolase. While BACH1 has previously exhibited regulation of a transketolase (*TKT*) (9), the effect of HrrA on the expression of *tkt* could not be conclusively determined in this study (see Table 2). Notably, however, transketolase, an important enzyme of the nonoxidative part of the pentose phosphate pathway (PPP), was recently shown to be required for cancer cell growth, helping the cells meet the high demand for NADPH (35).

Remarkably, HrrA binding was also observed upstream of both *gapA* and *gapB*, which encode glyceraldehyde-3-phosphate dehydrogenases (GapDHs) and are involved in glycolysis and gluconeogenesis, respectively. Previous studies have revealed that oxidative stress may block glycolysis by inhibiting glyceraldehyde-3-phosphate dehydrogenase (GapDH) in baker's yeast and mammalian cells (46, 47). Furthermore, GapDH of *C. diphtheriae* was recently shown to be redox-controlled by S-mycothiolation (48). Slight activation of *gapA* by HrrA may thus counteract an impaired glycolytic flux under conditions of heme stress.

Furthermore, several HrrA targets play a role in the biosynthesis and remodeling of the corynebacterial cell envelope, including *mepA* (a putative cell wall peptidase (49)); *ino1*, which is required for the synthesis of inositol-derived lipids (50); and *malR*, encoding a MarR-type regulator that is possibly involved in stress-responsive cell envelope remodeling (Hünnefeld & Frunzke, manuscript submitted). Taken together, these insights emphasize the important role of the HrrSA system in the control of heme stress responses.

Coordinated control of the respiratory chain

Among the most significantly affected targets in the Δ *hrrA* mutant were many genes encoding components of the respiratory chain (24), including all the genes constituting the cytochrome *bc₁-aa₃* branch of the respiratory chain (*ctaE-qcrCAB*, *ctaCF* and *ctaD*) (51); genes encoding the cytochrome *bd* branch (*cydAB* (24)); *ctaA* (52) and *ctaB* (53), encoding enzymes responsible for heme *a* synthesis; and *lldD* and *dld*, encoding lactate dehydrogenases that contribute to the reduced menaquinone pool (24).

In a recent study, Toyoda and Inui described the ECF sigma factor σ^C to be an important regulator of both branches of the *C. glutamicum* respiratory chain. The *ctaE-qcrCAB* operon was shown to be significantly downregulated after σ^C overexpression due to binding of the sigma factor to the antisense strand of the promoter (32). Here, we demonstrated that this repression is counteracted by HrrA, which not only represses *sigC* but also activates *ctaE-qcrCAB* expression. While the two proteins have antagonistic effects on the expression of the supercomplex, both σ^C and HrrA positively regulate the *cyd* operon, encoding the cytochrome *bd* branch of the respiratory chain (Figure 5).

Interestingly, a hierarchy in the regulon was reflected by the differences in the apparent K_d values of HrrA with P_{cydA} and P_{sigC} , which were two-fold lower than those with the promoter of *ctaE*. These findings were also consistent with the ChAP-Seq experiments, where the peaks upstream of *ctaE* and *ctaB* were among the highest peaks at T_0 and after 0.5 h (Figure 4A). These data suggest that under conditions of sufficient heme supply, production of the cytochrome *bc₁-aa₃* supercomplex is preferred, which is highly effective but requires the incorporation of six heme cofactors. Repression of *sigC* by HrrA and the relatively low affinity to the *cydAB* promoter results in delayed production of the *bd* branch. At high cell densities (mid-exponential phase), available heme is thus first channeled to the cytochrome *bc₁-aa₃* supercomplex before the cytochrome *bd* oxidase is used, which is less efficient but has a higher oxygen affinity.

There is further overlap between the HrrA and σ^C regulons in the case of *ctaB*, which encodes a farnesyltransferase, catalyzing the conversion of heme *b* to heme *a*. Because both HrrA and σ^C positively regulate *ctaB*, the expression of this gene

parallels that of the *cyd* operon, exhibiting delayed induction (Figure S6) in response to heme. This phenomenon is counterintuitive because the conversion of heme *b* to heme *a* is needed to fulfill the heme *a* requirement of the *bc₁-aa₃* supercomplex. In general, only a few studies have examined the transcriptional regulation of heme *a* synthesis in prokaryotes. In *B. subtilis*, *ctaA* and *ctaB* are regulated by the ResDE TCS in an oxygen-dependent but heme-independent manner (54). Furthermore, upon production of CtaA and CtaB of *B. subtilis* in *Escherichia coli*, the *in vivo* formation of a physiologically relevant complex was suggested that efficiently catalyzed the heme *b* to heme *a* conversion with heme *o* as intermediate (55). In *C. glutamicum*, further studies are needed to unravel the stoichiometry of this complex. For now, one can only speculate that cellular heme *a* stock is used to meet the initial cofactor demand of the *bc₁-aa₃* supercomplex. Subsequently, upregulation of the *ctaB-ctaA* synthesis pathway is needed to replenish these stores. This concept would foster a rapid response to potentially available external heme sources and may represent an important adaptive trait of pathogenic species.

Interference with other regulatory networks

Deletion of the *hrrA* gene led to more than 2-fold upregulation of 120 genes, while 154 genes were downregulated after the addition of heme. Several other genes were significantly affected but to a lesser extent. Remarkably, among the direct target genes controlled by HrrA, we identified several prominent global regulators, including the regulators of acetate metabolism *ramA* and *ramB* (56, 57); *malR*, which is involved in cell envelope remodeling (Hünnefeld & Frunzke, manuscript submitted); and *dtxR*, encoding the global iron-dependent regulator in corynebacterial species (34, 58). This finding is intriguing because it reveals the close association and reciprocal control between HrrA and DtxR. While DtxR represses *hrrA* transcription under conditions of sufficient iron supply (34), HrrA slightly upregulates *dtxR* expression (~1.5-fold) in response to heme.

Conclusion

Genome-wide analyses of targets controlled by prokaryotic transcription factors will change our view on many systems we believe to know. In this study, we provide an unprecedented insight into the systemic response to heme coordinated by the HrrSA TCS.

Given the many properties of this molecule, the complexity of this response is actually not surprising but paves the way for further functional analysis of HrrA targets with so far unknown functions.

MATERIALS AND METHODS

Bacterial strains and growth conditions

Bacterial strains used in this study are listed in Table S1. The *Corynebacterium glutamicum* strain ATCC 13032 was used as wild type (27) and cultivations were performed in liquid BHI (brain heart infusion, Difco BHI, BD, Heidelberg, Germany), as complex medium or CGXII (59) containing 2 % (w/v) glucose as minimal medium. The cells were cultivated at 30°C; if appropriate, 25 µg/ml kanamycin was added. *E. coli* (DH5α and BL21 (DE3)) was cultivated in Lysogeny Broth (Difco LB, BD, Heidelberg, Germany) medium at 37°C in a rotary shaker and for selection, 50 µg/ml kanamycin was added to the medium.

Recombinant DNA work and cloning techniques

Cloning and other molecular methods were performed according to standard protocols (60). As template, chromosomal DNA of *C. glutamicum* ATCC 13032 was used for PCR amplification of DNA fragments and was prepared as described previously (61). All sequencing and synthesis of oligonucleotides was performed by Eurofins Genomics (Ebersberg, Germany). For ChAP sequencing, the plasmid pJC1_ *P_{hrrSA}-hrrSA-twin-strep-P_{chrSA}-chrSA-his* was constructed after amplification of *hrrS-hrrA-twin-strep* and *chrS-chrA-his*, including promoter (500 bp upstream of the first gene) from stock plasmids, using the primers indicated in Table S2. The fragments were cloned into pJC1 using the created overhangs and Gibson assembly (62).

ChAP Sequencing – Sample preparation

The preparation of DNA for ChAP sequencing was adapted from (63). The *C. glutamicum* strain Δ *hrrSA*:*chrSA* was transformed with a plasmid carrying genes for both TCSs encoding tagged RRs (pJC1_ *P_{hrrSA}-hrrSA-twin-strep-P_{chrSA}-chrSA-his*). A preculture was inoculated in liquid BHI medium (25 µg/ml kanamycin) from a fresh BHI agar plate and incubated for 8-10 h at 30°C in a rotary shaker. After that, cells were transferred into a second preculture in CGXII medium containing 2 % (w/v) glucose and 0 µM FeSO₄ to starve the cells from iron. Protocatechuic acid (PCA), which was added to the medium, allowed the uptake of trace amounts of iron. From an overnight culture, six main cultures were inoculated to an OD₆₀₀ of 3.0 in 1 L CGXII medium containing 4 µM hemin as sole iron source. For the time point t=0, the cells were added to 1 L fresh CGXII containing no additional iron source. After 0 h, 0.5 h, 4 h, 9 h and 24 h, cells corresponding to an OD₆₀₀ of 3.5 in 1 L were harvested by centrifugation at 4 °C, 5000 x g and washed once in 20 ml CGXII. Subsequently, the cell pellet was resuspended in 20 ml CGXII containing 1 % (v/v) formaldehyde to crosslink the regulator protein to the DNA. After incubation for 20 min at RT, the cross linking was stopped by addition of glycine (125 mM), followed by an additional 5 minutes of incubation. After that, the cells were washed three times in buffer A (100

mM Tris-HCl, 1 mM EDTA, pH=8.0) and the pellets stored overnight at -80 °C. For cell disruption, the pellet was resuspended in buffer A containing "complete" protease inhibitor cocktail (Roche, Germany) and passed through a French pressure cell (SLM Aisco, Spectronic Instruments, Rochester, NY) five times at 207 MPa. The DNA was fragmented to ~500 bp by sonication (Branson Sonifier 250, Branson Ultrasonics Corporation, Connecticut, USA) and the supernatant was collected after ultra-centrifugation (150.000 x g, 4 °C, 1 h). The DNA-bound by the twin-Strep tagged HrrA protein was purified using Strep-Tactin XT Superflow column material (IBA Lifesciences, Göttingen, Germany) according to the supplier's manual (applying the gravity flow protocol, 1.5 ml column volume). Washing of the column was performed with buffer W (100 mM Tris-HCl, 1 mM EDTA, 150 mM NaCl, pH 8.0) and the tagged protein was eluted with buffer E (100 mM Tris-HCl, 1 mM EDTA, 150 mM NaCl, pH 8.0, added 50 mM D-Biotin). After purification, 1% (w/v) SDS was added to the elution fractions and the samples were incubated overnight at 65°C. For the digestion of protein, 400 µg/ml Proteinase K (AppliChem GmbH, Darmstadt, Germany) was added and incubated for 3 h at 55 °C. Subsequently, the DNA was purified as following: Roti-Phenol/Chloroform/Isoamyl alcohol (Carl Roth GmbH, Karlsruhe, Germany) was added to the samples in a 1:1 ratio and the organic phase was separated using Phase Lock Gel (PLG) tubes (VWR International GmbH, Darmstadt, Germany) according to the supplier's manual. Afterwards, the DNA was precipitated by adding ice cold ethanol (to a conc. of 70%) and centrifugation at 16.000xg, 4 °C for 10 min. The DNA was washed with ice cold 70% ethanol, then dried for 3 h at 50 °C and eluted in d₂O. The resulting DNA was used for library preparation and indexing using the TruSeq DNA PCR-free sample preparation kit (Illumina, California, USA) according to the manufacturer's instructions, only skipping fragmentation of the DNA. The resulting libraries were quantified using the KAPA library quant kit (Peqlab, Bonn, Germany) and normalized for pooling.

RNA Sequencing – Sample preparation

For RNA sequencing, *C. glutamicum* wild type and the \square *hrrA* mutant strain were cultivated under the same conditions as described for ChAP Sequencing. Both strains did not contain any plasmids and, hence, were cultivated without addition of antibiotics in biological duplicates. After 0 h (no heme), 0.5 h and 4 h, cells corresponding to an OD₆₀₀ of 3 in 0.1 L were harvested in falcon tubes filled with ice by centrifugation at 4 °C and 5000 x g for 10 minutes and the pellets were stored at -80 °C. For the preparation of the RNA, the pellets were resuspended in 800 µl RTL buffer (QIAGEN GmbH, Hilden, Germany) and the cells disrupted by 3 x 30 s silica bead beating, 6000 rpm (Precellys 24, VWR International GmbH, Darmstadt, Germany). After ultra-centrifugation (150.000 x g, 4 °C, 1 h), the RNA was purified using the RNeasy Mini Kit (QIAGEN GmbH, Hilden, Germany) according to the supplier's manual. Subsequently, the ribosomal RNA was removed by running twice the workflow of the RiboZero rRNA Removal Kit [Bacteria] (Illumina, California, USA) in succession. Between steps, the depletion of rRNA as well as the mRNA quality was analysed using the TapeStation 4200 (Agilent Technologies Inc, Santa Clara, USA). After removal of rRNA, the fragmentation of RNA, cDNA strand synthesis and indexing was carried out using the TruSeq Stranded mRNA Library Prep Kit

(Illumina, California, USA) according to the supplier's manual. Afterwards, the cDNA was purified using Agencourt AMPure XP magnetic beads (Beckman Coulter, Indianapolis, USA). The resulting libraries were quantified using the KAPA library quant kit (Peqlab, Bonn, Germany) and normalized for pooling.

Sequencing and sequence analysis

Pooled libraries were sequenced on a MiSeq (Illumina, California, USA) generating paired-end reads with a length of 2 x 75 bases. Data analysis and base calling were performed with the Illumina instrument software and stored as fastq output files. We then proceeded as follows:

ChAP-Seq analysis

The obtained DNA fragments of each sample (up to 2 µg) were used for library preparation and indexing using the TruSeq DNA PCR-free sample preparation kit according to the manufacturer's instruction, yet omitting the DNA size selection steps (Illumina, Chesterford, UK). The resulting libraries were quantified using the KAPA library quant kit (Peqlab, Bonn, Germany) and normalized for pooling. Sequencing of pooled libraries was performed on a MiSeq (Illumina) using paired-end sequencing with a read-length of 2 x 150 bases. Data analysis and base calling were accomplished with the Illumina instrument software and stored as fastq output files. The sequencing data obtained for each sample were imported into CLC Genomics Workbench (Version 9, Qiagen Aarhus A/S) for trimming and base quality filtering. The output was mapped to accession BX927147 as *C. glutamicum* reference genome (www.ncbi.nlm.nih.gov/pubmed/12948626). Genomic coverage was convoluted with second order Gaussian kernel. The kernel was truncated at 4 sigmas (that is all kernel values positioned further than 4 sigmas from the center were set to zero) and expanded to the "expected peak width". The expected peak width was estimated via the following procedure: 1) all the peaks higher than 3 mean coverage were detected 2) Points at which their coverage dropped below ½ of the maximal peak height were found and the distance between them was considered as a peak width 3) The "estimated peak width" was set equal to the median peak width. The convolution profile was scanned in order to find points where first derivative changes its sign from positive to negative (Figure S12). Each such point was considered as a potential peak and was assigned with a convolution score (that is convolution with second order Gaussian kernel centered at the peak position). Further we explored the distribution of the convolution scores. It appeared to resemble normal distribution, but with a heavy right tail. We assumed that this distribution is indeed bimodal of normal distribution (relatively low scores) representing 'noise' and a distribution of 'signal' (relatively high scores). We fit the Gaussian curve to the whole distribution (via `optimize.fit` function from SciPy package (64)) and set a score thresholds equal mean + 4 sigmas of the fitted distribution. Further filtering with this threshold provided estimated FDR (false discovery rate) of 0.004-0.013 depending on a sample. Filtered peaks were normalized to allow inter-sample comparisons. Sum of coverages of the detected peaks was negated from the total genomic coverage. The resulting difference was used as normalization coefficient; that is peak intensities were divided by this coefficient.

RNA-seq analysis

Sequencing reads quality was explored with the FastQC (65) tool. Since reads appeared to be of a good quality and didn't harbor significant fraction of adapters or overrepresented sequences, no preprocessing was undertaken. Identical reads were collapsed with a custom script in order to prevent gene levels' misquantification caused by PCR overamplification. Reads were mapped to the *C. glutamicum* genome (BX927147) with Bowtie2 (66). Bowtie2 was run with the following parameters: bowtie2 -1 [path to the reads, 1st mate] -2 [path to the reads, 2nd mate] -S [path to the mappings] -phred33 -sensitive-local -local -score-min C,90 -rdg 9,5 -rfg 9,5 -a -no-nal -l 40 -X 400 -no-mixed -ignorequals.

The reads mapped to multiple locations were split proportionally between parental genes. That is if 3 reads are mapped to gene A and gene B, expression of gene A is 10 and expression of gene B is 5, then 2 reads will go to gene A and 1 read to gene B. For each *C. glutamicum* gene (67) we assign an expression value equal to the average read coverage over the gene region. These expression values were then normalized to TPM (transcripts per million) values (68).

Furthermore, we analyzed which genes are significantly differentially expressed between conditions. We set combinatorial thresholds on normalized GEC (gene expression change) $[\log_2(\text{expr1} + \text{expr2}) / (\text{expr1} + \text{expr2})]$ and MGE (mean gene expression) $[\log_2((\text{expr1} + \text{expr2})/2)]$ where "expr1" is gene expression for the first condition and "expr2" for the second. Thresholds were set in a way to achieve maximal sensitivity while keeping FDR (false discovery rate) less than 0.05. FDR was estimated as $\text{GECintra} / (\text{GECintra} + \text{GECinter})$; where GECintra is a number of genes passed the thresholds based on intrasample GEC (that is gene expression change between the replicates for the same condition), GECinter is a number of genes passed the thresholds based on intersample GEC (that is gene expression change between two different conditions). Threshold function for GEC was defined as: $1 \mid \text{if } \text{MGE} < \text{C}; 2^{**} (-\text{A} * \text{MGE}) + \text{B} \mid \text{if } \text{MGE} \geq \text{C}$; where A, B, C are parameters to be adjusted. Parameters A, B, C were adjusted with genetic algorithm optimization approach to achieve maximal sensitivity in discovery of differentially expressed genes while keeping FDR below 0.05.

Accession numbers

All ChAP-Seq and RNA-Seq datasets were deposited in the GEO database under the accession number GSE120924.

Measurement of cell-associated hemin

The *C. glutamicum* strain $\Delta\text{hrrSA}\Delta\text{chrSA}$ (carrying the pJCI1_P_{hrrSA}-hrrSA-twin-strep_P_{chrSA}-chrSA-his plasmid) was cultivated in 4 μM hemin as described above (see ChAP Sequencing). To measure the cell-associated heme pool, CGXII minimal medium supplemented with 2% (w/v) glucose and 4 μM heme was inoculated to an OD₆₀₀ of 3.5. Samples were taken 0.5, 2, 4, 9 and 24 hours after addition of heme. Cells were harvested, resuspended in 100 mM Tris-HCl (pH 8) and adjusted to an OD₆₀₀ of 100. Cells cultivated in 4 μM FeSO₄

supplemented medium were taken as a control and harvested at the same time points. Absolute spectra of cells reduced with a spatula tip of sodium dithionite were measured at room temperature using the Jasco V560 with a silicon photodiode detector in combination with 5 mm light path cuvettes. Absorption values at 406 nm were normalized by subtracting the measured absorption values of Fe-cultivated cells.

Electrophoretic mobility shift assays (EMSA)

The promoter regions of HrrA target genes were chosen based on the ChAP-Seq analyses and comprised 50 bp up- and downstream of the maximal peak height (for primers see Table S2). For quantitative measurements, the DNA fragments were increased to 250 bp up- and downstream of the peak maximum. Before addition of DNA, HrrA was phosphorylated by incubation for 60 min with MBP-HrrSA Δ 1-248 in a ratio of 2:1 and 5 mM ATP. Binding assays were performed in a total volume of 20 μl using 15 nM DNA and increasing HrrA concentrations from 25 to 100 nM or 75 to 1500 nM, respectively. The binding buffer contained 20 mM Tris-HCl (pH 7.5), 50 mM KCl, 10 mM MgCl₂, 5% (v/v) glycerol, 0.5 mM EDTA and 0.005% (w/v) Triton X-100. After incubation for 20 min at room temperature, the reaction mixtures were loaded onto a 10% native polyacrylamide gel and subsequently stained using Sybr green I (Sigma Aldrich). The band intensities of unbound DNA were quantified using AIDA v.4.15 (Raytest GmbH, Germany) and Kd values calculated using GraphPad Prism 7.

Acknowledgements

We thank Eva Davoudi for fruitful discussions and critical reading of the manuscript. We thank Helga Etterich for her practical help with the sequencing experiments.

Funding

The authors acknowledge financial support by the German Research Foundation (FR 2759/4-1), the European Research Council (ERC-StG-2017, grant 757563) and by the Helmholtz Association (W2/W3-096).

Author contributions

MK, CFD, EP and JF designed the experiments. MK, CFD and UV performed the experiments. MK, CFD and AF analysed the data. AF and TP performed bioinformatics analysis of the sequencing data. MBA, MBO and JF supervised the project. MK and JF wrote the manuscript. MK, CFD and AF prepared the figures. MK, CFD, AF, UV, EP, TP, MBA, MBO and JF edited the manuscript.

REFERENCES

1. Ponka P. 1999. Cell biology of heme. *Am J Med Sci* 318:241-56.
2. Layer G, Reichelt J, Jahn D, Heinz DW. 2010. Structure and function of enzymes in heme biosynthesis. *Protein Science : A Publication of the Protein Society* 19:1137-1161.
3. Ajioka RS, Phillips JD, Kushner JP. 2006. Biosynthesis of heme in mammals. *Biochim Biophys Acta* 1763:723-36.
4. Anzaldi LL, Skaar EP. 2010. Overcoming the heme paradox: heme toxicity and tolerance in bacterial pathogens. *Infect Immun* 78:4977-89.
5. Huang W, Wilks A. 2017. Extracellular Heme Uptake and the Challenge of Bacterial Cell Membranes. *Annu Rev Biochem* 86:799-823.
6. Wilks A. 2002. Heme oxygenase: evolution, structure, and mechanism. *Antioxid Redox Signal* 4:603-14.
7. Hickman MJ, Winston F. 2007. Heme levels switch the function of Hap1 of *Saccharomyces cerevisiae* between transcriptional activator and transcriptional repressor. *Molecular and Cellular Biology* 27:7414-24.
8. Ogawa K, Sun J, Taketani S, Nakajima O, Nishitani C, Sassa S, Hayashi N, Yamamoto M, Shibahara S, Fujita H, Igarashi K. 2001. Heme mediates depression of Maf recognition element through direct binding to transcription repressor Bach1. *The EMBO journal* 20.
9. Warmatz HJ, Schmidt D, Manke T, Piccini I, Sultan M, Borodina T, Balzereit D, Wruck W, Soldatov A, Vingron M, Lehraich H, Yaspo ML. 2011. The BTB and CNC homology 1 (BACH1) target genes are involved in the oxidative stress response and in control of the cell cycle. *J Biol Chem* 286:23521-32.
10. Qi Z, Hamza I, O'Brian MR. 1999. Heme is an effector molecule for iron-dependent degradation of the bacterial iron response regulator (Irr) protein. *Proc Natl Acad Sci U S A* 96:13056-61.
11. Qi Z, O'Brian MR. 2002. Interaction between the bacterial iron response regulator and ferrochelatase mediates genetic control of heme biosynthesis. *Mol Cell* 9:155-62.
12. O'Brian MR. 2015. Perception and Homeostatic Control of Iron in the *Rhizobia* and Related Bacteria. *Annu Rev Microbiol* 69:229-45.
13. Torres VJ, Stauff DL, Pishchany G, Bezbradica JS, Gordy LE, Iurregui J, Anderson KL, Dunman PM, Joyce S, Skaar EP. 2007. A *Staphylococcus aureus* regulatory system that responds to host heme and modulates virulence. *Cell Host Microbe* 1:109-19.
14. Mike LA, Choby JE, Brinkman PR, Olive LQ, Dutter BF, Ivan SJ, Gibbs CM, Sulikowski GA, Stauff DL, Skaar EP. 2014. Two-component system cross-regulation integrates *Bacillus anthracis* response to heme and cell envelope stress. *PLoS Pathog* 10:e1004044.
15. Stauff DL, Skaar EP. 2009. The heme sensor system of *Staphylococcus aureus*. *Contrib Microbiol* 16:120-35.
16. Stauff DL, Skaar EP. 2009. *Bacillus anthracis* HssRS signalling to HrtAB regulates haem resistance during infection. *Mol Microbiol* 72:763-78.
17. Bibb LA, Kunkle CA, Schmitt MP. 2007. The ChrA-ChrS and HrrA-HrrS signal transduction systems are required for activation of the *hmuO* promoter and repression of the *hemA* promoter in *Corynebacterium diphtheriae*. *Infect Immun* 75:2421-31.
18. Frunzke J, Gatgens C, Brocker M, Bott M. 2011. Control of heme homeostasis in *Corynebacterium glutamicum* by the two-component system HrrSA. *J Bacteriol* 193:1212-21.
19. Heyer A, Gatgens C, Hentschel E, Kalinowski J, Bott M, Frunzke J. 2012. The two-component system ChrSA is crucial for haem tolerance and interferes with HrrSA in haem-dependent gene regulation in *Corynebacterium glutamicum*. *Microbiology* 158:3020-31.
20. Burgos JM, Schmitt MP. 2016. The ChrSA and HrrSA Two-Component Systems Are Required for Transcriptional Regulation of the *hemA* Promoter in *Corynebacterium diphtheriae*. *J Bacteriol* 198:2419-30.
21. Keppel M, Davoudi E, Gatgens C, Frunzke J. 2018. Membrane Topology and Heme Binding of the Histidine Kinases HrrS and ChrS in *Corynebacterium glutamicum*. *Frontiers in Microbiology* 9.
22. Ito Y, Nakagawa S, Komagata A, Ikeda-Saito M, Shiro Y, Nakamura H. 2009. Heme-dependent autophosphorylation of a heme sensor kinase, ChrS, from *Corynebacterium diphtheriae* reconstituted in protoliposomes. *FEBS Lett* 583:2244-8.
23. Hentschel E, Mack C, Gatgens C, Bott M, Brocker M, Frunzke J. 2014. Phosphatase activity of the histidine kinases ensures pathway specificity of the ChrSA and HrrSA two-component systems in *Corynebacterium glutamicum*. *Mol Microbiol* 92:1326-42.
24. Bott M, Niebisch A. 2003. The respiratory chain of *Corynebacterium glutamicum*. *J Biotechnol* 104:129-53.
25. Kao WC, Kleinschroth T, Nitschke W, Baymann F, Neehaul Y, Hellwig P, Richers S, Vonck J, Bott M, Hunte C. 2016. The obligate respiratory supercomplex from Actinobacteria. *Biochim Biophys Acta* 1857:1705-14.
26. Niebisch A, Bott M. 2001. Molecular analysis of the cytochrome *bc₁-aa₃* branch of the *Corynebacterium glutamicum* respiratory chain containing an unusual diheme cytochrome *c₁*. *Arch Microbiol* 175:282-94.
27. Kalinowski J, Bathe B, Bartels D, Bischoff N, Bott M, Burkovski A, Dusch N, Eggeling L, Eikmanns BJ, Gaigalat L, Goesmann A, Hartmann M, Huthmacher K, Kramer R, Linke B, McHardy AC, Meyer F, Mockel B, Pfefferle W, Puhler A, Rey DA, Ruckert C, Rupp O, Sahm H, Wendisch VF, Wiegand I, Tauch A. 2003. The complete *Corynebacterium glutamicum* ATCC 13032 genome sequence and its impact on the production of L-aspartate-derived amino acids and vitamins. *J Biotechnol* 104:5-25.
28. Ikeda M, Nakagawa S. 2003. The *Corynebacterium glutamicum* genome: features and impacts on biotechnological processes. *Appl Microbiol Biotechnol* 62:99-109.
29. Sone N, Nagata K, Kojima H, Tajima J, Kodera Y, Kanamaru T, Noguchi S, Sakamoto J. 2001. A novel hydrophobic diheme c-type cytochrome. Purification from *Corynebacterium glutamicum* and analysis of the QcrCBA operon encoding three subunit proteins of a putative cytochrome reductase complex. *Biochim Biophys Acta* 1503:279-90.
30. Teramoto H, Inui M, Yukawa H. 2013. OxyR acts as a transcriptional repressor of hydrogen peroxide-inducible antioxidant genes in *Corynebacterium glutamicum* R. *FEBS J* 280:3298-312.
31. Milse J, Petri K, Ruckert C, Kalinowski J. 2014. Transcriptional response of *Corynebacterium glutamicum* ATCC 13032 to hydrogen peroxide stress and characterization of the OxyR regulon. *J Biotechnol* 190:40-54.
32. Toyoda K, Inui M. 2016. The extracytoplasmic function sigma factor sigma(C) regulates expression of a branched quinol oxidation pathway in *Corynebacterium glutamicum*. *Molecular Microbiology* 100:486-509.
33. Morosov X, Davoudi CF, Baumgart M, Brocker M, Bott M. 2018. The copper-deprivation stimulant of *Corynebacterium glutamicum* comprises proteins for biogenesis of the actinobacterial cytochrome *bc₁-aa₃* supercomplex. *J Biol Chem* doi:10.1074/jbc.RA118.004117.
34. Wennerhold J, Bott M. 2006. The DtxR regulon of *Corynebacterium glutamicum*. *J Bacteriol* 188:2907-18.
35. Xu IM, Lai RK, Lin SH, Tse AP, Chiu DK, Koh HY, Law CT, Wong CM, Cai Z, Wong CC, Ng IO. 2016. Transketolase counteracts oxidative stress to drive cancer development. *Proc Natl Acad Sci U S A* 113:E725-34.

36. Arner ES, Holmgren A. 2000. Physiological functions of thioredoxin and thioredoxin reductase. *Eur J Biochem* 267:6102-9.
37. Alvarez-Peral FJ, Zaragoza O, Pedreno Y, Arguelles JC. 2002. Protective role of trehalose during severe oxidative stress caused by hydrogen peroxide and the adaptive oxidative stress response in *Candida albicans*. *Microbiology* 148:2599-606.
38. Pang YY, Schwartz J, Bloomberg S, Boyd JM, Horswill AR, Nauseef WM. 2014. Methionine sulfoxide reductases protect against oxidative stress in *Staphylococcus aureus* encountering exogenous oxidants and human neutrophils. *J Innate Immun* 6:353-64.
39. Bibb LA, King ND, Kunkle CA, Schmitt MP. 2005. Analysis of a heme-dependent signal transduction system in *Corynebacterium diphtheriae*: deletion of the *chrAS* genes results in heme sensitivity and diminished heme-dependent activation of the *hmuO* promoter. *Infect Immun* 73:7406-12.
40. Bibb LA, Schmitt MP. 2010. The ABC transporter HrtAB confers resistance to hemin toxicity and is regulated in a hemin-dependent manner by the ChrAS two-component system in *Corynebacterium diphtheriae*. *J Bacteriol* 192:4606-17.
41. Sun J, Hoshino H, Takaku K, Nakajima O, Muto A, Suzuki H, Tashiro S, Takahashi S, Shibahara S, Alam J, Taketo MM, Yamamoto M, Igarashi K. 2002. Hemoprotein Bach1 regulates enhancer availability of heme oxygenase-1 gene. *The EMBO journal* 21.
42. Ratliff M, Zhu W, Deshmukh R, Wilks A, Stojiljkovic I. 2001. Homologues of neisserial heme oxygenase in gram-negative bacteria: degradation of heme by the product of the *pigA* gene of *Pseudomonas aeruginosa*. *J Bacteriol* 183:6394-403.
43. Schmitt MP. 1997. Transcription of the *Corynebacterium diphtheriae hmuO* gene is regulated by iron and heme. *Infect Immun* 65:4634-41.
44. Hintze KJ, Katoh Y, Igarashi K, Theil EC. 2007. Bach1 repression of ferritin and thioredoxin reductase 1 is heme-sensitive in cells and in vitro and coordinates expression with heme oxygenase I, beta-globin, and NAD(P)H quinone (oxido) reductase I. *J Biol Chem* 282:34365-71.
45. Dhakshinamoorthy S, Jain AK, Bloom DA, Jaiswal AK. 2005. Bach1 competes with Nrf2 leading to negative regulation of the antioxidant response element (ARE)-mediated NAD(P)H:quinone oxidoreductase 1 gene expression and induction in response to antioxidants. *J Biol Chem* 280:16891-900.
46. Kuehne A, Emmert H, Soehle J, Winnefeld M, Fischer F, Wenck H, Gallinat S, Terstegen L, Lucius R, Hildebrand J, Zamboni N. 2015. Acute Activation of Oxidative Pentose Phosphate Pathway as First-Line Response to Oxidative Stress in Human Skin Cells. *Molecular Cell* 59:359-71.
47. Ralsler M, Wamelink MM, Latkolik S, Jansen EE, Lehrach H, Jakobs C. 2009. Metabolic reconfiguration precedes transcriptional regulation in the antioxidant response. *Nat Biotechnol* 27:604-5.
48. Hillion M, Imber M, Pedre B, Bernhardt J, Saleh M, Loi VV, Maaß S, Becher D, Astolfi Rosado L, Adrian L, Weise C, Hell R, Wirtz M, Messens J, Antelmann H. 2017. The glyceraldehyde-3-phosphate dehydrogenase GapDH of *Corynebacterium diphtheriae* is redox-controlled by protein S-mycothiolation under oxidative stress. *Scientific Reports* 7:5020.
49. Möker N, Brocker M, Schaffer S, Kramer R, Morbach S, Bott M. 2004. Deletion of the genes encoding the MtrA-MtrB two-component system of *Corynebacterium glutamicum* has a strong influence on cell morphology, antibiotics susceptibility and expression of genes involved in osmoprotection. *Molecular Microbiology* 54:420-38.
50. Baumgart M, Luder K, Grover S, Gatgens C, Besra GS, Frunzke J. 2013. IpsA, a novel LacI-type regulator, is required for inositol-derived lipid formation in *Corynebacterium* and *Mycobacterium*. *BMC Biol* 11:122.
51. Niebisch A, Bott M. 2003. Purification of a cytochrome *bc₁a* supercomplex with quinol oxidase activity from *Corynebacterium glutamicum*. Identification of a fourth subunit of cytochrome *aa3* oxidase and mutational analysis of diheme cytochrome *c1*. *J Biol Chem* 278:4339-46.
52. Mueller JP, Taber HW. 1989. Isolation and sequence of *ctaA*, a gene required for cytochrome *aa3* biosynthesis and sporulation in *Bacillus subtilis*. *J Bacteriol* 171:4967-78.
53. Svensson B, Lubben M, Hederstedt L. 1993. *Bacillus subtilis* CtaA and CtaB function in haem A biosynthesis. *Mol Microbiol* 10:193-201.
54. Paul S, Zhang X, Hulett FM. 2001. Two ResD-controlled promoters regulate *ctaA* expression in *Bacillus subtilis*. *J Bacteriol* 183:3237-46.
55. Brown BM, Wang Z, Brown KR, Cricco JA, Hegg EL. 2004. Heme O synthase and heme A synthase from *Bacillus subtilis* and *Rhodobacter sphaeroides* interact in *Escherichia coli*. *Biochemistry* 43:13541-8.
56. Aucher M, Cramer A, Huser A, Ruckert C, Emer D, Schwarz P, Arndt A, Lange C, Kalinowski J, Wendisch VF, Eikmanns BJ. 2011. RamA and RamB are global transcriptional regulators in *Corynebacterium glutamicum* and control genes for enzymes of the central metabolism. *J Biotechnol* 154:126-39.
57. Shah A, Blombach B, Gauttam R, Eikmanns BJ. 2018. The RamA regulon: complex regulatory interactions in relation to central metabolism in *Corynebacterium glutamicum*. *Appl Microbiol Biotechnol* 102:5901-5910.
58. Schiering N, Tao X, Zeng H, Murphy JR, Peto GA, Ringe D. 1995. Structures of the apo- and the metal ion-activated forms of the diphtheria toxin repressor from *Corynebacterium diphtheriae*. *Proc Natl Acad Sci U S A* 92:9843-50.
59. Keilhauer C, Eggeling L, Sahn H. 1993. Isoleucine synthesis in *Corynebacterium glutamicum*: molecular analysis of the *ilvB-ilvN-ilvC* operon. *Journal of Bacteriology* 175:5595-5603.
60. Sambrook J, RD. 2001. *Molecular Cloning: A Laboratory Manual*, 3rd edn. . NY: Cold Spring Harbor Laboratory Press.
61. Eikmanns BJ, Thum-Schmitz N, Eggeling L, Ludtke KU, Sahn H. 1994. Nucleotide sequence, expression and transcriptional analysis of the *Corynebacterium glutamicum gltA* gene encoding citrate synthase. *Microbiology* 140 (Pt 8):1817-28.
62. Gibson DG, Young L, Chuang RY, Venter JC, Hutchison CA, 3rd, Smith HO. 2009. Enzymatic assembly of DNA molecules up to several hundred kilobases. *Nat Methods* 6:343-5.
63. Pfeifer E, Hünnefeld M, Popa O, Polen T, Köhlhoyer D, Baumgart M, Frunzke J. 2016. Silencing of cryptic prophages in *Corynebacterium glutamicum*. *Nucleic Acids Research* 44:10117-10131.
64. Jones E, Oliphant T, Peterson P. 2001. SciPy: Open source scientific tools for Python <http://www.scipy.org/>.
65. Andrews S. 2010. FASTQC. A quality control tool for high throughput sequence data.
66. Langmead B, Salzberg SL. 2012. Fast gapped-read alignment with Bowtie 2. *Nat Methods* 9:357-9.
67. Baumgart M, Unthan S, Kloss R, Radek A, Polen T, Tenhaef N, Müller MF, Kubel A, Siebert D, Brühl N, Marin K, Hans S, Kramer R, Bott M, Kalinowski J, Wiechert W, Seibold G, Frunzke J, Ruckert C, Wendisch VF, Noack S. 2018. *Corynebacterium glutamicum* Chassis C1*: Building and Testing a Novel Platform Host for Synthetic Biology and Industrial Biotechnology. *ACS Synth Biol* 7:132-144.
68. Pachter L. 2011. Models for transcript quantification from RNA-Seq. *Conference Proceedings*.

4. References

- Aft, R. L. and Mueller, G. C. (1984). Hemin-mediated oxidative degradation of proteins. *J Biol Chem*, 259 (1): 301-5.
- Ajioka, R. S., Phillips, J. D. and Kushner, J. P. (2006). Biosynthesis of heme in mammals. *Biochim Biophys Acta*, 1763 (7): 723-36. doi: 10.1016/j.bbamcr.2006.05.005.
- Albanesi, D., Martin, M., Trajtenberg, F., Mansilla, M. C., Haouz, A., Alzari, P. M., de Mendoza, D. and Buschiazzo, A. (2009). Structural plasticity and catalysis regulation of a thermosensor histidine kinase. *Proc Natl Acad Sci U S A*, 106 (38): 16185-90. doi: 10.1073/pnas.0906699106.
- Andrews, S. C. (1998). Iron storage in bacteria. *Adv Microb Physiol*, 40: 281-351.
- Andrews, S. C., Robinson, A. K. and Rodriguez-Quinones, F. (2003). Bacterial iron homeostasis. *FEMS Microbiol Rev*, 27 (2-3): 215-37.
- Anzaldi, L. L. and Skaar, E. P. (2010). Overcoming the heme paradox: heme toxicity and tolerance in bacterial pathogens. *Infect Immun*, 78 (12): 4977-89. doi: 10.1128/iai.00613-10.
- Aravind, L., Anantharaman, V., Balaji, S., Babu, M. M. and Iyer, L. M. (2005). The many faces of the helix-turn-helix domain: transcription regulation and beyond. *FEMS Microbiol Rev*, 29 (2): 231-62. doi: 10.1016/j.femsre.2004.12.008.
- Baker, M. D., Wolanin, P. M. and Stock, J. B. (2006). Signal transduction in bacterial chemotaxis. *Bioessays*, 28 (1): 9-22. doi: 10.1002/bies.20343.
- Baumgart, M., Luder, K., Grover, S., Gätgens, C., Besra, G. S. and Frunzke, J. (2013). IpsA, a novel LacI-type regulator, is required for inositol-derived lipid formation in *Corynebacteria* and *Mycobacteria*. *BMC Biol*, 11: 122. doi: 10.1186/1741-7007-11-122.
- Beauchene, N. A., Mettert, E. L., Moore, L. J., Keles, S., Willey, E. R. and Kiley, P. J. (2017). O₂ availability impacts iron homeostasis in *Escherichia coli*. *Proc Natl Acad Sci U S A*. doi: 10.1073/pnas.1707189114.
- Bhate, M. P., Molnar, K. S., Goulian, M. and DeGrado, W. F. (2015). Signal transduction in histidine kinases: insights from new structures. *Structure*, 23 (6): 981-94. doi: 10.1016/j.str.2015.04.002.
- Bibb, L. A., King, N. D., Kunkle, C. A. and Schmitt, M. P. (2005). Analysis of a heme-dependent signal transduction system in *Corynebacterium diphtheriae*: deletion of the *chrAS* genes results in heme sensitivity and diminished heme-dependent activation of the *hmuO* promoter. *Infect Immun*, 73 (11): 7406-12. doi: 10.1128/iai.73.11.7406-7412.2005.
- Bibb, L. A., Kunkle, C. A. and Schmitt, M. P. (2007). The ChrA-ChrS and HrrA-HrrS signal transduction systems are required for activation of the *hmuO* promoter and repression of the *hemA* promoter in *Corynebacterium diphtheriae*. *Infect Immun*, 75 (5): 2421-31. doi: 10.1128/iai.01821-06.
- Bibb, L. A. and Schmitt, M. P. (2010). The ABC transporter HrtAB confers resistance to heme toxicity and is regulated in a heme-dependent manner by the ChrAS two-component system in *Corynebacterium diphtheriae*. *J Bacteriol*, 192 (18): 4606-17. doi: 10.1128/jb.00525-10.
- Borzelleca, J. F. (2000). Paracelsus: herald of modern toxicology. *Toxicol Sci*, 53 (1): 2-4.
- Bott, M. and Niebisch, A. (2003). The respiratory chain of *Corynebacterium glutamicum*. *J Biotechnol*, 104 (1-3): 129-53.
- Boyd, J., Oza, M. N. and Murphy, J. R. (1990). Molecular cloning and DNA sequence analysis of a diphtheria tox iron-dependent regulatory element (*dtxR*) from *Corynebacterium diphtheriae*. *Proc Natl Acad Sci U S A*, 87 (15): 5968-72.
- Braun, V. (2001). Iron uptake mechanisms and their regulation in pathogenic bacteria. *Int J Med Microbiol*, 291 (2): 67-79. doi: 10.1078/1438-4221-00103.

- Burbulys, D., Trach, K. A. and Hoch, J. A. (1991). Initiation of sporulation in *B. subtilis* is controlled by a multicomponent phosphorelay. *Cell*, 64 (3): 545-52.
- Burgos, J. M. and Schmitt, M. P. (2016). The ChrSA and HrrSA Two-Component Systems Are Required for Transcriptional Regulation of the *hema* Promoter in *Corynebacterium diphtheriae*. *J Bacteriol*, 198 (18): 2419-30. doi: 10.1128/jb.00339-16.
- Camacho, C., Coulouris, G., Avagyan, V., Ma, N., Papadopoulos, J., Bealer, K. and Madden, T. L. (2009). BLAST+: architecture and applications. *BMC Bioinformatics*, 10: 421. doi: 10.1186/1471-2105-10-421.
- Camadro, J. M. and Labbe, P. (1988). Purification and properties of ferrochelatase from the yeast *Saccharomyces cerevisiae*. Evidence for a precursor form of the protein. *J Biol Chem*, 263 (24): 11675-82.
- Capra, E. J. and Laub, M. T. (2012). Evolution of two-component signal transduction systems. *Annu Rev Microbiol*, 66: 325-47. doi: 10.1146/annurev-micro-092611-150039.
- Carpenter, B. M., Whitmire, J. M. and Merrell, D. S. (2009). This is not your mother's repressor: the complex role of *fur* in pathogenesis. *Infect Immun*, 77 (7): 2590-601. doi: 10.1128/iai.00116-09.
- Catlett, N. L., Yoder, O. C. and Turgeon, B. G. (2003). Whole-genome analysis of two-component signal transduction genes in fungal pathogens. *Eukaryot Cell*, 2 (6): 1151-61.
- Chan, C., Paul, R., Samoray, D., Amiot, N. C., Giese, B., Jenal, U. and Schirmer, T. (2004). Structural basis of activity and allosteric control of diguanylate cyclase. *Proc Natl Acad Sci U S A*, 101 (49): 17084-9. doi: 10.1073/pnas.0406134101.
- Chang, P., Li, W., Shi, G., Li, H., Yang, X., Xia, Z., Ren, Y., Li, Z., Chen, H. and Bei, W. (2018). The *VraSR* regulatory system contributes to virulence in *Streptococcus suis* via resistance to innate immune defenses. *Virulence*, 9 (1): 771-782. doi: 10.1080/21505594.2018.1428519.
- Cheung, J. and Hendrickson, W. A. (2008). Crystal structures of C4-dicarboxylate ligand complexes with sensor domains of histidine kinases DcuS and DctB. *J Biol Chem*, 283 (44): 30256-65. doi: 10.1074/jbc.M805253200.
- Cho, B. K., Barrett, C. L., Knight, E. M., Park, Y. S. and Palsson, B. O. (2008). Genome-scale reconstruction of the Lrp regulatory network in *Escherichia coli*. *Proc Natl Acad Sci U S A*, 105 (49): 19462-7. doi: 10.1073/pnas.0807227105.
- Choby, J. E. and Skaar, E. P. (2016). Heme Synthesis and Acquisition in Bacterial Pathogens. *J Mol Biol*, 428 (17): 3408-28. doi: 10.1016/j.jmb.2016.03.018.
- Contreras, H., Chim, N., Credali, A. and Goulding, C. W. (2014). Heme uptake in bacterial pathogens. *Curr Opin Chem Biol*, 19: 34-41. doi: 10.1016/j.cbpa.2013.12.014.
- Cornelis, P., Wei, Q., Andrews, S. C. and Vinckx, T. (2011). Iron homeostasis and management of oxidative stress response in bacteria. *Metallomics*, 3 (6): 540-9. doi: 10.1039/c1mt00022e.
- Cuthbertson, L. and Nodwell, J. R. (2013). The TetR family of regulators. *Microbiol Mol Biol Rev*, 77 (3): 440-75. doi: 10.1128/mmbr.00018-13.
- Davis, M. C., Kesthely, C. A., Franklin, E. A. and MacLellan, S. R. (2017). The essential activities of the bacterial sigma factor. *Can J Microbiol*, 63 (2): 89-99. doi: 10.1139/cjm-2016-0576.
- Dhakshinamoorthy, S., Jain, A. K., Bloom, D. A. and Jaiswal, A. K. (2005). Bach1 competes with Nrf2 leading to negative regulation of the antioxidant response element (ARE)-mediated NAD(P)H:quinone oxidoreductase 1 gene expression and induction in response to antioxidants. *J Biol Chem*, 280 (17): 16891-900. doi: 10.1074/jbc.M500166200.
- Diensthuber, R. P., Bommer, M., Gleichmann, T. and Moglich, A. (2013). Full-length structure of a sensor histidine kinase pinpoints coaxial coiled coils as signal transducers and modulators. *Structure*, 21 (7): 1127-36. doi: 10.1016/j.str.2013.04.024.

- Drazek, E. S., Hammack, C. A. and Schmitt, M. P. (2000). *Corynebacterium diphtheriae* genes required for acquisition of iron from haemin and haemoglobin are homologous to ABC haemin transporters. *Mol Microbiol*, 36 (1): 68-84.
- Fernandez, A., Lechardeur, D., Derre-Bobillot, A., Couve, E., Gaudu, P. and Gruss, A. (2010). Two coregulated efflux transporters modulate intracellular heme and protoporphyrin IX availability in *Streptococcus agalactiae*. *PLoS Pathog*, 6 (4): e1000860. doi: 10.1371/journal.ppat.1000860.
- Ferris, H. U., Dunin-Horkawicz, S., Hornig, N., Hulko, M., Martin, J., Schultz, J. E., Zeth, K., Lupas, A. N. and Coles, M. (2012). Mechanism of regulation of receptor histidine kinases. *Structure*, 20 (1): 56-66. doi: 10.1016/j.str.2011.11.014.
- Ferris, H. U., Coles, M., Lupas, A. N. and Hartmann, M. D. (2014). Crystallographic snapshot of the *Escherichia coli* EnvZ histidine kinase in an active conformation. *J Struct Biol*, 186 (3): 376-9. doi: 10.1016/j.jsb.2014.03.014.
- Francez-Charlot, A., Frunzke, J., Reichen, C., Ebnetter, J. Z., Gourion, B. and Vorholt, J. A. (2009). Sigma factor mimicry involved in regulation of general stress response. *Proc Natl Acad Sci U S A*, 106 (9): 3467-72. doi: 10.1073/pnas.0810291106.
- Fritz, G., Dintner, S., Treichel, N. S., Radeck, J., Gerland, U., Mascher, T. and Gebhard, S. (2015). A New Way of Sensing: Need-Based Activation of Antibiotic Resistance by a Flux-Sensing Mechanism. *MBio*, 6 (4). doi: 10.1128/mBio.00975-15.
- Frunzke, J., Gatgens, C., Brocker, M. and Bott, M. (2011). Control of heme homeostasis in *Corynebacterium glutamicum* by the two-component system HrrSA. *J Bacteriol*, 193 (5): 1212-21. doi: 10.1128/jb.01130-10.
- Galperin, M. Y., Nikolskaya, A. N. and Koonin, E. V. (2001). Novel domains of the prokaryotic two-component signal transduction systems. *FEMS Microbiol Lett*, 203 (1): 11-21.
- Galperin, M. Y. (2005). A census of membrane-bound and intracellular signal transduction proteins in bacteria: bacterial IQ, extroverts and introverts. *BMC Microbiol*, 5: 35. doi: 10.1186/1471-2180-5-35.
- Galperin, M. Y. (2010). Diversity of structure and function of response regulator output domains. *Curr Opin Microbiol*, 13 (2): 150-9. doi: 10.1016/j.mib.2010.01.005.
- Gao, R., Mack, T. R. and Stock, A. M. (2007). Bacterial response regulators: versatile regulatory strategies from common domains. *Trends Biochem Sci*, 32 (5): 225-34. doi: 10.1016/j.tibs.2007.03.002.
- Gourion, B., Rossignol, M. and Vorholt, J. A. (2006). A proteomic study of *Methylobacterium extorquens* reveals a response regulator essential for epiphytic growth. *Proc Natl Acad Sci U S A*, 103 (35): 13186-91. doi: 10.1073/pnas.0603530103.
- Grant, R. A., Filman, D. J., Finkel, S. E., Kolter, R. and Hogle, J. M. (1998). The crystal structure of Dps, a ferritin homolog that binds and protects DNA. *Nat Struct Biol*, 5 (4): 294-303.
- Gushchin, I., Melnikov, I., Polovinkin, V., Ishchenko, A., Yuzhakova, A., Buslaev, P., Bourenkov, G., Grudinin, S., Round, E., Balandin, T., Borshchevskiy, V., Willbold, D., Leonard, G., Buldt, G., Popov, A. and Gordeliy, V. (2017). Mechanism of transmembrane signaling by sensor histidine kinases. *Science*, 356 (6342). doi: 10.1126/science.aah6345.
- Hamza, I., Chauhan, S., Hassett, R. and O'Brian, M. R. (1998). The bacterial irr protein is required for coordination of heme biosynthesis with iron availability. *J Biol Chem*, 273 (34): 21669-74.
- Heinemann, I. U., Jahn, M. and Jahn, D. (2008). The biochemistry of heme biosynthesis. *Arch Biochem Biophys*, 474 (2): 238-51. doi: 10.1016/j.abb.2008.02.015.
- Helmann, J. D. (1999). Anti-sigma factors. *Curr Opin Microbiol*, 2 (2): 135-41. doi: 10.1016/s1369-5274(99)80024-1.
- Hentschel, E., Mack, C., Gatgens, C., Bott, M., Brocker, M. and Frunzke, J. (2014). Phosphatase activity of the histidine kinases ensures pathway specificity of the ChrSA and HrrSA two-component systems in *Corynebacterium glutamicum*. *Mol Microbiol*, 92 (6): 1326-42. doi: 10.1111/mmi.12633.

- Hentschel, E. (2015). Interaction of the two-component systems HrrSA and ChrSA in *Corynebacterium glutamicum*. *Gesundheit/Health (Forschungszentrum Jülich; Heinrich-Heine-Universität Düsseldorf)*, 79: 56-76.
- Herzberg, M., Kaye, I. K., Peti, W. and Wood, T. K. (2006). YdgG (TqsA) controls biofilm formation in *Escherichia coli* K-12 through autoinducer 2 transport. *J Bacteriol*, 188 (2): 587-98. doi: 10.1128/jb.188.2.587-598.2006.
- Heyer, A., Gatgens, C., Hentschel, E., Kalinowski, J., Bott, M. and Frunzke, J. (2012). The two-component system ChrSA is crucial for haem tolerance and interferes with HrrSA in haem-dependent gene regulation in *Corynebacterium glutamicum*. *Microbiology*, 158 (Pt 12): 3020-31. doi: 10.1099/mic.0.062638-0.
- Hickman, M. J. and Winston, F. (2007). Heme levels switch the function of Hap1 of *Saccharomyces cerevisiae* between transcriptional activator and transcriptional repressor. *Mol Cell Biol*, 27 (21): 7414-24. doi: 10.1128/mcb.00887-07.
- Hillion, M., Imber, M., Pedre, B., Bernhardt, J., Saleh, M., Loi, V. V., Maaß, S., Becher, D., Astolfi Rosado, L., Adrian, L., Weise, C., Hell, R., Wirtz, M., Messens, J. and Antelmann, H. (2017). The glyceraldehyde-3-phosphate dehydrogenase GapDH of *Corynebacterium diphtheriae* is redox-controlled by protein S-mycothiolation under oxidative stress. *Scientific Reports*, 7 (1): 5020. doi: 10.1038/s41598-017-05206-2.
- Hintze, K. J., Katoh, Y., Igarashi, K. and Theil, E. C. (2007). Bach1 repression of ferritin and thioredoxin reductase1 is heme-sensitive in cells and in vitro and coordinates expression with heme oxygenase1, beta-globin, and NADP(H) quinone (oxido) reductase1. *J Biol Chem*, 282 (47): 34365-71. doi: 10.1074/jbc.M700254200.
- Hon, T., Lee, H. C., Hu, Z., Iyer, V. R. and Zhang, L. (2005). The Heme Activator Protein Hap1 Represses Transcription by a Heme-Independent Mechanism in *Saccharomyces cerevisiae*. *Genetics*, 169 (3): 1343-52.
- Ishihama, A. (2010). Prokaryotic genome regulation: multifactor promoters, multitarget regulators and hierarchic networks. *FEMS Microbiol Rev*, 34 (5): 628-45. doi: 10.1111/j.1574-6976.2010.00227.x.
- Jacob, F. and Monod, J. (1961). Genetic regulatory mechanisms in the synthesis of proteins. *J Mol Biol*, 3: 318-56.
- Jensen, R. B., Wang, S. C. and Shapiro, L. (2002). Dynamic localization of proteins and DNA during a bacterial cell cycle. *Nat Rev Mol Cell Biol*, 3 (3): 167-76. doi: 10.1038/nrm758.
- Jeon, B., Wang, Y., Hao, H., Barton, Y. W. and Zhang, Q. (2011). Contribution of CmeG to antibiotic and oxidative stress resistance in *Campylobacter jejuni*. *J Antimicrob Chemother*, 66 (1): 79-85. doi: 10.1093/jac/dkq418.
- Jochmann, N., Kurze, A. K., Czaja, L. F., Brinkrolf, K., Brune, I., Huser, A. T., Hansmeier, N., Puhler, A., Borovok, I. and Tauch, A. (2009). Genetic makeup of the *Corynebacterium glutamicum* LexA regulon deduced from comparative transcriptomics and in vitro DNA band shift assays. *Microbiology*, 155 (Pt 5): 1459-77. doi: 10.1099/mic.0.025841-0.
- Johnston, A. W., Todd, J. D., Curson, A. R., Lei, S., Nikolaidou-Katsaridou, N., Gelfand, M. S. and Rodionov, D. A. (2007). Living without Fur: the subtlety and complexity of iron-responsive gene regulation in the symbiotic bacterium *Rhizobium* and other alpha-proteobacteria. *Biometals*, 20 (3-4): 501-11. doi: 10.1007/s10534-007-9085-8.
- Kaspar, S. and Bott, M. (2002). The sensor kinase CitA (DpiB) of *Escherichia coli* functions as a high-affinity citrate receptor. *Arch Microbiol*, 177 (4): 313-21. doi: 10.1007/s00203-001-0393-z.
- Kazmierczak, M. J., Wiedmann, M. and Boor, K. J. (2005). Alternative Sigma Factors and Their Roles in Bacterial Virulence. *Microbiology and Molecular Biology Reviews*, 69 (4): 527-543. doi: 10.1128/MMBR.69.4.527-543.2005.
- Keppel, M., Davoudi, C. F., Filipchuk, A., Viets, U., Pfeifer, E., Baumgart, M., Bott, M. and Frunzke, J. (2018a). HrrSA orchestrates a systemic response to heme and determines prioritisation of terminal cytochrome oxidase expression. *Submitted*.
- Keppel, M., Davoudi, E., Gätgens, C. and Frunzke, J. (2018b). Membrane Topology and Heme Binding of the Histidine Kinases HrrS and ChrS in *Corynebacterium glutamicum*. *Front Microbiol*, 9 (183). doi: 10.3389/fmicb.2018.00183.

- Keppel, M., Piepenbreier, H., Gätgens, C., Fritz, G. and Frunzke, J. (2018c). Toxic but tasty - Temporal dynamics and network architecture of heme-responsive two-component signalling in *Corynebacterium glutamicum*. *In revision: Mol Micro*.
- Kim, H. J., Khalimonchuk, O., Smith, P. M. and Winge, D. R. (2012). Structure, function, and assembly of heme centers in mitochondrial respiratory complexes. *Biochim Biophys Acta*, 1823 (9): 1604-16. doi: 10.1016/j.bbamcr.2012.04.008.
- Kinoshita, E., Kinoshita-Kikuta, E., Takiyama, K. and Koike, T. (2006). Phosphate-binding tag, a new tool to visualize phosphorylated proteins. *Mol Cell Proteomics*, 5 (4): 749-57. doi: 10.1074/mcp.T500024-MCP200.
- Kirby, A. E., King, N. D. and Connell, T. D. (2004). RhuR, an extracytoplasmic function sigma factor activator, is essential for heme-dependent expression of the outer membrane heme and hemoprotein receptor of *Bordetella avium*. *Infect Immun*, 72 (2): 896-907.
- Kuehne, A., Emmert, H., Soehle, J., Winnefeld, M., Fischer, F., Wenck, H., Gallinat, S., Terstegen, L., Lucius, R., Hildebrand, J. and Zamboni, N. (2015). Acute Activation of Oxidative Pentose Phosphate Pathway as First-Line Response to Oxidative Stress in Human Skin Cells. *Mol Cell*, 59 (3): 359-71. doi: 10.1016/j.molcel.2015.06.017.
- Kumar, S. and Bandyopadhyay, U. (2005). Free heme toxicity and its detoxification systems in human. *Toxicol Lett*, 157 (3): 175-88. doi: 10.1016/j.toxlet.2005.03.004.
- Kusumoto, K., Sakiyama, M., Sakamoto, J., Noguchi, S. and Sone, N. (2000). Menaquinol oxidase activity and primary structure of cytochrome *bd* from the amino-acid fermenting bacterium *Corynebacterium glutamicum*. *Arch Microbiol*, 173 (5-6): 390-7.
- Kusumoto, T., Aoyagi, M., Sugiyama, T. and Sakamoto, J. (2015). Monitoring the enzyme expression in a respiratory chain of *Corynebacterium glutamicum* in a copper ion-supplemented culture medium. *Biosci Biotechnol Biochem*, 79 (2): 223-9. doi: 10.1080/09168451.2014.968089.
- Laub, M. T. and Goulian, M. (2007). Specificity in two-component signal transduction pathways. *Annu Rev Genet*, 41: 121-45. doi: 10.1146/annurev.genet.41.042007.170548.
- Lavrrar, J. L. and McIntosh, M. A. (2003). Architecture of a fur binding site: a comparative analysis. *J Bacteriol*, 185 (7): 2194-202.
- Layer, G., Reichelt, J., Jahn, D. and Heinz, D. W. (2010). Structure and function of enzymes in heme biosynthesis. *Protein Science : A Publication of the Protein Society*, 19 (6): 1137-1161. doi: 10.1002/pro.405.
- Leeper, F. J. (1985). The biosynthesis of porphyrins, chlorophylls, and vitamin B12. *Nat Prod Rep*, 2 (6): 561-80.
- Leonardo, M. R. and Forst, S. (1996). Re-examination of the role of the periplasmic domain of EnvZ in sensing of osmolarity signals in *Escherichia coli*. *Mol Microbiol*, 22 (3): 405-13. doi: 10.1046/j.1365-2958.1996.1271487.x.
- Létoffé, S., Delepelaire, P. and Wandersman, C. (2006). The housekeeping dipeptide permease is the *Escherichia coli* heme transporter and functions with two optional peptide binding proteins. *Proc Natl Acad Sci U S A*, 103 (34): 12891-6. doi: 10.1073/pnas.0605440103.
- Li, T., Bonkovsky, H. L. and Guo, J.-t. (2011). Structural analysis of heme proteins: implications for design and prediction. *BMC Structural Biology*, 11 (1): 13. doi: 10.1186/1472-6807-11-13.
- Lodish, H., Berk, A., Zipursky, L., Matsudaira, P., Baltimore, D. and Darnell, J. (2000). *Molecular Cell Biology*. 4th edition. Section 16.2, Electron Transport and Oxidative Phosphorylation. New York, Available from: <https://www.ncbi.nlm.nih.gov/books/NBK21475/>.
- Marchler-Bauer, A., Bo, Y., Han, L., He, J., Lanczycki, C. J., Lu, S., Chitsaz, F., Derbyshire, M. K., Geer, R. C., Gonzales, N. R., Gwadz, M., Hurwitz, D. I., Lu, F., Marchler, G. H., Song, J. S., Thanki, N., Wang, Z., Yamashita, R. A., Zhang, D., Zheng, C., Geer, L. Y. and Bryant, S. H. (2017). CDD/SPARCLE: functional classification of proteins via subfamily domain architectures. *Nucleic Acids Res*, 45 (D1): D200-d203. doi: 10.1093/nar/gkw1129.

- Marger, M. D. and Saier, M. H., Jr. (1993). A major superfamily of transmembrane facilitators that catalyse uniport, symport and antiport. *Trends Biochem Sci*, 18 (1): 13-20.
- Mascher, T., Helmann, J. D. and Unden, G. (2006). Stimulus perception in bacterial signal-transducing histidine kinases. *Microbiol Mol Biol Rev*, 70 (4): 910-38. doi: 10.1128/mmbr.00020-06.
- Mascher, T. (2013). Signaling diversity and evolution of extracytoplasmic function (ECF) sigma factors. *Curr Opin Microbiol*, 16 (2): 148-55. doi: 10.1016/j.mib.2013.02.001.
- McCleary, W. R. and Stock, J. B. (1994). Acetyl phosphate and the activation of two-component response regulators. *J Biol Chem*, 269 (50): 31567-72.
- McNutt, M., Bradford, M., Drazen, J., Hanson, R. B., Howard, B., Jamieson, K. H., Kiermer, V., Magoulias, M., Marcus, E., Pope, B. K., Schekman, R., Swaminathan, S., Stang, P. and Verma, I. (2017). Transparency In Authors' Contributions And Responsibilities To Promote Integrity In Scientific Publication. doi: 10.1101/140228 %J bioRxiv.
- Mechaly, A. E., Sassoon, N., Betton, J. M. and Alzari, P. M. (2014). Segmental helical motions and dynamical asymmetry modulate histidine kinase autophosphorylation. *PLoS Biol*, 12 (1): e1001776. doi: 10.1371/journal.pbio.1001776.
- Merchant, A. T. and Spatafora, G. A. (2014). A role for the DtxR family of metalloregulators in gram-positive pathogenesis. *Mol Oral Microbiol*, 29 (1): 1-10. doi: 10.1111/omi.12039.
- Mike, L. A., Choby, J. E., Brinkman, P. R., Olive, L. Q., Dutter, B. F., Ivan, S. J., Gibbs, C. M., Sulikowski, G. A., Stauff, D. L. and Skaar, E. P. (2014). Two-component system cross-regulation integrates *Bacillus anthracis* response to heme and cell envelope stress. *PLoS Pathog*, 10 (3): e1004044. doi: 10.1371/journal.ppat.1004044.
- Milse, J., Petri, K., Ruckert, C. and Kalinowski, J. (2014). Transcriptional response of *Corynebacterium glutamicum* ATCC 13032 to hydrogen peroxide stress and characterization of the OxyR regulon. *J Biotechnol*, 190: 40-54. doi: 10.1016/j.jbiotec.2014.07.452.
- Möker, N., Brocker, M., Schaffer, S., Kramer, R., Morbach, S. and Bott, M. (2004). Deletion of the genes encoding the MtrA-MtrB two-component system of *Corynebacterium glutamicum* has a strong influence on cell morphology, antibiotics susceptibility and expression of genes involved in osmoprotection. *Mol Microbiol*, 54 (2): 420-38. doi: 10.1111/j.1365-2958.2004.04249.x.
- Morosov, X., Davoudi, C. F., Baumgart, M., Brocker, M. and Bott, M. (2018). The copper-deprivation stimulon of *Corynebacterium glutamicum* comprises proteins for biogenesis of the actinobacterial cytochrome *bc₁-aa₃* supercomplex. *J Biol Chem*. doi: 10.1074/jbc.RA118.004117.
- Myers, K. S., Yan, H., Ong, I. M., Chung, D., Liang, K., Tran, F., Keles, S., Landick, R. and Kiley, P. J. (2013). Genome-scale analysis of *Escherichia coli* FNR reveals complex features of transcription factor binding. *PLoS Genet*, 9 (6): e1003565. doi: 10.1371/journal.pgen.1003565.
- Niebisch, A. and Bott, M. (2001). Molecular analysis of the cytochrome *bc₁-aa₃* branch of the *Corynebacterium glutamicum* respiratory chain containing an unusual diheme cytochrome *c₁*. *Arch Microbiol*, 175 (4): 282-94.
- Niebisch, A. and Bott, M. (2003). Purification of a cytochrome *bc₁-aa₃* supercomplex with quinol oxidase activity from *Corynebacterium glutamicum*. Identification of a fourth subunit of cytochrome *aa₃* oxidase and mutational analysis of diheme cytochrome *c₁*. *J Biol Chem*, 278 (6): 4339-46. doi: 10.1074/jbc.M210499200.
- Nilsson, R., Schultz, I. J., Pierce, E. L., Soltis, K. A., Naranuntarat, A., Ward, D. M., Baughman, J. M., Paradkar, P. N., Kingsley, P. D., Culotta, V. C., Kaplan, J., Palis, J., Paw, B. H. and Mootha, V. K. (2009). Discovery of genes essential for heme biosynthesis through large-scale gene expression analysis. *Cell Metab*, 10 (2): 119-30. doi: 10.1016/j.cmet.2009.06.012.
- Ogawa, K., Sun, J., Taketani, S., Nakajima, O., Nishitani, C., Sassa, S., Hayashi, N., Yamamoto, M., Shibahara, S., Fujita, H. and Igarashi, K. (2001). Heme mediates derepression of Maf recognition element through direct binding to transcription repressor Bach1. *The EMBO journal*, 20. doi: 10.1093/emboj/20.11.2835.

- Olson, E. R., Duniak, D. S., Jurss, L. M. and Poorman, R. A. (1991). Identification and characterization of *dppA*, an *Escherichia coli* gene encoding a periplasmic dipeptide transport protein. *J Bacteriol*, 173 (1): 234-44.
- Pannen, D., Fabisch, M., Gausling, L. and Schnetz, K. (2016). Interaction of the RcsB Response Regulator with Auxiliary Transcription Regulators in *Escherichia coli*. *J Biol Chem*, 291 (5): 2357-70. doi: 10.1074/jbc.M115.696815.
- Pappenheimer, A. M. and Johnson, S. J. (1936). Studies in Diphtheria Toxin Production. I: The Effect of Iron and Copper. *British Journal of Experimental Pathology*, 17 (5): 335-341.
- Park, D. M., Akhtar, M. S., Ansari, A. Z., Landick, R. and Kiley, P. J. (2013). The bacterial response regulator ArcA uses a diverse binding site architecture to regulate carbon oxidation globally. *PLoS Genet*, 9 (10): e1003839. doi: 10.1371/journal.pgen.1003839.
- Parkinson, J. S. and Kofoid, E. C. (1992). Communication modules in bacterial signaling proteins. *Annu Rev Genet*, 26: 71-112. doi: 10.1146/annurev.ge.26.120192.000443.
- Parkinson, J. S. (1993). Signal transduction schemes of bacteria. *Cell*, 73 (5): 857-71.
- Pazy, Y., Motaleb, M. A., Guarnieri, M. T., Charon, N. W., Zhao, R. and Silversmith, R. E. (2010). Identical phosphatase mechanisms achieved through distinct modes of binding phosphoprotein substrate. *Proc Natl Acad Sci U S A*, 107 (5): 1924-9. doi: 10.1073/pnas.0911185107.
- Peuser, V., Remes, B. and Klug, G. (2012). Role of the Irr protein in the regulation of iron metabolism in *Rhodobacter sphaeroides*. *PLoS One*, 7 (8): e42231. doi: 10.1371/journal.pone.0042231.
- Pi, H. and Helmann, J. D. (2017). Sequential induction of Fur-regulated genes in response to iron limitation in *Bacillus subtilis*. *Proc Natl Acad Sci U S A*, 114 (48): 12785-12790. doi: 10.1073/pnas.1713008114.
- Pi, H. and Helmann, J. D. (2018). Genome-wide characterization of the Fur regulatory network reveals a link between catechol degradation and bacillibactin metabolism in *Bacillus subtilis*. doi: 10.1101/364588 %J bioRxiv.
- Pohl, E., Haller, J. C., Mijovilovich, A., Meyer-Klaucke, W., Garman, E. and Vasil, M. L. (2003). Architecture of a protein central to iron homeostasis: crystal structure and spectroscopic analysis of the ferric uptake regulator. *Mol Microbiol*, 47 (4): 903-15.
- Ponka, P. (1999). Cell biology of heme. *Am J Med Sci*, 318 (4): 241-56.
- Qi, Z., Hamza, I. and O'Brian, M. R. (1999). Heme is an effector molecule for iron-dependent degradation of the bacterial iron response regulator (Irr) protein. *Proc Natl Acad Sci U S A*, 96 (23): 13056-61.
- Qi, Z. and O'Brian, M. R. (2002). Interaction between the bacterial iron response regulator and ferrochelatase mediates genetic control of heme biosynthesis. *Mol Cell*, 9 (1): 155-62.
- Rudolph, G., Semini, G., Hauser, F., Lindemann, A., Friberg, M., Hennecke, H. and Fischer, H. M. (2006). The Iron control element, acting in positive and negative control of iron-regulated *Bradyrhizobium japonicum* genes, is a target for the Irr protein. *J Bacteriol*, 188 (2): 733-44. doi: 10.1128/jb.188.2.733-744.2006.
- Salvi, M., Schomburg, B., Giller, K., Graf, S., Unden, G., Becker, S., Lange, A. and Griesinger, C. (2017). Sensory domain contraction in histidine kinase CitA triggers transmembrane signaling in the membrane-bound sensor. *Proc Natl Acad Sci U S A*, 114 (12): 3115-3120. doi: 10.1073/pnas.1620286114.
- Santos, J. L. and Shiozaki, K. (2001). Fungal histidine kinases. *Sci STKE*, 2001 (98): re1. doi: 10.1126/stke.2001.98.re1.
- Schagger, H. (2002). Respiratory chain supercomplexes of mitochondria and bacteria. *Biochim Biophys Acta*, 1555 (1-3): 154-9.
- Schelder, S., Zaade, D., Litsanov, B., Bott, M. and Brocker, M. (2011). The two-component signal transduction system CopRS of *Corynebacterium glutamicum* is required for adaptation to copper-excess stress. *PLoS One*, 6 (7): e22143. doi: 10.1371/journal.pone.0022143.

- Scheu, P. D., Witan, J., Rauschmeier, M., Graf, S., Liao, Y. F., Ebert-Jung, A., Basche, T., Erker, W. and Unden, G. (2012). CitA/CitB two-component system regulating citrate fermentation in *Escherichia coli* and its relation to the DcuS/DcuR system in vivo. *J Bacteriol*, 194 (3): 636-45. doi: 10.1128/jb.06345-11.
- Schmitt, M. P. and Holmes, R. K. (1991). Iron-dependent regulation of diphtheria toxin and siderophore expression by the cloned *Corynebacterium diphtheriae* repressor gene *dtxR* in *C. diphtheriae* C7 strains. *Infect Immun*, 59 (6): 1899-904.
- Seo, S. W., Kim, D., Latif, H., O'Brien, E. J., Szubin, R. and Palsson, B. O. (2014). Deciphering Fur transcriptional regulatory network highlights its complex role beyond iron metabolism in *Escherichia coli*. *Nat Commun*, 5: 4910. doi: 10.1038/ncomms5910.
- Sidote, D. J., Barbieri, C. M., Wu, T. and Stock, A. M. (2008). Structure of the *Staphylococcus aureus* AgrA LytTR domain bound to DNA reveals a beta fold with an unusual mode of binding. *Structure*, 16 (5): 727-35. doi: 10.1016/j.str.2008.02.011.
- Silversmith, R. E. (2010). Auxiliary phosphatases in two-component signal transduction. *Curr Opin Microbiol*, 13 (2): 177-83. doi: 10.1016/j.mib.2010.01.004.
- Stauff, D. L. and Skaar, E. P. (2009a). *Bacillus anthracis* HssRS signalling to HrtAB regulates haem resistance during infection. *Mol Microbiol*, 72 (3): 763-78. doi: 10.1111/j.1365-2958.2009.06684.x.
- Stauff, D. L. and Skaar, E. P. (2009b). The heme sensor system of *Staphylococcus aureus*. *Contrib Microbiol*, 16: 120-35. doi: 10.1159/000219376.
- Steele, K. H., O'Connor, L. H., Burpo, N., Kohler, K. and Johnston, J. W. (2012). Characterization of a ferrous iron-responsive two-component system in nontypeable *Haemophilus influenzae*. *J Bacteriol*, 194 (22): 6162-73. doi: 10.1128/jb.01465-12.
- Stock, A. M., Robinson, V. L. and Goudreau, P. N. (2000). Two-component signal transduction. *Annu Rev Biochem*, 69: 183-215. doi: 10.1146/annurev.biochem.69.1.183.
- Stojiljkovic, I., Kumar, V. and Srinivasan, N. (1999). Non-iron metalloporphyrins: potent antibacterial compounds that exploit haem/Hb uptake systems of pathogenic bacteria. *Mol Microbiol*, 31 (2): 429-42.
- Storz, G., Vogel, J. and Wassarman, K. M. (2011). Regulation by small RNAs in bacteria: expanding frontiers. *Mol Cell*, 43 (6): 880-91. doi: 10.1016/j.molcel.2011.08.022.
- Sun, J., Hoshino, H., Takaku, K., Nakajima, O., Muto, A., Suzuki, H., Tashiro, S., Takahashi, S., Shibahara, S., Alam, J., Taketo, M. M., Yamamoto, M. and Igarashi, K. (2002). Hemoprotein Bach1 regulates enhancer availability of heme oxygenase-1 gene. *The EMBO journal*, 21. doi: 10.1093/emboj/cdf516.
- Svensson, B., Lubben, M. and Hederstedt, L. (1993). *Bacillus subtilis* CtaA and CtaB function in haem A biosynthesis. *Mol Microbiol*, 10 (1): 193-201.
- Teramoto, H., Inui, M. and Yukawa, H. (2013). OxyR acts as a transcriptional repressor of hydrogen peroxide-inducible antioxidant genes in *Corynebacterium glutamicum* R. *Febs j*, 280 (14): 3298-312. doi: 10.1111/febs.12312.
- Teramoto, H., Yukawa, H. and Inui, M. (2015). Copper homeostasis-related genes in three separate transcriptional units regulated by CsoR in *Corynebacterium glutamicum*. *Appl Microbiol Biotechnol*, 99 (8): 3505-17. doi: 10.1007/s00253-015-6373-z.
- Tiwari, S., Jamal, S. B., Hassan, S. S., Carvalho, P. V. S. D., Almeida, S., Barh, D., Ghosh, P., Silva, A., Castro, T. L. P. and Azevedo, V. (2017). Two-Component Signal Transduction Systems of Pathogenic Bacteria As Targets for Antimicrobial Therapy: An Overview. *Frontiers in Microbiology*, 8: 1878. doi: 10.3389/fmicb.2017.01878.
- Toyoda, K. and Inui, M. (2016). The extracytoplasmic function sigma factor sigma(C) regulates expression of a branched quinol oxidation pathway in *Corynebacterium glutamicum*. *Mol Microbiol*, 100 (3): 486-509. doi: 10.1111/mmi.13330.
- Ulrich, L. E., Koonin, E. V. and Zhulin, I. B. (2005). One-component systems dominate signal transduction in prokaryotes. *Trends Microbiol*, 13 (2): 52-6. doi: 10.1016/j.tim.2004.12.006.

- Wakeman, C. A., Stauff, D. L., Zhang, Y. and Skaar, E. P. (2014). Differential activation of *Staphylococcus aureus* heme detoxification machinery by heme analogues. *J Bacteriol*, 196 (7): 1335-42. doi: 10.1128/jb.01067-13.
- Wanner, B. L. and Chang, B. D. (1987). The phoBR operon in *Escherichia coli* K-12. *J Bacteriol*, 169 (12): 5569-74.
- Warnatz, H. J., Schmidt, D., Manke, T., Piccini, I., Sultan, M., Borodina, T., Balzereit, D., Wruck, W., Soldatov, A., Vingron, M., Lehrach, H. and Yaspo, M. L. (2011). The BTB and CNC homology 1 (BACH1) target genes are involved in the oxidative stress response and in control of the cell cycle. *J Biol Chem*, 286 (26): 23521-32. doi: 10.1074/jbc.M111.220178.
- Weiss, V., Kramer, G., Dunnebier, T. and Flotho, A. (2002). Mechanism of regulation of the bifunctional histidine kinase NtrB in *Escherichia coli*. *J Mol Microbiol Biotechnol*, 4 (3): 229-33.
- Wennerhold, J. and Bott, M. (2006). The DtxR regulon of *Corynebacterium glutamicum*. *J Bacteriol*, 188 (8): 2907-18. doi: 10.1128/jb.188.8.2907-2918.2006.
- West, A. H., Martinez-Hackert, E. and Stock, A. M. (1995). Crystal structure of the catalytic domain of the chemotaxis receptor methylesterase, CheB. *J Mol Biol*, 250 (2): 276-90. doi: 10.1006/jmbi.1995.0376.
- Wilks, A. (2002). Heme oxygenase: evolution, structure, and mechanism. *Antioxid Redox Signal*, 4 (4): 603-14. doi: 10.1089/15230860260220102.
- Wilks, A. and Ikeda-Saito, M. (2014). Heme utilization by pathogenic bacteria: not all pathways lead to biliverdin. *Acc Chem Res*, 47 (8): 2291-8. doi: 10.1021/ar500028n.
- Willett, J. W. and Kirby, J. R. (2012). Genetic and Biochemical Dissection of a HisKA Domain Identifies Residues Required Exclusively for Kinase and Phosphatase Activities. *PLoS Genetics*, 8 (11): e1003084. doi: 10.1371/journal.pgen.1003084.
- Wolanin, P. M., Thomason, P. A. and Stock, J. B. (2002). Histidine protein kinases: key signal transducers outside the animal kingdom. *Genome Biol*, 3 (10): Reviews3013.
- Xu, I. M., Lai, R. K., Lin, S. H., Tse, A. P., Chiu, D. K., Koh, H. Y., Law, C. T., Wong, C. M., Cai, Z., Wong, C. C. and Ng, I. O. (2016). Transketolase counteracts oxidative stress to drive cancer development. *Proc Natl Acad Sci U S A*, 113 (6): E725-34. doi: 10.1073/pnas.1508779113.
- Zenke-Kawasaki, Y., Dohi, Y., Katoh, Y., Ikura, T., Ikura, M., Asahara, T., Tokunaga, F., Iwai, K. and Igarashi, K. (2007). Heme induces ubiquitination and degradation of the transcription factor Bach1. *Molecular and cellular biology*, 27. doi: 10.1128/mcb.02415-06.
- Zhang, L. and Hach, A. (1999). Molecular mechanism of heme signaling in yeast: the transcriptional activator Hap1 serves as the key mediator. *Cell Mol Life Sci*, 56 (5-6): 415-26.
- Zhao, R., Collins, E. J., Bourret, R. B. and Silversmith, R. E. (2002). Structure and catalytic mechanism of the *E. coli* chemotaxis phosphatase CheZ. *Nat Struct Biol*, 9 (8): 570-5. doi: 10.1038/nsb816.
- Zitomer, R. S., Carrico, P. and Deckert, J. (1997). Regulation of hypoxic gene expression in yeast. *Kidney Int*, 51 (2): 507-13.

5. Appendix

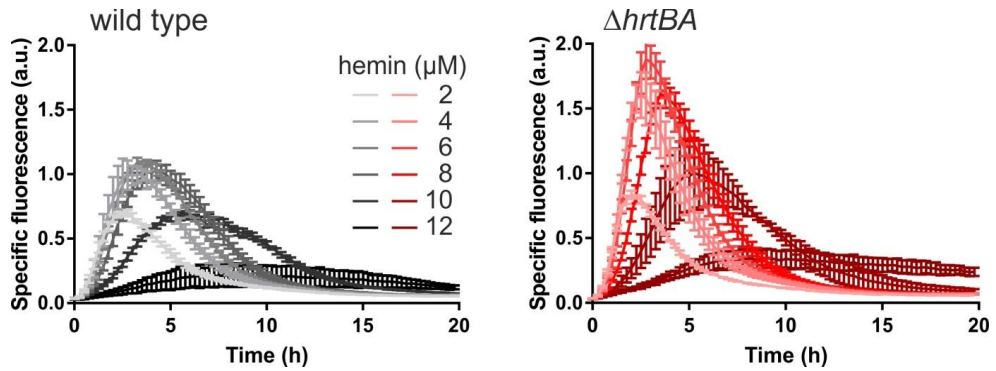


Figure S1: Reporter screening, P_{hrtBA}

Reporter output of *C. glutamicum* wild type and $\Delta hrtBA$ mutant strains carrying the vector pJC1_ P_{hrtBA} -*eyfp*. Cells were inoculated in CGXII minimal medium with 2% (w/v) glucose containing hemin in varying concentrations as iron source. For further information on target gene reporter screenings, see Keppel *et al.* (2018c).

P_{hrrS} -*eyfp*

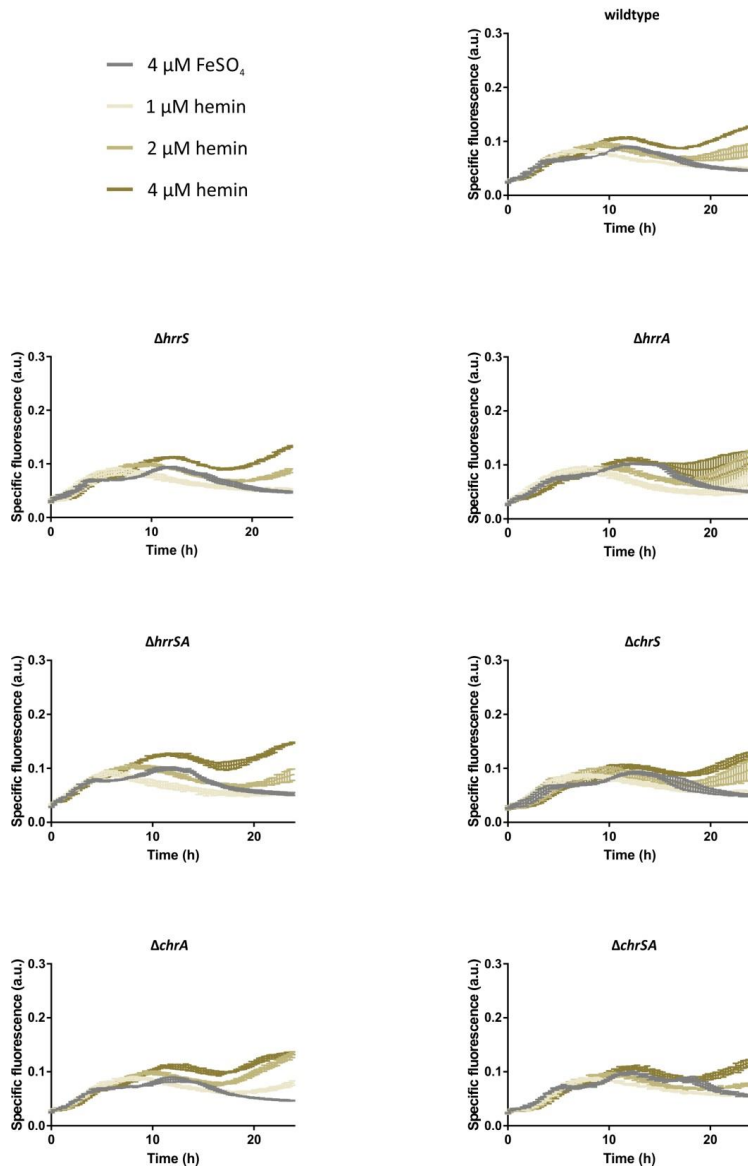


Figure S2: Reporter screening, P_{hrrS}

Reporter output of *C. glutamicum* wild type and mutant strains carrying the vector pJC1_ P_{hrrS} -*eyfp*. Cells were inoculated in CGXII minimal medium with 2% (w/v) glucose containing either hemin or FeSO_4 as iron source.

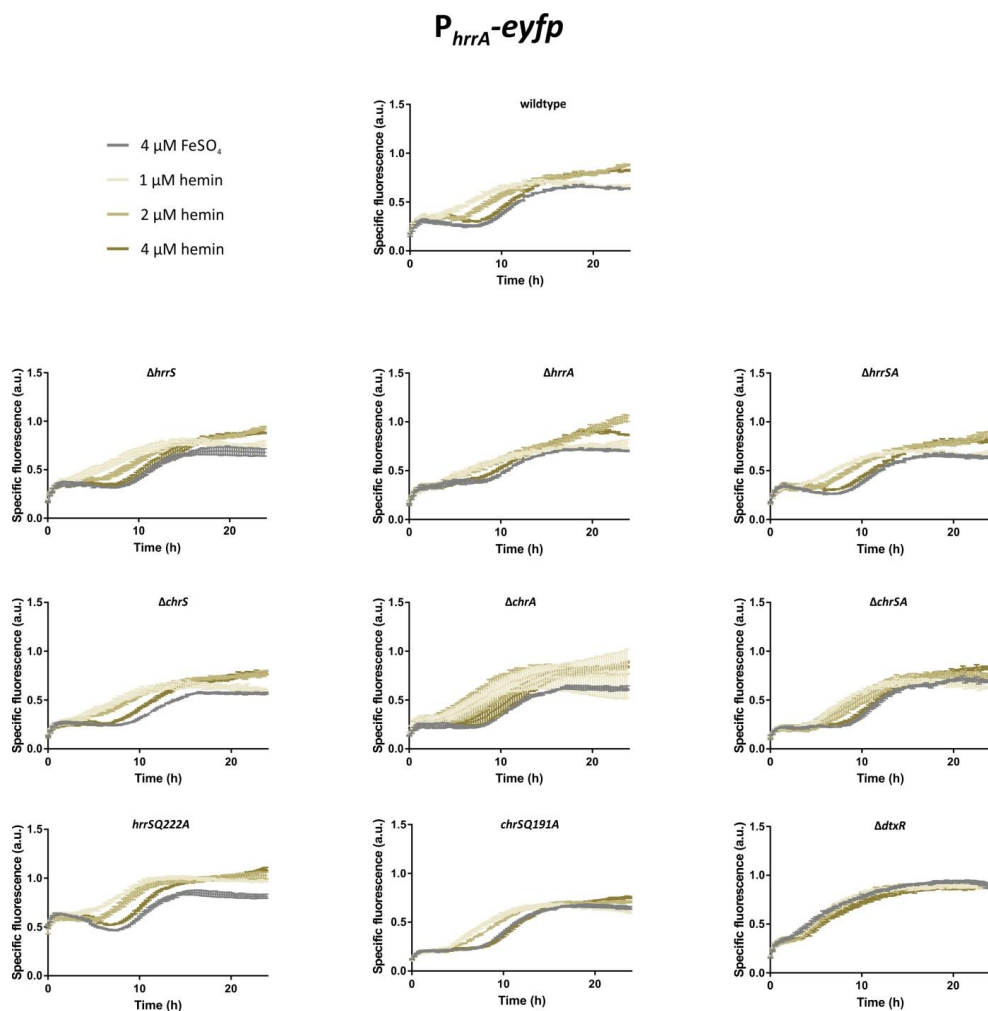


Figure S3: Reporter screening, P_{hrrA}

Reporter output of *C. glutamicum* wild type and mutant strains carrying the vector pJC1_P_{hrrA}-*eyfp*. Cells were inoculated in CGXII minimal medium with 2% (w/v) glucose containing either hemin or FeSO_4 as iron source.

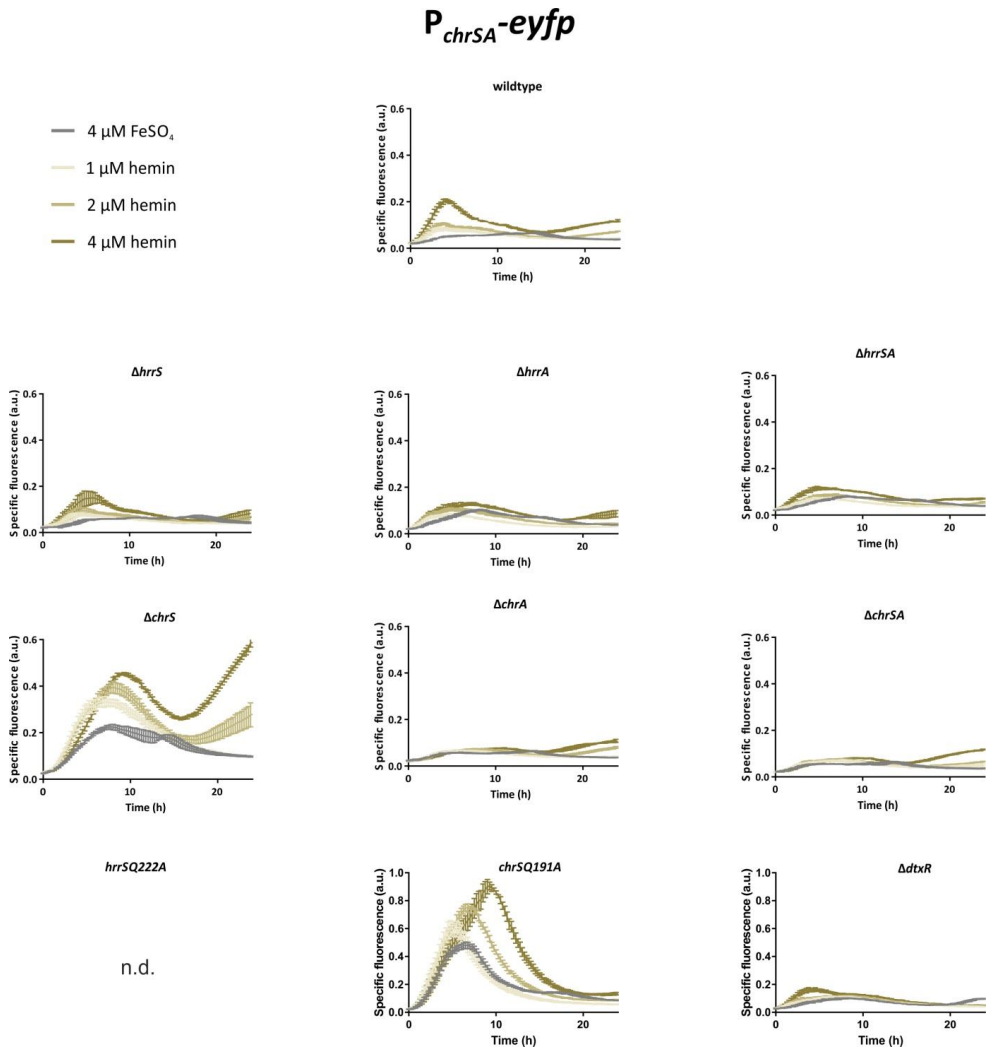


Figure S4: Reporter screening, P_{chrSA}

Reporter output of *C. glutamicum* wild type and mutant strains carrying the vector pJC1_ $P_{chrSA-eyfp}$. Cells were inoculated in CGXII minimal medium with 2% (w/v) glucose containing either hemin or FeSO_4 as iron source.

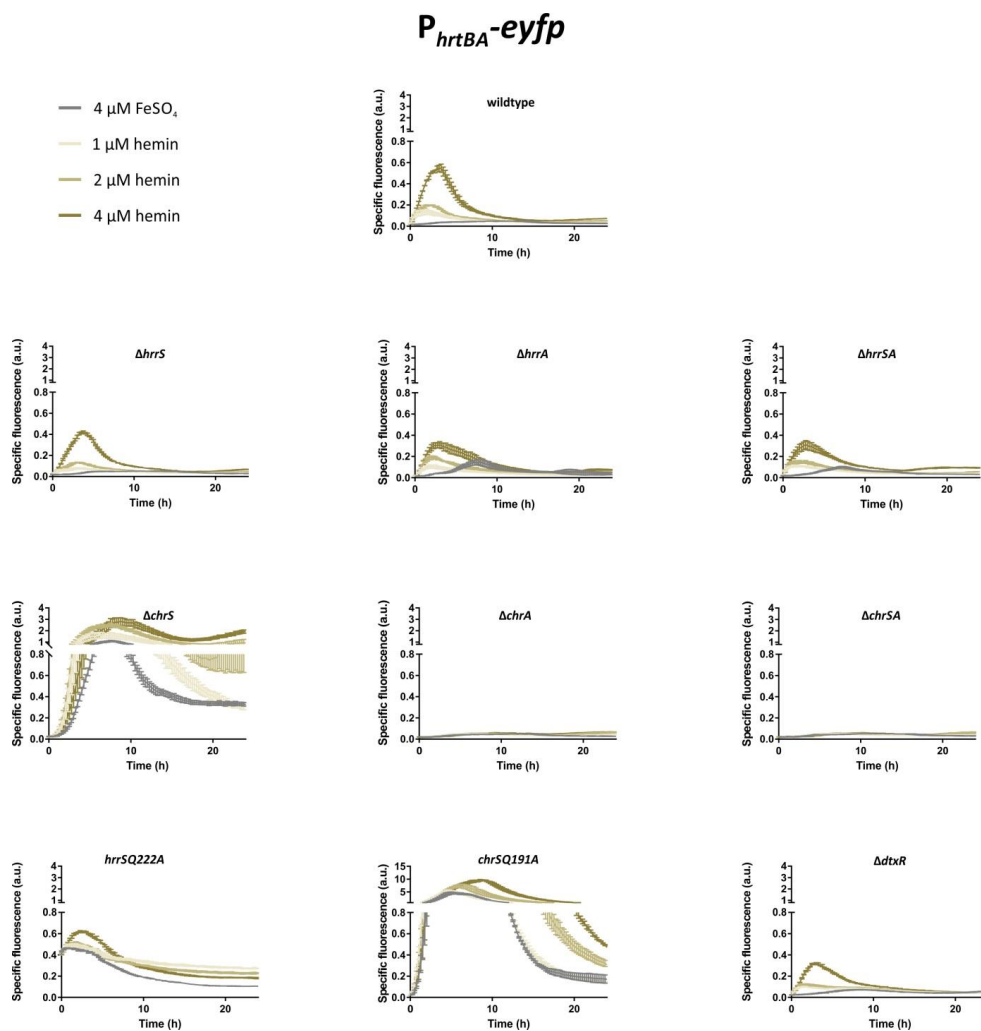


Figure S5: Reporter screening, P_{hrtBA}

Reporter output of *C. glutamicum* wild type and mutant strains carrying the vector pJC1- P_{hrtBA} -*eyfp*. Cells were inoculated in CGXII minimal medium with 2% (w/v) glucose containing either hemin or FeSO_4 as iron source.

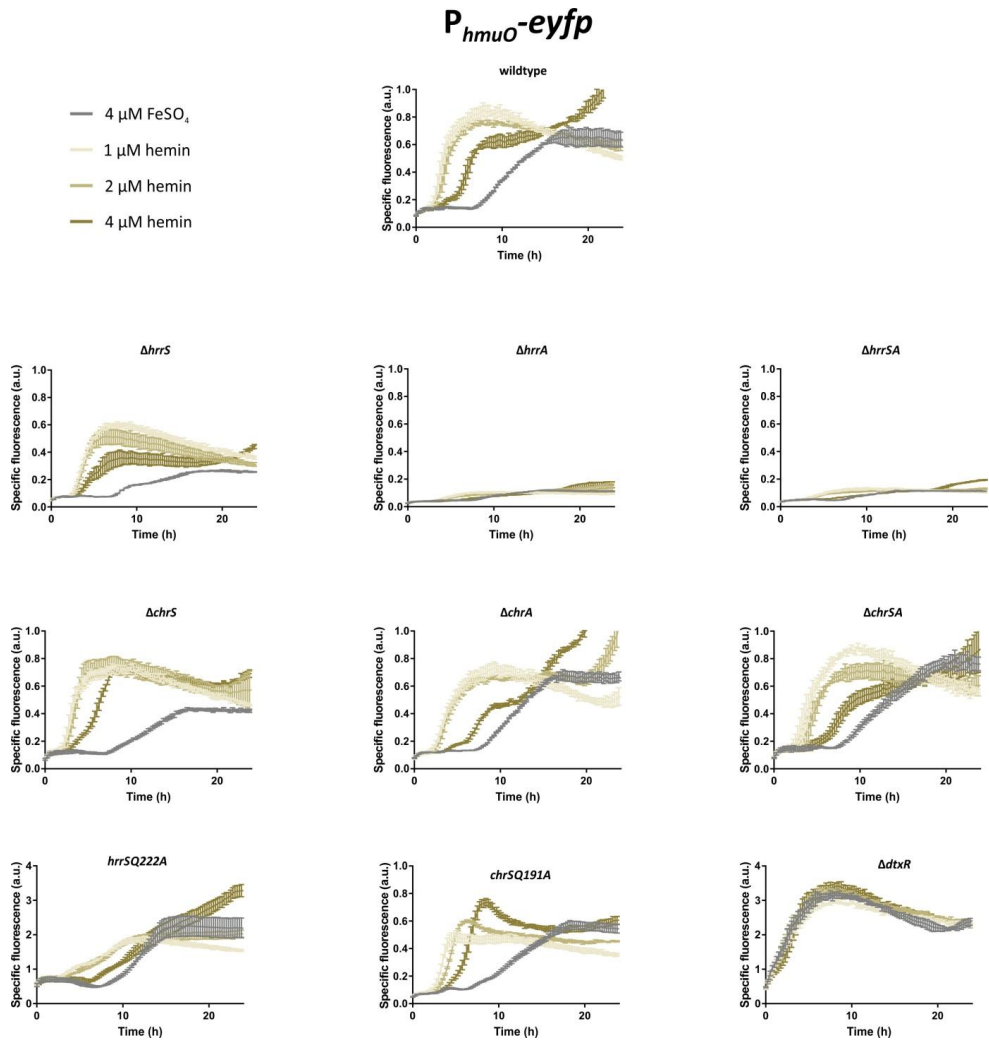


Figure S6: Reporter screening, P_{hmuO}

Reporter output of *C. glutamicum* wild type and mutant strains carrying the vector pJC1_ P_{hmuO} -*eyfp*. Cells were inoculated in CGXII minimal medium with 2% (w/v) glucose containing either hemin or FeSO_4 as iron source

5.1 Supplement “Membrane Topology and Heme Binding of the Histidine Kinases HrrS and ChrS”



Supplementary Material

Membrane topology and heme binding of the histidine kinases HrrS and ChrS in *Corynebacterium glutamicum*

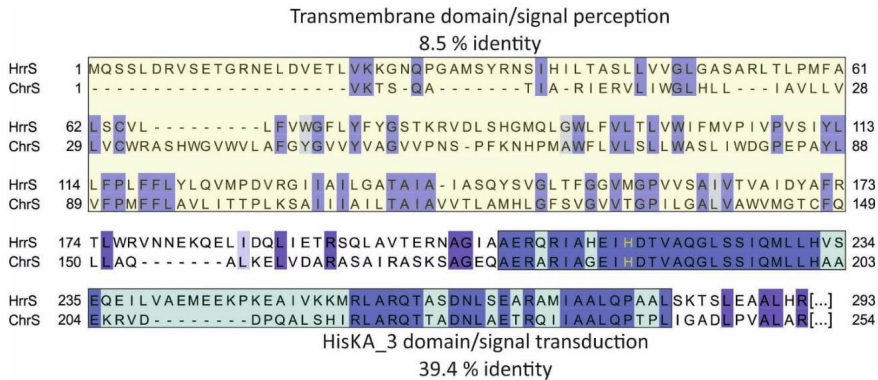
Marc Keppel¹, Eva Davoudi¹, Cornelia Gätgens¹, and Julia Frunzke^{1*}

¹Institute of Bio- und Geosciences, IBG-1: Biotechnology, Forschungszentrum Jülich, 52425 Jülich, Germany

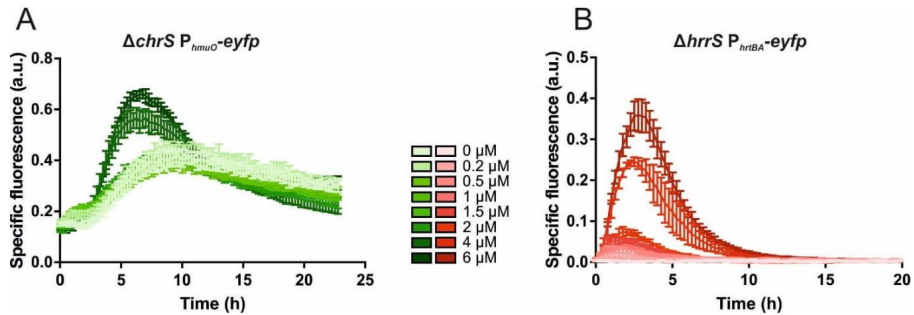
*Corresponding author: Julia Frunzke; Email: j.frunzke@fz-juelich.de; Phone: +49 2461 615430

Supplementary Material

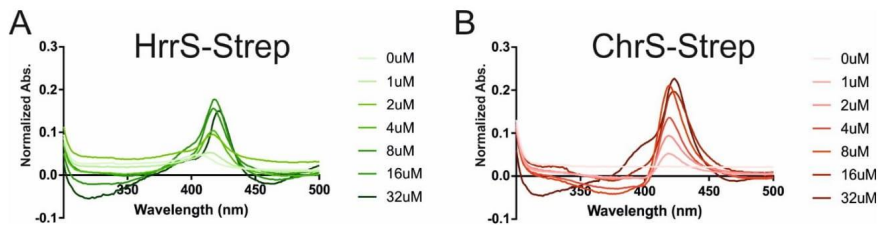
- 1 Supplementary Data
- 2 Supplementary Figures and Tables
- 2.1 Supplementary Figures



Supplementary Figure S1 - Amino acid sequence alignment of the histidine kinases HrrS and ChrS of *C. glutamicum*. The alignment was performed using Clustal Omega and jalview. Sequences were obtained from the NCBI database (<https://blast.ncbi.nlm.nih.gov>).



Supplementary Figure S2 - Promoter profiling in $\Delta hrrS$ and $\Delta chrS$ deletion mutants. The *C. glutamicum* mutant $\Delta chrS$ or $\Delta hrrS$ were transformed with the target gene reporter pJC1- $P_{hmuO-eyfp}$ or pJC1- $P_{hrrBA-eyfp}$, respectively. Cells were cultivated in a microbioreactor system (Biolector) in CGXII minimal medium with 2% (w/v) glucose containing 0-6 μM hemin. The specific fluorescence was referenced against the reporter output of strains showing background level of the particular reporter construct as described previously ($\Delta hrrSA / pJC1-P_{hmuO-eyfp}$ and $\Delta chrSA / pJC1-P_{hrrBA-eyfp}$ (Hentschel et al., 2014)).

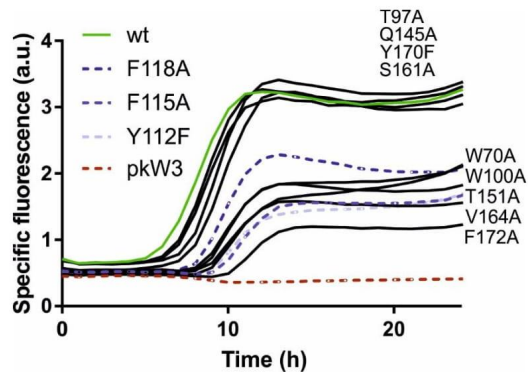


Supplementary Figure S3 - UV-Vis analysis of the heme binding properties of HrrS and ChrS. For hemin binding assays, different amounts of hemin were titrated to 10 μM of purified HrrS or ChrS protein to a final concentration of 0, 2, 4, 8, 16 and 32 μM . The mixture was incubated for 5 min at RT and then analyzed by UV-visual spectroscopy. The resulting absorption was referenced against the absorption of buffer containing only DDM micelles without protein.

Supplementary Material

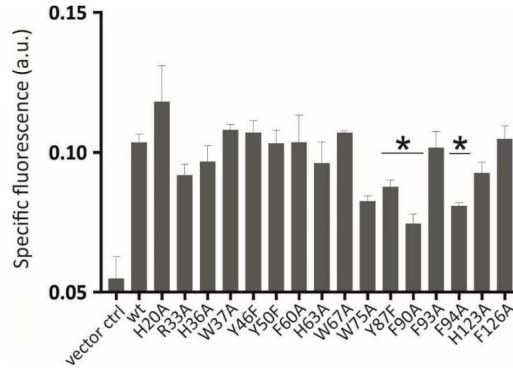
C. glutamicum	1	MQSSLDR	-----VSETGRN-----ELDVETLVKKGNGPGAMYSRNS	THITASLTVVGLG	-----ASARLTL	MFAL	62	
C. pseudogenitulum	1	-----	-----MRTGHIITAGLVVGF	-----	-----TSARML	SQLI	1	
C. aurumcum	1	MG-SWASEHP	-----TVAKPMPITGA-AKEGSR	-----WR-MTSTLDORSVESDALRNC	-----HVIITATLLVVA	IF-----	TVRRLPLWQGL	73
C. diptheriae	1	MQSSLDFEKPSGT	-----SHLTGTD	-----LDVSHHTGRPAALYRSMV	-----LTVALLVSL	-----	GVVSL-DRRS	64
C. difcens	1	MQSSLDR	-----GQDSMRN-----ELDVENLRGGGPGAMYSRNS	-----HITATLVVGLG	-----	-----ASARLPL	PMFAV	62
C. pseudotuberculosis	1	MLRSLDPDPPNSARLPERHGSDGK	AGDPTLGLFDVTDGSR	-----D-----GHLEAHAGGPGAALYRRAMN	-----ITVLLIVS	-----	GVVRL-DTR	58
C. silicenos	1	-----	-----M-----VHLEDHVGPGAALYRRAMN	-----LTMVLLIVS	-----	-----	GVVRL-DTR	58
C. matruchotii	1	-----	-----MKSNGLEASKSNI	-----A-----GDVSTYDSQPGAAFRAMN	-----LTVALLVSL	-----	AAVRTGDV	59
C. glaucanonylium	1	-----	-----MATNRHAGPFSYTVG	-----HIITALLAVTVA	-----	-----	TSLTVLI	62
C. lipophilum	1	-----	-----MTRSRL-----VK-----LDSQPREVDNKLDTG	-----HITVLSL	-----	-----	ALLQMLNS	50
C. gentium	1	-----	-----MVSTV-----SAESGRDRVAGLPDNRALDTG	-----AALTVALLVSLG	-----	-----	GVFRMHIS	53
C. subcolastricum	1	-----	-----KPSDSKMKVVALNRWAVLSMGLHLMAL	-----LMAVAVIV	-----	-----	RDG-W	59
C. glutamicum	1	-----	-----MREDSRL-----FR-MMSTIEGRSPDTEALRNL	-----	-----	-----	HTVRLPLWQ	53
C. glutamicum	1	-----	-----	-----HMLITAVL	-----	-----	RASHW	23
C. glutamicum	1	-----	-----MIYRGGVKTSGAT	-----IARIERVL	-----	-----	IWGLHLL	47
C. glutamicum	1	-----	-----MMHRE-----KPSDSKMKVVALNRWAVLSMGLHLMAL	-----LMAVAVIV	-----	-----	RDG-W	59
C. areolatum	1	-----	-----MNEPDRTHLSAQPVTGKLSHGLWGLQVLMIGL	-----LILVAV	-----	-----	RATHPMTW	49
C. amycolatum	1	-----	-----MDPTNLRNSQWLLRFALDVLVLLAVCV	-----	-----	-----	PPQWR	1
C. resistens	1	-----	-----MIGRKAMHGHLEARSVDQLDRWVTLGHS	-----LHLLVFL	-----	-----	ILAVTVA	52
C. lipophilum	1	-----	-----MTSRL-----VK-----LDSQPREVDNKLDTG	-----HITVLSL	-----	-----	ALLQMLNS	50
C. pseudotuberculosis	1	-----	-----MRPHIQ	-----LITL	-----	-----	RVSLHMF	46
C. glutamicum	63	CVLLFVWGFVYFSTKRRVD	-----LSHGDLQGLFVLTWVFP	-----IPVYS	-----	-----	VMPDPRG	173
C. pseudogenitulum	31	-----	-----WARPVRYLWCLISLVWADLP	-----VAPAA	-----	-----	PLVFLVTLDMAG	113
C. aurumcum	74	NLLLVSAFVAVYFGGSAYLE	-----LPRVARYGWMV	-----LTVLWADL	-----	-----	VAPAA	156
C. diptheriae	65	VAVILSALFALFYAA-AAVSHR	-----RAMWTKAML	-----LITLVWVFL	-----	-----	PIIPVSI	147
C. difcens	63	CVLLFVWGFVYFGSSRRVT	-----FAHTKQLAW	-----FVLTWVWML	-----	-----	PIIPVSI	145
C. pseudotuberculosis	46	IHAVLSAFFALYSL-IVLQY	-----TKLWD	-----LILLAA	-----	-----	TLVWVLP	171
C. silicenos	46	IHAVLSAFFALYSL-IVLQY	-----TRLWQL	-----LFGAL	-----	-----	TLVWVLP	171
C. matruchotii	60	VAVILCILFAFFYTM-AVTRIR	-----DRMLK	-----KIMWAGL	-----	-----	TAVVW	142
C. glaucanonylium	43	VSF LAVITFGA IYAGNHFFHQ	-----LNSTQHLWAF	-----GTLW	-----	-----	LILLPHLS	125
C. lipophilum	51	HIVLSIFAFLLFYGLVEMPR	-----WGRAGAGW	-----LMLTGMW	-----	-----	ADMMV	134
C. gentium	54	LVLVLIITFGG IYSGFALQMR	-----WNA	-----IARV	-----	-----	WMLALTAVVW	124
C. tuberculostearicum	42	NLLLVSAFVAVYFGGSAYLE	-----LPRVARYGWMV	-----LTVLWADL	-----	-----	VAPAA	156
C. glutamicum	54	NLLLVSAFVAVYFGGSAYLE	-----LPRVARYGWMV	-----LTVLWADL	-----	-----	VAPAA	156
C. glutamicum	48	-----LAFYGVVYVAGVVPNS	-----	-----PFKNHPMAW	-----	-----	FLVLSLWASL	126
C. lipophilum	50	-----VALCFIYVMGLW	-----	-----RPTWL	-----	-----	WLTVL	117
C. areolatum	50	-----GLGVFWLVCYGRVTR	-----	-----W	-----	-----	LGAPTFW	128
C. amycolatum	41	-----YAAFLAVYIGDSVYGR	-----	-----IRGR	-----	-----	HRHDVANEAL	134
C. resistens	53	-----GAFAYASGRIL	-----	-----PQRL	-----	-----	WMLALVLCW	124
C. lipophilum	51	HIVLSIFAFLLFYGLVEMPR	-----WGRAGAGW	-----LMLTGMW	-----	-----	ADMMV	134
C. pseudotuberculosis	47	-----TLALGLGAFYMGFTAWENRFRGDN	-----	-----DPMPL	-----	-----	SGWMLVITL	131
C. glutamicum	146	YSVGLTFGVWGFVYFSTKRRVD	-----LSHGDLQGLFVLTWVFP	-----IPVYS	-----	-----	VMPDPRG	173
C. pseudogenitulum	114	IPGGLTFGVWGFVYFSTKRRVD	-----LSHGDLQGLFVLTWVFP	-----IPVYS	-----	-----	VMPDPRG	173
C. aurumcum	157	IPGGLTFGVWGFVYFSTKRRVD	-----LSHGDLQGLFVLTWVFP	-----IPVYS	-----	-----	VMPDPRG	173
C. diptheriae	146	YVPGVLTGQVWGFVYFSTKRRVD	-----LSHGDLQGLFVLTWVFP	-----IPVYS	-----	-----	VMPDPRG	173
C. pseudotuberculosis	172	MP-DLTLGAVMPLVYFSTKRRVD	-----LSHGDLQGLFVLTWVFP	-----IPVYS	-----	-----	VMPDPRG	173
C. silicenos	129	MP-DLTLGAVMPLVYFSTKRRVD	-----LSHGDLQGLFVLTWVFP	-----IPVYS	-----	-----	VMPDPRG	173
C. matruchotii	143	RA-HLTVGAVMPLVYFSTKRRVD	-----LSHGDLQGLFVLTWVFP	-----IPVYS	-----	-----	VMPDPRG	173
C. glaucanonylium	126	IPGTITGAVMPLVYFSTKRRVD	-----LSHGDLQGLFVLTWVFP	-----IPVYS	-----	-----	VMPDPRG	173
C. lipophilum	134	VPTGLTFGVWGFVYFSTKRRVD	-----LSHGDLQGLFVLTWVFP	-----IPVYS	-----	-----	VMPDPRG	173
C. gentium	137	IPGGLTFGVWGFVYFSTKRRVD	-----LSHGDLQGLFVLTWVFP	-----IPVYS	-----	-----	VMPDPRG	173
C. subcolastricum	125	IPGGLTFGVWGFVYFSTKRRVD	-----LSHGDLQGLFVLTWVFP	-----IPVYS	-----	-----	VMPDPRG	173
C. stratum	137	IPGGLTFGVWGFVYFSTKRRVD	-----LSHGDLQGLFVLTWVFP	-----IPVYS	-----	-----	VMPDPRG	173
C. glutamicum	103	AMHLGFSVGVVTFILGALVAVWVGTFCFLLAD	-----	-----AL	-----	-----	KELV	192
C. glutamicum	127	AMHLGFSVGVVTFILGALVAVWVGTFCFLLAD	-----	-----AL	-----	-----	KELV	192
C. lipophilum	119	-----VYGGDGLSIFVAVVATVYVGGVGF	-----	-----LHRE	-----	-----	AKARALD	226
C. areolatum	127	VGHIGWNI	-----	-----IGAV	-----	-----	VAVT	226
C. amycolatum	135	AVHPTLFGVWGFVYFSTKRRVD	-----LSHGDLQGLFVLTWVFP	-----IPVYS	-----	-----	VMPDPRG	173
C. resistens	125	ARHLGWSVGVVTFILGALVAVWVGTFCFLLAD	-----	-----AL	-----	-----	KELV	192
C. lipophilum	134	VPTGLTFGVWGFVYFSTKRRVD	-----LSHGDLQGLFVLTWVFP	-----IPVYS	-----	-----	VMPDPRG	173
C. pseudotuberculosis	138	ARPEDRVLLGDLGILIGACFSVAIYGGVYV	-----	-----ND	-----	-----	AMHYRQVA	237

Supplementary Figure S4 - Sequence alignment of HrrS (top) and ChrS (bottom) of different *Corynebacteriaceae*. Alignment was performed using Clustal Omega and Jalview. Sequences were obtained from the NCBI database (<https://blast.ncbi.nlm.nih.gov>). Asterisks mark amino acids analyzed by alanine-scanning of HrrS (Figure 4) and ChrS (Figure S6). The conserved trio (Y112-F115-F118, in *C. glutamicum* HrrS) of aromatic residues are highlighted in yellow. Exchange of the respective residues resulted in an almost abolished heme-binding of HrrS *in vitro* (Figure 5 and 6).

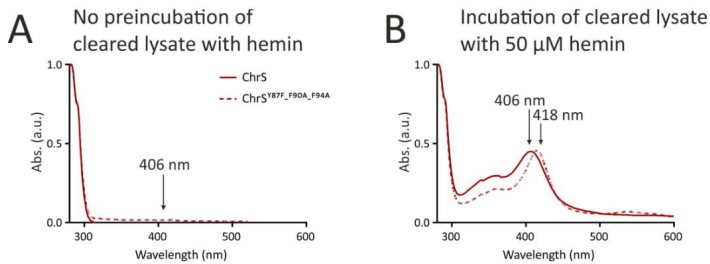


Supplementary Figure S5 - Alanine scanning of the transmembrane domain of HrrS reveals putative heme binding residues. The *C. glutamicum* mutant strain $\Delta hrrS\Delta chrS$ was transformed with the target gene reporter pECXC99E- P_{hmuO} -*eyfp* and the pKW3 plasmid either containing wild type *hrrS* under its native promoter (wt) or one of fifteen *hrrS* variants, encoding the histidine kinase with a single amino acid exchange. All proteins contained a C-terminal FLAG tag fusion for western blot analysis. Cells were cultivated in a microbioreactor system (Biolector) in CGXII minimal medium with 2% (w/v) glucose containing 2.5 μ M hemin.

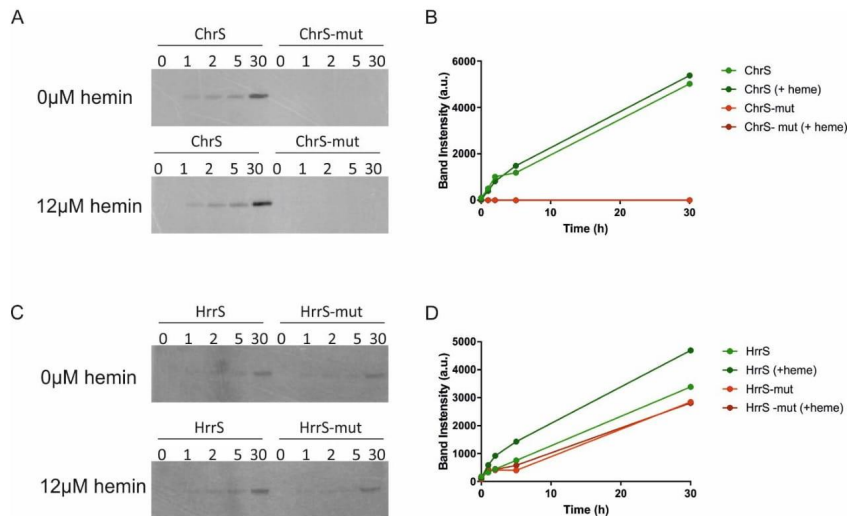
Supplementary Material



Supplementary Figure S6 - Alanine scanning of the transmembrane domain of ChrS revealed amino acid residues putatively involved in heme binding. A *C. glutamicum* $\Delta hrrS\Delta chrS$ mutant strain was transformed with the target gene reporter pJC1_PhrtBA-eyfp (kanamycin resistance) and either containing wild type *chrS* under native promoter (labeled wt) or one of fifteen *chrS* variants, encoding the histidine kinase with a single amino acid exchange. Cells were cultivated in the BioLector system in CGXII minimal medium with 2% (w/v) glucose containing 2.5 μM hemin. The peak specific fluorescence (fluorescence signal per backscatter signal, given in arbitrary units, a.u.) after 4 h is shown in the graph. The data represent average values of three independent biological replicates.



Supplementary Figure S7 - Heme/hemin binding properties of purified ChrS and ChrSY87A-F90A-F94A. ChrS is not co-purified together with heme from the *E. coli* lysate, but shows significant heme binding properties after incubation with 50 μM hemin in the *E. coli* crude extract. The membrane proteins were purified by the means of a C-terminal Strep-tag and analyzed the UV/Visible double beam spectrophotometer UV-1601 PC (Shimadzu, Kyoto, Japan).



Supplementary Figure S8 - Autophosphorylation of full length histidine kinases HrrS-Strep and ChrS-Strep. Immediately after purification, both kinases were incubated with $0.25 \mu\text{M} [\gamma\text{-}^{33}\text{P}]\text{-ATP}$ (10 mCi/ml ; PerkinElmer, USA) mixed with $80 \mu\text{M}$ non-radioactive ATP. The mixture was incubated for up to 30 min and at different time points aliquots were removed and the phosphorylation state was analyzed on storage phosphor imaging films (Fuji Photo Film Co., Tokyo, Japan) and with a Typhoon Trio Scanner (GE Healthcare, Germany).

$12 \mu\text{M}$ of purified HrrS/HrrSY112F-F115A-F118A (C) and ChrS/ChrSY87A-F90A-F94A (A) either with (top) or without (bottom) addition of hemin. B and D: Band intensities were analyzed with Fiji ImageJ (<https://fiji.sc/>).

2.2 Supplementary Tables

Supplementary Table S1. Bacterial strains and plasmids.

Strain or plasmid	Relevant characteristics	Source or reference
<i>E. coli</i>		
DH5 α	<i>fhuA2 lac(del)U169 phoA glnV44</i> $\Phi 80'$ <i>lacZ(del)M15 gyrA96 recA1 relA1 endA1 thi-1</i> <i>hsdR17</i> ; for general cloning purposes	Invitrogen

Supplementary Material

TG-1	K-12 <i>glnV44 thi-1 Δ(lac-proAB) Δ(mcrB-hsdSM)5, (r_K⁻m_K⁻) F' [traD36 proAB⁺ lacI^q lacZΔM15]; for <i>phoA/lacZ</i> assays</i>	Lucigen
BL21(DE3)	B F ⁻ <i>ompT gal dcm lon hsdS_B(r_B⁻m_B⁻) λ(DE3 [lacI lacUV5-T7p07 ind1 sam7 nin5]) [malB⁺]_{K-12}(λ^S); overexpression of membrane proteins.</i>	(Studier & Moffatt, 1986)
<i>C. glutamicum</i>		
ATCC 13032	Wildtype strain <i>Corynebacterium glutamicum</i>	(Kinoshita <i>et al.</i> , 2004)
ATCC Δ <i>hrrS</i> Δ <i>chrS</i>	13032 Deletion mutant of the two genes encoding the HKs HrrS and ChrS	(Hentschel <i>et al.</i> , 2014)
ATCC Δ <i>hrrS</i>	13032 Deletion mutant of the open reading frame (orf) encoding the HK HrrS	(Hentschel <i>et al.</i> , 2014)
ATCC Δ <i>chrS</i>	13032 Deletion mutant of the orf encoding the HK ChrS	(Hentschel <i>et al.</i> , 2014)
Plasmids		
pJC1_P _{<i>hmuO</i>} - <i>eyfp</i>	Target gene reporter for the HrrSA system	(Heyer <i>et al.</i> , 2012)
pJC1_P _{<i>hrrBA</i>} - <i>eyfp</i>	Target gene reporter for the ChrSA system	(Heyer <i>et al.</i> , 2012)
pEC-XC99E_P _{<i>hmuO</i>} - <i>eyfp</i>	Alternative target gene reporter for the HrrSA system with chloramphenicol resistance. Amplification of the P _{<i>hmuO</i>} - <i>eyfp</i> fragment (Oligo 42 and 43) and ligation into the pEC-XC99E vector backbone.	This work
pT7-5- <i>phoA</i>	Expression plasmid for <i>E. coli</i> , carries <i>phoA</i> as 3' extension behind the MCS, kindly supplied by the laboratories of G. Uden	(Bauer <i>et al.</i> , 2011)
pT7-5- <i>lacZ</i>	Expression plasmid for <i>E. coli</i> , carries <i>lacZ</i> as 3' extension behind the MCS	(Bauer <i>et al.</i> , 2011)
pT7-5- <i>hrrS-phoA</i> (<i>hrrSA30-hrrSE424</i>)	The pT7-5 plasmid was digested with <i>Bam</i> HI and <i>Nhe</i> I and 20 different truncated versions of <i>hrrS</i> were amplified (Oligo 1-21), digested with the	This work

	same restriction enzymes and ligated into the linearized plasmid.	
pT7-5_ <i>hrrS-lacZ</i> (<i>hrrSA30-hrrSE424</i>)	See construction of pT7-5_ <i>hrrS-phoA</i>	This work
pT7-5_ <i>chrS-phoA</i> (<i>chrSE12-chrSA160</i>)	The pT7-5 plasmid was digested with <i>Bam</i> HI and <i>Nhe</i> I and 20 different truncated versions of <i>chrS</i> were amplified (Oligo 22–41), digested with the same restriction enzymes and ligated into the linearized plasmid	This work
pT7-5_ <i>chrS-lacZ</i> (<i>chrSE12-chrSA160</i>)	See construction of pT7-5_ <i>chrS-phoA</i>	This work
pET24b- <i>hrrS-Cstrep</i>	IPTG inducible expression plasmid for the overexpression of <i>hrrS-strep</i> (full-length) in <i>E. coli</i> BL21. Amplification of <i>hrrS</i> wt from chromosomal DNA with the oligonucleotides 44 and 45, ligation into pET24b <i>via</i> Gibson assembly.	This work
pET24b- <i>chrS-Cstrep</i>	IPTG inducible expression plasmid for the overexpression of <i>chrS-strep</i> (full-length) in <i>E. coli</i> BL21. Amplification of <i>chrS</i> wt from chromosomal DNA with the oligonucleotides 46 and 47, ligation into pET24b <i>via</i> Gibson assembly.	This work
pET24b- <i>hrrSY112F-F115A-F118A-Cstrep</i>	Single mutations were introduced into the plasmid <i>via</i> the “quik-change-lightning” kit (Agilent Genomics, Santa Clara, United States) and for the triple mutations additional rounds of mutagenesis were performed	This work
pET24b- <i>chrSY87F-F90A-F94A-Cstrep</i>	Single mutations were introduced into the plasmid <i>via</i> the “quik-change-lightning” kit (Agilent Genomics, Santa Clara, United States) and for the triple mutations additional rounds of mutagenesis were performed	This work
pKW3	Expression plasmid; containing a high copy number ori for <i>E. coli</i> and a low copy number ori for <i>C. glutamicum</i>	(Eggeling <i>et al.</i> , 1998)

Supplementary Material

pKW3_ <i>hrrS</i> -flag	<i>hrrS</i> including native promoter (~300 Bp upstream of ATG) was amplified with the oligonucleotides 106 and 107 and cut with <i>EcoRI</i> and <i>BamHI</i> . pKW3 was linearized with <i>EcoRI</i> and <i>BamHI</i> and the PCR fragment ligated to generate the circular plasmid.	This work
pKW3_ <i>hrrS</i> -flag (<i>hrrSW70A-F172A</i>)	16 single mutations were introduced into the pKW3_ <i>hrrS</i> -flag plasmid to generate 16 different single mutation expression plasmids. Mutations were introduced into the plasmid <i>via</i> the “quick-change-lightning” kit (Agilent Genomics, Santa Clara, USA) and the oligonucleotides 48 - 79 as described in material and methods.	This work
pJC1_P _{<i>hrrBA</i>} - <i>eyfp</i> _ <i>chrS</i> -flag (<i>chrSH20A-F126A</i>)	16 single mutations were introduced into the pJC1_P _{<i>hrrBA</i>} - <i>eyfp</i> _ <i>chrS</i> -flag plasmid to generate 16 different single mutation expression plasmids. Mutations were introduced into the plasmid <i>via</i> the “quick-change-lightning” kit (Agilent Genomics, Santa Clara, USA).	This work

Supplementary Table S2. Oligonucleotides used in this study. Restriction sites are underlined.

#	Oligonucleotide	Sequence
PhoA/LacZ Screening		
1	<i>hrrS</i> _phoA-lacZ_fw	GCGC <u>GGATCC</u> ATGCAGTCAAGCCTAGATCG
2	<i>hrrS</i> -A30_phoA/lacZ_rv	GCGC <u>GCTAGC</u> CGCGCCCGTTGATTCCTTC
3	<i>hrrS</i> -H38_phoA/lacZ_rv	GCGC <u>GCTAGC</u> GTGGATACTGTTGCGATAGCTC
4	<i>hrrS</i> -A42_phoA/lacZ_rv	GCGC <u>GCTAGC</u> GGCTGTCAAATGTGGATAC
5	<i>hrrS</i> -A51_phoA/lacZ_rv	GCGC <u>GCTAGC</u> AGTCCCAACCCACGACCAG
6	<i>hrrS</i> -L55_phoA/lacZ_rv	GCGC <u>GCTAGC</u> CAGGCGGGCGGAAGCTCCCAAC
7	<i>hrrS</i> -G77_phoA/lacZ_rv	GCGC <u>GCTAGC</u> TCCATAGAAGTACAGAAAACCC
8	<i>hrrS</i> -L84_phoA/lacZ_rv	GCGC <u>GCTAGC</u> CAAATCTACGCGTTGGTTGATC
9	<i>hrrS</i> -G87_phoA/lacZ_rv	GCGC <u>GCTAGC</u> GCCGTGGCTCAAATCTACGC
10	<i>hrrS</i> -Q89_phoA/lacZ_rv	GCGC <u>GCTAGC</u> CTGCATGCCGTGGCTCAAATC
11	<i>hrrS</i> -L96_phoA/lacZ_rv	GCGC <u>GCTAGC</u> CAGCACAAACAGCCAGCCCAG
12	<i>hrrS</i> -L114_phoA/lacZ_rv	GCGC <u>GCTAGC</u> CAGCAGATAAATGGACACGG
13	<i>hrrS</i> -L117_phoA/lacZ_rv	GCGC <u>GCTAGC</u> CAGCGGGAACAGCAGATAAATGG
14	<i>hrrS</i> -L122_phoA/lacZ_rv	GCGC <u>GCTAGC</u> TAGATAGAGGAAAAACAGCG
15	<i>hrrS</i> -A133_phoA/lacZ_rv	GCGC <u>GCTAGC</u> CGCAATAATGCCTCTCACGT
16	<i>hrrS</i> -A143_phoA/lacZ_rv	GCGC <u>GCTAGC</u> CCCCACGGAATACTGGCTG

17	hrrS-Q145_phoA/lacZ_rv	GCGCGCTAGCCTGGCTGGCAATCGCAATCG
18	hrrS-A171_phoA/lacZ_rv	GCGCGCTAGCCGCGTAATCAATAGCCACGG
19	hrrS-E181_phoA/lacZ_rv	GCGCGCTAGCTTCATTATTACCCGCCACAAC
20	hrrS-H214_phoA/lacZ_rv	GCGCGCTAGCATGCGCAATACGTTGACGTTT
21	hrrS-E424_phoA/lacZ_rv	GCGCGCTAGCCTCATCGTCAGTTGGAGAAC
22	chrS-E18_phoA/lacZ_rv	GCGCGCTAGCCTCAATTCGGGGCATGGTC
23	chrS-A30_phoA/lacZ_rv	GCGCGCTAGCGGCAATGAGTAAATGCAATC
24	chrS-S41_phoA/lacZ_rv	GCGCGCTAGCGCTGGCACGCCAACACACCAAC
25	chrS-A49_phoA/lacZ_rv	GCGCGCTAGCAGCGAGCACCCACACACCCC
26	chrS-G59_phoA/lacZ_rv	GCGCGCTAGCACCCGCCACATAAACACCG
27	chrS-F66_phoA/lacZ_rv	GCGCGCTAGCAAACGGCGAATTCGGGACCAC
28	chrS-L77_phoA/lacZ_rv	GCGCGCTAGCAGCACAAGAAACCACGCCATAG
29	chrS-G88_phoA/lacZ_rv	GCGCGCTAGCTCCATCCCAAATCAGGCTCG
30	chrS-F96_phoA/lacZ_rv	GCGCGCTAGCAAAACACCAAATACGAGGCTCC
31	chrS-F100_phoA/lacZ_rv	GCGCGCTAGCGAAAAACATCGGAAACACC
32	chrS-F104_phoA/lacZ_rv	GCGCGCTAGCCAACACTGCGAGGAAAAACATC
33	chrS-K110_phoA/lacZ_rv	GCGCGCTAGCTTTCAGCGGTGTCGTGATCAAC
34	chrS-A112_phoA/lacZ_rv	GCGCGCTAGCCGCGGATTTTCAGCGGTGTCG
35	chrS-A116_phoA/lacZ_rv	GCGCGCTAGCTGCAATGATGATCGCGGATTTTAC
36	chrS-A122_phoA/lacZ_rv	GCGCGCTAGCCGCGATCGCCGTCAGTATTG
37	chrS-A127_phoA/lacZ_rv	GCGCGCTAGCAGCCAACGTAACCCGCGCATC
38	chrS-F132_phoA/lacZ_rv	GCGCGCTAGCAAACCCAGGTGCATAGCCAAC
39	chrS-G135_phoA/lacZ_rv	GCGCGCTAGCGCCAAACAGAAAACCCAGGTG
40	chrS-L156_phoA/lacZ_rv	GCGCGCTAGCTAACTGAAAAACAGTACCC
41	chrS-A167_phoA/lacZ_rv	GCGCGCTAGCTGCGTCGACAAGCTCCTTTAAG
pECXC99E reporter		
42	PhmuO_fw	GCGCCATATGCTAGCGAAGTTCTTGAAGTG
43	PhmuO_rv	GCGCGTCGACTTATCTAGACTGTACAGCTCG
Overexpression plasmids HrrS/ChrS-Strep		
44	hrrS_Cstrep_fw	ACTTTAAGAAGGAGATATACATATGATGCAGTCAAGCCTAGATCG
45	hrrS_Cstrep_rv	CCTGAAAATACAGGTTCTCGCTAGCCTCATCGTCAGTTGGAGAAC
46	chrS_Cstrep_fw	ACTTTAAGAAGGAGATATACATATGGTGAAAACCTAGCCAAGCGACC
47	chrS_Cstrep_rv	CCTGAAAATACAGGTTCTCGCTAGCCTTATCTTGGTCCCTTTGTGG
Point mutations hrrS/chrS		
48	hrrS-W70_A_fw	ATAGAAGTACAGAAAACCCGCCACAACAACAGCACGCAC
49	hrrS-W70_A_rv	GTGCGTGTGTTGTTTGTGGCGGGTTTCTGTACTTCTAT
50	hrrS-Y74_A_fw	CGTTTGGTTGATCCATAGAAGGCCAGAAAACCCACACAAACAA
51	hrrS-Y74_A_rv	TTGTTTGTGTGGGGTTTCTGCGCTTCTATGGATCAACCAAAACG
52	hrrS-T97A-fw	CTGGCTGTTTGTGCTGGCGCTGGTGTGGATTTT
53	hrrS-T97A-rv	AAAATCCACACCAGCGCCAGCACAACAACAGCCAG
54	hrrS-W100_A_fw	GATCGGCACCATAAAAAATCGCCACCAGCGTCAGCACAAAC
55	hrrS-W100_A_rv	GTTTGTGCTGACGCTGGTGGCGATTTTTATGGTGCCGATC
56	hrrS-Y112A_fw	GCGGGAACAGCAGAGCAATGGACACGGGCAGGATC
57	hrrS-Y112A_rv	GATCGTGCCCGTGTCCATTGCTCTGCTGTTCCCGC

Supplementary Material

58	hrrS-Y112F-fw	CGATCGTGCCCGTGTCATTTTCTGCTGTCC
59	hrrS-Y112F-rv	GGAACAGCAGAAAAATGGACACGGGCACGATCG
60	hrrS-F115A-fw	CGTGTCATTATCTGCTGGCCCCGCTGTTTTCTCTAT
61	hrrS-F115A-rv	ATAGAGGAAAAACAGCGGGGCCAGCAGATAAATGGACACG
62	hrrS-F118_A_fw	CACCTGTAGATAGAGGAAAGCCAGCGGGAACAGCAGATAA
63	hrrS-F118_A_rv	TTATCTGCTGTTCCCGCTGGCTTTCCTCTATCTACAGGTG
64	hrrS-F119_A_fw	CACCTGTAGATAGAGGGCAAACAGCGGGAACAGCAGATAA
65	hrrS-F119_A_rv	TTATCTGCTGTTCCCGCTGTTTGCCCTCTATCTACAGGTG
66	hrrS-Y121_A_fw	GTCAGGCATCACCTGTAGAGCGAGGAAAAACAGCGGGAAC
67	hrrS-Y121_A_rv	GTTCCCGCTGTTTTCTCGCTCTACAGGTGATGCCTGAC
68	hrrS-Q145A-fw	GATTGCGATTGCCAGCGCGTATTCCGTGGGGTTG
69	hrrS-Q145A-rv	CAACCCACGGAATACCGCGTGGCAATCGCAATC
70	hrrS-T151A-fw	GTATCCGTGGGGTTGGCCTTTGGTGGTGTGAT
71	hrrS-T151A-rv	ATCACACCACAAAGGCCAACCCACGGAATAC
72	hrrS-S161A-fw	GGGTCCGGTGGTCTGCTGCGATCGTGAC
73	hrrS-S161A-rv	GTCACGATCGCAGCGACCACCGGACCC
74	hrrS-V164_A_fw	CAATAGCCACGGTCGCGATCGCAGAGACC
75	hrrS-V164_A_rv	GGTCTCTGCGATCGCGACCGTGGCTATTG
76	hrrS-Y170F-fw	GTGACCGTGGCTATTGATTTCCGCTTCCGC
77	hrrS-Y170F-rv	GCGGAACGCGAAATCAATAGCCACGGTCCAC
78	hrrS-F172A-fw	GGCTATTGATTACGCGGCCCGCACGTTGTGGCGG
79	hrrS-F172A-rv	CCGCCACAACGTGCGGGCCGCGTAATCAATAGCC
80	chrS-H20A-fw	GAGAGTCTCATTTGGGGATTGGCTTTACTATTGCCGTTTTGTTG
81	chrS-H20A-rv	CAACAAAACGGCAATGAGTAAAGCCAATCCCCAAATGAGAACTCTC
82	chrS-H36A-fw	GTTGGCGTGCCAGCGCTTGGGGTGTGTGGG
83	chrS-H36A-rv	CCCACACACCCCAAGCGCTGGCACGCCAAC
84	chrS-W37A-fw	TGGCGTGCCAGCCATGCGGGTGTGTGGGT
85	chrS-W37A-rv	ACCCACACACCCGCATGGCTGGCACGCCA
86	chrS-Y46F-fw	TGGGTGCTCGTTTTGGCTTTGGCGTGGTT
87	chrS-Y46F-rv	AACCACGCCAAAAGCCAAAAGCGAGCACCCA
88	chrS-F60A-fw	GTGGTCCCGAATTGCGCGGCTAAGAATCACCTATGGC
89	chrS-F60A-rv	GCCATAGGGTGATTCTTAGCCGGCGAATTCGGGACCAC
90	chrS-H63A-fw	TCCCGAATTCGCCGTTAAGAAATGCCCTATGGCGTG
91	chrS-H63A-rv	CACGCCATAGGGGCATTCTTAAACGGCGAATTCGGGA
92	chrS-W67A-fw	TAAGAATCACCTATGGCGGCGTTTTCTTGTGCTGAGTTTG
93	chrS-W67A-rv	CAAACCTCAGCACAAGAAACGCCCATAGGGTGATTTCTTA
94	chrS-W75A-fw	CTTGTGCTGAGTTTGTGGCGGCGAGCCTGATTTGGG
95	chrS-W75A-rv	CCCAAATCAGGCTCGCCGCCAACAAACTCAGCACAAG
96	chrS-Y87F-fw	GACCGGAGCCTGCGTTTTTTGGTGTTCGGAT
97	chrS-Y87F-rv	ATCGGAAACACAAAAACGCAGGCTCCGGTC
98	chrS-F90A-fw	GAGCCTGCGTATTGGTGGCTCCGATGTTTTCTCGC
99	chrS-F90A-rv	GCGAGGAAAAACATCGGAGCCACCAAATACGCAGGCTC
100	chrS-F93A-fw	CGTATTTGGTGTTCGGATGGCTTTCCTCGCAGTGTGTATCA

101	chrS-F93A-rv	TGATCAACACTGCGAGGAAAGCCATCGGAAACACCAAATACG
102	chrS-H123A-fw	GTGGTTACGTTGGCTATGGCCCTGGGGTTTTCTGTTGG
103	chrS-H123A-rv	CCAACAGAAAACCCAGGGCCATAGCCAACGTAACCAC
104	chrS-F126A-fw	GGCTATGCACCTGGGGGCTTCTGTTGGCGTTGTC
105	chrS-F126A-rv	GACAACGCCAACAGAAGCCCCCAGGTGCATAGCC
Generation of pKW3_P_{hrrS}-hrrS-flag		
106	<i>PhrrS-hrrS_fw</i>	TATAG GAATTC CGGCGACCCAGTCGGTGC
107	<i>PhrrS-hrrS_rv</i> (FLAG)	GCGC GGATCC TTACTTGTGTCATCGTCTTTGTAGTCCTCATCGTCAGT TGGAGAACTTAG

Supplementary Material

Supplementary Table S3. Number of transmembrane helices (TMHs) predicted by several different online tools. The transmembrane domain of both HKs was analyzed using six different online tools for the prediction of membrane spanning helices: TopPredII (Claros & von Heijne, 1994), TMPred (Hofman & Stoffel, 1993), Hmmtop (Tusnady & Simon, 2001), Minnou polyview (Porollo *et al.*, 2004), CBS TMHMM (Krogh *et al.*, 2001), DAS (Cserzo *et al.*, 1997), Mpex (Snider *et al.*, 2009), TOPCONS (Tsirigos *et al.*, 2015) and Phobius (Kall *et al.*, 2007). TopPredII predicted three and five helices for HrrS and ChrS, respectively, but suggested a forth (or sixth) helix with lower probability. The prediction of Hmmtop and TOPCONS were in line with the experimental data and are highlighted in yellow.

Links: TopPredII [<https://bioweb.pasteur.fr/seqanal/interfaces/toppred.html>], TMPred [https://www.ch.embnet.org/software/TMPRED_form.html], HMMTOP [www.enzim.hu/hmmtop/], Minnou polyview [<http://minnou.cchmc.org/>], CBS TMHMM [www.cbs.dtu.dk/services/TMHMM/], DAS [tmdas.bioinfo.se/], Mpex [<http://blanco.biomol.uci.edu/mpex/>], TOPCONS [<http://topcons.cbr.su.se>] and Phobius [<http://phobius.sbc.su.se>].

Program	HrrS	ChrS
	predicted TMHs	predicted TMHs
TopPredII	3(4?)	5(6?)
TMpred	3	5
HMMTOP	6	6
Minnou polyview	7	5
CBS TMHMM	4	5
DAS	5	5
Mpex	5	5
TOPCONS	6	6
Phobius	5	6

$$\text{Miller units} = 1000 * \frac{\text{Abs}_{420} - 1,7 * \text{Abs}_{550}}{\text{time (min)} * \text{Abs}_{600}}$$

Formula S1: Calculation of alkaline phosphatase and β -galactosidase activity in miller units.

3 References

Bauer, J., Fritsch, M. J., Palmer, T. & Unden, G. (2011). Topology and accessibility of the transmembrane helices and the sensory site in the bifunctional transporter DcuB of *Escherichia coli*. *Biochemistry* **50**, 5925-5938.

Claros, M. G. & von Heijne, G. (1994). TopPred II: an improved software for membrane protein structure predictions. *Computer applications in the biosciences : CABIOS* **10**, 685-686.

Cserzo, M., Wallin, E., Simon, I., von Heijne, G. & Elofsson, A. (1997). Prediction of transmembrane alpha-helices in prokaryotic membrane proteins: the dense alignment surface method. *Protein engineering* **10**, 673-676.

Eggeling, L., Oberle, S. & Sahn, H. (1998). Improved L-lysine yield with *Corynebacterium glutamicum*: use of *dapA* resulting in increased flux combined with growth limitation. *Applied microbiology and biotechnology* **49**, 24-30.

Hentschel, E., Mack, C., Gatgens, C., Bott, M., Brocker, M. & Frunzke, J. (2014). Phosphatase activity of the histidine kinases ensures pathway specificity of the ChrSA and HrrSA two-component systems in *Corynebacterium glutamicum*. *Molecular microbiology* **92**, 1326-1342.

Heyer, A., Gatgens, C., Hentschel, E., Kalinowski, J., Bott, M. & Frunzke, J. (2012). The two-component system ChrSA is crucial for haem tolerance and interferes with HrrSA in haem-dependent gene regulation in *Corynebacterium glutamicum*. *Microbiology (Reading, England)* **158**, 3020-3031.

Hofman, K. & Stoffel, W. (1993). A database of membrane spanning proteins segments. *Journal of Biological Chemistry* **374**.

Kall, L., Krogh, A. & Sonnhammer, E. L. (2007). Advantages of combined transmembrane topology and signal peptide prediction--the Phobius web server. *Nucleic acids research* **35**, W429-432.

Kinoshita, S., Udaka, S. & Shimono, M. (2004). Studies on the amino acid fermentation. Part 1. Production of L-glutamic acid by various microorganisms. *The Journal of general and applied microbiology* **50**, 331-343.

Supplementary Material

Krogh, A., Larsson, B., von Heijne, G. & Sonnhammer, E. L. (2001). Predicting transmembrane protein topology with a hidden Markov model: application to complete genomes. *Journal of molecular biology* **305**, 567-580.

Porollo, A. A., Adamczak, R. & Meller, J. (2004). POLYVIEW: a flexible visualization tool for structural and functional annotations of proteins. *Bioinformatics (Oxford, England)* **20**, 2460-2462.

Snider, C., Jayasinghe, S., Hristova, K. & White, S. H. (2009). MPEx: a tool for exploring membrane proteins. *Protein science : a publication of the Protein Society* **18**, 2624-2628.

Studier, F. W. & Moffatt, B. A. (1986). Use of bacteriophage T7 RNA polymerase to direct selective high-level expression of cloned genes. *Journal of molecular biology* **189**, 113-130.

Tsirigos, K. D., Peters, C., Shu, N., Kall, L. & Elofsson, A. (2015). The TOPCONS web server for consensus prediction of membrane protein topology and signal peptides. *Nucleic acids research* **43**, W401-407.

Tusnady, G. E. & Simon, I. (2001). The HMMTOP transmembrane topology prediction server. *Bioinformatics (Oxford, England)* **17**, 849-850.

5.2 Supplement “Toxic but Tasty - Temporal Dynamics and Network Architecture of Heme-Responsive Two-Component Signalling”

Supplementary Information

Toxic but tasty - Temporal dynamics and network architecture of heme-responsive two-component signalling in *Corynebacterium glutamicum*

Marc Keppel^{1#}, Hannah Piepenbreier^{2#}, Cornelia Gätgens¹, Georg Fritz² and Julia Frunzke^{1*}

Content

Figure S1: Growth curves after application of additional heme pulses.

Figure S2: Additional heme pulses do not prime P_{hrrBA} .

Figure S3: Electrophoretic Mobility Shift Assays (EMSAs) reveal crucial nucleotides for HrrA binding to the operator.

Figure S4: Control of P_{hmuO} by HrrA and DtxR.

Figure S5: The *in vitro* data suggest a cross-phosphatase activity of HrrS which did not result in a model that quantitatively fits to the behavior of the $\Delta chrS$ mutant *in vivo* data

Figure S6: An increased phosphatase activity of HrrS prevents a delayed P_{hmuO} activation by HrrA~P.

General supplement file S1: In depth description of the mathematical models and equations

Table S1: Bacterial strains used in this study.

Table S2: Oligonucleotides used in this study.

Table S3: Plasmids used in this study.

Table S4: Parameters used in the mathematical model of the *C. glutamicum* heme detoxification module.

Table S5: Additional parameters used in the mathematical model of the *C. glutamicum* heme utilization module.

Table S6: Transformation of the units within the mathematical models.

Pulsing experiments, biomass

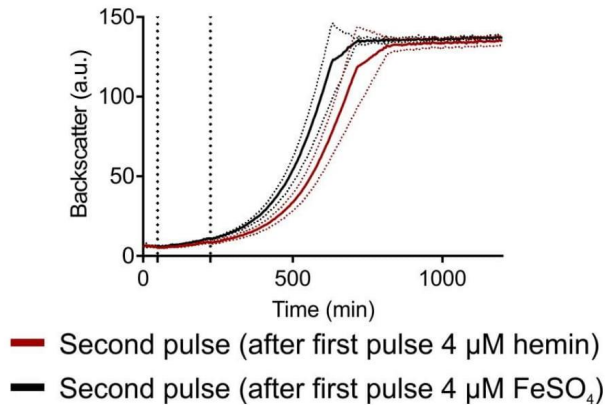


Figure S1: Growth curves after application of additional heme pulses

C. glutamicum cells were transformed with the target gene reporter $\text{pJC1_P}_{hrtBA}\text{-eyfp}$ and starved from iron overnight as described in material and methods. Subsequently, the cells were inoculated in CGXII minimal medium with 2% (w/v) glucose containing no iron source and transferred to the microbioreactor system (Biolector) where eYfp fluorescence (=reporter output) and backscatter (biomass) was measured in 5 minutes intervals. After 45 min, hemin (red line) or FeSO_4 (black line) was added to a final concentration of 4 μM . A second pulse of 4 μM hemin was applied to both cultures after 225 min.

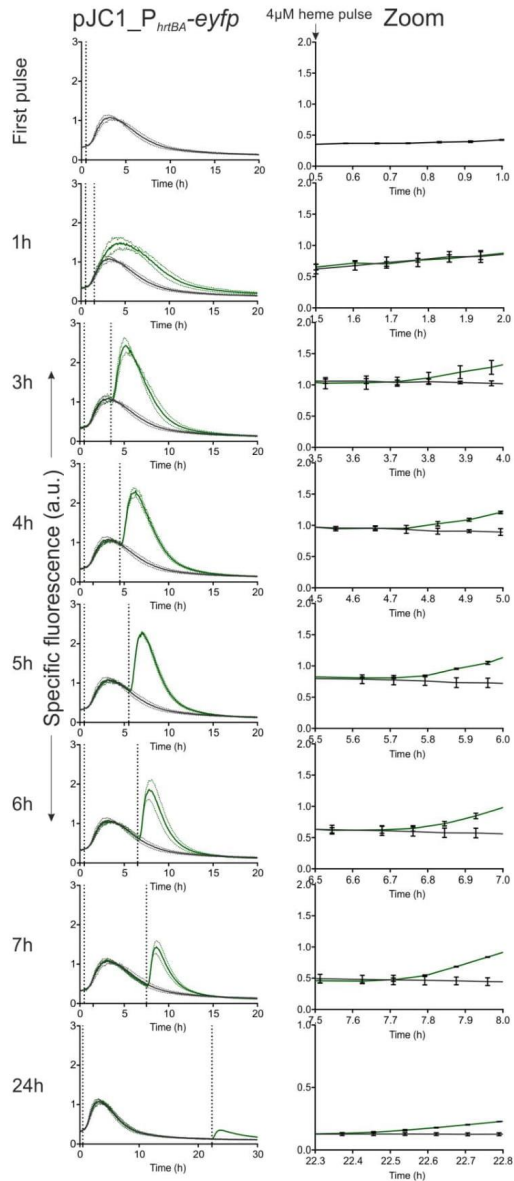


Figure S2: Additional heme pulses do not prime P_{hrtBA} .

C. glutamicum cells were transformed with the target gene reporter pJC1_ P_{hrtBA} -*eyfp* and starved from iron overnight as described in material and methods. Subsequently, the cells were inoculated in CGXII minimal medium with 2% (w/v) glucose containing no iron source and transferred to the microbioreactor system (Biolector) where eYfp fluorescence (=reporter output) and backscatter

(biomass) was measured in 5 minutes intervals. After 30 min, hemin was added to a final concentration of 4 μM . A second pulse of 4 μM hemin (resulting in a final hemin concentration of 8 μM) was applied after 1h, 3h, 4h 5h, 6h, 7h or 24h, respectively.

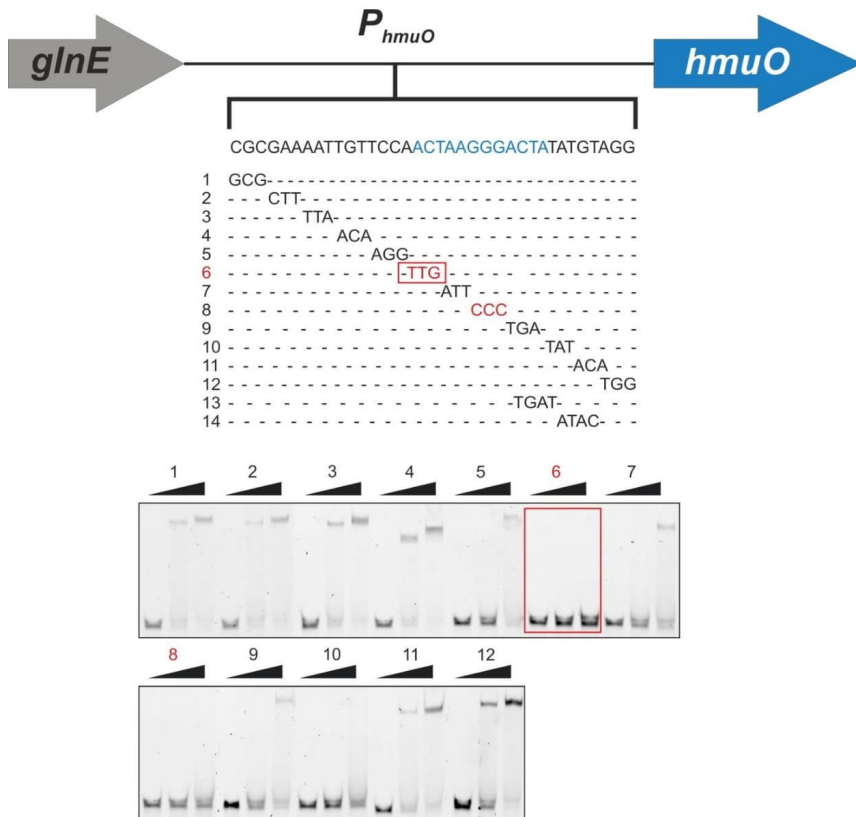


Figure S3: Electrophoretic Mobility Shift Assays (EMSAs) reveal crucial nucleotides for HrrA binding to the operator.

For all EMSAs, 36 Bp of mutated DNA fragments (100 ng) were used and purified HrrA-His protein was applied in 0, 10 and 30-fold molecular excess for each sample. Mutation 6 (ACT::TTG) and mutation 8 (GGG::CCC) led to strongly reduced binding of HrrA to P_{hmuO} and similar P_{hmuO} -*eyfp* output like observed in a $\Delta hrrA$ deletion mutant (Fig. S5B).

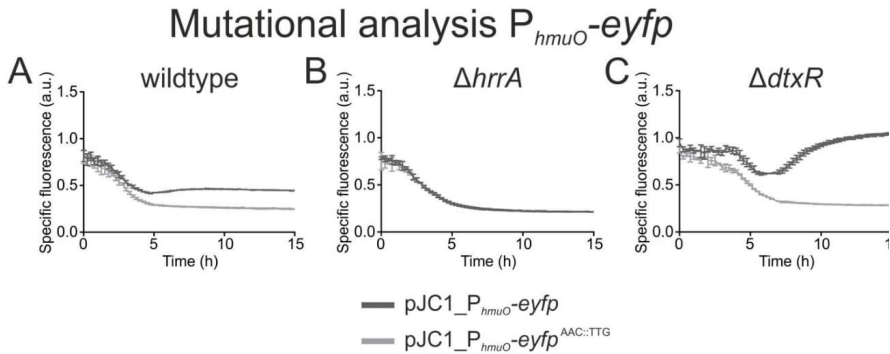


Figure S4: Control of P_{hmuO} by HrrA and DtxR.

HrrA binding was abolished by introducing the AAC::TTG mutation into the P_{hmuO} -*eyfp* reporter. After iron starvation overnight, the three strains (A: wildtype, B: $\Delta hrrA$ and C: $\Delta dtxR$) were inoculated in BHI complex medium supplemented with 4 μ M hemin and the specific fluorescence (eYFP-fluorescence/backscatter) was recorded in 15 minutes intervals. The strains were grown in BHI complex medium as the $\Delta dtxR$ strain grows poorly in CGXII medium.

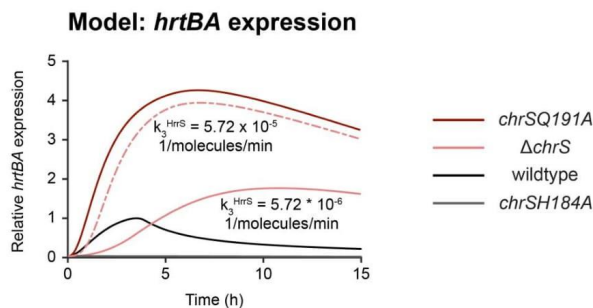


Figure S5: The *in vitro* data suggest a cross-phosphatase activity of HrrS which did not result in a model that quantitatively fits to the behavior of the $\Delta chrS$ mutant *in vivo* data

Setting k_3^{HrrS} to 5.72×10^{-5} 1/molecules/min as expected from the *in vitro* data in (Hentschel et al., 2014) led to an excessive response of P_{hrtBA} in the $\Delta chrS$ mutant (dashed red line). A reduced cross-phosphatase activity of HrrS by a factor of 10 reproduces the mutant behaviour quantitatively (solid red line).

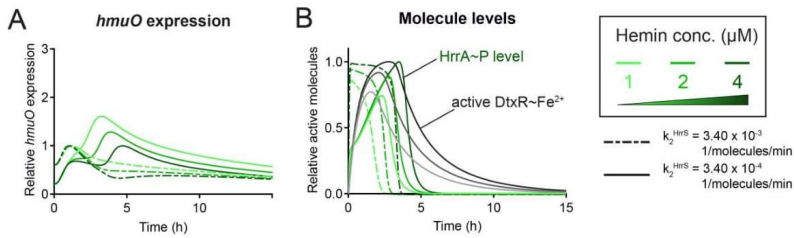


Figure S6: An increased phosphatase activity of HrrS prevents a delayed P_{hmuO} activation by HrrA~P.

Setting k_2^{HrrS} to 3.40×10^{-3} 1/molecules/min as expected from the *in vitro* data in (Hentschel et al., 2014) did not result in a model that quantitatively fits to the behaviour of the *in vivo* data in wild-type. The strong phosphatase activity decreases HrrAP levels immediately after stimulus reduction and no delayed P_{hmuO} activation is possible. Decreasing k_2^{HrrS} about a factor of 10 improved the ability to reproduce the *in vivo* behaviour.

Description of mathematical models

The heme detoxification and utilization network contains different layers of regulation that have to be considered within the mathematical model.

Bacterial growth kinetics

The overall flux of the stimulus heme through the network represents the first layer that was quantified within the model. As the cells are heavily iron-starved, heme is used as alternative iron source for growth. Based on the experimental growth curves, we included the assumption of heme-dependent effects on the growth rate of *C. glutamicum* into our model and ended up with a growth rate $\gamma(t)$ that varies over the time, according to hemin uptake via the heme importer HmuTUV and incorporation into biomass. Thus, bacterial growth could be described based on an effective Michaelis-Menten expression:

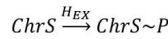
$$\frac{d[\text{cells}]}{dt} = \beta * \frac{[H_{IN}]}{K_M^{CON} + [H_{IN}]} * [\text{cells}]$$

$[H_{IN}]$ is the internal heme concentration and the Michaelis-Menten term with its Michaelis constant K_M^{CON} and the maximal growth rate β functions as an effective description of the heme consumption via diverse enzymatic reactions.

Stimulus perception and signalling in the two-component systems

As a second layer of regulation, the dynamics within the TCSs were quantified. According to the reporter assays, we assumed a constitutive expression and thereby production of HrrS, while the phosphorylated response regulator HrrA activates the production of HrrA and HmuO. Besides, ChrS, ChrA and HrtBA production is dependent from ChrA. We expected a production of the non-phosphorylated form exclusively, both in case of the histidine kinases as well as the response regulators. Given that no information is available about the copy number of the heme importer HmuTUV, we assumed a constant number of transporter molecules independent from time and hemin levels. Both kinases, HrrS and ChrS, phosphorylate their cognate and non-cognate response regulator (Hentschel et al., 2014) in

response to external heme as their stimulus (Keppel, Davoudi, Gätgens, & Frunzke, 2018). In the following, we will give the quantification of different reactions for ChrSA as an example but the description is identical for HrrSA. Following this approach of Groban and co-workers (Groban, Clarke, Salis, Miller, & Voigt, 2009), we described the transition from the non-phosphorylated form into the phosphorylated one of the histidine kinases and the response regulators but did not quantify the phosphotransfer in detail. Thus, we expected the autophosphorylation of the kinases (ChrS) in response to stimulus perception

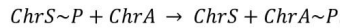


and described the reaction by

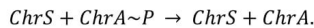
$$\frac{d[ChrS\sim P]}{dt} = I_{ChrS}(H_{EX}) [ChrS],$$

while $I_{ChrS}(H_{EX}) = k_+^{ChrS} * \frac{[H_{EX}]}{K_{H_{EX}} + [H_{EX}]}$ describes the autophosphorylation rate, dependent on the external heme concentration. The autophosphorylation threshold is given by $K_{H_{EX}}$, while k_+^{ChrS} determine the speed of the autophosphorylation reaction. $[ChrS]$ and $[ChrS\sim P]$ describe the concentration of the phosphorylated or non-phosphorylated form of the kinase.

A phosphorylated kinase (ChrS~P) can donate its phosphate to the response regulator



During the reverse process of dephosphorylation of the response regulator, the phosphate is not passed back to the kinase



The phosphorylation and dephosphorylation of ChrA was expected to follow second order kinetics, which were quantified by the rate constants k_i :

$$\frac{d[ChrA\sim P]}{dt} = k_1^{ChrS} * [ChrS\sim P] * [ChrA] - k_2^{ChrS} * [ChrS] * [ChrA\sim P]$$

The phosphotransfer from $ChrS\sim P$ to $ChrA$ is determined by the rate constant k_1^{ChrS} , while the reverse reaction ($ChrS$ dephosphorylates $ChrA\sim P$) occurs with a rate dependent on the rate constant k_2^{ChrS} . Cross-phosphorylation of both kinases to their non-cognate response

regulators was expected, cross-dephosphorylation could not be observed previously and was therefore not included into the model.

Regulatory dynamics of target genes

The target gene activation of the phosphorylated response regulators represents the third layer of regulation and a mathematical description based on thermodynamic modelling quantified the observed transcriptional regulation. Following the approach of Bintu and co-workers (Bintu et al., 2005), the activation of gene expression from the P_{HrtBA} and the P_{chrSA} promoter by phosphorylated ChrA could then be formulated in terms of $ChrA\sim P$ concentrations, such that the dynamic equation for the HrtBA protein levels, $[HrtBA]$, read:

$$\frac{d[HrtBA]}{dt} = \alpha * \left(\frac{1 + \omega \left(\frac{[ChrA\sim P]}{\kappa} \right)^n}{1 + \left(\frac{[ChrA\sim P]}{\kappa} \right)^n} \right) - \gamma * [HrtBA]$$

We assumed a basal protein production with an effective rate α and dilution with a rate proportional to γ for all components within the systems according to growth. The basal production of the proteins is a combined representation of the processes of transcription and translation, justified by the fact that e.g. mRNA maturation and degradation proceed on much faster time-scales than the signalling and target gene regulation within the system and were therefore not relevant for the investigated dynamics. The ratio of maximal to basal promoter activity is defined as the fold-change ω (Bintu et al., 2005). K in turn represents a measurement of the concentration of phosphorylated response regulator ChrA at which P_{HrtBA} is activated and the hill coefficient n reflects all forms of cooperativity in ChrA binding to the promoter. According to the fact that we based our mathematic model on the experimental data of the performed reporter assays, we discriminated within our model between the proteins of the systems itself and the reporter output that reflects the production of detectable fluorescence proteins based on the original promoter activity. To this end, we formulated one equation for the regulated protein production and one equation for the corresponding YFP production each and integrated an effective parameter for YFP bleaching and degradation

processes in the latter equation. The dynamic equations for all components can be found in M1 and M2.

Model parameters

In order to calibrate the model, various parameters concerning the cell growth as well as the dynamics within the TCSs could be fixed to their physiological values based on experimental data. The remaining ones were adjusted within physiological intervals to reproduce the experimental data of promoter activity within the mathematical model (for further descriptions see Tables S4 and S5 and Fig. S5/S6).

Mutant simulations

For the purpose of predicting the behaviour of several mutants within the model of the heme detoxification module, we adapted the individual parameters of the mathematic equations to the experimentally given scenarios. For the wild type, we simulated the time-dependent dynamics based on the complete set of parameters we fixed within our model. To knock out a protein in the model, we set the participating rate constants of the protein-based reactions as well as the initial concentrations to zero. In case of the $\Delta chrS$ mutant, we set the basal concentration $ChrS_{INI}$ as well as the rate constants for phosphorylation (k_1^{ChrS}) and dephosphorylation (k_2^{ChrS}) to zero. Within the phosphatase mutant *chrSQ191A*, the dephosphorylation step of ChrA is not possible. Thus, we exclusively chose k_2^{ChrS} to zero. In contrast, inhibition of ChrS kinase activity (*chrSH186A*) leads to a lack in the ability of autophosphorylation of ChrS and thereby the option of phosphotransfer to the response regulator ChrA. Disrupting the autophosphorylation of ChrS could be simulated by setting k_+^{ChrS} to zero. In addition, the lack of phosphotransfer could be quantified by $k_1^{ChrS} = 0$.

Model equations M1: ODEs of the mathematical model of the *C. glutamicum* heme detoxification module

Variables within the model:

Name	Description
H_{EX}	External heme
H_{IN}	Internal heme
$cells$	Cells of <i>C. glutamicum</i>
$ChrS$	Unphosphorylated histidine kinase ChrS
$ChrS\sim P$	Autophosphorylated histidine kinase ChrS
$HrrS$	Unphosphorylated histidine kinase HrrS
$HrrS\sim P$	Autophosphorylated histidine kinase HrrS
$ChrA$	Unphosphorylated response regulator ChrA
$ChrA\sim P$	Phosphorylated response regulator ChrA
$HrtBA$	Heme exporter HrtBA
$ChrS_{TOT}\text{-YFP}$	YFP proteins corresponding to the total amount of the kinase ChrS (The production is under the control of P_{chrSA} promoter)
$ChrA_{TOT}\text{-YFP}$	YFP proteins corresponding to the total amount of the response regulator ChrA (The production is under the control of P_{chrSA} promoter)
$HrtBA\text{-YFP}$	YFP proteins corresponding to the total amount of the heme exporter HrtBA (The production is under the control of P_{hrtBA} promoter)

ODEs:

$$\frac{d[H_{EX}]}{dt} = -v_{max}^{IMP} \frac{[H_{EX}]}{K_M^{IMP} + [H_{EX}]} [cells] + k_{cat}^{HrtBA} [HrtBA] \frac{[H_{IN}]}{K_M^{HrtBA} + [H_{IN}]} [cells] \quad (1)$$

$$\frac{d[H_{IN}]}{dt} = v_{max}^{IMP} \frac{[H_{EX}]}{K_M^{IMP} + [H_{EX}]} - v_{max}^{CON} \frac{[H_{IN}]}{K_M^{CON} + [H_{IN}]} - k_{cat}^{HrtBA} [HrtBA] \frac{[H_{IN}]}{K_M^{HrtBA} + [H_{IN}]} - \gamma [H_{IN}] \quad (2)$$

$$\frac{d[cells]}{dt} = \beta \frac{[H_{IN}]}{K_M^{CON} + [H_{IN}]} [cells] \quad (3)$$

$$\frac{d[ChrS]}{dt} = \gamma [ChrS_{IN1}] \left(\frac{1 + \omega_{P_{chrSA}}^{ChrA} \left(\frac{[ChrA - P]}{K_P^{ChrA}} \right)^{n_{P_{chrSA}}^{ChrA}}}{1 + \left(\frac{[ChrA - P]}{K_P^{ChrA}} \right)^{n_{P_{chrSA}}^{ChrA}}} \right) - k_+^{ChrS} [ChrS] \frac{[H_{EX}]}{K_{H_{EX}} + [H_{EX}]} + k_1^{ChrS} [ChrS\sim P][ChrA] - \gamma [ChrS] \quad (4)$$

$$\frac{d[ChrS\sim P]}{dt} = k_+^{ChrS} [ChrS] \frac{[H_{EX}]}{K_{H_{EX}} + [H_{EX}]} - k_1^{ChrS} [ChrS\sim P][ChrA] - \gamma [ChrS\sim P] \quad (5)$$

$$\frac{d[HrrS]}{dt} = \gamma [HrrS_{TOT}] - k_+^{HrrS} [HrrS] \frac{[H_{EX}]}{K_{H_{EX}} + [H_{EX}]} + k_3^{HrrS} [HrrS\sim P][ChrA] - \gamma [HrrS] \quad (6)$$

$$\frac{d[HrrS\sim P]}{dt} = k_+^{HrrS} [HrrS] \frac{[H_{EX}]}{K_{H_{EX}} + [H_{EX}]} - k_3^{HrrS} [HrrS\sim P][ChrA] - \gamma [HrrS\sim P] \quad (7)$$

$$\begin{aligned} \frac{d[ChrA]}{dt} = & \gamma[ChrA_{INI}] \left(\frac{1 + \omega_{P_{chrSA}^{ChrA}} \left(\frac{[ChrA - P]}{K_{P_{chrSA}^{ChrA}}} \right)^{n_{P_{chrSA}^{ChrA}}}}{1 + \left(\frac{[ChrA - P]}{K_{P_{chrSA}^{ChrA}}} \right)^{n_{P_{chrSA}^{ChrA}}}} \right) - k_1^{ChrS}[ChrS \sim P][ChrA] + k_2^{ChrS}[ChrS][ChrA \sim P] \\ & - k_3^{HrrS}[HrrS \sim P][ChrA] - \gamma[ChrA] \end{aligned} \quad (8)$$

$$\frac{d[ChrA \sim P]}{dt} = k_1^{ChrS}[ChrS \sim P][ChrA] + k_2^{ChrS}[ChrS][ChrA \sim P] - k_3^{HrrS}[HrrS \sim P][ChrA] - \gamma[ChrA \sim P] \quad (9)$$

$$\frac{d[HrtBA]}{dt} = \gamma[HrtBA_{INI}] \left(\frac{1 + \omega_{P_{hrtBA}^{ChrA}} \left(\frac{[ChrA - P]}{K_{P_{hrtBA}^{ChrA}}} \right)^{n_{P_{hrtBA}^{ChrA}}}}{1 + \left(\frac{[ChrA - P]}{K_{P_{hrtBA}^{ChrA}}} \right)^{n_{P_{hrtBA}^{ChrA}}}} \right) - \gamma[HrtBA] \quad (10)$$

$$\frac{d[ChrS_{TOT} - YFP]}{dt} = \gamma[ChrS_{INI}] \left(\frac{1 + \omega_{P_{chrSA}^{ChrA}} \left(\frac{[ChrA - P]}{K_{P_{chrSA}^{ChrA}}} \right)^{n_{P_{chrSA}^{ChrA}}}}{1 + \left(\frac{[ChrA - P]}{K_{P_{chrSA}^{ChrA}}} \right)^{n_{P_{chrSA}^{ChrA}}}} \right) - (\gamma + k_{bl})[ChrS_{TOT} - YFP] \quad (11)$$

$$\frac{d[ChrA_{TOT} - YFP]}{dt} = \gamma[ChrA_{INI}] \left(\frac{1 + \omega_{P_{chrSA}^{ChrA}} \left(\frac{[ChrA - P]}{K_{P_{chrSA}^{ChrA}}} \right)^{n_{P_{chrSA}^{ChrA}}}}{1 + \left(\frac{[ChrA - P]}{K_{P_{chrSA}^{ChrA}}} \right)^{n_{P_{chrSA}^{ChrA}}}} \right) - (\gamma + k_{bl})[ChrA_{TOT} - YFP] \quad (12)$$

$$\frac{d[HrtBA - YFP]}{dt} = \gamma[HrtBA_{INI}] \left(\frac{1 + \omega_{P_{hrtBA}^{ChrA}} \left(\frac{[ChrA - P]}{K_{P_{hrtBA}^{ChrA}}} \right)^{n_{P_{hrtBA}^{ChrA}}}}{1 + \left(\frac{[ChrA - P]}{K_{P_{hrtBA}^{ChrA}}} \right)^{n_{P_{hrtBA}^{ChrA}}}} \right) - (\gamma + k_{bl})[HrtBA - YFP] \quad (13)$$

Model equations M2: ODEs of the mathematical model of the *C. glutamicum* heme utilization module

Variables within the model:

Name	Description
H_{EX}	External heme
H_{IN}	Internal heme
$cells$	Cells of <i>C. glutamicum</i>
$ChrS$	Unphosphorylated histidine kinase ChrS
$ChrS\sim P$	Autophosphorylated histidine kinase ChrS
$HrrS$	Unphosphorylated histidine kinase HrrS
$HrrS\sim P$	Autophosphorylated histidine kinase HrrS
$HrrA$	Unphosphorylated response regulator HrrA
$HrrA\sim P$	Phosphorylated response regulator HrrA
$HmuO$	Heme oxygenase HmuO
$DtxR^*$	Activated form of the iron repressor DtxR
$DtxR$	Non-activated form of the iron repressor DtxR
$HrrA_{TOT}\text{-YFP}$	YFP proteins corresponding to the total amount of the response regulator HrrA (The production is under the control of P_{hrrA} promoter)
$HmuO\text{-YFP}$	YFP proteins corresponding to the total amount of heme oxygenase HmuO (The production is under the control of P_{hmuO} promoter)

ODEs:

$$\frac{d[H_{EX}]}{dt} = -v_{max}^{IMP} \frac{[H_{EX}]}{K_M^{IMP} + [H_{EX}]} [cells] \quad (14)$$

$$\frac{d[H_{IN}]}{dt} = v_{max}^{IMP} \frac{[H_{EX}]}{K_M^{IMP} + [H_{EX}]} - k_{cat}^{CON} ([E^{CON}] + [HmuO]) \frac{[H_{IN}]}{K_M^{CON} + [H_{IN}]} - \gamma[H_{IN}] \quad (15)$$

$$\frac{d[cells]}{dt} = \beta^1 k_{cat}^{CON} ([E^{CON}] + [HmuO]) \frac{[H_{IN}]}{K_M^{CON} + [H_{IN}]} [cells] \quad (16)$$

$$\frac{d[ChrS]}{dt} = \gamma[ChrS_{TOT}] - k_+^{ChrS} [ChrS] \frac{[H_{EX}]}{K_{H_{EX}} + [H_{EX}]} + k_3^{ChrS} [ChrS\sim P][ChrA] - \gamma[ChrS] \quad (17)$$

$$\frac{d[ChrS\sim P]}{dt} = k_+^{ChrS} [ChrS] \frac{[H_{EX}]}{K_{H_{EX}} + [H_{EX}]} - k_3^{ChrS} [ChrS\sim P][ChrA] - \gamma[ChrS\sim P] \quad (18)$$

$$\frac{d[HrrS]}{dt} = \gamma[HrrS_{TOT}] - k_+^{HrrS} [HrrS] \frac{[H_{EX}]}{K_{H_{EX}} + [H_{EX}]} + k_1^{HrrS} [HrrS\sim P][ChrA] - \gamma[HrrS] \quad (19)$$

$$\frac{d[HrrS\sim P]}{dt} = k_+^{HrrS} [HrrS] \frac{[H_{EX}]}{K_{H_{EX}} + [H_{EX}]} - k_1^{HrrS} [HrrS\sim P][ChrA] - \gamma[HrrS\sim P] \quad (20)$$

$$\frac{d[HrrA]}{dt} = \gamma[HrrA_{INI}] \left(\frac{1 + \omega_{P_{HrrA}}^{HrrA} \left(\frac{[HrrA - P]}{K_{P_{HrrA}}^{HrrA}} \right)^{n_{P_{HrrA}}^{HrrA}}}{1 + \left(\frac{[HrrA - P]}{K_{P_{HrrA}}^{HrrA}} \right)^{n_{P_{HrrA}}^{HrrA}} + \left(\frac{DtxR_{TOT} \frac{[H_{IN}]}{K_{H_{IN}} + [H_{IN}]} }{K_{P_{HrrA}}^{DtxR}} \right)^{n_{P_{HrrA}}^{DtxR}}} \right) - k_1^{HrrS}[HrrS \sim P][HrrA] + k_2^{HrrS}[HrrS][HrrA \sim P] - k_3^{ChrS}[ChrS \sim P][HrrA] - \gamma[HrrA] \quad (21)$$

$$\frac{d[ChrA \sim P]}{dt} = k_1^{HrrS}[HrrS \sim P][HrrA] - k_2^{HrrS}[HrrS][HrrA \sim P] + k_3^{ChrS}[ChrS \sim P][HrrA] - \gamma[HrrA \sim P] \quad (22)$$

$$\frac{d[HmuO]}{dt} = \gamma[HmuO_{INI}] \left(\frac{1 + \omega_{P_{HmuO}}^{HrrA} \left(\frac{[HrrA - P]}{K_{P_{HmuO}}^{HrrA}} \right)^{n_{P_{HmuO}}^{HrrA}}}{1 + \left(\frac{[HrrA - P]}{K_{P_{HmuO}}^{HrrA}} \right)^{n_{P_{HmuO}}^{HrrA}} + \left(\frac{DtxR_{TOT} \frac{[H_{IN}]}{K_{H_{IN}} + [H_{IN}]} }{K_{P_{HmuO}}^{DtxR}} \right)^{n_{P_{HmuO}}^{DtxR}}} \right) - \gamma[HmuO] \quad (23)$$

$$\frac{d[HrrA_{TOT} - YFP]}{dt} = \gamma[HrrA_{INI}] \left(\frac{1 + \omega_{P_{HrrA}}^{HrrA} \left(\frac{[HrrA - P]}{K_{P_{HrrA}}^{HrrA}} \right)^{n_{P_{HrrA}}^{HrrA}}}{1 + \left(\frac{[HrrA - P]}{K_{P_{HrrA}}^{HrrA}} \right)^{n_{P_{HrrA}}^{HrrA}} + \left(\frac{DtxR_{TOT} \frac{[H_{IN}]}{K_{H_{IN}} + [H_{IN}]} }{K_{P_{HrrA}}^{DtxR}} \right)^{n_{P_{HrrA}}^{DtxR}}} \right) - (\gamma + k_{bl})[HrrA_{TOT} - YFP] \quad (24)$$

$$\frac{d[HmuO - YFP]}{dt} = \gamma[HmuO_{INI}] \left(\frac{1 + \omega_{P_{HmuO}}^{HrrA} \left(\frac{[HrrA - P]}{K_{P_{HmuO}}^{HrrA}} \right)^{n_{P_{HmuO}}^{HrrA}}}{1 + \left(\frac{[HrrA - P]}{K_{P_{HmuO}}^{HrrA}} \right)^{n_{P_{HmuO}}^{HrrA}} + \left(\frac{DtxR_{TOT} \frac{[H_{IN}]}{K_{H_{IN}} + [H_{IN}]} }{K_{P_{HmuO}}^{DtxR}} \right)^{n_{P_{HmuO}}^{DtxR}}} \right) - (\gamma + k_{bl})[HmuO - YFP] \quad (25)$$

DtxR activation:

$$DtxR_{TOT} = DtxR + DtxR^* \quad (26)$$

$$DtxR^* = DtxR_{TOT} \frac{[H_{IN}]}{K_{H_{IN}} + [H_{IN}]} \quad (27)$$

$$DtxR = DtxR_{TOT} \left(1 - \frac{[H_{IN}]}{K_{H_{IN}} + [H_{IN}]} \right) \quad (28)$$

Supplementary Table S1. Bacterial strains used in this study.

Strain or plasmid	Relevant characteristics	Source reference	or
<i>Escherichia coli</i>			
DH5 α	<i>fhuA2 lac(del)U169 phoA glnV44 Φ80' lacZ(del)M15 gyrA96 recA1 relA1 endA1 thi-1 hsdR17</i> ; for general cloning purposes	Invitrogen	
BL21(DE3)	B F ⁻ <i>ompT gal dcm lon hsdS_B(r_B⁻m_B⁻) λ(DE3 [<i>lacI lacUV5-T7p07 ind1 sam7 nin5</i>] [<i>malB'</i>]_{K-12}(λ^S); overexpression of proteins.</i>	(Studier & Moffatt, 1986)	
<i>Corynebacterium glutamicum</i>			
ATCC 13032	<i>C. glutamicum</i> wild type strain	(Kinoshita, Udaka, & Shimono, 2004)	
ATCC 13032 Δ <i>hrrS</i>	Deletion mutant of the open reading frame (orf) encoding the HK HrrS	(Hentschel et al., 2014)	
ATCC <i>hrrSQ222A</i>	13032 Phosphatase=OFF mutant of <i>hrrS</i>	(Hentschel et al., 2014)	
ATCC 13032 Δ <i>chrS</i>	Deletion mutant of the orf encoding the HK ChrS	(Hentschel et al., 2014)	
ATCC <i>chrSQ191A</i>	13032 Phosphatase=OFF mutant of <i>hrrS</i>	(Hentschel et al., 2014)	
ATCC <i>chrSH186A</i>	13032 Kinase=OFF mutant of <i>chrS</i>	This study	
ATCC 13032 Δ <i>dtxR</i>	Deletion mutant of the orf encoding DtxR	(Wennerhold & Bott, 2006)	
ATCC 13032 Δ <i>hrrA</i>	Deletion mutant of the orf encoding the RR HrrA	(Frunzke, Gatgens, Brocker, & Bott, 2011)	

Supplementary Table S2. Oligonucleotides used in this study. Restriction sites mutations are underlined.

#	Name	Sequence	Special feature
1	<i>chrS-fw</i>	GCGCAAGCTTGTGAAAAGTCCAAAGCGAC	<i>HindIII</i> RS
2	<i>chrS-rv</i>	TATACCCGGGTCACCTTATCTTGGTCCTTTTG	<i>SmaI</i> RS
3	<i>chrSH186A</i>	CCACAGTGTCAGCTATTTTCGCCCGCTATGCGGGC	Mutation <i>H186A</i>
4	<i>chrSH186A</i>	GCCCGCATAGCGGGCGAAATAGCTGACACTGTGG	Mutation <i>H186A</i>
5	<i>P_{hmuO}^{AAC::TTG}</i>	CACACCTACATATAGTCCCTTA <u>CA</u> AGGAACAATTTTCCGCAACTTTGG	Mutation <i>P_{hmuO}</i>
6	<i>P_{hmuO}^{AAC::TTG}</i>	CCAAAGTTGCGGAAAATTGTCC <u>TTG</u> TAAGGGACTATATGTAGGTGG	Mutation <i>P_{hmuO}</i>

Supplementary Table S3. Plasmids used in this study. If plasmids were constructed in this study, primers used are indicated in Table S2.

Reporter plasmids				
#	Name	Resistance	Source	Primer used
1	pJC1_ <i>PhrtBA-eyfp</i>	Kanamycin	(Heyer et al., 2012)	
2	pJC1_ <i>PhmuO-eyfp</i>	Kanamycin	(Heyer et al., 2012)	
3	pJC1_ <i>PhmuO-eyfp^{AAC::TTG}</i>	Kanamycin	This study	#5, #6

Plasmids for genomic intergrations			
4	pK19_ΔchrS ^{wt} ::chrSH184A	Kanamycin	This study
			Cloning: #1, #2 Mut.: #3, #4

Supplementary Table S4. Parameters used in the mathematical model of the *C. glutamicum* heme detoxification module.

Parameter	Notation	Value	Source
Maximal velocity of heme import via heme transporter HmuTUV	v_{max}^{IMP}	9.83×10^3 molecules/min/cell	Adjusted to match the average growth curve (Fig. 2)
Michaelis-Menten constant for heme import via heme transporter HmuTUV	K_M^{IMP}	1.19×10^{13} molecules	
Maximal velocity of heme consumption via diverse enzymes	v_{max}^{CON}	7.86×10^3 molecules/min/cell	
Michaelis-Menten constant for heme consumption via diverse enzymes	K_M^{CON}	1.84×10^6 molecules/cell	
Growth parameter	β	0.04 1/min	
Initial OD	OD_{INI}	$2.2 \sim 6.6 \times 10^7$ cells	
Autophosphorylation threshold of ChrS/HrrS	$K_{H_{EX}}$	1.2×10^{13} molecules	Adjusted to guarantee approximately maximal autophosphorylation rate even for the lowest hemin concentration
Autophosphorylation rate of ChrS	k_+^{ChrS}	1 1/min	Adjusted to match a rate of autophosphorylation as expected in (Groban et al., 2009), taking the ChrS/HrrS levels into account.
Autophosphorylation rate of HrrS	k_+^{HrrS}	1 1/min	
Effective rate constants of phosphorylation reaction of the cognate kinase ChrS on ChrA	k_1^{ChrS}	3.98×10^{-3} 1/molecules/min	Correspond to the <i>in vitro</i> data in (Hentschel et al., 2014), multiplied by a factor of 10 due to the observation of (Gao & Stock, 2017; Kremling, Kremling, & Bettenbrock, 2009), that <i>in vitro</i> rates are often about 10^1 - 10^2 -fold lower than the actual <i>in vivo</i> ones.
Effective rate constants of dephosphorylation reaction of the cognate kinase ChrS on ChrA	k_2^{ChrS}	3.76×10^{-2} 1/molecules/min	
Effective rate constants of phosphorylation reaction of the non-cognate kinase HrrS on ChrA	k_3^{HrrS}	5.72×10^{-6} 1/molecules/min	Correspond to the <i>in vitro</i> data in (Hentschel et al., 2014), decreased by a factor of 10, suggested by Fig.S5.
Initial ChrS concentration	$ChrS_{INI}$	100 molecules/cell	Correspond to reference values for total numbers in <i>E. coli</i> for several two-component systems (Cai & Inouye, 2002; Gao & Stock, 2013; Li, Burkhardt, Gross, & Weissman, 2014): Numbers of histidine kinases are within a physiological range of 10^1 - 10^3 and response regulators range between 10^2 and 10^4 . A 1:1 stoichiometry is assumed for ChrS and ChrA due to the fact that they are within one operon.
Initial ChrA concentration	$ChrA_{INI}$	100 molecules/cell	
Total HrrS concentration	$HrrS_{TOT}$	100 molecules/cell	
Initial HrtBA concentration	$HrtBA_{INI}$	10 molecules/cell	Arbitrary choice
Turnover rate of heme exporter HrtBA	k_{cat}^{HrtBA}	20 molecules/min/transporter	Adjusted to counteract the import rate under maximal <i>hrtBA</i> expression
Michaelis-Menten constant for	K_M^{HrtBA}	8×10^5 molecules/cell	

heme export via HrrBA			
Fold-change of P _{chrSA} promoter	$\omega_{P_{chrSA}}^{ChrA}$	70	Suggested by wildtype data in Fig. S1a; within physiological range of 1-10 ⁴ (see e.g. (Lutz & Bujard, 1997)) for promoters with high dynamic range)
Fold-change of P _{hrrBA} promoter	$\omega_{P_{hrrBA}}^{ChrA}$	150	
P _{chrSA} activation threshold	$K_{P_{chrSA}}^{ChrA}$	75 molecules/cell	Correspond to the total levels of ChrA~P
P _{hrrBA} activation threshold	$K_{P_{hrrBA}}^{ChrA}$	75 molecules/cell	
Hill coefficient P _{chrSA}	$n_{P_{chrSA}}^{ChrA}$	1	Assuming no cooperativity in promoter binding
Hill coefficient P _{hrrBA}	$n_{P_{hrrBA}}^{ChrA}$	1	
Effective rate constant of YFP bleaching and protein degradation	k_{bl}	0.001 1/min	Arbitrary choice

Supplementary Table S5. Additional parameters used in the mathematical model of the *C. glutamicum* heme utilization module (all other parameters are taken from the model of *C. glutamicum* heme detoxification module, cf. Supplementary Table S4).

Parameter	Notation	Value	Source
Growth parameter	β'	5×10^{-6} 1/molecules	Adjusted to match the growth rate we observed in the model of <i>C. glutamicum</i> heme detoxification module
Effective rate constants of phosphorylation reaction of the cognate kinase HrrS on HrrA	k_1^{HrrS}	3.76×10^{-3} 1/molecules/min	Correspond to the <i>in vitro</i> data in (Hentschel et al., 2014), multiplied by a factor of 10 due to the observation of (Gao & Stock, 2017; Kremling et al., 2009), that <i>in vitro</i> rates are often about 10 ¹ -10 ² -fold lower than the actual <i>in vivo</i> ones.
Effective rate constants of dephosphorylation reaction of the cognate kinase HrrS on HrrA	k_2^{HrrS}	3.40×10^{-4} 1/molecules/min	Correspond to the <i>in vitro</i> data in (Hentschel et al., 2014), decreased by a factor of 10, suggested by Fig. S5.
Effective rate constants of phosphorylation reaction of the non-cognate kinase ChrS on HrrA	k_3^{ChrS}	1.40×10^{-3} 1/molecules/min	Correspond to the <i>in vitro</i> data in (Hentschel et al., 2014), multiplied by a factor of 10 due to the observation of (Gao & Stock, 2017; Kremling et al., 2009), that <i>in vitro</i> rates are often about 10 ¹ -10 ² -fold lower than the actual <i>in vivo</i> ones.
Total HrrS concentration	$HrrS_{TOT}$	100 molecules/cell	Reference values for total numbers in <i>E. coli</i> for several TCS: Numbers of histidine kinases are within a physiological range of 10 ¹ -10 ³ and response regulators range between 10 ² and 10 ⁴ (Cai & Inouye, 2002; Gao & Stock, 2013; Li et al., 2014).
Initial HrrA concentration	$HrrA_{INI}$	100 molecules/cell	
Total ChrS concentration	$ChrS_{TOT}$	100 molecules/cell	
Initial HmuO concentration	$HmuO_{INI}$	100 molecules/cell	Arbitrary choice
Turnover rate of heme consumption via HmuO and	k_{cat}^{CON}	6.04 molecules/min/transporter	Adjusted to match the maximal

diverse other enzymes			
Concentration of other enzymes responsible for heme consumption next to HmuO	E^{CON}	1000 molecules/cell	velocity (v_{max}^{CON}) and total reaction rate of consumption we observed in the model of <i>C. glutamicum</i> heme detoxification module
Michaelis-Menten constant for heme consumption via HmuO and diverse other enzymes	K_M^{CON}	1.84×10^6 molecules/cell	
Total DtxR concentration	$DtxR_{TOT}$	1000 molecules/cell	Arbitrary choice
Activation threshold of DtxR	K_{HIN}	8×10^5 molecules/cell	Adjusted to guarantee a sufficient activation of iron repressor DtxR for the highest hemin concentration.
Fold-change of P_{HrrA} promoter	$\omega_{P_{HrrA}}^{HrrA}$	5	Suggested by wildtype data in Fig. S1a; within physiological range of $1-10^4$ (see e.g. (Lutz & Bujard, 1997) for promoters with high dynamic range)
Fold-change of P_{HmuO} promoter	$\omega_{P_{HmuO}}^{HrrA}$	50	Correspond to the total levels of ChrA~P and activated DtxR. Experimental Data suggest a significant higher activation via HrrA than the repression via DtxR on P_{HrrA}
P_{HrrA} activation threshold	$K_{P_{HrrA}}^{HrrA}$	100 molecules/cell	
P_{HmuO} activation threshold	$K_{P_{HmuO}}^{HrrA}$	300 molecules/cell	
P_{HmuO} threshold of DtxR repression	$K_{P_{HmuO}}^{DtxR}$	300 molecules/cell	
P_{HrrA} threshold of DtxR repression	$K_{P_{HrrA}}^{DtxR}$	500 molecules/cell	
Hill coefficient of HrrA binding to P_{HrrA}	$n_{P_{HrrA}}^{HrrA}$	1	Assuming no cooperativity in promoter binding on P_{HrrA}
Hill coefficient of HrrA binding to P_{HmuO}	$n_{P_{HmuO}}^{HrrA}$	1	
Hill coefficient of DtxR binding to P_{HmuO}	$n_{P_{HmuO}}^{DtxR}$	7	Adjusted to have a strong repressive effect on P_{HmuO}/P_{HrrBA}
Hill coefficient of DtxR binding to P_{HrrA}	$n_{P_{HrrA}}^{DtxR}$	7	

Supplementary Table S6. Transformation of the units within the mathematical models

Experimental unit	Unit within the mathematical models	Source
OD = 1	$\sim 3 \times 10^8$ cells/mL	(Unthan et al., 2015)
Heme [μM] in the growth medium	$\sim 6 \times 10^{13}$ molecules heme in the growth medium	Assuming a reaction volume of $\sim 100 \mu L$
Free heme [μM] in the cell	~ 1000 heme molecules/cell	Corresponds to a cell size of $\sim 1 \mu m^3$ [REF]

Supporting References

- Bintu, L., Buchler, N. E., Garcia, H. G., Gerland, U., Hwa, T., Kondev, J., & Phillips, R. (2005). Transcriptional regulation by the numbers: models. *Curr Opin Genet Dev*, 15(2), 116-124. doi: 10.1016/j.gde.2005.02.007
- Cai, S. J., & Inouye, M. (2002). EnvZ-OmpR interaction and osmoregulation in *Escherichia coli*. *J Biol Chem*, 277(27), 24155-24161. doi: 10.1074/jbc.M110715200
- Frunzke, J., Gatgens, C., Brocker, M., & Bott, M. (2011). Control of heme homeostasis in *Corynebacterium glutamicum* by the two-component system HrrSA. *J Bacteriol*, 193(5), 1212-1221. doi: 10.1128/jb.01130-10
- Gao, R., & Stock, A. M. (2013). Evolutionary tuning of protein expression levels of a positively autoregulated two-component system. *PLoS Genet*, 9(10), e1003927. doi: 10.1371/journal.pgen.1003927
- Gao, R., & Stock, A. M. (2017). Quantitative Kinetic Analyses of Shutting Off a Two-Component System. *MBio*, 8(3). doi: 10.1128/mBio.00412-17
- Groban, E. S., Clarke, E. J., Salis, H. M., Miller, S. M., & Voigt, C. A. (2009). Kinetic buffering of cross talk between bacterial two-component sensors. *J Mol Biol*, 390(3), 380-393. doi: 10.1016/j.jmb.2009.05.007
- Hentschel, E., Mack, C., Gatgens, C., Bott, M., Brocker, M., & Frunzke, J. (2014). Phosphatase activity of the histidine kinases ensures pathway specificity of the ChrSA and HrrSA two-component systems in *Corynebacterium glutamicum*. *Mol Microbiol*, 92(6), 1326-1342. doi: 10.1111/mmi.12633
- Heyer, A., Gatgens, C., Hentschel, E., Kalinowski, J., Bott, M., & Frunzke, J. (2012). The two-component system ChrSA is crucial for haem tolerance and interferes with HrrSA in haem-dependent gene regulation in *Corynebacterium glutamicum*. *Microbiology*, 158(Pt 12), 3020-3031. doi: 10.1099/mic.0.062638-0
- Keppel, M., Davoudi, E., Gätgens, C., & Frunzke, J. (2018). Membrane Topology and Heme Binding of the Histidine Kinases HrrS and ChrS in *Corynebacterium glutamicum*. *Front Microbiol*, 9(183). doi: 10.3389/fmicb.2018.00183
- Kinoshita, S., Udaka, S., & Shimono, M. (2004). Studies on the amino acid fermentation. Part 1. Production of L-glutamic acid by various microorganisms. *J Gen Appl Microbiol*, 50(6), 331-343.
- Kremling, A., Kremling, S., & Bettenbrock, K. (2009). Catabolite repression in *Escherichia coli*- a comparison of modelling approaches. *FEBS J*, 276(2), 594-602. doi: 10.1111/j.1742-4658.2008.06810.x
- Li, G. W., Burkhardt, D., Gross, C., & Weissman, J. S. (2014). Quantifying absolute protein synthesis rates reveals principles underlying allocation of cellular resources. *Cell*, 157(3), 624-635. doi: 10.1016/j.cell.2014.02.033
- Lutz, R., & Bujard, H. (1997). Independent and tight regulation of transcriptional units in *Escherichia coli* via the LacR/O, the TetR/O and AraC/I1-I2 regulatory elements. *Nucleic Acids Res*, 25(6), 1203-1210.
- Studier, F. W., & Moffatt, B. A. (1986). Use of bacteriophage T7 RNA polymerase to direct selective high-level expression of cloned genes. *J Mol Biol*, 189(1), 113-130.
- Unthan, S., Baumgart, M., Radek, A., Herbst, M., Siebert, D., Bruhl, N., . . . Noack, S. (2015). Chassis organism from *Corynebacterium glutamicum*--a top-down approach to identify and delete irrelevant gene clusters. *Biotechnol J*, 10(2), 290-301. doi: 10.1002/biot.201400041

Wennerhold, J., & Bott, M. (2006). The DtxR regulon of *Corynebacterium glutamicum*. *J Bacteriol*, *188*(8), 2907-2918. doi: 10.1128/jb.188.8.2907-2918.2006

5.3 Supplement “HrrSA orchestrates a systemic response to heme and determines prioritization of terminal cytochrome oxidase expression”

1 Supplement to:

2 **HrrSA orchestrates a systemic response to heme and determines**
3 **prioritisation of terminal cytochrome oxidase expression**

4 Marc Keppel^{1#}, Cedric-Farhad Davoudi^{1#}, Andrei Filipchuk^{1#}, Ulrike Viets¹, Eugen Pfeifer¹, Tino
5 Polen¹, Meike Baumgart¹, Michael Bott¹, and Julia Frunzke^{1*}

6

7 ¹Institute of Bio- und Geosciences, IBG-1: Biotechnology, Forschungszentrum Jülich, 52425
8 Jülich, Germany

9

10 *Corresponding author:

11 Julia Frunzke; Email: j.frunzke@fz-juelich.de; Phone: +49 2461 615430

12 [#]These authors contributed equally to this work.

13 **Content**

14 **Table S1:** Bacterial strains and plasmids used in this study.

15 **Table S2:** Oligonucleotides used in this study.

16 **Table S3:** Full Dataset, binding peaks HrrA and transcriptome analysis wild type and $\Delta hrrA$
17 (separate file)

18

19

20 **Figure S1:** Global binding pattern of HrrA in the *C. glutamicum* genome in response to hemin
21 addition

22 **Figure S2:** Distribution of distances from HrrA binding peaks centers to the closest gene start
23 site (translation start site, TLS).

24 **Figure S3:** HrrA binding to selected target promotor regions.

25 **Figure S4:** Derivation of a HrrA binding motif revealed a weakly conserved palindromic
26 sequence.

27 **Figure S5:** Discoloration of *C. glutamicum* cells after addition of heme.

28 **Figure S6:** HrrA coordinates expression of *ctaA* and *ctaB* in response to heme.

29 **Figure S7:** Dynamic range of HrrA association upon addition of external heme

30 **Figure S8:** Binding affinity of HrrA to selected target promoters.

31 **Figure S9:** Time-resolved differential gene expression analysis.

32 **Figure S10:** HrrA-dependent *hmuO* expression in response to heme.

33 **Figure S11:** Alignment of HrrA orthologs of *C. glutamicum* and *C. diphtheriae*.

34 **Figure S12:** Schematic overview of the convolution profiling.

35 **Supplement**36 **Strains, plasmids and oligonucleotides used in this study.**

37 **Table S1: Bacterial strains and plasmids used in this study.** Oligonucleotides used for the
 38 construction of the plasmids are listed in Table S2.

Strain	Relevant characteristics	Reference
<i>Escherichia coli</i>		
DH5 α	<i>fhuA2 lac(del)U169 phoA glnV44 Φ80' lacZ(del)M15 gyrA96 recA1 relA1 endA1 thi-1 hsdR17</i> ; for general cloning purposes	Invitrogen
BL21(DE3)	B F ⁻ <i>ompT gal dcm lon hsdS_B(r_B⁻m_B⁻)</i> λ (DE3 [<i>lacI</i> ¹ <i>lacUV5-T7p07 ind1 sam7 nin5</i>]) [<i>malB</i> [*]] _{K-12} (λ ^S); overexpression of proteins.	
<i>Corynebacterium glutamicum</i>		
<i>C. glutamicum</i> ATCC13032	Biotin-auxotrophic wild type strain	²
<i>C. glutamicum</i> Δ <i>hrrA</i>	Derivative of ATCC13032 with in-frame deletion of the <i>hrrA</i> gene	³
<i>C. glutamicum</i> Δ <i>hrrSA</i> Δ <i>chrSA</i>	Derivative of ATCC13032 with in-frame deletions of the <i>hrrS</i> (cg3248) and <i>hrrA</i> (cg3247) genes and the <i>chrSA</i> (cg2201-cg2200) operon.	⁴
Plasmid		
Name	Resistance	Source
pJC1	Kanamycin	⁵
pJC1_ <i>P</i> _{<i>hrrSA</i>} - <i>hrrSA</i> - <i>twin</i> - <i>strep</i> - <i>P</i> _{<i>chrSA</i>} - <i>chrSA</i> - <i>his</i>	Kanamycin	This study

39 Table S2: Oligonucleotides used in this study.

#	Name	Sequence
1	<i>hrrSA-twin-strep-fw</i>	TTTTGCGTTTCTACAAACTCTTTTGTAGAGACCAAGATTCTGG
2	<i>hrrSA-twin-strep-rv</i>	CTGTAAAACGACGGCCAGTACTAGTCTATTTTTTCGAACTGCGGGTG
3	<i>chrSA-his-fw</i>	CAGCGACGCCGACGGGGATCCCTACTACACTACATCATGCGCAGTAG
4	<i>chrSA-his-rv</i>	AGTAATCCAGAATCTTGGTCTTAACAAAAGAGTTTGTAGAAACG
5	<i>P_{hmuO}</i> (EMSA) fw	GAGAAATCCTCACGCTCAC
6	<i>P_{hmuO}</i> (EMSA) rv	GGTGGGAGCCCCAAGTTG
7	<i>P_{ctaE}</i> (EMSA) fw	CCCAAAGTGGTTCCGCAGG
8	<i>P_{ctaE}</i> (EMSA) rv	ACGCCTTTTATTCGGGTTC
9	<i>P_{pck}</i> (EMSA) fw	CTTTCTATGGAGATGATCG
10	<i>P_{pck}</i> (EMSA) rv	CGATTTAAATGGACCCTAAAC
11	<i>P_{ramB}</i> (EMSA) fw	CCTGCGCAAAGTTGCTCCCTG
12	<i>P_{ramB}</i> (EMSA) rv	CTCACAGGATACCGATCCGAAC
13	<i>P_{cg1080}</i> (EMSA) fw	CGCTCCTCTGTGGGATTTGTC
14	<i>P_{cg1080}</i> (EMSA) rv	GCCTTCACTCCCTCAAAC
15	<i>P_{xerC}</i> (EMSA) fw	CTTAGGCTTGCTCACACAC
16	<i>P_{xerC}</i> (EMSA) rv	AATGCGGAAATGCCATAAAACC
17	<i>P_{cg3402}</i> (EMSA) fw	CATAGGGGTATAGCCTTGAG
18	<i>P_{cg3402}</i> (EMSA) rv	CAGTGTGCGCAGGTCATGCC
19	<i>P_{ctaC}</i> (EMSA) fw	GGAATACCTAAAGTCTAGGC
20	<i>P_{ctaC}</i> (EMSA) rv	GTAGGAACGTAGGGGTAAG
21	<i>P_{sigC/kata}</i> (EMSA) fw	GGTCACCATAAAGTGTGTAG
22	<i>P_{sigC/kata}</i> (EMSA) rv	GCCACCAATAATCAGCCC
23	<i>P_{cyd}</i> (EMSA) fw	GTCCCGCTCACAGCTTAAC
24	<i>P_{cyd}</i> (EMSA) rv	GGTGACTTGCAACAAGGGG
25	<i>P_{trpS}</i> (EMSA) fw	GACTTGTTTACCCAAGCAATAC
26	<i>P_{trpS}</i> (EMSA) rv	CCGGTGAGGCAACATTTACC
27	<i>P_{htaA}</i> (EMSA) fw	GTCATGATGGCGTCTCGGGC
28	<i>P_{htaA}</i> (EMSA) rv	GTAATCAACGCACAATG

Table S3: Partial Dataset of genome wide HrrA binding (ChAP-Seq) and time resolved transcriptome analysis of *C. glutamicum* wild type and Δ hrrA (RNA-Seq). For ChAP-Seq analysis, the strain *C. glutamicum* Δ hrrSA Δ chrSA harboring the plasmid pJC1_PhrrSA-hrrSA-twin-strep_PchrSA-chrSA-his was cultivated in CGXII minimal medium supplemented with 2% (w/v) glucose and 4 μ M hemin and was harvested at different time points as described in Figure 1. For RNA-Seq, wild type cells and a Δ hrrA were cultivated accordingly and harvested 0 h, 0.5 h and 4 h after hemin addition. For RNA-Seq analysis strains contained no plasmids and consequently no antibiotics were added to the medium. Column 1 and 2 show the locus and gene name and column 3 indicates the distance of the peak maximum to the translational start site of the gene in column 1/2. For all known transcriptional start sites, the distance to the TSS is indicated in column 4. In grey (5-10), ChAP-Seq peak intensities are indicated at 0 h, 0.5 h, 2 h, 4 h, 9 h and 24 h after hemin addition. In green (11-13) and red (14-16), the measured mRNA levels of the corresponding genes in the wild type strain (green) and a Δ hrrA strain are shown (in transcripts per million, mean of two biological replicates). All further information can be found in the full Table in Keppel *et al.* (2018a).

cg number	Gene name	Distance ATG	Distance to TSS	ChAP-Seq T=0	T=0.5	T=2	T=4	T=9	T=24	mRNA wt t=0	mRNA wt t=0.5	mRNA wt t=4	mRNA Δ hrrA t=0	mRNA Δ hrrA t=0.5	mRNA Δ hrrA t=4
cg0019		24	24	1.4	4.7	2.1	1.3	1.0	1.0	21.0	20.8	23.5	28.5	21.6	15.2
cg0046		129	unknown	1.3	3.1	1.0	1.0	1.0	1.0	273.3	179.3	181.8	171.5	177.1	256.8
cg0061	<i>rodA</i>	389	unknown	1.7	8.7	2.6	1.0	1.0	1.0	141.2	331.2	212.2	159.7	157.7	148.7
cg0074		203	unknown	2.6	12.1	4.1	2.9	1.0	1.0	7.0	1.5	9.2	4.9	2.2	6.3
cg0076		245	unknown	3.2	18.9	8.2	3.1	1.0	1.5	21.7	5.7	15.2	11.3	3.6	11.8
cg0104	<i>codA</i>	72	41	1.0	3.4	2.1	1.0	1.0	1.0	196.4	30.3	35.4	57.2	64.4	21.5
cg0109	<i>lip1</i>	199	199	1.0	6.1	1.0	1.6	1.0	1.0	135.2	108.0	66.7	145.0	157.0	41.0
cg0113	<i>ureA</i>	585	561	3.2	21.4	5.5	1.9	1.0	1.0	391.8	157.5	111.5	155.0	204.3	89.3
cg0134	<i>abgB</i>	76	0	1.0	3.8	1.3	1.0	1.0	1.2	96.7	63.7	207.1	52.6	45.1	108.9
cg0142	<i>sixA</i>	253	253	1.0	4.4	1.0	1.7	1.0	1.0	32.9	29.5	42.2	36.2	40.2	32.2
cg0152		30	20	1.0	3.3	1.0	1.0	1.0	1.0	20.1	13.0	16.3	17.9	11.8	15.1
cg0153	<i>hde</i>	313	unknown	2.5	4.4	2.3	1.6	1.0	1.9	19.2	16.7	28.6	19.7	19.7	15.0
cg0163		438	unknown	2.4	12.0	4.2	2.2	1.6	1.0	160.3	290.8	172.4	53.3	48.0	84.1
cg0204	<i>iolG</i>	246	unknown	3.5	16.8	5.9	3.0	2.2	1.9	20.4	38.2	55.9	24.3	25.2	35.8
cg0219		251	unknown	1.1	3.9	2.0	1.0	1.7	1.0	40.8	40.5	35.4	49.1	66.8	22.9
cg0222		413	unknown	4.1	11.0	5.9	3.0	1.0	1.0	41.6	27.1	35.8	20.8	23.7	20.9
cg0222		30	unknown	1.0	3.8	2.0	1.0	1.0	1.0	41.6	27.1	35.8	20.8	23.7	20.9
cg0247		202	202	1.0	17.2	4.6	1.0	1.0	1.0	38.8	20.2	27.0	35.1	32.9	22.3
cg0296	<i>dnaZX</i>	56	56	1.0	5.1	2.2	1.0	1.0	1.0	183.7	140.0	225.0	131.2	137.8	181.2
cg0306	<i>lysC</i>	40	4	3.5	12.2	7.7	4.1	4.3	6.3	578.7	576.4	655.1	680.0	919.0	730.8
cg0309	<i>sigC</i>	38	unknown	7.8	25.4	12.8	5.0	7.1	4.8	37.5	28.1	79.5	74.8	124.4	118.7
cg0319	<i>arsC2 (arsX)</i>	70	unknown	1.0	6.8	2.9	1.0	1.0	1.0	83.0	112.1	32.8	72.4	47.4	24.2
cg0335		447	447	1.0	3.1	1.0	1.6	1.0	1.0	99.0	95.2	143.5	121.9	125.0	113.9
cg0337	<i>whcA (whiB4)</i>	125	21	1.0	6.4	4.6	1.6	1.0	1.0	1149.5	986.9	1054.7	709.3	702.9	648.4
cg0359		468	327	1.0	3.1	1.9	1.0	1.0	1.6	573.5	562.7	658.7	483.6	663.5	542.4
cg0382		259	unknown	0.9	7.8	2.5	1.0	1.0	1.0	23.7	44.3	21.9	21.0	27.2	11.7
cg0389		31	unknown	2.4	15.2	4.7	1.7	1.0	1.0	368.0	157.6	247.8	275.8	213.8	157.0
cg0390		387	unknown	3.5	6.6	3.5	2.1	1.0	3.0	92.6	92.5	52.4	55.5	85.7	41.9
cg0411		238	unknown	1.1	4.4	1.0	1.1	1.0	1.0	150.3	72.0	32.7	59.9	80.3	34.1
cg0415	<i>ptpA2</i>	696	1023	1.3	8.0	3.2	1.0	1.0	1.0	311.2	176.8	498.8	272.4	229.8	476.3
cg0420		354	272	4.8	25.6	12.2	4.7	1.0	1.0	178.4	88.3	136.7	61.4	78.0	45.7
cg0422	<i>murA</i>	701	651	3.0	14.1	6.2	2.4	1.0	2.8	221.0	151.3	206.6	223.7	136.7	196.5
cg0423	<i>murB</i>	2	unknown	2.1	18.7	5.4	1.9	1.0	2.1	219.5	148.5	240.5	205.2	122.3	210.4
cg0431		76	unknown	2.0	6.9	2.2	1.0	1.0	1.0	93.6	58.7	64.3	65.7	46.4	52.3
cg0432		49	594	3.8	29.3	6.0	1.9	1.0	1.2	238.1	186.5	242.2	194.1	156.2	214.2
cg0437	<i>wzy</i>	303	unknown	3.5	30.3	10.1	3.7	2.1	1.3	149.3	115.5	201.3	83.3	117.4	153.8

cg0438		65	15	2.1	8.5	4.8	1.5	1.0	3.0	399.7	345.9	433.0	364.2	378.1	251.8
cg0444	<i>ramB</i>	224	224	9.7	26.7	18.0	7.1	12.7	13.5	641.0	690.2	441.8	329.1	413.1	301.9
cg0453		45	unknown	2.1	5.4	3.8	1.0	1.0	1.6	212.1	301.0	475.9	411.8	531.9	398.6
cg0465		95	unknown	2.4	10.4	4.0	1.9	1.0	1.7	5.5	1.1	8.3	3.8	1.0	10.8
cg0475		386	386	13.8	34.4	16.7	7.2	8.3	12.0	588.0	681.2	1518.0	1042.4	1302.8	1540.3
cg0497	<i>hemA</i>	26	17	6.4	25.8	14.6	5.5	3.1	5.2	111.1	469.9	129.2	599.2	727.3	263.6
cg0500	<i>qsuR</i>	19	unknown	4.3	22.3	8.8	3.6	2.4	2.0	37.3	24.6	19.4	21.1	19.4	13.4
cg0505		462	462	2.1	6.2	1.0	1.3	1.0	1.0	76.6	57.8	77.2	119.3	88.5	40.0
cg0505		7	7	1.3	4.8	3.3	1.3	1.0	1.0	76.6	57.8	77.2	119.3	88.5	40.0
cg0516	<i>hemE</i>	60	60	10.8	33.7	19.6	7.9	6.1	5.0	54.6	32.9	51.2	275.3	273.6	249.9
cg0517	<i>hemY</i>	642	447	3.0	6.4	3.9	1.0	1.0	1.0	63.5	36.3	91.7	202.5	244.4	284.7
cg0556	<i>menG (ubiE)</i>	61	61	2.5	6.8	1.0	1.3	1.0	1.0	132.0	77.8	176.0	155.6	132.8	173.2
cg0557		33	unknown	2.5	7.0	4.0	2.4	2.9	2.1	23.4	24.1	27.0	32.0	52.8	41.1
cg0566	<i>gabT</i>	227	unknown	1.8	4.2	2.2	1.0	1.0	1.1	3.1	3.9	3.1	2.8	3.3	3.1
cg0612	<i>dkg</i>	120	120	1.5	4.8	1.0	1.0	1.0	1.0	76.4	60.2	137.1	95.1	107.3	68.7
cg0614		145	unknown	1.0	4.5	1.0	1.0	1.0	1.0	75.8	189.2	50.7	69.2	136.1	32.3
cg0617		629	unknown	3.7	15.3	5.5	1.9	1.0	1.0	219.6	670.2	82.7	145.8	343.0	51.8
cg0636	<i>creB</i>	33	unknown	4.4	28.5	9.0	3.0	1.0	1.0	48.8	48.0	17.9	39.6	29.4	12.5
cg0636	<i>creB</i>	453	unknown	3.5	12.2	4.7	1.9	1.7	1.7	48.8	48.0	17.9	39.6	29.4	12.5
cg0645	<i>creJ (cytP)</i>	678	unknown	1.3	5.1	1.8	1.0	1.0	1.0	4.5	1.8	16.0	2.1	1.7	6.4
cg0656	<i>rplQ</i>	1	unknown	2.2	6.1	3.4	1.6	1.0	1.0	1323.1	721.0	2899.2	1339.1	1385.0	3899.9
cg0671		696	unknown	3.8	12.3	4.6	1.8	1.0	1.0	7.6	2.1	8.3	3.2	3.9	3.0
cg0673	<i>rplM</i>	13	104	1.6	5.7	2.9	1.0	1.0	2.4	1686.2	1495.2	3974.2	2555.6	2381.4	5428.0
cg0688		38	38	5.1	16.1	8.6	4.0	5.5	6.1	47.7	39.8	108.3	61.8	71.3	86.2
cg0752		511	388	1.6	3.5	1.0	1.0	1.0	1.0	107.4	130.8	271.1	148.5	177.2	371.0
cg0753		106	106	7.7	29.0	16.4	5.7	3.3	5.0	278.2	365.7	329.4	476.8	563.7	199.4
cg0778		42	6	4.9	15.2	8.5	2.9	1.0	2.1	126.0	77.7	108.5	141.4	115.5	149.1
cg0831	<i>tusG</i>	25	unknown	2.6	23.4	6.6	2.1	0.9	1.0	140.9	125.0	428.3	122.7	122.0	385.2
cg0842		35	unknown	1.0	3.3	1.0	1.0	1.0	1.4	21.0	21.3	114.6	33.7	40.2	87.0
cg0844		3	unknown	1.7	9.2	3.8	1.9	1.0	1.5	55.2	67.4	209.5	73.8	83.2	166.0
cg0875		56	unknown	2.6	6.3	3.1	1.9	1.0	2.6	3.6	3.8	3.4	2.0	3.0	1.6
cg0879		60	unknown	1.0	7.0	1.0	1.0	1.8	1.0	25.5	13.1	20.5	6.7	16.6	31.7
cg0880		49	unknown	5.8	13.2	5.2	3.0	1.0	4.7	64.3	43.1	59.8	72.4	67.2	49.3
cg0908		157	unknown	1.8	33.8	5.5	1.0	1.0	1.0	18.3	21.6	24.9	29.4	24.9	17.3
cg0928		277	unknown	1.0	5.6	1.0	1.2	1.0	1.7	819.4	41.5	224.7	119.2	21.7	752.8
cg0931		369	369	3.5	7.6	4.8	1.0	3.8	3.1	26.2	16.8	7.5	16.3	12.0	5.4
cg0931		34	34	2.1	4.8	2.4	1.5	1.0	1.0	26.2	16.8	7.5	16.3	12.0	5.4
cg0950	<i>fkpA</i>	684	621	5.0	12.4	4.4	2.8	1.0	4.8	662.5	526.2	1121.2	677.8	902.8	1376.1
cg0951	<i>accD3</i>	84	43	4.9	25.9	10.3	2.7	1.9	1.0	488.6	701.6	375.5	126.5	148.0	114.8
cg0986	<i>amtR</i>	414	unknown	2.4	13.5	3.3	2.3	1.0	1.0	263.8	233.6	221.3	196.1	279.4	231.8
cg0996	<i>cgfR2</i>	120	116	1.5	6.4	2.5	1.3	1.0	1.0	221.1	218.7	193.3	207.2	204.4	125.1
cg1017	<i>metS</i>	1	unknown	1.0	3.5	1.0	1.0	1.0	1.0	612.9	545.6	419.0	551.7	132.2	383.1
cg1044		445	445	1.5	3.6	1.7	1.0	1.0	1.0	261.9	181.7	641.7	440.0	412.9	444.4
cg1050		60	unknown	8.6	24.6	13.3	5.0	3.0	1.0	48.1	25.8	87.0	97.4	111.1	161.1
cg1052	<i>cmt3</i>	249	205	2.2	6.2	2.3	1.9	1.0	2.1	86.1	64.8	72.2	70.3	84.9	41.4
cg1069	<i>gapB (gapX)</i>	284	204	3.4	3.5	1.0	1.0	1.0	2.8	72.8	92.4	509.6	84.1	288.5	481.9
cg1076	<i>glmU</i>	118	76	1.0	3.8	1.0	1.0	1.0	1.0	285.1	226.7	718.8	249.7	330.3	665.7

cg1077		17	unknown	14.7	41.8	18.9	10.5	15.4	13.6	4.3	2.8	6.8	21.7	24.3	20.4
cg1077		424	unknown	1.0	7.7	1.0	1.0	1.0	1.0	4.3	2.8	6.8	21.7	24.3	20.4
cg1086		257	unknown	1.0	4.8	1.0	1.0	1.0	1.0	78.6	39.8	53.3	58.3	59.0	40.7
cg1087		59	33	3.6	16.9	8.3	2.2	2.1	2.6	182.7	263.3	656.8	439.7	333.2	367.6
cg1105	<i>lysI</i>	517	517	2.2	4.2	2.3	1.6	1.6	2.6	22.5	13.8	12.9	19.0	16.9	10.7
cg1145	<i>fumC (fum)</i>	109	72	2.2	4.0	3.0	1.9	1.0	1.5	639.1	692.5	1421.6	634.5	1145.9	1466.3
cg1233		494	494	1.5	3.9	1.7	1.0	1.0	1.0	55.3	70.7	64.7	69.6	75.9	37.3
cg1233		33	33	1.0	3.8	1.0	1.0	1.1	1.0	55.3	70.7	64.7	69.6	75.9	37.3
cg1272	<i>cseE</i>	132	67	1.0	4.2	1.0	1.0	1.0	1.0	978.8	1099.2	464.4	1055.0	1012.8	280.6
cg1289		546	unknown	1.6	4.7	1.6	1.0	1.0	1.0	12.7	30.2	12.8	7.8	23.1	13.1
cg1292		105	unknown	4.1	10.7	4.3	1.9	4.3	2.8	80.2	28.5	331.7	72.8	38.8	312.0
cg1301	<i>cydA</i>	177	72	10.3	17.9	12.5	5.2	8.8	8.3	29.1	113.5	423.4	163.6	70.3	71.4
cg1301	<i>cydA</i>	571	466	1.0	17.0	3.8	1.0	1.0	1.0	29.1	113.5	423.4	163.6	70.3	71.4
cg1328		98	41	1.0	3.1	1.0	1.2	1.0	1.0	70.2	121.9	89.7	92.5	122.2	76.5
cg1334	<i>lysA</i>	116	unknown	5.8	12.8	5.2	2.4	1.0	5.1	315.7	318.8	501.9	257.1	319.3	563.0
cg1346	<i>mog</i>	528	495	1.0	7.7	3.0	1.3	1.0	1.0	94.4	84.8	200.7	100.5	97.1	143.2
cg1346	<i>mog</i>	476	443	2.7	7.7	1.0	1.0	1.0	2.2	94.4	84.8	200.7	100.5	97.1	143.2
cg1355	<i>prfA</i>	606	unknown	1.9	4.3	1.9	1.4	1.0	1.0	484.3	214.2	377.0	415.6	242.7	452.8
cg1449		608	unknown	1.1	3.3	1.0	1.2	1.0	1.0	265.5	114.3	138.4	124.3	119.3	119.8
cg1449		139	unknown	2.0	3.1	2.0	1.0	1.0	1.3	265.5	114.3	138.4	124.3	119.3	119.8
cg1454		303	unknown	1.7	7.6	2.0	1.0	1.0	1.0	81.0	122.6	94.2	115.0	134.9	63.7
cg1459		696	unknown	2.6	9.2	4.1	1.5	1.8	1.0	258.7	135.2	327.4	200.4	231.9	399.4
cg1464		125	unknown	1.9	3.1	1.0	1.0	1.1	1.0	12.9	21.7	20.7	7.1	11.6	21.3
cg1474		552	unknown	1.3	3.0	1.6	1.1	1.0	1.0	46.3	52.8	67.2	41.4	38.1	45.5
cg1484		23	4	1.0	7.2	1.0	1.6	1.0	1.0	96.8	183.1	95.5	132.8	176.8	102.7
cg1516		32	unknown	1.0	6.9	3.3	1.6	1.6	1.0	11.8	19.2	19.9	11.4	12.6	13.8
cg1526		29	unknown	1.5	4.5	2.3	1.4	1.0	1.0	3.0	1.2	2.0	3.1	2.0	1.4
cg1531	<i>rpsA</i>	391	241	2.6	6.5	4.1	1.0	2.1	2.1	1712.6	1757.9	3842.6	1882.6	2389.0	4889.1
cg1538	<i>coaE</i>	150	150	3.5	22.3	4.6	1.4	1.0	1.0	797.2	513.3	474.7	654.2	468.2	340.2
cg1568	<i>ugpA</i>	253	unknown	1.0	4.3	1.0	1.0	1.5	1.0	28.7	18.2	16.9	22.6	14.8	9.1
cg1603		42	unknown	1.0	5.6	2.0	1.0	1.0	1.0	263.2	359.7	316.8	200.9	336.3	295.4
cg1607		49	unknown	1.5	5.8	1.0	1.0	1.0	1.2	177.8	108.9	110.2	165.7	144.2	90.1
cg1628		18	2	1.9	3.9	2.3	1.0	1.0	2.3	56.9	186.8	18.1	38.0	333.2	29.4
cg1668		177	unknown	1.0	5.5	2.6	1.0	1.0	1.0	148.4	119.0	154.7	187.3	200.7	225.6
cg1691	<i>arc (mpa)</i>	50	unknown	1.6	5.1	2.1	1.6	1.0	1.0	434.6	346.3	190.7	340.0	291.0	155.1
cg1695		188	unknown	9.3	22.6	9.9	5.5	9.0	11.2	289.4	414.5	162.4	159.1	198.5	58.6
cg1702		345	345	1.0	3.0	1.0	1.3	1.6	1.0	10.9	7.1	15.7	15.3	11.7	7.3
cg1728		91	21	1.0	3.2	1.6	1.0	1.0	1.1	120.9	93.2	129.4	126.7	133.3	103.9
cg1731		140	140	4.6	21.0	7.8	2.9	5.3	5.0	453.9	312.9	715.7	378.1	468.8	503.5
cg1734	<i>hemH</i>	16	16	14.4	52.9	24.7	9.0	9.3	13.3	75.5	65.5	147.7	688.9	1029.3	663.1
cg1736		95	2	4.7	12.2	6.1	2.3	1.0	1.0	46.3	29.2	35.1	35.9	34.0	25.2
cg1767		19	19	9.2	31.9	16.1	5.7	4.3	7.9	40.0	15.9	45.8	123.5	131.7	123.8
cg1773	<i>ctaB</i>	204	43	1.8	5.0	1.0	1.2	1.0	1.0	92.2	70.9	298.0	69.7	95.8	110.1
cg1774	<i>tkt</i>	16	1	8.5	147.0	12.6	2.2	1.0	1.0	964.4	724.7	1241.6	954.6	721.5	1156.9
cg1791	<i>gapA (gap)</i>	287	104	3.6	4.4	3.7	1.0	1.0	4.8	6163.6	3596.8	6243.6	8801.8	2867.2	4950.7
cg1796	<i>ribX</i>	63	unknown	1.0	11.0	1.0	1.0	1.3	1.0	284.1	404.0	286.2	283.0	424.2	324.7
cg1801	<i>rpe</i>	38	38	2.6	15.6	6.0	1.0	1.0	1.0	337.8	365.3	421.5	335.8	363.9	397.7

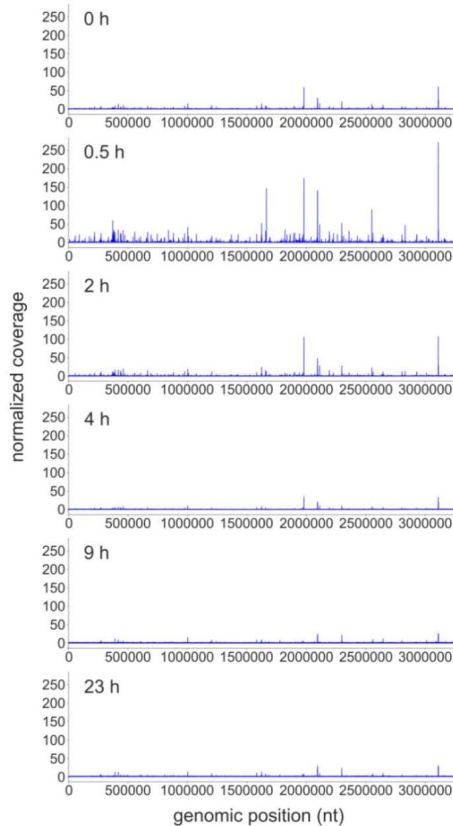
cg1811	<i>lhf</i>	74	19	1.6	4.1	2.1	1.0	1.0	1.2	1586.5	1798.5	2336.7	1840.0	2223.8	2148.1
cg1867	<i>secD</i>	321	172	1.3	4.1	1.8	1.4	1.0	1.0	102.9	88.2	287.3	73.9	88.1	292.7
cg1893	<i>act4</i>	445	unknown	1.0	4.3	1.0	1.0	1.0	1.9	134.2	85.4	97.6	115.9	96.6	72.3
cg1904		7	unknown	1.0	3.9	1.0	1.0	1.0	1.0	248.4	180.2	284.3	193.7	195.1	222.4
cg1924		137	unknown	2.0	10.7	1.0	1.5	1.0	1.3	1.9	3.3	#NV	3.3	2.9	#NV
cg1926		30	unknown	1.7	4.9	2.5	1.5	1.0	2.0	73.2	42.8	37.2	37.5	67.6	30.0
cg1942		402	unknown	1.3	4.3	1.0	1.0	1.7	1.0	9.4	21.0	17.9	7.3	8.6	17.1
cg1944		43	14	3.3	35.1	9.4	1.0	1.0	1.0	16.1	15.8	13.6	35.7	22.5	13.0
cg1945		577	116	1.0	8.3	2.7	1.0	1.0	1.0	34.4	17.4	23.8	28.3	19.8	17.4
cg1946		99	unknown	1.0	3.1	1.0	1.0	1.0	1.0	53.8	57.3	30.5	40.3	48.2	27.4
cg1956	<i>recJ</i>	1	unknown	1.3	3.6	2.2	0.9	1.0	1.0	14.8	12.7	16.1	20.4	21.7	17.8
cg1959	<i>priP</i>	26	unknown	4.3	21.3	6.8	2.6	1.0	1.0	4.6	2.5	2.5	3.5	2.5	2.0
cg1981		598	unknown	1.0	6.2	1.0	1.0	1.0	1.0	12.4	6.7	5.8	8.9	5.4	4.2
cg1981		433	unknown	1.0	6.2	1.0	1.5	1.2	1.0	12.4	6.7	5.8	8.9	5.4	4.2
cg1981		12	unknown	1.0	3.5	1.0	1.0	1.0	1.0	12.4	6.7	5.8	8.9	5.4	4.2
cg2003		170	unknown	1.3	4.2	1.0	1.0	1.0	1.0	45.2	60.5	34.8	71.5	44.6	24.4
cg2005		246	unknown	7.2	24.2	7.4	1.6	1.0	1.0	15.4	14.2	11.5	16.0	13.9	9.0
cg2005		531	unknown	1.0	12.5	4.3	1.0	1.0	1.0	15.4	14.2	11.5	16.0	13.9	9.0
cg2007		177	unknown	1.7	3.3	1.0	1.0	1.0	1.0	10.3	6.9	10.4	8.0	6.0	6.8
cg2021		263	unknown	2.2	9.9	2.7	1.0	1.0	1.5	14.5	12.3	8.8	11.3	10.4	6.3
cg2030		586	543	1.0	7.1	1.5	1.0	1.0	1.0	64.2	60.5	38.4	44.1	43.9	33.2
cg2031		181	unknown	1.6	5.3	2.7	1.4	1.0	1.0	88.6	108.3	74.9	91.0	68.5	59.7
cg2037		19	unknown	2.3	7.1	3.9	1.0	2.1	1.0	86.6	89.5	77.9	77.0	93.3	66.6
cg2045		222	unknown	1.3	6.3	2.1	1.0	0.8	1.0	15.4	12.4	42.4	24.0	24.3	46.5
cg2047		13	78	1.0	4.0	1.3	1.0	1.0	1.0	49.3	121.5	78.9	237.2	467.6	61.3
cg2051		33	14	4.5	24.2	8.9	2.1	1.0	1.7	180.3	286.1	140.0	197.9	206.5	116.7
cg2059		156	unknown	1.7	11.8	2.3	1.0	1.0	1.5	13.7	7.8	12.8	20.5	9.4	11.6
cg2061	<i>psp3</i>	155	121	1.0	3.1	1.0	1.0	1.0	1.0	39.0	35.2	40.1	45.1	37.0	49.1
cg2063		40	unknown	1.0	4.9	2.4	1.0	1.9	1.0	22.3	16.9	10.8	15.7	12.0	6.9
cg2069	<i>psp1</i>	33	17	1.0	4.4	2.9	1.0	1.0	1.0	69.4	49.0	45.8	71.8	52.7	37.9
cg2071	<i>int2</i>	82	618	3.5	10.3	4.3	2.7	1.0	3.3	86.7	90.1	137.1	94.0	191.0	217.9
cg2077	<i>oftC</i>	268	268	2.3	14.3	2.9	1.0	1.0	1.0	248.8	302.5	120.8	147.5	239.3	103.9
cg2078	<i>msrB</i>	282	unknown	1.0	3.0	1.0	1.2	1.0	1.0	538.4	1894.3	303.9	438.3	1183.0	327.1
cg2079		134	15	8.6	22.2	9.9	5.5	6.7	7.5	170.0	104.9	436.1	593.0	731.7	1573.5
cg2091	<i>ppgK</i>	202	202	58.9	174.4	105.8	35.7	2.7	6.3	453.5	426.4	833.1	464.8	475.5	476.9
cg2092	<i>sigA (rpoD)</i>	29	115	1.0	3.9	1.7	1.3	1.0	1.0	687.2	1215.9	598.1	541.9	774.5	573.4
cg2103	<i>dtxR</i>	579	310	1.0	3.3	1.6	1.0	2.4	1.0	666.9	702.5	468.0	548.9	529.8	318.5
cg2121	<i>ptsH</i>	31	unknown	1.9	4.2	1.9	1.0	1.0	1.0	2665.7	2945.4	2311.5	3242.5	1233.2	1896.9
cg2155		333	333	3.6	15.8	4.8	2.0	1.0	1.0	442.3	353.3	372.1	600.7	598.2	312.7
cg2171	<i>pptA</i>	448	unknown	1.0	5.4	1.6	1.0	1.0	1.6	98.1	111.7	86.0	123.5	97.4	74.6
cg2181	<i>oppA</i>	274	217	4.1	6.7	6.3	2.6	4.7	4.1	1255.6	128.3	1864.6	407.8	129.1	1460.9
cg2187		221	unknown	1.8	5.7	1.8	1.3	1.0	1.0	84.8	53.1	39.5	34.7	37.1	38.6
cg2188		55	2	1.0	3.0	1.0	1.0	1.0	1.0	119.0	93.3	60.9	60.8	67.1	51.4
cg2195		166	61	2.7	11.7	4.0	2.0	2.4	2.0	6384.2	8528.4	11102.6	8391.4	11066.7	11490.2
cg2197		0	1	1.0	6.5	1.7	1.0	1.5	1.0	244.5	126.1	333.4	170.0	196.4	311.8
cg2199	<i>pbp2a</i>	131	131	1.0	30.7	21.0	1.0	1.0	1.0	233.9	358.9	121.4	124.6	255.1	112.0
cg2200	<i>chrA (cgtR8)</i>	326	unknown	29.2	140.9	47.7	20.5	1.0	1.0	79.3	770.3	69.2	31.6	578.3	116.5

cg2201	<i>chrS (cgtS8)</i>	32	unknown	29.4	141.1	40.5	21.8	1.0	29.7	36.6	481.4	23.3	11.0	352.6	56.6
cg2201	<i>chrS (cgtS8)</i>	424	unknown	1.0	27.7	21.2	1.0	1.0	1.0	36.6	481.4	23.3	11.0	352.6	56.6
cg2206	<i>ispG</i>	236	190	2.1	3.9	1.5	1.4	1.0	1.0	524.6	842.9	566.4	398.5	585.2	449.4
cg2221	<i>tsf</i>	4	4	1.0	4.2	1.9	1.5	1.0	1.0	694.7	580.5	2069.5	795.7	774.8	2124.6
cg2224	<i>xerC</i>	134	31	15.5	49.1	28.4	10.6	4.4	9.4	41.0	25.6	29.6	40.5	39.7	32.0
cg2241	<i>tex</i>	149	149	1.4	9.7	3.2	1.0	1.0	1.0	96.4	46.4	119.9	70.3	72.2	98.4
cg2247		534	464	1.0	4.0	1.9	1.3	1.0	1.4	415.5	1108.7	264.4	352.6	724.0	270.6
cg2274		58	55	1.0	10.4	2.0	1.5	1.0	1.0	247.5	244.8	420.6	204.8	271.1	360.2
cg2290		221	unknown	1.0	3.8	1.8	1.0	1.0	1.0	93.3	60.5	35.0	58.2	47.9	27.7
cg2305	<i>hisD</i>	383	290	1.7	7.1	3.0	1.0	1.5	1.7	215.3	200.9	347.8	234.3	362.7	419.5
cg2310	<i>glgX</i>	307	307	1.0	3.1	1.0	1.0	1.0	1.0	206.5	178.4	297.4	175.5	175.1	203.8
cg2311		88	88	4.4	19.9	5.6	3.0	2.7	1.0	96.2	48.4	128.1	44.3	45.9	156.6
cg2337		421	379	1.0	9.9	3.1	1.0	1.0	1.0	799.6	894.0	371.9	858.6	1230.5	533.7
cg2337		264	222	1.0	9.0	1.0	1.0	1.0	1.0	799.6	894.0	371.9	858.6	1230.5	533.7
cg2338	<i>dnaE1</i>	607	607	1.2	4.0	1.0	1.0	1.3	1.0	269.0	389.3	216.5	382.3	383.6	179.0
cg2343		26	unknown	5.2	24.9	9.5	3.0	1.3	1.0	122.9	154.6	85.8	113.5	123.1	62.2
cg2373	<i>murF</i>	133	unknown	1.4	23.1	1.9	1.3	0.8	1.0	200.5	160.2	175.8	194.8	141.7	151.9
cg2403	<i>qcrB</i>	221	unknown	1.6	4.8	2.1	1.0	1.2	1.0	1474.9	4043.9	1898.9	501.6	1147.1	1176.0
cg2406	<i>ctaE</i>	324	324	20.3	52.9	28.1	11.0	20.7	23.3	3792.2	4388.5	1723.4	907.8	1375.2	995.2
cg2406	<i>ctaE</i>	616	616	1.0	29.3	1.0	1.0	1.0	1.0	3792.2	4388.5	1723.4	907.8	1375.2	995.2
cg2406	<i>ctaE</i>	27	27	1.0	17.9	1.0	1.0	1.0	1.0	3792.2	4388.5	1723.4	907.8	1375.2	995.2
cg2409	<i>ctaC</i>	259	73	5.7	16.1	8.6	4.0	6.2	5.9	2600.7	3428.4	2548.1	976.8	1329.5	1313.3
cg2423	<i>lipA</i>	163	69	1.0	18.4	1.0	1.0	1.0	1.0	652.1	1614.9	429.7	638.5	1617.6	442.8
cg2445	<i>hmuO</i>	150	44	3.1	10.4	4.5	1.0	1.0	3.7	178.5	77.0	249.1	7.8	9.1	18.2
cg2445	<i>hmuO</i>	587	481	1.0	4.3	1.0	1.6	1.0	1.0	178.5	77.0	249.1	7.8	9.1	18.2
cg2473	<i>acpM</i>	593	593	4.8	31.4	9.7	3.1	1.0	1.0	181.4	134.9	234.0	238.8	263.1	169.2
cg2478	<i>pbp6</i>	26	26	1.5	5.0	2.1	1.0	1.0	1.0	537.8	475.3	154.5	218.9	259.2	106.0
cg2491		162	unknown	1.0	4.0	1.0	1.0	1.0	1.0	94.1	86.0	125.1	89.9	129.9	123.2
cg2496		1	1	3.2	11.4	4.3	2.3	1.0	2.6	123.4	105.0	132.8	115.5	137.1	108.5
cg2523	<i>malQ</i>	94	94	1.8	4.7	2.9	1.0	1.0	1.0	1568.4	1124.7	1268.4	1040.2	947.1	996.7
cg2537	<i>brnQ</i>	336	unknown	2.9	6.6	1.0	1.6	1.7	3.2	171.9	129.2	143.0	148.8	177.7	163.3
cg2542		546	unknown	1.0	3.8	1.0	1.3	1.0	1.0	51.0	56.1	43.9	50.1	46.7	36.4
cg2546		194	173	4.3	18.3	6.8	2.2	3.8	2.6	5.2	4.0	11.4	3.1	3.5	15.5
cg2557		538	unknown	1.6	3.4	1.4	1.0	1.1	1.0	24.4	19.5	109.0	14.6	20.6	121.2
cg2566		132	unknown	1.4	5.5	2.3	1.0	1.0	1.3	29.8	19.4	59.3	21.2	13.6	29.5
cg2579		13	unknown	1.0	6.0	2.1	1.0	1.0	1.0	246.1	167.2	229.7	135.4	150.9	169.5
cg2592		140	140	1.0	4.8	1.8	1.0	1.0	1.0	91.1	82.9	130.9	129.4	173.5	144.4
cg2593		170	91	1.6	3.5	1.0	1.0	2.1	1.0	124.3	101.4	120.9	100.0	122.8	91.9
cg2601		327	unknown	3.5	3.6	2.8	2.9	1.0	3.6	57.7	26.4	31.3	38.9	29.3	21.2
cg2641	<i>benR</i>	229	229	6.3	20.8	6.8	2.8	1.0	1.0	22.8	25.0	42.9	20.6	22.6	19.4
cg2675		34	unknown	1.0	89.9	22.9	7.2	4.3	4.4	549.6	1308.3	17.1	808.4	378.7	58.5
cg2675		9	unknown	13.4	89.9	22.9	7.2	4.3	1.0	549.6	1308.3	17.1	808.4	378.7	58.5
cg2680	<i>argD2</i>	271	229	2.8	6.5	3.3	1.3	1.9	1.0	157.7	179.9	202.2	104.3	126.0	168.1
cg2685		13	16	7.0	25.0	13.0	5.0	10.3	8.3	142.6	68.6	76.2	108.2	115.4	123.9
cg2701	<i>musI</i>	523	523	1.0	4.4	2.1	1.7	1.0	1.5	578.8	391.0	635.7	362.6	413.2	664.5
cg2745		455	455	2.2	3.2	2.3	1.0	1.0	1.0	62.8	54.5	71.9	86.6	62.1	34.4
cg2747	<i>mepA</i>	69	unknown	1.4	4.1	2.1	1.0	1.5	1.0	94.6	118.3	173.8	305.9	102.2	67.7

cg2761	<i>cpdA</i>	310	310	4.4	11.8	4.7	1.7	1.0	1.0	98.2	165.2	166.3	87.0	209.8	117.7
cg2766		555	555	1.8	4.2	2.0	1.4	1.0	1.0	313.6	243.4	159.0	292.3	273.4	122.6
cg2780	<i>ctaD</i>	314	202	10.9	21.8	11.6	5.7	11.8	10.0	2992.2	5262.4	3087.5	1582.8	2519.5	1714.3
cg2786	<i>nrpE</i>	8	unknown	2.8	13.5	4.3	1.0	1.0	1.0	249.5	300.9	390.7	225.0	214.1	389.7
cg2823		347	unknown	1.0	9.9	2.8	1.4	1.0	1.4	2.6	1.7	1.5	2.1	1.4	0.9
cg2829	<i>murA2</i>	269	unknown	2.0	3.6	1.0	1.0	1.0	1.3	218.5	132.8	260.0	205.1	186.0	208.8
cg2831	<i>ramA</i>	42	19	1.8	5.0	2.3	1.0	1.9	2.9	223.2	240.4	130.2	148.6	173.8	195.4
cg2857	<i>purF</i>	19	19	1.0	8.1	1.0	1.4	1.3	1.2	404.9	374.1	261.5	455.7	791.0	346.2
cg2867	<i>mpx</i>	56	56	1.4	5.6	1.0	1.0	1.0	1.2	273.5	469.1	295.1	184.5	162.8	199.3
cg2944	<i>ispF</i>	540	unknown	4.7	3.8	2.9	1.0	1.0	2.0	190.6	131.5	199.8	155.2	170.0	165.7
cg2949		122	60	6.7	22.3	12.7	5.7	7.1	5.2	707.2	979.7	1539.3	483.6	833.9	937.9
cg2953	<i>vdh</i>	42	unknown	1.5	7.0	2.4	1.0	1.6	1.6	57.0	29.0	144.7	42.5	47.4	102.4
cg2977		408	408	1.0	4.4	1.0	1.0	1.0	1.0	444.0	424.7	281.2	406.6	432.4	218.9
cg3054	<i>purT</i>	241	205	1.0	3.3	2.6	1.6	1.0	1.2	187.4	190.9	212.9	136.2	132.6	147.7
cg3068	<i>fda</i>	20	9	3.1	20.5	7.7	2.7	1.0	1.0	978.6	631.5	1696.7	1271.8	1048.7	1758.1
cg3068	<i>fda</i>	423	305	1.0	6.3	2.2	1.0	1.0	1.0	978.6	631.5	1696.7	1271.8	1048.7	1758.1
cg3069		54	5	5.4	22.5	12.5	3.6	2.6	3.3	234.1	217.7	310.7	352.7	309.8	220.6
cg3097	<i>hspR</i>	393	unknown	1.0	3.1	1.0	1.0	1.0	1.0	87.0	419.1	271.5	69.3	227.8	248.3
cg3101		626	unknown	1.0	7.1	1.0	2.2	1.0	2.7	378.5	414.6	309.7	99.9	120.0	171.0
cg3101		25	unknown	1.8	7.1	3.5	2.2	1.0	2.1	378.5	414.6	309.7	99.9	120.0	171.0
cg3115	<i>cysD</i>	106	unknown	1.0	6.7	2.6	1.0	1.0	1.0	4453.1	5001.1	35.0	3477.3	3194.4	397.8
cg3118	<i>cysl</i>	498	446	1.0	3.7	1.0	1.5	1.0	1.0	5918.5	6455.9	54.8	4787.0	3972.1	476.6
cg3127	<i>tctC</i>	37	unknown	2.3	3.4	1.0	1.0	1.0	1.0	7.3	9.2	26.4	8.1	8.3	14.0
cg3156	<i>htaD</i>	151	unknown	5.7	17.3	8.6	3.9	7.3	4.2	6.3	0.9	48.1	2.6	0.7	23.5
cg3170		66	unknown	1.6	10.4	3.6	1.0	1.0	1.0	24.2	20.6	16.4	20.7	17.2	12.6
cg3173		0	unknown	2.7	6.6	3.4	2.2	1.0	2.1	322.9	203.0	303.9	238.8	206.5	267.7
cg3175		217	unknown	3.1	9.2	4.1	1.0	1.0	1.4	61.4	45.0	70.9	55.5	65.0	60.7
cg3182	<i>cop1</i>	198	13	1.0	4.0	3.1	1.0	1.0	1.0	537.5	663.0	1163.6	974.8	1214.0	923.4
cg3194		369	unknown	2.9	5.1	3.3	1.0	2.6	2.5	21.5	7.6	41.0	15.4	10.4	27.8
cg3199		158	unknown	2.7	5.0	1.0	2.1	2.8	1.9	49.2	28.5	77.5	31.7	41.6	67.2
cg3226		213	140	2.0	3.7	2.2	1.0	1.0	2.0	2480.6	547.0	79.3	1092.9	169.4	145.6
cg3226		622	549	4.2	5.5	3.3	1.0	6.2	2.0	2480.6	547.0	79.3	1092.9	169.4	145.6
cg3245		695	unknown	1.0	24.9	22.9	1.0	1.0	1.0	12.0	10.7	10.9	8.4	11.1	6.7
cg3247	<i>hrrA</i> (<i>cgtR11</i>)	108	26	60.4	271.4	107.2	34.1	1.0	30.8	78.8	50.7	214.3	0.1	0.0	0.2
cg3248	<i>hrrS</i> (<i>cgtS11</i>)	474	unknown	1.0	33.4	26.7	1.0	1.0	1.0	67.3	65.5	47.7	59.3	60.2	35.3
cg3249		419	419	1.0	20.5	18.6	15.8	1.0	1.0	28.2	17.3	27.5	18.2	25.5	21.0
cg3283		58	unknown	1.0	7.3	1.0	1.0	1.0	2.5	750.3	943.5	21.9	446.8	416.9	19.7
cg3315	<i>malR</i>	91	23	1.5	5.2	1.6	1.0	1.0	1.0	114.2	200.8	877.2	234.4	440.1	582.5
cg3317		29	unknown	2.5	9.5	4.8	2.1	1.0	2.6	132.1	204.2	212.7	208.5	322.2	352.1
cg3323	<i>ino1</i>	156	100	4.9	7.6	4.5	2.3	5.2	2.6	433.9	210.2	1216.8	283.8	674.5	1848.2
cg3357	<i>trpP</i>	91	91	1.3	4.0	1.0	1.0	1.0	1.0	184.5	426.6	114.2	172.7	338.6	121.4
cg3378	<i>cg3378</i>	60	unknown	1.0	3.8	2.6	1.0	1.0	1.9	6.6	16.4	18.4	16.9	34.6	13.3
cg3389		143	34	1.0	3.2	1.0	2.0	1.0	1.9	111.7	24.0	59.5	84.1	15.4	47.2
cg3402		13	5	2.8	18.4	7.5	2.9	1.0	2.5	1413.6	2492.6	27.0	1756.9	1175.2	23.0
cg3411		18	2	2.0	10.3	3.8	1.5	1.0	1.4	1511.1	5172.0	121.8	2499.8	3220.4	98.1
cg3422	<i>trxB</i>	5	11	1.0	5.8	1.0	1.0	1.0	1.0	839.4	1791.5	546.6	819.4	1000.3	460.0
cg4002		564	unknown	1.0	4.8	1.0	1.0	1.9	1.0	9.4	10.5	24.5	11.6	9.1	8.3

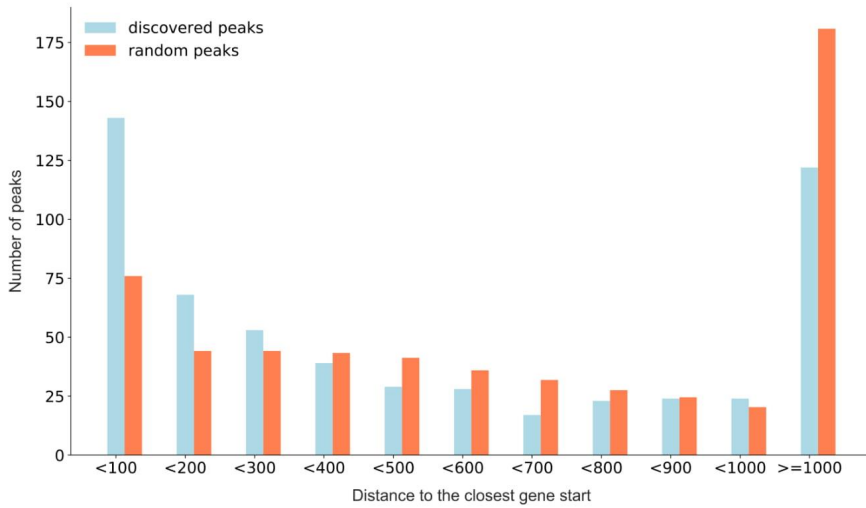
40 **Supplementary Figures**

41



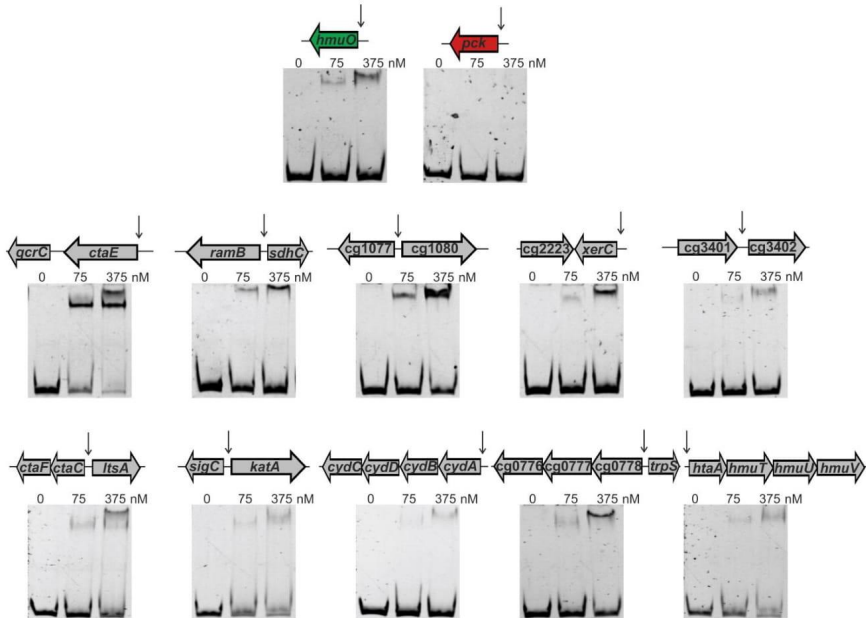
42

43 **Figure S1: Global binding pattern of HrrA in the *C. glutamicum* genome in response to hemin**
44 **addition.** Genomic coverage (number of reads covering a particular genomic position) was
45 normalized to the average coverage of the regions not harbouring binding peaks. Thus, depicted
46 peak intensities are comparable between different time points. The strain *C. glutamicum* $\Delta hrrSA$
47 $\Delta chrSA$ harbouring the plasmid pJC1_ P_{hrrSA} -*hrrSA*-*twin-strep*- P_{chrSA} -*chrSA*-*his* was cultivated in
48 CGXII minimal medium (lacking $FeSO_4$) supplemented with 2% (w/v) glucose and 4 μM hemin
49 was added at 0 h. Cells were harvested at different time points as described in Figure 1.



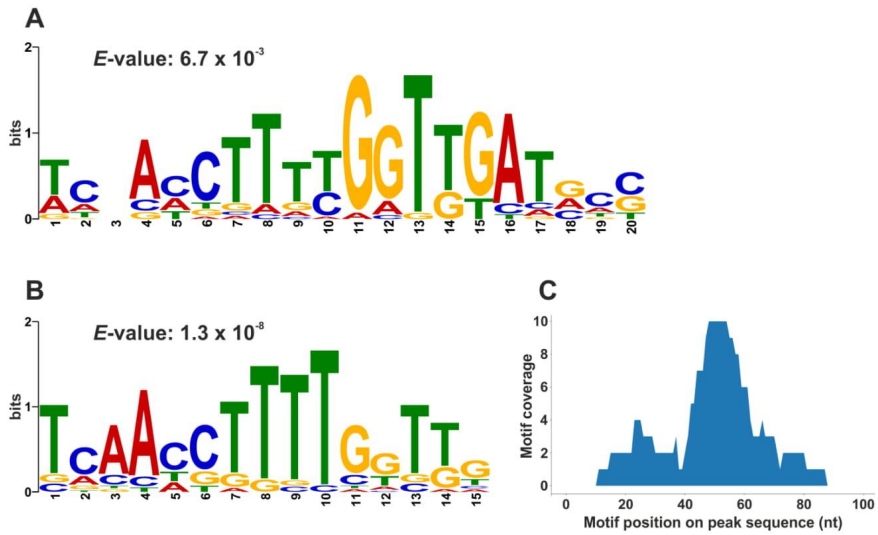
50

51 **Figure S2: Distribution of distances from HrrA binding peaks centers to the closest gene start**
52 **site (translation start site, TLS).** As a background (red color), random peaks of the same width
53 as real ones were generated. Random peak generation was performed 100 times and resulting
54 distance distributions were then averaged into a single background distribution.



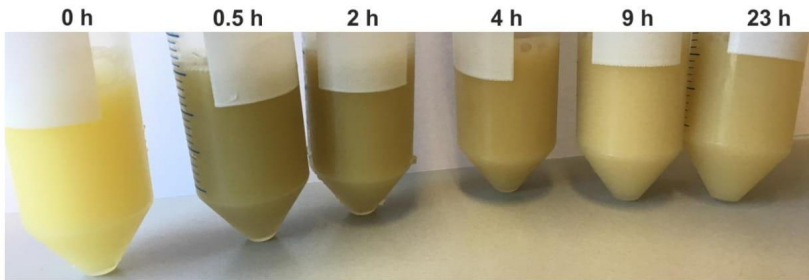
55

56 **Figure S3: HrrA binding to selected target promoter regions.** Protein-DNA interactions were
 57 validated by electrophoretic mobility shift assays (EMSA) using 15 nM DNA fragments covering
 58 50 bp up- and downstream of the maximal ChAP-Seq peak height and an increasing protein
 59 monomer concentration of 0, 75 and 375 nM. The genomic location of the maximal peak height
 60 found in the ChAP-Seq experiments is indicated by an arrow. As control, the promoter regions
 61 of *hmuO* (positive control) and *pck* (negative control) were used.



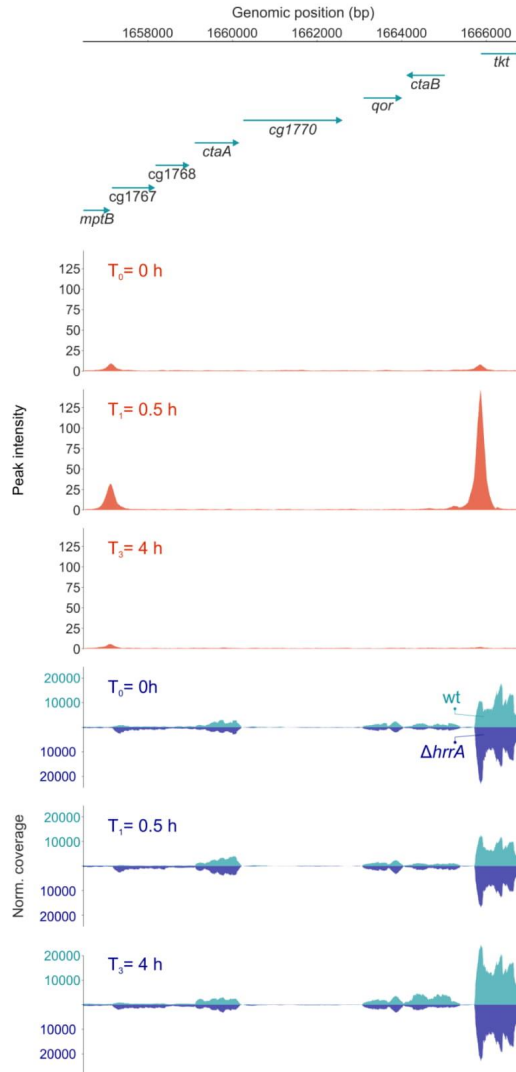
62

63 **Figure S4: Derivation of a HrrA binding motif revealed a weakly conserved palindromic**
 64 **sequence.** Sequences of the top 20 peaks (T_0) (A) or 100 bp of the tested EMSA DNA fragments
 65 (Figure S2) (B) were used for a MEME v.5 analysis (<http://meme-suite.org>). (C) Shown is the
 66 position of identified motif sequences within the analysed peak sequences used in (B). The
 67 majority of HrrA motifs centre at the position of the peak maximum (at 50 nt).



68

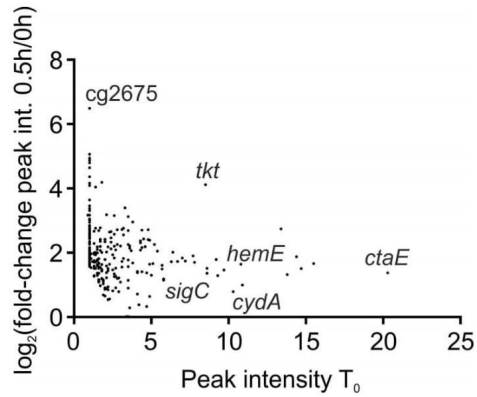
69 **Figure S5: Visual inspection of *C. glutamicum* cells before and after addition of heme.** Iron-
70 starved *C. glutamicum* wild type cells were cultivated in CGXII medium (2 % (w/v) glucose,
71 without FeSO_4) and cells were harvested at different time points before and after the addition
72 of 4 μM heme. Cell pellets were subsequently resuspended in Tris-buffer (100 mM Tris-HCl,
73 1 mM EDTA, pH 8.0) and adjusted to an OD_{600} of 3.5.



74

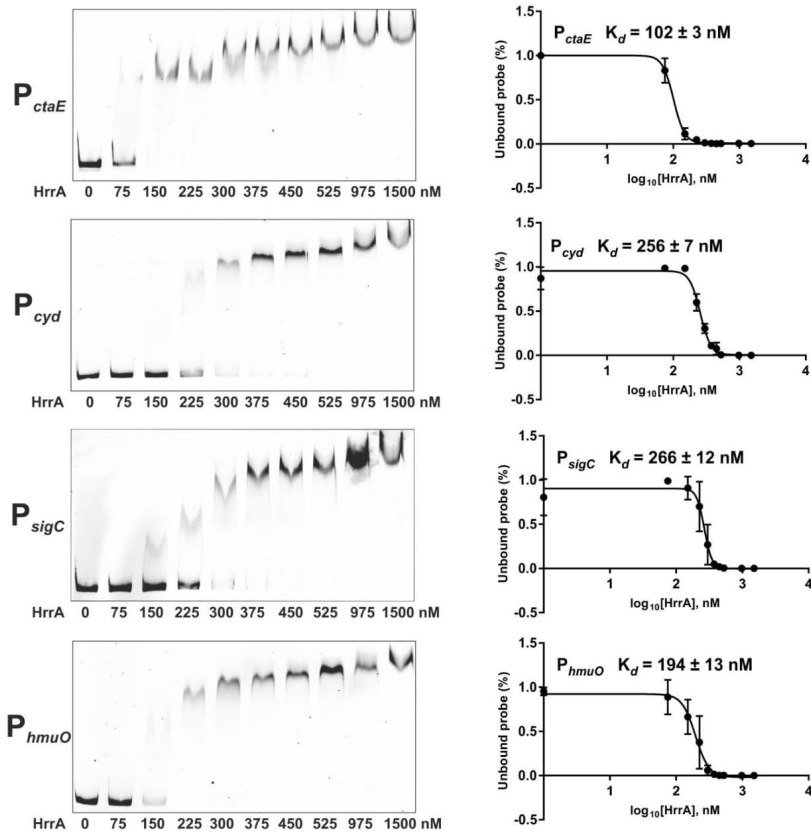
75 **Figure S6: HrrA coordinates expression of *ctaA* and *ctaB* in response to heme.** Shown are the
 76 ChAP-Seq (orange) and RNA-Seq (blue) results focusing on the *ctaA* and *ctaB* locus in the
 77 genome of *C. glutamicum*. Depicted is the genomic region between *mptb* (cg1766) and *tkr*
 78 (cg1774). For the cultivation, CGXII medium supplemented with 2% (w/v) glucose and 4 μ M
 79 hemin was inoculated with iron starved cells from a stationary culture and adjusted to an OD_{600}
 80 of 3.5. Samples were analysed at the indicated time points as described in material and
 81 methods.

10



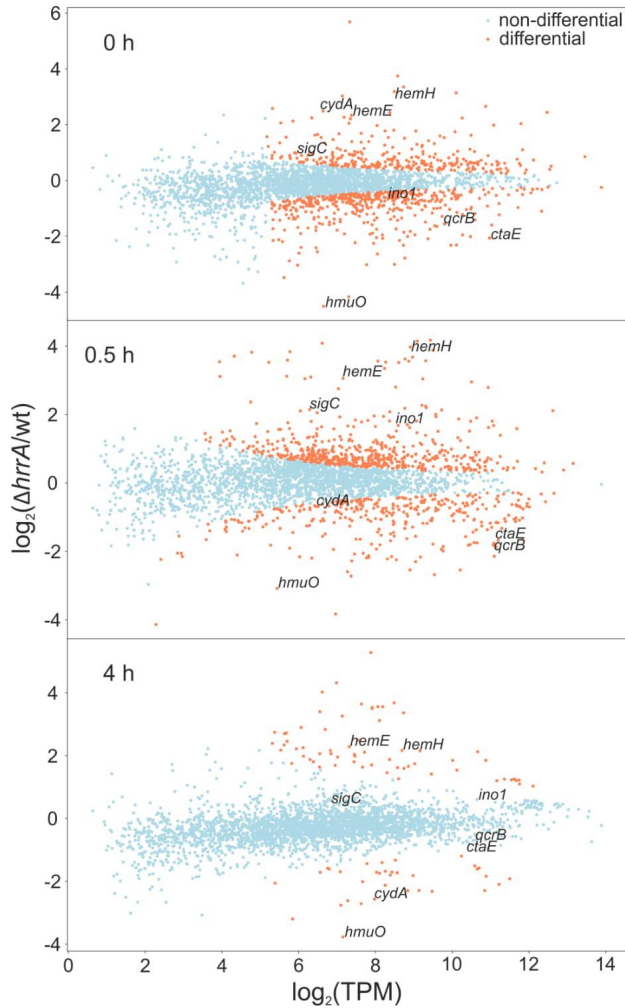
82

83 **Figure S7: Dynamic range of HrrA association upon addition of external heme.** ChAP-Seq
84 analysis revealed that targets that are moderately bound before stimulus addition show a
85 generally higher fold-change in HrrA association than targets sequences that showed already a
86 high coverage at T_0 . The log₂ of the fold change of the normalized peak intensities was
87 calculated ($T_{0.5}$ versus T_0) and plotted against the peak intensity at time point T_0 (before stimulus
88 addition). For details on cultivation and ChAP-Sequencing, see material and methods and Figure
89 1.



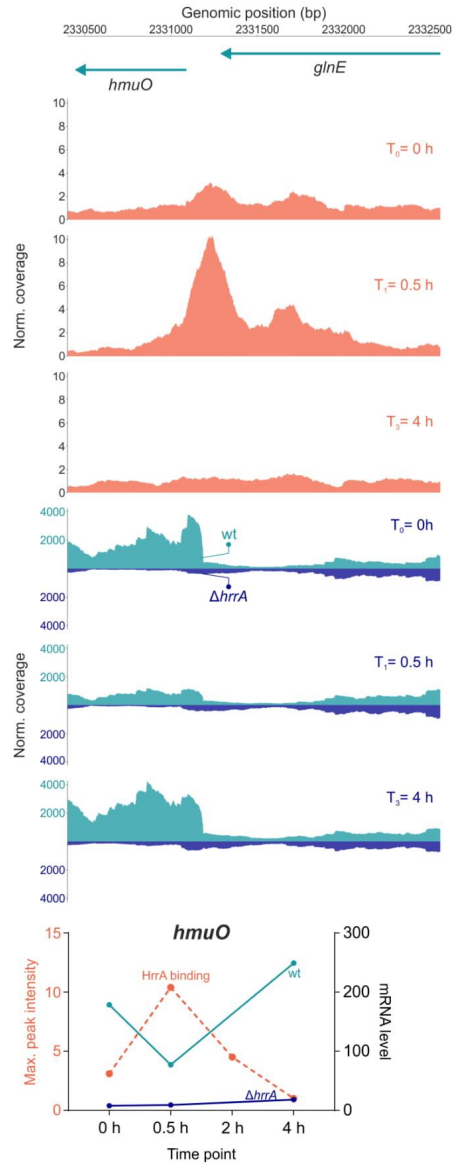
90

91 **Figure S8: Binding affinity of HrrA to selected target promoters.** Depicted are representative
 92 images of quantitative EMSAs used for analysis of protein-DNA interaction and the calculation
 93 of HrrA affinities to the different promoters. For the analyses, 15 nM DNA fragments covering
 94 250 bp up- and downstream of the maximal ChAP-Seq peak height were used with an increasing
 95 monomeric protein concentration. Determination of unbound DNA in EMSA studies allowed the
 96 calculation of HrrA binding affinities to different target promoters. Quantification of unbound
 97 DNA band intensities was performed using AIDA v.4.15 (Raytest GmbH, Germany) and K_d values
 98 were calculated using GraphPad Prism 7.



99

100 **Figure S9: Time-resolved differential gene expression analysis.** Shown is the \log_2 fold change in
 101 gene expression ($\Delta hrrA$ versus wild type) along with a \log_2 mean expression (expression
 102 averaged for $\Delta hrrA$ and WT samples) in transcripts per million (TPM). Orange dots represent
 103 significantly differentially expressed genes with an empirical FDR < 0.05 (see material and
 104 methods). Wild type and $\Delta hrrA$ *C. glutamicum* strains were grown in CGXII medium (without
 105 FeSO_4) supplemented with 2% (w/v) glucose and 4 μM hemin (T_0 is prior addition of hemin; for
 106 details on cultivation and sample preparation see material and methods).



107
108
109
110
111
112
113

Figure S10: HrrA-dependent *hmuO* expression in response to heme. Shown are the ChAP-Seq (orange) and RNA-Seq (blue) results focusing on the *hmuO* locus in the genomic region between *hmuO* (cg2445) and *glnE* (cg2446). For the cultivation, CGXII medium supplemented with 2% (w/v) glucose and 4 μ M hemin was inoculated with iron starved cells from a stationary culture and adjusted to an OD₆₀₀ of 3.5. Samples were analysed at the indicated time points as described in material and methods.

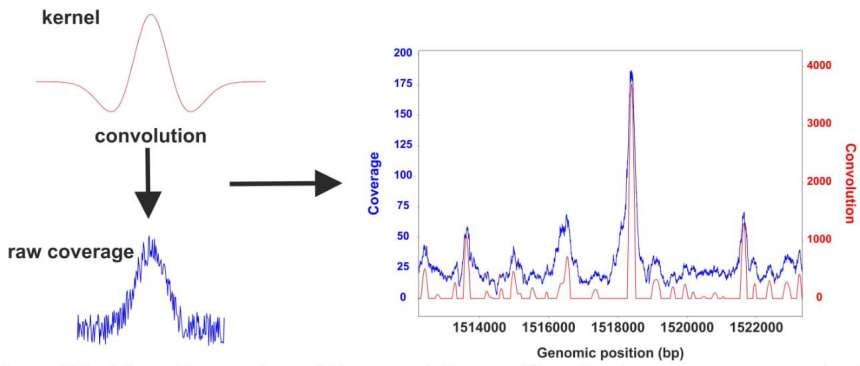
HrrA (87% identity)

	<i>C. diphtheriae</i> HrrA	1	MIRVLLADDHEIVRLGLRAVLESAEDI	EV	IGEVATAEAAIAAAQAGGID	49		
	<i>C. glutamicum</i> HrrA	1	MIRVLLADDHEIVRLGLRAVLESAEDI	EV	VEVSTAEAVQAAQEGGID	49		
	<i>C. diphtheriae</i> HrrA	50	VILM ^P DLRFGPGVQGT	KL	TSGADATAAIRRMDNPP	EVLVVTNYDTDADI	98	
	<i>C. glutamicum</i> HrrA	50	VILM ^P DLRFGPGVQGT	QV	STGADATAAIKRNI	DNPPKVLVVTNYDTDTDI	98	
	<i>C. diphtheriae</i> HrrA	99	LGAIEAGALGYMLKDAPPE	ELLA	AAVRSAAEGDTAL	SPTVANRLMSRVRA	147	
	<i>C. glutamicum</i> HrrA	99	LGAIEAGALGYLLKDAPPE	S	ELLA	AAVRSAAEGDSTLSPM	VANRLMTRVRT	147
	<i>C. diphtheriae</i> HrrA	148	PRNSLTPRELEVLLKLVAGGSSNRD	IGRRL	LLSEATVKSHLVHIYDKLGV	196		
	<i>C. glutamicum</i> HrrA	148	PKTSLTPRELEVLLKLVAGGSSNRD	IGRIL	FLSEATVKSHLVHIYDKLGV	196		
	<i>C. diphtheriae</i> HrrA	197	RSRTSAVAIAREQVL			212		
114	<i>C. glutamicum</i> HrrA	197	RSRTSAVAAREQGL			212		

115 **Figure S11: Alignment of HrrA orthologs of *C. glutamicum* and *C. diphtheria*.** The alignment was
 116 generated with Clustal Omega (<https://www.ebi.ac.uk/Tools/msa/clustalo/>) and visualized using
 117 Jalview (<http://www.jalview.org/>). Indicated in purple are identical amino acids and in yellow
 118 are the aspartate residues which become phosphorylated by HrrS.

119

120



121

122 **Figure S12: Schematic overview of the convolution profiling.** Read coverage was convolved
123 with negative second order Gaussian kernel. The convolved read coverage was then scanned to
124 discover the local maxima (peaks).

125

References

- 1 Studier, F. W. & Moffatt, B. A. Use of bacteriophage T7 RNA polymerase to direct selective high-level expression of cloned genes. *Journal of molecular biology* **189**, 113-130 (1986).
- 2 Kalinowski, J., Bathe, B., Bartels, D., Bischoff, N., Bott, M., Burkovski, A., Dusch, N., Eggeling, L., Eikmanns, B. J., Gaigalat, L., Goesmann, A., Hartmann, M., Huthmacher, K., Kramer, R., Linke, B., McHardy, A. C., Meyer, F., Mockel, B., Pfefferle, W., Puhler, A., Rey, D. A., Ruckert, C., Rupp, O., Sahm, H., Wendisch, V. F., Wiegrabe, I. & Tauch, A. The complete *Corynebacterium glutamicum* ATCC 13032 genome sequence and its impact on the production of L-aspartate-derived amino acids and vitamins. *Journal of biotechnology* **104**, 5-25 (2003).
- 3 Frunzke, J., Gatgens, C., Bocker, M. & Bott, M. Control of heme homeostasis in *Corynebacterium glutamicum* by the two-component system HrrSA. *Journal of bacteriology* **193**, 1212-1221, doi:10.1128/jb.01130-10 (2011).
- 4 Heyer, A., Gatgens, C., Hentschel, E., Kalinowski, J., Bott, M. & Frunzke, J. The two-component system ChrSA is crucial for haem tolerance and interferes with HrrSA in haem-dependent gene regulation in *Corynebacterium glutamicum*. *Microbiology (Reading, England)* **158**, 3020-3031, doi:10.1099/mic.0.062638-0 (2012).
- 5 Cremer, J., Eggeling, L. & Sahm, H. Cloning the *dapA dapB* cluster of the lysine-secreting bacterium *Corynebacterium glutamicum*. *Molecular and General Genetics MGG* **220**, 478-480, doi:10.1007/bf00391757 (1990).

Acknowledgement

I would like to express my special thanks to Prof. Dr. Julia Frunzke, for sharing the exciting and interesting project, for the constant interest in my work, the great discussions and her support in every respect.

Furthermore, I would like to thank Prof. Dr. Georg Groth for agreeing to be my co-supervisor.

I would like to thank all colleagues involved in the cooperation projects; Hannah Piepenbreier and Dr. Georg Fritz for the astounding work on the modelling of the two-component signaling and Cedric Davoudi, Dr. Andrei Filipchuk, Dr. Eugen Pfeifer, Dr. Tino Polen, Dr. Meike Baumgart and Prof. Dr. Michael Bott for fruitful discussions and valuable inputs regarding the HrrSA regulon.

I would like to thank Nguyen Van Nhi Le for her great work during her Bachelor thesis, which I had the chance to supervise.

Furthermore, I would particularly like to express my thanks to Cornelia Gätgens for her excellent technical support and Ulrike Viets for her great help on the ChAP-Seq and RNA-Seq dataset.

A special thanks to current and former group members of "Team Frunzke", especially Dr. Eva Davoudi, Dr. Andrei Filipchuk, Dr. Eugen Pfeifer, Aël Hardy, Max Hünnefeld, Roberto Stella, Johanna Wiechert, Larissa Kever, Aileen Krüger, Raphael Freiherr Von Boeselager, Isabell Huber, Cornelia Gätgens and Ulrike Viets. Thank you for creating the best working atmosphere one could wish for!

Special thanks also to my proof readers, for their time and valuable input: Dr. Eva Davoudi, Dorottya Keppel and Florian Küst.

Ich danke meiner Familie, die immer für mich da war und ist. Danke an Anna und meine Eltern, Frank und Karin, dafür, dass Ihr an mich glaubt.

Ich danke meiner Frau Dorottya. Für Alles.

Eidesstattliche Erklärung

Hiermit versichere ich an Eides Statt, dass die Dissertation von mir selbständig und ohne unzulässige fremde Hilfe unter Beachtung der „Grundsätze zur Sicherung guter wissenschaftlicher Praxis an der Heinrich-Heine-Universität Düsseldorf“ erstellt worden ist. Die Dissertation wurde in der vorgelegten oder in ähnlicher Form noch bei keiner anderen Institution eingereicht. Ich habe bisher keine erfolglosen Promotionsversuche unternommen.

Marc Keppel, 29.10.2018

Band / Volume 191

Absolute scale off-axis electron holography of thin dichalcogenide crystals at atomic resolution

F. Winkler (2019), xxiii, 187 pp

ISBN: 978-3-95806-383-9

Band / Volume 192

High-resolution genome and transcriptome analysis of *Gluconobacter oxydans* 621H and growth-improved strains by next-generation sequencing

A. Kranz (2019), III, 182 pp

ISBN: 978-3-95806-385-3

Band / Volume 193

Group IV (Si)GeSn Light Emission and Lasing Studies

D. Stange (2019), vi, 151 pp

ISBN: 978-3-95806-389-1

Band / Volume 194

Construction and analysis of a spatially organized cortical network model

J. Senk (2019), 245 pp

ISBN: 978-3-95806-390-7

Band / Volume 195

Large-scale Investigations of Non-trivial Magnetic Textures in Chiral Magnets with Density Functional Theory

M. Bornemann (2019), 143 pp

ISBN: 978-3-95806-394-5

Band / Volume 196

Neutron scattering

Experimental Manuals of the JCNS Laboratory Course held at Forschungszentrum Jülich and at the Heinz-Maier-Leibnitz Zentrum Garching edited by T. Brückel, S. Förster, G. Roth, and R. Zorn (2019), ca 150 pp

ISBN: 978-3-95806-406-5

Band / Volume 197

Topological transport in non-Abelian spin textures from first principles

P. M. Buhl (2019), vii, 158 pp

ISBN: 978-3-95806-408-9

Band / Volume 198

Shortcut to the carbon-efficient microbial production of chemical building blocks from lignocellulose-derived D-xylose

C. Brüsseler (2019), X, 62 pp

ISBN: 978-3-95806-409-6

Band / Volume 199

Regulation and assembly of the cytochrome *bc*₁-*aa*₃ supercomplex in *Corynebacterium glutamicum*

C.-F. Davoudi (2019), 135 pp

ISBN: 978-3-95806-416-4

Band / Volume 200

Variability and compensation in Alzheimer's disease across different neuronal network scales

C. Bachmann (2019), xvi, 165 pp

ISBN: 978-3-95806-420-1

Band / Volume 201

Crystal structures and vibrational properties of chalcogenides: the role of temperature and pressure

M. G. Herrmann (2019), xi, 156 pp

ISBN: 978-3-95806-421-8

Band / Volume 202

Current-induced magnetization switching in a model epitaxial Fe/Au bilayer

P. Gospodarič (2019), vi, 120, XXXVIII pp

ISBN: 978-3-95806-423-2

Band / Volume 203

Network architecture and heme-responsive gene regulation of the two-component systems HrrSA and ChrSA

M. Keppel (2019), IV, 169 pp

ISBN: 978-3-95806-427-0

Weitere **Schriften des Verlags im Forschungszentrum Jülich** unter
<http://www.zb1.fz-juelich.de/verlagextern1/index.asp>

Schlüsseltechnologien / Key Technologies
Band / Volume 203
ISBN 978-3-95806-427-0

Mitglied der Helmholtz-Gemeinschaft

